

**NONLINEAR OPTICAL PROPERTIES OF ORGANIC AND
POLYMER SYSTEMS: THEORETICAL AND
EXPERIMENTAL INVESTIGATIONS**

*Thesis submitted to
Cochin University of Science and Technology
in partial fulfilment of the requirements
of the Degree of*

Doctor of Philosophy

in

Chemistry

Under the faculty of Science

by

Elizabeth C V



**DEPARTMENT OF APPLIED CHEMISTRY
COCHIN UNIVERSITY OF SCIENCE AND TECHNOLOGY
KOCHI-22, INDIA**

September 2010

*Dedicated to
My Family,
Teachers and Friends.....*

COCHIN UNIVERSITY OF SCIENCE AND TECHNOLOGY
DEPARTMENT OF APPLIED CHEMISTRY


Dr. K. SREEKUMAR
Professor

CUSAT campus
Kochi-682022
Kerala, India
Tel: 0484-2575804
0484-2421530
Email: ksk@cusat.ac.in

CERTIFICATE

This is to certify that the thesis entitled “**Nonlinear Optical Properties of Organic and Polymer Systems: Theoretical and Experimental Investigations**” submitted for the award of the Degree of Doctor of Philosophy of the Cochin University of Science and Technology, is a record of original research work carried out by Ms. Elizabeth C V under my supervision and guidance in the Department of Applied Chemistry, and further that it has not formed the part of any other thesis previously.

Kochi-22
29.09.2010

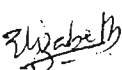


Dr. K. Sreekumar
(Supervising Teacher)

DECLARATION

I hereby declare that the thesis entitled **“Nonlinear Optical Properties of Organic and Polymer Systems: Theoretical and Experimental Investigations”** submitted for the award of Ph. D. Degree, is based on the original work done by me under the guidance of Dr. K. Sreekumar, Professor, Department of Applied Chemistry, Cochin University of Science And Technology and further that it has not previously formed the basis for the award of any other degree.

Kochi-22
29.09.2010


Elizabeth C V

*He has looked with favor on the lowliness of his servant...
the Mighty one has done great things for me
(Luke 1: 48-49)*

Acknowledgement

Dr. K Sreekumar - My supervising guide and Head of the Department - For his constant inspiration and guidance all through this work

Prof. K Girish Kumar - Former Head of the Department and Doctoral committee member - For the assistance during period of research

Prof. M R Prathapachandra Kurup - Former Head of the Department - For the help and for all the facilities

All the faculty members and non-teaching staff of the department - For their timely help and co-operation

Prof. Swapan K Pati, JNCASR, Bangalore - Our collaborator

Prof. P K Das, IISc, Bangalore - For NLO measurements

Dr. Ayan Datta, IISER Trivandrum; Dr. Manoj, IIITMK Trivandrum - For their valuable discussions and suggestions

STIC - CUSAT, NRC- IISc - Bangalore, SAIF - IIT Madras, NIIST - Trivandrum, Department of Physics-CUSAT - For Spectral Analysis

My Labmates - For their love and co-operation

Friends from Theoretical Science Unit, JNCASR, Bangalore - For their help during my work in JNCASR

Athulya hostel inmates - For their love, support and help

Friends of Department of Applied Chemistry - For their help and care

Research scholars from Department of Physics, Polymer Science and Rubber Technology Department, International School of Photonics - For their help during research

Friends and Teachers from Mar Thoma College, Perumbavoor, Sree Sankara Vidhyapeedam College, Valayanchirangara, C M S College Kottayam - For their love support and blessings

DRDO and CUSAT - For financial support to carry out the research work

My family - For their love, prayers, patience, support and interest

Elizabeth

PREFACE

The development of materials with high nonlinear optical (NLO) properties is a key to control the propagation of light by optical means. In particular, the response of the materials to the electric field has found tremendous application in designing materials for NLO devices. These devices are being used in numerous applications, from lasers to optical switches and electronics. Some of the best NLO properties are displayed by organic and polymer systems. These materials are of great interest because of their low cost, ease of fabrication and integration into devices. The necessary and essential conditions for the existence of second order nonlinear optics include the attainment of charge and spatial asymmetry. Such requirements are best met by dipolar, highly polarizable donor-acceptor systems, showing charge transfer between electron donating and electron withdrawing groups. When such structures extend to macroscopic dimensions, the poling of chromophores can be achieved through chemical synthesis, and there is no need for external poling. The permanent dipole moment of such structures can be very large because of the coherent addition of dipole moments achieved by a high degree of polar order.

Another way of ensuring noncentrosymmetry in polymer system is the incorporation of chiral molecules in polymer structure. Optically pure materials, which have only left-handed or right-handed symmetry, are inherently noncentrosymmetric. Such compounds are, in fact, readily available in the nature (amino acids, sugars and alkaloids are well known examples existing only in a single enantiomer). Thus polymers with these molecules are expected to be NLO active. The present work emphasizes chirality as an efficient tool to synthesize new class of second order nonlinear optical polymers. The nonlinear optical properties of polymers have been studied theoretically and experimentally.

Objectives of the present study

1. Theoretical investigation of NLO properties of organic molecules and polymers.
2. Theoretical designing of bifunctional and multifunctional polymers with high second-order NLO properties.

3. Synthesis and characterization of the designed bifunctional and multifunctional polyesters and polyurethanes.
4. Experimental evaluation of NLO efficiency of the polymers.
5. Theoretical and experimental correlations.

Chapter 1: Nonlinear optical properties of organic and polymer systems

This chapter presents a general introduction on the nonlinear optical (NLO) properties, theoretical background and various applications of NLO materials. It also gives a brief review of the important nonlinear optical polymers such as side chain, main chain, guest host systems, crosslinked systems etc. developed with high NLO coefficients.

Chapter 2: Computational studies on the stability and spectroscopic properties of porphyrin, chlorin, bacteriochlorin and their few metal complexes

This chapter discusses the stability of metal incorporated porphyrin, chlorin and bacteriochlorin. The metals with +2 oxidation state (Be, Mg, Ca, Sr, Ba, Zn and Cd) are used for the stability studies. The theoretical calculations were done to investigate the metal-ligand stability by means of Density Functional Theory and Time Dependent Density Functional Theory. Various spectroscopic properties (UV-Vis, IR, Raman) including NLO properties of metal free and metal incorporated porphyrin, chlorin and bacteriochlorin were investigated. This chapter mainly describes the effect of changes in electronic structure, bond order, formation energy, aromaticity and charge distribution on the stability of the metal encapsulated complexes. The stability order of metal complexes is predicted.

Chapter 3: Nonlinear optical properties of organic molecules: Theoretical investigation

This chapter describes the theoretical calculation of NLO properties of organic molecules. The chapter is divided into four parts. The first part deals with nonlinear optical properties of chromophore (D- π -A) and bichromophore (D- π -A-A- π -D) systems by making use of DFT and semiempirical calculations. Second part of this chapter deals with the odd-even effects in D-A groups of amidodiols obtained by the aminolysis of ϵ -caprolactone. Extensive theoretical evaluation was done on the effect of spacer length enhancement on the second-order NLO properties of twin donor-acceptor molecules having amido units bridged by CH₂

spacers. ZINDO/CV method was adopted for the NLO property calculations. The third part describes the odd even effect of D-A groups of amidodiols obtained by the aminolysis of γ -butyrolactones. The fourth part of this chapter deals with the theoretical investigation on the Diels-Alder reactions of fulgides with maleic anhydride. The spectroscopic properties of fulgides obtained by the Stobbe condensation of acetone, acetophenone and benzophenone with diethyl succinate and the theoretical studies regarding the feasibility of Diels-Alder reaction with maleic anhydride were performed by computational methods. DFT/B3LYP/6-31G (d, p) basis set was used for the theoretical evaluation of the transition states.

Chapter 4: Nonlinear optical polymers from natural resources: Theoretical and experimental studies on cardanol based polyurethanes

This chapter describes the synthesis of a series of polyurethanes incorporating chiral and achiral diols obtained from natural resources. The bifunctional and multifunctional polymers were designed computationally and the NLO activity was predicted. The achiral diol used for polymer synthesis was prepared by the condensation of formaldehyde with cardanol. The bifunctional and multifunctional polymers were synthesized by varying the composition of chiral and achiral diols. The NLO activity of the chiral polyurethanes was determined experimentally and the chapter concludes with correlating the experimental and theoretical results.

Chapter 5: Nonlinear optical properties of main chain chiral polyurethanes containing bisazo chromophores: Theoretical and experimental investigations

Chapter 5 deals with the theoretical and experimental studies of polyurethanes having main chain chirality and push-pull (donor-acceptor) azobenzene moiety. The azo polymers were designed as the polyaddition product of chromophores 2, 4-toluene diisocyanate (TDI) with azo diols, bis (4-hydroxy phenylazo)-2, 2'- dinitrodiphenylmethane, bis (8-hydroxy quinolinazo)-2, 2'-dinitro- diphenylmethane, bis (4-hydroxy-3-methylphenylazo)-2, 2'-dinitrodiphenylmethane (obtained by the diazo coupling of 4, 4' diamino-2, 2'-dinitrodiphenylmethane with phenol, 8-hydroxy quinoline and o-Cresol) and chiral diols (isosorbide, (2R, 3R)-diethyl tartrate and isomannide) with 2, 4-toluene diisocyanate. The SHG efficiency of the polyurethanes was found to be considerably high as predicted by theoretical calculations.

Chapter 6: Main chain chiral polyesters with amidodiol monomers derived from γ -Butyrolactone: Theoretical and experimental investigations

This chapter deals with the theoretical and experimental investigation of nonlinear optical properties of polyesters obtained by the condensation polymerization of terephthaloyl chloride with chiral diols and achiral diols. The polyesters were computationally designed and NLO properties of the bifunctional and multifunctional polymers were studied using ZINDO/CV methods. The designed polymer molecules were synthesized and the SHG efficiency of the molecules was evaluated. One part of the chapter describes the polyester synthesis using isosorbide as chiral moiety. The amidodiol obtained by the aminolysis of γ -Butyrolactone was used as the achiral diol for the present synthesis. The second and third parts of the chapter deal with synthesis of polyesters from (2R, 3R)-diethyl tartrate and isomannide as chiral molecules and SHG efficiency was experimentally determined.

Chapter 7: Main chain chiral polyurethanes with amidodiol monomers derived from ϵ -Caprolactone: Theoretical and experimental investigations

This chapter discusses the NLO properties of chiral polyurethanes obtained by the polyaddition of achiral amidodiol and chiral diols with 2, 4-toluene diisocyanate. The amidodiol monomers used for the synthesis was prepared by the aminolysis of ϵ -Caprolactone. The polymers were first designed and the NLO properties were predicted by computational tools. The designed bifunctional and multifunctional polyurethanes were synthesized by varying the chiral-achiral diol compositions. The SHG efficiency of the polymers predicted by theoretical calculations correlated with the experimental measurements

Chapter 8: Conclusions

This chapter presents the summary and important conclusions of the work done. References are given to the end of each chapter.

CONTENTS

Chapter 1:	Nonlinear optical properties of organic and polymer systems	1
Chapter 2:	Computational studies on the stability and spectroscopic properties of porphyrin, chlorin, bacteriochlorin and their few metal complexes	53
Chapter 3:	Nonlinear optical properties of organic molecules: Theoretical investigations	78
Chapter 4:	Nonlinear optical polymers from natural resources: Theoretical and experimental studies on cardanol-based polyurethanes	109
Chapter 5:	Nonlinear optical properties of main chain chiral polyurethanes containing bisazo chromophores: Theoretical and experimental investigations	136
Chapter 6:	Main chain chiral polyesters with amidodiol monomers derived from γ -Butyrolactone: Theoretical and experimental investigations	171
Chapter 7:	Main chain chiral polyurethanes with amidodiol monomers derived from ϵ -Caprolactone: Theoretical and experimental investigations	206
Chapter 8:	Summary	244

Chapter 1

**NONLINEAR OPTICAL PROPERTIES OF ORGANIC AND
POLYMER SYSTEMS***Abstract*

The review deals with recent and important developments in the field of organic polymers for second-order nonlinear optics. Second order nonlinear optical (NLO) properties of polymeric materials have attracted a lot of attention, especially for potential applications such as fast wave guides, electrooptic (EO) modulation and frequency-doubling devices. The review provides a survey of NLO active polymeric materials with a brief introduction which comprises the principles and the origin of nonlinear optics, chirality, donor-acceptor chromophores and the various kinds of polymeric materials for nonlinear optics, including guest-host systems, side chain polymers, main chain polymers, crosslinked polymers and chiral polymers.

1. 1. Introduction

Nonlinear electromagnetic phenomena occur when the response of a medium (including the electric polarization and its time derivative, the current density or the magnetisation) is a nonlinear function of the applied electric and magnetic field amplitudes¹. Earlier, nonlinear responses were observed with the application of dc or low frequency electric and magnetic fields. Pockels and Kerr effects, Raman Scattering etc. were some of the earlier nonlinear optical effects.

Nonlinear optics refers to any light-induced change in the optical properties of a material. Its domain encompasses those phenomena for which electric and magnetic intensities of higher powers than the first play a dominant role². Nonlinear optics is the basis of all the fledging photonic technologies^{3, 4}, where light works with or even replaces electrons in applications traditionally carried out by microelectronics. Nonlinear optics has applications in the domain of optoelectronics and photonics^{5, 6}, and materials with high nonlinear optical properties are used in high performance electro optic switching elements for telecommunication and optical information processing. Inorganic materials,⁶

organometallic compounds,⁷ liquid crystals,⁸ organic molecules and polymers⁹ have been investigated for their nonlinear optical properties.

The nonlinear optical phenomena were demonstrated after the invention of laser in 1960. By 1961, optical harmonics were already being generated and other nonlinear phenomena such as sum and difference frequency mixing, the optical Kerr effect, four-wave mixing, stimulated scattering (Raman and Brillouin) and self-induced transparency, soon followed¹⁰. Franken et al¹¹ were the first to demonstrate SHG of light in 1961. They used pulses of a ruby laser, first realised by Maiman¹² in 1960 and on the passage of the ruby laser pulse (3-kw pulse of red light, 694.3nm) through a quartz crystal, some ultraviolet photons at twice the frequency (347.15 nm) were generated.

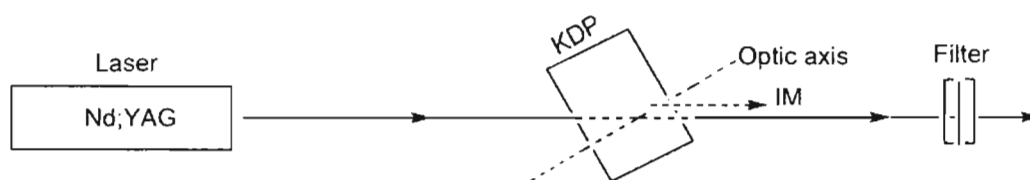


Figure 1. 1: Schematic illustration of optical frequency doubling using KDP crystal. IM is the index matched direction at an angle of θ to the optic axis.

This led to the development of inorganic materials such as lithium niobate (LNB), potassium titanyl phosphate (KTP), potassium dihydrogen phosphate etc. Maker¹³ et al and Giordmaine¹⁴ soon showed how the second harmonic generation would be enhanced by many orders of magnitude by phase matching of the fundamental and harmonic wave with the compensation of colour dispersion by birefringence in an anisotropic KDP crystal (**Figure 1. 1**).

1. 1. 1. Polymers for optical devices

Organic polymers have a number of desirable properties, which make them materials of choice for optical devices. Organic materials are intrinsically fast (electronic response, femto second response) due to the virtual process of polarizing electrons, and have low dielectric constants, which permit low capacitance leading to high-speed devices. They could have exceptionally high nonlinear activity resulting in improved device performance and can be tailored by conventional synthetic methods to meet specific requirements (e.g.: transparency at particular wavelength and stability at particular temperature).

They offer many processing options towards desired device formats, which should reduce the cost of active devices and are found to be more adept at manipulating light than their inorganic counter parts. They are also easy to prepare, process and fabricate into devices. Also they can be readily integrated with semiconductor electronics and fiber-optic transmission lines. As a result, polymeric materials promise to make optoelectronic technologies more practical and wide spread. They could make major impacts on telecommunication¹⁵, optical signal processing, computing and data storage¹⁶. As polymer based electro optic modulators and switches begin to enter the market, other applications are waiting in the wings.

1. 2. Theory of nonlinear optics

Before the invention of laser, under the ordinary experience of every day life, the optical properties and parameters of a medium were independent of the intensity of light that permitted observation of the optical phenomena such as reflection, refraction, diffraction, absorption, and scattering. This is the realm of what is called linear optics. The invention of laser gave rise to the study of optics at high intensities, leading to new phenomena not seen with ordinary light such as the generation of new colors from monochromatic light in a transparent crystal, or self-focusing of an optical beam in a homogeneous liquid. At the intensities used to generate these types of effects, the usual optical parameters of materials cannot be considered constant but become functions of light intensity. The science of optics in this regime is called nonlinear optics. This is because of the reason that the field strength of the conventional light source used before the advent of lasers, were much smaller than the field strength of atomic and inter-atomic fields. The electric charges in matter are held in equilibrium by atomic fields of the order 10^8 - 10^9 V/cm, and anharmonicity in their motion can only be observed by using perturbing fields that are not negligible compared to these values. Due to coherence, the laser beam can be focused to an area $A \approx \lambda^2$. If the laser wavelength is assumed to be 1μ , then $A = 10^{12}$ m² and hence $J_E \approx 10^{18}$ MW/m² giving $E \approx 3 \times 10^{10}$ V/m which is within the range of atomic field. At such high fields, the relationship between the electric polarization P and the field strength E ceases to be linear and some interesting nonlinear effects come to the fore^{17, 18}.

When a ray of light of frequency ν strikes a material system, the elementary particles of which it is made of are influenced in their relative motion and begin to oscillate with the frequency ν . By this induced polarization, the material system is transformed into a secondary emitter like an antenna. The simple assumption concerning such a scattering process is that electric field component of the electromagnetic radiation induces an oscillating dipole in the molecule, the magnitude of which is proportional to the electric field. If an elastic or linear scattering occurs, no net energy is transferred from the radiation to the molecule, i.e., the molecule will be in the same energy state before and after the scattering. However, during the time of scattering, the molecule is not in a pure stationary state. But it is in a time dependent, non-stationary state, which may be described as a superposition of many stationary states. The duration of such a scattering process may be estimated from the angular frequency of the interacting radiation. If it is ω , the time for such an interaction lasts is $\tau=1/\omega$. In spite of this very short time, the molecule can interact several times with the radiation. As a direct consequence, the radiation-induced polarization consists of a major part, which depends on the first power of field strength, but may also contain nonlinear contributions, which are proportional to the radiation field to second, third or even higher order. Thus the induced polarization consists of a variety of contributions giving rise to very fast secondary re-emission, i.e., scattering at different frequencies^{11, 17-20}.

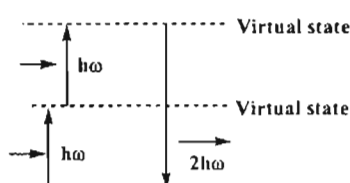


Figure 1. 2: Schematic representation of second harmonic generation

Nonlinear interaction between electromagnetic radiation and matter can be described in quantum mechanical terms as multi photon process. In multi photon process an interaction between radiation and matter accompanied by absorption or emission or both, of not less than two photons per elementary act is observed. Second harmonic generation is a three-photon process as shown in **Figure 1. 2**. Two photons, each with energy $h\omega$, are absorbed and one photon

with energy $2\hbar\omega$ is emitted. The state of the quantum system remains unaltered. This gives an impression that two colliding photons merge “directly” into a single one. The levels shown in the figure by dotted lines are the “virtual levels”.

1.3. Electromagnetic basis of nonlinear optics²¹

Ordinary matter consists of a collection of positively charged cores (of atoms or molecules) and surrounded by negatively charged electrons. Light interacts primarily with matter via the valence electrons in the outer shells of electron orbital. The fundamental parameter in this light-matter interaction theory is the electronic polarization of the material induced by light. When an electric field is applied to a dielectric medium (of neutral electric charge), a separation of bound charges is induced. Within the electric-dipole approximation, this separation of charge results in a collection of induced dipole moments μ , which, as designated, may be rapidly oscillating if induced by a rapidly varying applied field.

$$\mu = -er \quad (1)$$

where e the electric charge, r the displacement induced by the electric field.

The electric polarization P is defined as the net average dipole moment per unit volume and is given by

$$P = N \langle \mu \rangle \quad (2)$$

where N is the number of microscopic dipoles per unit volume, and the angular bracket indicates an ensemble average over all the dipoles in the medium. In what follows, any permanent dipole within the medium will be ignored since they will not be oscillating at optical frequencies and hence will not radiate electromagnetic waves.

By the principle of causality (the relationship between causes and effects), P must be a function of the applied field E . To an excellent approximation, at the low intensity levels of natural light sources, the relation of the applied field is linear i.e. proportional to the applied field. This is the regime of linear optics. The most general form of the electric polarization for a homogeneous medium is given by

$$P_L(r, t) = \int_{-\infty}^{\infty} \int_{-\infty}^{\infty} \chi^{(1)}(r - r', t - t') \cdot E(r', t') dr' dt' \quad (3)$$

The equation is in cgs system. In SI system the equation should be multiplied with $\epsilon_0=8.85 \times 10^{-12}$ farad/meter, the electric permittivity of free space, where the subscript L signifies a linear polarization. $\chi^{(1)}(r-r', t-t')$ is the linear dielectric response tensor. The functional form of $\chi^{(1)}$ reflects the principles of space and time invariance²². In other words, the polarization response of the medium does not depend on whether (in an absolute sense) the driving field is applied, or not, but only on the time, since it was applied. Consequently, $\chi^{(1)}(r-r', t-t')$ must be defined in such a way that it vanishes when $t-t' < 0$ to preserve causality. Similarly, the polarization response in a homogeneous medium does not depend on the absolute position in space of the applied field, but only on the distance away from this position. A non zero value of $\chi^{(1)}(r-r', t-t')$ for $r \neq r'$ is called a non local response. If there is no response except within a small neighborhood where $r \approx r'$, then the response is called local. This is equivalent to saying that the linear dielectric response tensor has a δ -function dependence. For the vast majority of problems in nonlinear optics, the media of interest produces approximately a local response. Consequently we shall ignore the spatial dependence of $\chi^{(1)}$.

The form of the linear dielectric response tensor allows a simpler relation to be made between the Fourier transforms of the polarization and the applied field,

$$P_L(\omega) = \chi^{(1)}(\omega) \cdot E(\omega) \quad (4)$$

where $\chi^{(1)}(\omega)$, the linear susceptibility tensor, is the Fourier transform of the linear dielectric response tensor. The tensor relation in equation (4) can also be written as

$$P_{L,I}(\omega) = \sum_J \chi_{IJ}^{(1)}(\omega) E_J(\omega) \quad (5)$$

where the subscript I signifies the i^{th} Cartesian coordinate ($l = x, y, z$) and the sum is over $J=x, y, z$. The tensor $\chi^{(1)}(\omega)$ thus has nine components. In an isotropic medium, there is only one independent, non-zero component, and the susceptibility is written as a scalar quantity, $\chi^{(1)}(\omega)$. This can be represented in the molecular (microscopic) level as

$$\langle \mu(\omega) \rangle = \alpha^{(1)}(\omega) \cdot E_{\text{local}}(\omega), \quad (6)$$

where $\alpha^{(1)}$ is the molecular polarizability, E_{local} is the local electric field (at the molecule), which is a superposition of the applied field E and the net field due to the surrounding dipoles. An analytical expression for the local field can be

obtained for isotropic and cubic medium. The relationship between the susceptibility and the polarizability for this media is given by

$$\chi^{(1)} = \left(\frac{n^2 + 2}{3} \right) N\alpha^{(1)} \quad (7)$$

The quantity $f(\omega) = [n^2(\omega) + 2]/3$ is called the local field factor.

The nonlinear optical phenomena arise from the break down of equation 4 at sufficiently intense fields. As the applied field strength increases, the polarization of the medium is no longer linear. Only after the advent of the laser could optical fields of sufficient intensity be produced to observe this effect¹¹. To account for the "nonlinearity" of the medium response, the induced polarization is given as a power series expansion in the applied electric field.

It is assumed that the nonlinear polarization can be written as

$$P = P_L + P_{NL} \quad (8)$$

$$P_{NL} = P^{(2)} + P^{(3)} \quad (9)$$

$$P^{(2)}(r, t) = \int_{-\infty}^{\infty} \int_{-\infty}^{\infty} \chi^{(2)}(t-t', t-t'') : E(r, t') E(r, t'') dt' dt'' \quad (10)$$

$$P^{(3)}(r, t) = \int_{-\infty}^{\infty} \int_{-\infty}^{\infty} \int_{-\infty}^{\infty} \chi^{(3)}(t-t', t-t'', t-t''') : E(r, t') E(r, t'') E(r, t''') dt' dt'' dt''' \quad (11)$$

It is important that the field in the equations above is the total applied field, which can be a superposition of many fields of different frequencies. $\chi^{(n)}$ is called nth order dielectric response, and is a tensor of rank n+1. As for the linear dielectric response, it is assumed that the response is local and hence the spatial dependence of $\chi^{(n)}$ is suppressed.

If the applied field is a superposition of monochromatic or quasi monochromatic waves, then it is possible to write expressions analogous to equations (10) and (11) in terms of Fourier transforms of the nonlinear polarization, fields, and the dielectric response tensor, provided the frequency dependence of the Fourier transform of $\chi^{(n)}$ is slowly varying in the region of each Fourier components (e.g., its various laser frequencies), then, the nonlinear polarization will consist of several terms oscillating at various combination frequencies. For example, if the total field consists of two waves oscillating at frequencies ω_1 and ω_2 , the second-order nonlinear polarization will have components oscillating at $2\omega_1$, $2\omega_2$, $\omega_1+\omega_2$, and $\omega_1-\omega_2$ and dc terms at zero

frequency. Similarly, with three fields oscillating at frequencies $\omega_1, \omega_2, \omega_3$, the third-order polarization will oscillate at $3\omega_1, 3\omega_2, 3\omega_3, \omega_1+\omega_2+\omega_3, \omega_1+\omega_2-\omega_3$, etc.

Thus, applying Fourier transform, the equation (10) can be written as follows. Consider a second-order polarization oscillating at ω_3 due to the presence of fields oscillating at frequencies ω_1 and ω_2 with $\omega_3 = \omega_1 + \omega_2$. Then the i^{th} Cartesian component of the complex polarization amplitude is expressed as

$$P_i^{(2)}(\omega_1) = D^{(2)} \sum_{JK} \chi_{iJK}^{(2)}(-\omega_1; \omega_2, \omega_3) E_J(\omega_2) E_K(\omega_3) \quad (12)$$

$$D^{(2)} = \begin{cases} 1 & \text{for indistinguishable fields} \\ 2 & \text{for distinguishable fields.} \end{cases}$$

where $\chi^{(2)}(-\omega_3; \omega_1, \omega_2)$ is the second order susceptibility and Fourier transform of $\chi^{(2)}(t)$. The form of equation (12) allows for the possibility that the frequencies ω_1 and ω_2 are equal or equal in magnitude and opposite in sign. In this case, there may actually be only one field present, and the degeneracy factor $D^{(2)}$ takes this into account. This notation is easily extended to higher orders. When three frequencies $\omega_1, \omega_2, \omega_3$ are present, the third-order polarization at $\omega_4 = \omega_1 + \omega_2 + \omega_3$ is given by

$$P_i^{(3)}(\omega_1) = D^{(3)} \sum_{JKL} \chi_{iJKL}^{(3)}(-\omega_1; \omega_2, \omega_3, \omega_4) E_J(\omega_2) E_K(\omega_3) E_L(\omega_4) \quad (13)$$

where degeneracy factors, in this case, becomes

$$D^{(3)} = \begin{cases} 1 & \text{all fields indistinguishable} \\ 3 & \text{two fields indistinguishable} \\ 6 & \text{all fields distinguishable} \end{cases}$$

This form of third-order polarization allows for various combination frequencies, even when only two fields are present, such as $\omega_1+2\omega_2$, or $2\omega_1-\omega_2$, etc. the degeneracy factor is just due to the number of different ways in which the products of the Fourier components appear in the expansion of the total field to some power.

Hence the total polarization can be represented as

$$P_i(\omega_1) = \sum_J \chi_{iJ}^{(1)}(-\omega_1; \omega_2) E_J(\omega_2) + \frac{1}{2} \sum_{JK} \chi_{iJK}^{(2)}(-\omega_1; \omega_2, \omega_3) E_J(\omega_2) E_K(\omega_3) + \frac{1}{6} \sum_{JKL} \chi_{iJKL}^{(3)}(-\omega_1; \omega_2, \omega_3, \omega_4) E_J(\omega_2) E_K(\omega_3) E_L(\omega_4) + \dots \quad (14)$$

The macroscopic susceptibilities are related to the corresponding molecular susceptibilities by local field corrections (f)²³ and the molecular number density (N)²⁰

$$\chi_{ij}^{(1)} = N \sum_{ij} f_i \langle \cos \theta_{ii} \rangle f_j \langle \cos \theta_{jj} \rangle \alpha_{ij} \quad (15)$$

$$\chi_{ijk}^{(2)} = N \sum_{ijk} f_i \langle \cos \theta_{ii} \rangle f_j \langle \cos \theta_{jj} \rangle f_k \langle \cos \theta_{kk} \rangle \beta_{ijk} \quad (16)$$

$$\chi_{ijkl}^{(3)} = N \sum_{ijkl} f_i \langle \cos \theta_{ii} \rangle f_j \langle \cos \theta_{jj} \rangle f_k \langle \cos \theta_{kk} \rangle f_l \langle \cos \theta_{ll} \rangle \gamma_{ijkl} \quad (17)$$

where the variables, i, j, k and l now span the molecular axes, and the angle between the macroscopic axis I and microscopic i is denoted as θ_{ii} . The local field factors are essentially correct for the difference between an applied field that would be felt by the molecule in free space and the local field detected in a material. These factors usually take the form of the well known Onsager²⁴ or Lorentz²⁵ correction fields. The microscopic polarization (p_i) can then be expressed as

$$p_i(\omega_1) = \sum_j \alpha_{ij}(-\omega_1; \omega_2) E_j(\omega_2) + \frac{1}{2} \sum_{jk} \beta_{ijk}(-\omega_1; \omega_2, \omega_3) E_j(\omega_2) E_k(\omega_3) + \frac{1}{6} \sum_{jkl} \gamma_{ijkl}(-\omega_1; \omega_2, \omega_3, \omega_4) E_j(\omega_2) E_k(\omega_3) E_l(\omega_4) + \dots \quad (18)$$

The manifestation of nonlinear optical behavior can be clearly seen by substituting a sinusoidal field $E = E_0 + E_1 \cos \omega t$ in to the polarization. Substituting this in equation (14) gives:

$$P = (E_0 + E \cos \omega t) \chi^{(1)} + (E_0 + E \cos \omega t)^2 \chi^{(2)} + (E_0 + E \cos \omega t)^3 \chi^{(3)} + \dots \quad (19)$$

Rearranging the equation,

$$P = (\chi^{(1)} E_0 + \chi^{(2)} E_0^2 + \chi^{(3)} E_0^3) + (\chi^{(1)} E_1 + 2\chi^{(2)} E_0 E_1 + 3\chi^{(3)} E_0^2 E_1) \cos \omega t + (\chi^{(2)} E_1^2 + 3\chi^{(3)} E_0 E_1^2) \cos^2 \omega t + (\chi^{(3)} E_1^3) \cos^3 \omega t + \dots \quad (20)$$

Using Trigonometric relations, $\cos^2 \omega t = (1 + \cos 2\omega t)/2$, $\cos^3 \omega t = (\cos 3\omega t + 3\cos \omega t)/4$, equation (20) becomes

$$P = \chi^{(1)} [E_0 + E_1 \cos \omega t] + \chi^{(2)} [E_0^2 + (1/2)E_1^2 + 2E_0 E_1 \cos \omega t] + (1/2)E_1^2 \cos 2\omega t + \chi^{(3)} [E_0^3 + (3/2)E_0 E_1^2 + 3E_0^2 E_1 \cos \omega t] + (3/4)E_1^3 \cos 2\omega t + 3/2 E_0 E_1^2 \cos 2\omega t + (3/4)E_1^3 \cos 3\omega t + \dots \quad (21)$$

The 1st term in the brackets for all $\chi^{(n)}$ are constant factors. They give rise to a dc field across the medium.

1. 4. Second order nonlinear optical processes

This section explains the processes associated with the $\chi^{(2)}$ in detail. From equation (21),

$$P^{(2)} = \chi^{(2)}[E_0^2 + (1/2)E_1^2 + 2E_0E_1 \cos \omega t] + (1/2)E_1^2 \cos 2\omega t \quad (22)$$

The coefficients E_0 , E_1 corresponds to the linear electro-optic effect and is represented as $\chi^{(2)}(-\omega; \omega, 0)$. The sign attached to a frequency is negative if the photon is emitted and positive, if it is absorbed. The last term, which is square in the ac electric field and has a frequency of 2ω is known as second harmonic generation (SHG) process.

Consider that two coherent light waves of unequal frequencies ω_1 and ω_2 are traveling in the material, then the 2nd and 4th terms in the previous equation (22) becomes

$$\chi^{(2)}(1/2)E_1^2[\cos(\omega_1 - \omega_2) + \cos(\omega_1 + \omega_2)] \quad (23)$$

Thus it contains two frequencies, $(\omega_1 + \omega_2)$ and $(\omega_1 - \omega_2)$. This phenomenon is known as optical mixing. While $(\omega_1 + \omega_2)$ is called sum frequency generation (SFG), $(\omega_1 - \omega_2)$ is called the difference-frequency generation (DFG). The second harmonic generation (SHG) process, actually, is a special case of SFG, where the frequencies of the photons from the incident beams are equal ($\omega_1 = \omega_2$). Similarly, optical rectification (OR) is a special case of DFG for $(\omega_1 = \omega_2)$. Thus OR susceptibility, is represented as $\chi^{(2)}(0; \omega, -\omega)$.

Three-wave mixing (two inputs and one output) is known as a parametric process, if the initial state and the final state of the system remain unchanged after interaction with light. This is because, in an emission process, the system comes back to the same state after emission. The same is not true for an absorption process where the initial and final states differ. The most prominent example of a non-parametric process is two-photon absorption. Various processes in nonlinear optical spectroscopy are listed in **Table 1. 1**. Parametric processes can be used to make various devices. For example, Optical Generators can produce a wave of higher (up-conversion) or lower frequency (down-conversion) than the initial frequency. In Parametric Amplifiers three waves interact at frequency ω_1 , ω_2 and ω_3 , so that one wave at frequency ω grows at the expense of the input frequency called the pump frequency. A very important device using parametric amplification is the Optical Parametric Oscillator. In this

device, one uses a single pump source as an input and the output intensity can be controlled by changing the positions of the two mirrors surrounding the material.

Table 1. 1: Some important processes involving Nonlinear Optical Spectroscopy

Process	Order	Frequency relation
Linear Response	1	$-\omega; \omega$
Pockels Effect (EO effect)	2	$-\omega; \omega, 0$
Sum Mixing	2	$-\omega_a; \omega_1, \omega_2$
Second Harmonic Generation (SHG)	2	$2\omega; \omega, \omega$
Optical Rectification (OR)	2	$0; \omega; -\omega$
Intensity- dependent refractive index	3	$-\omega; \omega, -\omega, \omega$
Optical Kerr Effect	3	$-\omega_1; \omega_2, -\omega_2, \omega_1$
Dc Kerr Effect	3	$-\omega; 0, 0, \omega$
Two-photon Absorption (TPA)	3	$-\omega_1; \omega_2, \omega_2, \omega_1$
Third Harmonic Generation (THG)	3	$3\omega; \omega, \omega, \omega$
Coherent anti-stokes Raman scattering	3	$-(2\omega_1, -\omega_2); \omega_1, \omega_1, -\omega_2$
General four Wave mixing (FWM)	3	$-\omega_a; \omega_1, \omega_2, \omega_3$
Three-Photon Absorption (TPA)	5	$-\omega_1; \omega_2, -\omega_3, \omega_3, \omega_2, \omega_1$
n^{th} Harmonic Generation	n	$n\omega; \omega, \omega, \dots, \omega$
Multi-photon Absorption	$2n-1$	$-\omega; \dots, -\omega, \omega, \dots, \omega$

Owing to the spherical nature of nearly all molecular structures, and the differing atomic charges, δ^+ and δ^- , that each element possesses relative to each other in a given molecule, the overall polarization inevitably has a net direction, i.e. it is anisotropic. The relative orientation of a molecule with respect to others with in the repeating (unit cell) crystal-lattice motif is also important, since the SHG effect is a supramolecular rather than a molecular one. This polarization anisotropy is therefore three dimensional and thus (beyond the molecule) dependent upon supramolecular symmetry. The associated mathematics of the symmetry considerations is therefore very much involved, since the SHG effect is a third rank tensor. But it is only the results that are important here: in total

the symmetry conditions dictate that SHG active compounds can only occur in 18 out of the 32 crystallographic point groups.¹⁹

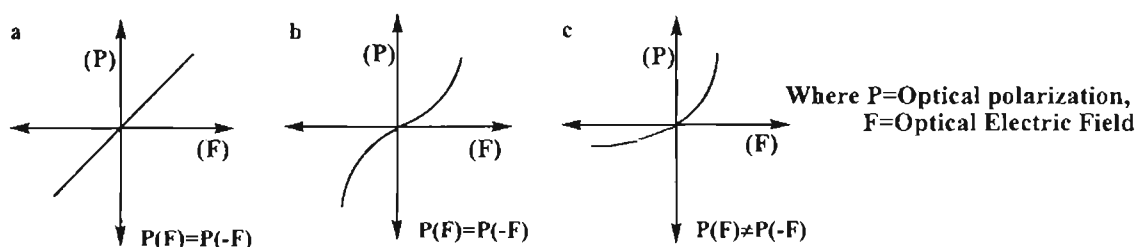


Figure 1. 3: Symmetry requirements for second-order process showing the dissipation of the optical polarization. a. Linear, b. Centrosymmetric nonlinear, c. Non-centrosymmetric nonlinear

In 1962 Kleinman found that in many nonlinear processes where all the interacting frequencies are far away from resonance, energy is simply exchanged between the fields and not dissipated in the medium^{26, 27}. Thus, the dispersion of the $\chi^{(n)}$ is negligible and therefore the susceptibility tensors are invariant under any permutation of their Cartesian indices. For instance, in the $\chi^{(2)}$, the symmetry relations give rise to

$$\chi_{ijk}^{(2)} = \chi_{ikj}^{(2)} = \chi_{jik}^{(2)} = \chi_{jki}^{(2)} = \chi_{kij}^{(2)} = \chi_{kji}^{(2)} \quad (24)$$

Thus due to Kleinman symmetry relations, the number of independent components of $\chi^{(2)}$ reduces from 27 to 10 and that of $\chi^{(3)}$ from 81 to 15.

Thus for a medium to exhibit frequency conversion process mediated by $\chi^{(2)}$, the medium must have $\chi^{(2)} \neq 0$. This condition requires that at a molecular level the nonlinear coefficient β must be nonzero. Furthermore, the orientationally averaged sum of β gives rise to the macroscopic $\chi^{(2)}$ should not be zero. These two conditions lead to the following symmetry requirements for the realization of $\chi^{(2)} \neq 0$. The molecules are non-centrosymmetric (do not possess an inversion symmetry), β -being an odd rank (3rd rank) tensor-is not zero.

A molecular design often used to make molecules with large β values is D- π -conjugation-A. This is the one in which the molecular unit involving π -conjugation is connected to an electron donor, D, at one end and to an electron acceptor group, A, at the other end. The donor-acceptor systems show charge transfer between electron donating and electron withdrawing groups. Effective NLO polymers were obtained by the incorporation of highly active

chromophore molecules which have a large molecular hyperpolarizability β . Factors such as increased length, increased planarity and overall increased conjugation and the strength of donors and acceptors (i.e., the Hammett substituent-constant parameters) all play significant roles in nonlinear optics and are amenable to design.

1. 5. NLO chromophores

NLO chromophores are molecules with electron donor and acceptor conjugated π -systems²⁸. The π conjugated system could be azobenzene, stilbene, biphenyl, heterocycles, polyenes etc. The electron acceptors and donors that can be attached to a π -conjugated system are as follows: Acceptor Groups: NO₂, COOH, CN, CHO, CONH₂, CONHR, CONR, CONR₂, SO₂R, CF₃, COCH₃, CH=C(CN)₂ etc and donor Groups: NH₂, NHR, NR₂, F, Cl, Br, OR, OH, C(CH₃)₃, COOR etc.

Ouder and Chemla suggested a two-state model to guide the design of second-order NLO chromophores²⁹

$$\beta = \frac{(\mu_{ee} - \mu_{gg})(\mu_{ge})^2}{(E_{ge})^2}$$

where μ and E are the dipole matrix element and transition energy, respectively, between the ground state (g) and the excited state (e). In fact, molecules for second order NLO applications were based simply upon aromatic π - electron systems asymmetrically end capped with electron donating and accepting groups which impart the directional bias. By the development of the EFISHG technique and by two level model, several one dimensional charge transfer systems with good NLO properties were developed during the 1980s. Typical examples of such systems are p-nitroaniline (PNA) and dimethyl- amino nitrostilbene (DANS). In DANS, the two benzene rings and the double bond provide the conjugated π - system and the polarizable electrons, the dimethylamino group acts as the donor and the nitro group acts as the acceptor which is shown in **Figure 1. 4**. DANS was considered to be quite nonlinear at that time and is still being used as a typical benchmark to evaluate NLO properties of other molecules³⁰. Attempts carried out to increase the nonlinearity were usually aimed at increasing the donor-acceptor strength or increasing the

length of the conjugation bridge³¹. In addition, chromophores with other types of conjugation bridges have been investigated. Many of these systems fall into the category of substituted benzenes, biphenyls, stilbenes, azostilbenes and tolans³²⁻³⁴.

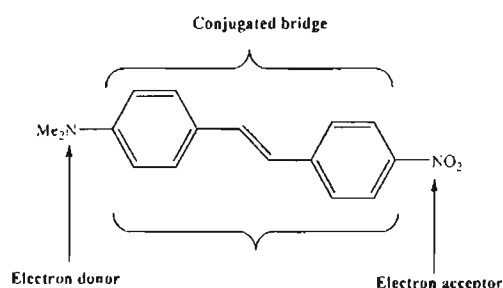


Figure 1. 4: Dimethylamino nitro stilbene(DANS)

Schmidt et al. reported 2-dicyanomethylidene-4, 5, 5-trimethyl-2, 5-dihydrofuran group as a strong acceptor in second-order NLO chromophores which possess high β , excellent thermal stability and when incorporated in a PMMA film results in a high value of electro-optic coefficient r_{33} ³⁵. Rutkis et al. studied the NLO efficiency of the poled host-guest films of eight different dimethylamino benzylidene 1, 3-indandione (DMABI) (**Figure 1. 5**) derivative chromophores which resulted in high NLO efficiency.³⁶

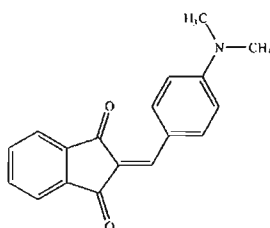


Figure 1. 5: Structure of DMABI

Azo dyes are widely used as chromophores for organic nonlinear optics (NLO) in modern technology. Rezaeifard et al.³⁷ reported the synthesis of several varieties of azo chromophores and their characteristics. Sreekumar et al. developed biphenolic azo diol chromophores, bis (4-hydroxy phenylazo)-2, 2'-dinitro diphenylmethane and bis (4-hydroxy phenylazo)-2, 2'-dinitrodiphenylsulfone³⁸⁻⁴⁰, the structure are shown in (**Figure 1. 6**).

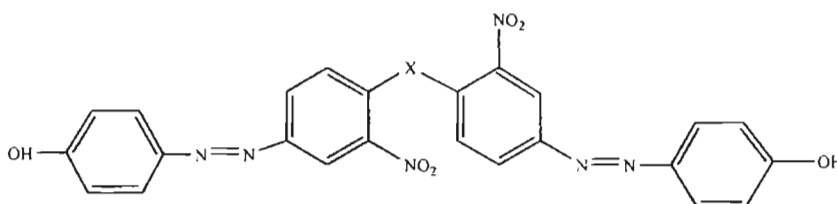


Figure 1. 6: Bis (4-hydroxy phenylazo)-2, 2'-dinitrodiphenylmethane with $X=CH_2, SO_2$

Disperse Red 1 (**Figure 1. 7**) and its derivatives are widely exploited as a side chain chromophore in the field of nonlinear optics.

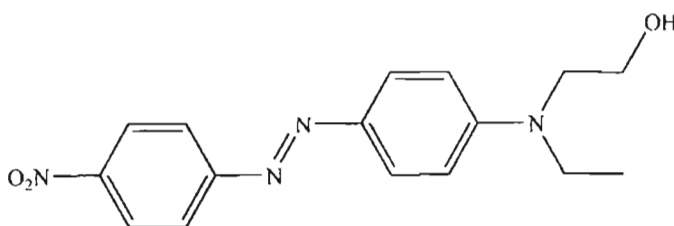


Figure 1. 7: Disperse Red 1 chromophore

Odobel et al.⁴¹ used DR1 chromophore as the active NLO unit for the successful preparation of new EO materials based on hyperbranched dendritic polymers. Although hyperbranched polymers have been known since 1950s⁴², their use for EO application has been reported only recently⁴³⁻⁴⁴. They proposed three types of organization for the chromophores for a branched material like main chain, side chain and peripheral form.

1. 6. Polymers as second-order nonlinear optical materials

The nonlinear optical response of a material can be used to make a variety of all-optical devices and the material criteria depend on the need for each specific device. Optical quality, transparency, tailorable refractive index, the ability to make specialized structures with the materials (such as thin films and fibers) and nonlinear susceptibility are some important properties that make an ideal NLO material.

Polymers are now considered as the most important specialty materials, as they combine the nonlinear optical properties of conjugated π -electron systems with the feasibility of creating new materials with appropriate optical and structural properties. Polymers that contain NLO active chromophores are promising candidates due to several advantages that are linked with polymers⁴⁵.

They provide tremendous architectural flexibility to tailor the desired photonics functions and material performance. Polymers provide ease of processing and they are compatible to metal, glasses, ceramics and other substrates. They can be chemically modified to generate new materials. Also, polymers are environmentally stable and robust materials and are also tough and lightweight¹⁷. As a result of all these, nonlinear optical polymers have received considerable attention in the development of photonic, and optoelectronic based technologies for high speed data processing, transmission and storage in the past two decades.⁴⁶⁻⁴⁸

Nonlinear optical chromophores can be incorporated into the macroscopic environment by several ways. The most important and most widely used is the incorporation of dipolar chromophores into a polymer host by simply dissolving the chromophore into a polymeric material (guest-host systems), by covalently attaching the chromophores to a polymeric backbone (side-chain polymers) or by incorporating the chromophores into the backbone of the polymer (main-chain polymers).

1.7. Guest-host systems

Guest-host (GH) systems were the first organic materials investigated, in which SHG was induced by noncentrosymmetric ordering of NLO chromophores under electrical poling. The main problem of guest host systems is the decrease of the glass transition temperature of the host (polymer) dramatically due to plasticization by the guest (chromophore)⁴⁹. GH systems are also undesirable because the chromophores are labile; at elevated temperatures they diffuse to the surface of the film and evaporate or sublime. However, GH systems offer several advantages: they can use a wide variety of noncentrosymmetric NLO chromophores for SHG activity, ease of processing into thin film by coating, dipping, and lithography, ease of fabrication onto a large area of substrate of any dimensions, inexpensive production of NLO materials, wide range of operating frequencies and low dielectric constant^{50, 51}. A guest-host system is generally prepared by mixing a NLO dye, possessing large molecular hyperpolarisability β , into an amorphous polymer matrix of high optical transparency. NLO dye is dissolved in the polymer host using a

common solvent; spin coated as a film to the substrate and the films are dried under vacuum. It is then poled at elevated temperatures.

Meredith et al.⁵² in 1982 reported SHG active guest-host system by doping a side chain liquid crystal polymer with 4-(dimethylamino)-4'-nitrostilbene. The poled-polymer approach in an amorphous system was first demonstrated by dissolving (N-ethyl-N-(2-hydroxyethyl) amino-4'-nitroazobenzene) (DRI) in poly (methyl methacrylate) (PMMA)⁵³ (Figure 1. 8).

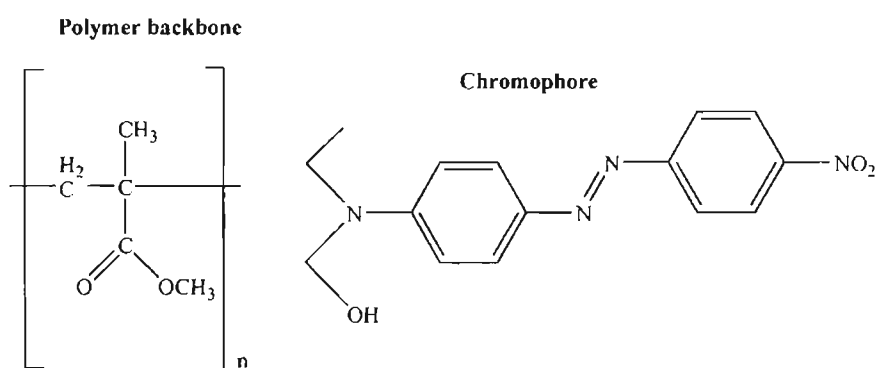


Figure 1. 8: Polymer backbone and azo chromophore

Wu et al. developed guest-host system with good temporal stability and high T_g polyimide at a high temperature⁵⁴. Guest chromophores were typically introduced into solutions of polyamic acids which was processible into thin films. Thermal and chemical imidisation under a poling field at temperatures up to 360°C have resulted in impressive temporal stability at 200-300°C^{54, 55}. Petsalakis et al. developed crosslinked host polymers to improve the temporal stability of a guest-host system and in a composite of 4-N, N-dimethyl-4'-nitrostilbene (DANS) with a highly crosslinked epoxy network, good temporal stability at room temperature was achieved⁵⁶. (Figure 1. 9)

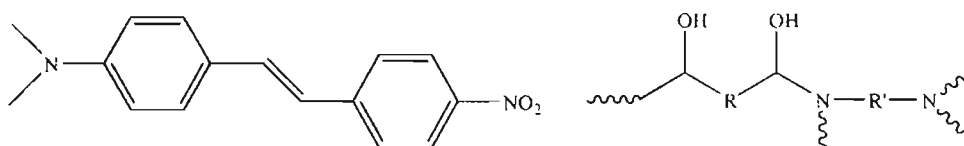


Figure 1. 9: 4- N, N-dimethyl-4'-nitrostilbene (DANS)

Physical aging of guest host systems was demonstrated by Lee et al⁵⁷. Physical aging can reduce the free volume of the polymer or change the

distribution of free volume and size and therefore, physical aging seems to be a good technique for improving the stability of polymers. Boyd et al.⁵⁸ suggested that large dopant molecules were effective in preventing the decay of SHG activity and large dopant molecules with high thermal stability^{59, 60} were reported. Although high temporal stability can be achieved with high T_g host polymers, problems such as low solubility, thermal degradation, sublimation and the plasticizing effect of the guest molecules have prevented the attainment of both high stability and nonlinearity⁶¹. So in guest-host nonlinear optical polymers, the primary factor influencing the relaxation state is the T_g of the doped system. Because of this observation, high T_g thermoplastic polyimides were used as hosts⁶².

Recent investigations have confirmed the suitability of disposable recycled polystyrene⁶³ as a host polymer to accommodate NLO active chromophores (guest molecules) that can lead to cheap NLO active device materials. Nonlinear optical properties of a guest host system consisting of the chromophore (Lemke's dye) embedded in poly (bisphenol A carbonate) matrix were studied and the polymer system formed a good optical quality, regular and slightly birefringent thin films.⁶⁴

The phase stability and photorefractive properties of the guest-host system of poly (N-vinyl carbazole) (PVK)-based photorefractive polymer composite was achieved by modifying the structure of a nonlinear optical chromophore, 4-butoxy-3-propyl-1-(4'-nitrophenyazo) benzene. The shelf life of a sample with a modified NLO chromophore, 4-(2-ethylhexyloxy)3-propyl-1-(4'-nitrophenyazo) benzene was extended by more than five months even though it had a low glass transition temperature (T_g) of -19°C . This material also had a short photorefractive response time constant of 33 ms and a high diffraction efficiency of 49% at an electric field of $100\text{V}/\mu\text{m}$ and a total writing intensity of $942\text{mW}/\text{cm}^2$. These desirable characteristics are due to the plasticizer nature of chromophore, which enhanced the orientation of the NLO chromophore and secondly, the solubility of the chromophore in the polymer matrix was increased, inhibiting crystallization and providing high optical quality⁶⁵.

Zang et al. used some conjugated polymers to functionalize single walled carbon nanotubes and the experimental results showed that different polymer backbones had considerable influence on the nonlinear optical properties of

carbon nanotubes. It is one of the recent works based on guest-host systems as nanotubes⁶⁶.

1.8. Side-chain polymer systems

An NLO chromophore may be covalently bonded as a pendant group to the polymer backbone directly or through a spacer group. Functionalized polyalkylacrylates are the most studied polymer systems for nonlinear optics⁶¹. The good optical and dielectric properties of PMMA and the synthetic accessibility of its derivatives have contributed to the great demand for the acrylates. Works on co-and homopolymers of functionalized polyacrylates demonstrated that large nonlinearity was possible due to the much higher number density compared with guest-host systems⁶⁷⁻⁷⁰(**Figure 1. 10**).

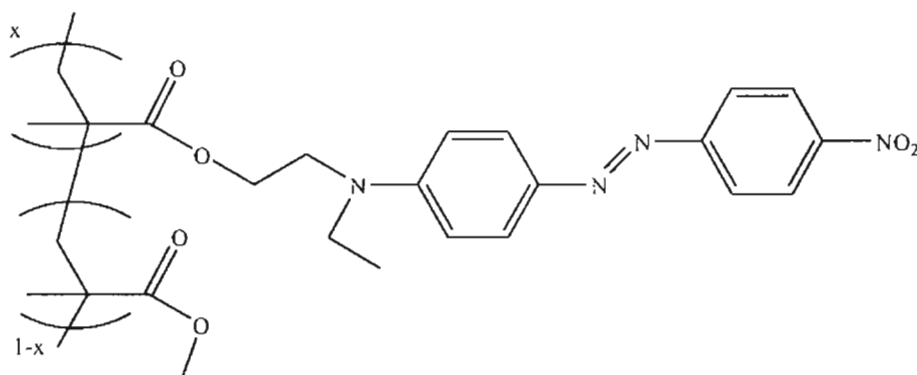


Figure 1. 10: DRI functionalized methacrylate copolymer⁶⁷

Poled polymers with polystyrene type backbones were obtained which showed good optical and dielectric properties, relatively high T_g and ease of functionalization. Functionalized polystyrenes have been obtained via polymer reaction⁷¹ and polymerization of functionalized vinyl monomers⁷² (**Figure 1. 11**).

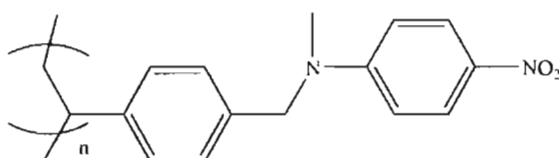


Figure 1. 11: Poly-4-[N-methyl-N-(4'-nitrophenyl) aminomethyl] styrene⁷¹

Yin et al.⁷³ have reported a second order nonlinear optical poly (ester amide) possessing good organo solubility, excellent film-forming property, high glass transition temperature and high thermal stability. Side chain polyimides

are now widely used, as they have high glass transition temperatures leading to high thermal and temporal stabilities^{58-60, 67-70} and make them good choices for applications in photonic devices. Peng et al.⁷⁴, Yang et al.⁷⁵ and Yu et al.^{76, 77} have designed side chain polyimides with dialkylamino nitrostilbene and dialkylaminomethyl sulfonyl stilbene (**Figure 1. 12**).

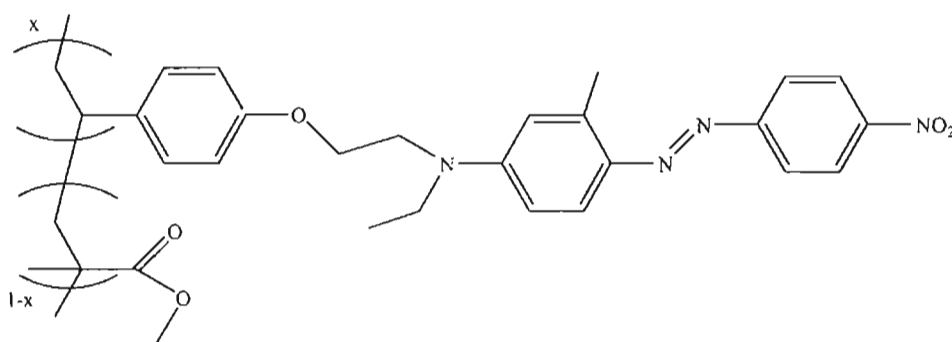


Figure 1. 12: Styrene/p-[4-nitro-4'-(N-ethyl-N-2-oxyethyl)azobenzene] methyl styrene copolymer⁷²

Roviello et al. synthesized side chain polyurethanes with large molecular hyperpolarizabilities by the reaction of ethylenic and azo bridged (N, N-diethanol-4-[4-[(4-nitrophenyl) azo]-2,5-dimethoxyphenyl] azo) aniline, N, N-diethanol-4-[3-methyl-4-[2,5-dimethoxy-4-[(4-nitrophenyl) azo] phenyl] azo] phenyl] azo) aniline, N, N-diethanol-4-[4-[2-[4-[2-(4-nitrophenyl)ethenyl]-2,5-dimethoxy phenyl] ethenyl] phenyl] azo) aniline etc. and such other push pull chromophoric monomers with toluene diisocyanate⁷⁸.

Azobenzene-containing side-chain photorefractive polyphosphazene P3-P8 were obtained via a post-azo coupling reaction. The photorefractive polymers obtained showed high glass transition temperature and good optical transparency. The polyphosphazenes possessed relatively large magnitude of photoinduced birefringence⁷⁹. The polymers with structurally isomeric and free-radically polymerizable methacrylates bearing azo-naphthol group in the side chain spaced away from the backbone by a hexamethylene spacer and substituted at 4-position with electron-withdrawing and donating substituents were reported for NLO applications and their photo-isomerization properties were studied. The results revealed that these polymers possessed potential applications in nonlinear optics⁸⁰.

Ju et al. synthesized a polyimide with two aromatic hydroxyls in the repeat unit by condensation polymerization between 2, 2-bis (3-amino-4-hydroxyphenyl) hexafluoropropane and oxydiphthalic anhydride followed by imidization reaction. Mitsunobu coupling was carried out to incorporate the NLO chromophore into the polyimide backbone, resulted a side-chain polymer with T_g at 168°C and thermal stability up to 370°C. The polymer solution was spin coated on the ITO glass to produce an optical quality film. The electro-optic coefficient of the film was obtained using 1.55 μm laser source, giving 31 pm/V with an electrical poling field of 1 MV/cm⁸¹.

Chen et al. reported a side chain polymer by using the bis fluoro NLO chromophore monomer, 4-[(4-cyanophenyl) diazenyl] phenyl-2, 6-difluorobenzoate, azobenzene-functionalized poly (aryl ether) (azo-PAE) was prepared via a nucleophilic aromatic substitution polycondensation. The results showed that azo-PAE had high glass transition temperature, good thermal stability and large nonlinear susceptibility⁸²(Figure 1. 13).

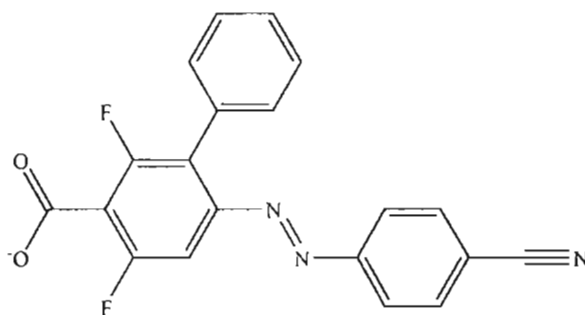


Figure 1. 13: 4-[(4-cyanophenyl) diazenyl] phenyl-2, 6-difluorobenzoate NLO chromophore incorporated in polyimide backbone⁸²

Zhao et al. reported NLO side-chain polymers, obtained by attaching the NLO chromophore to a hydroxyl containing polymer BPAN resulted in a good performance of BPAN, such as good film formation property and crosslinkability. Crosslinked poled polymer with even higher content of NLO chromophore was obtained by taking the same kind of NCO-containing chromophore as crosslinking agent⁸³.

Golemme et al.⁸⁴ developed the homopolymers and copolymers which are multifunctional side chain polymers exhibiting chiral, semiconducting, photochromic and nonlinear optical (azo aromatic moieties) properties. The high T_g , non-poled photorefractive polymers were advised for a variety of

applications ranging from holography to image processing. Li et al.⁸⁵ proposed the synthesis of azobenzene containing side chain homopolymers and copolymers with controllable molecular weight by means of atom transfer radical polymerization. The influence of push pull electronic effect of chromophores to the macroscopic NLO properties of homopolymers and copolymers were explained in detail.

A broad variety of side chain NLO polymers have been demonstrated through post functionalization of commercially available polymers using the Mitsunobu reaction, azo coupling, tricyanovinylolation, Knoevenagel condensation and acid and base catalyzed esterification. More recently, the click chemistry based Diels Alder reaction has emerged as a powerful strategy to construct NLO polymers. Jen et al. conducted a systematic study for constructing high-performance NLO polymers via Diels Alder based click chemistry. By using the DA reaction, highly nonlinear and chemically sensitive phenyltetraene based NLO chromophores were incorporated into side chain polymers to achieve good processibility, large NLO coefficients and excellent thermal stability⁸⁶.

1. 9. Main chain polymer systems

In main chain polymers, a high concentration of NLO chromophores can be introduced by covalently functionalised polymers. The polymers containing covalently attached NLO chromophore show increased stability towards relaxation after poling. A main chain polymer may show improved tensile and mechanical properties, relative to a side chain polymer⁸⁷. Main chain polymers, which contain chromophores in a head-to-tail arrangement within the polymer backbone, were used as nonlinear optical materials and the potential advantages include high temporal stability and a poling enhancement resulting from the backbone correlated dipole orientation. Low T_g , low solubility and high crystallinity of the main chain polymers were the major difficulties encountered^{88- 91}. The 'accordion' polymer approach, in which the polymer backbone is folded like an accordion with the chromophoric segments in head-to-tail arrangement, showed encouraging results⁹². Despite rather low nonlinearity, a T_g of 143°C and room temperature temporal stability of the polar order were reported⁹³. A random main chain polymer in which the

chromophoric backbone consisted of a statistical mixture of head-to-head, tail-to-tail and head-to-tail arrangements, showed better results^{94,95}. When the results from the random main-chain polymer systems are compared to those obtained from an acrylate side-chain copolymer with similar T_g and chromophoric content, similar poling efficiency (within 80%) was shown⁹⁶. The temporal stability of the polar order is also similar in both polymers. This suggests that the degree of coupling between the polymer backbone motion and the chromophoric orientation are similar for both side-chain and main-chain polymers, despite their considerable structural differences⁶¹.

Kim et al. reported a novel T-type polyester containing dioxynitro stilbenyl groups as the NLO chromophores obtained by the polycondensation of 2, 5-di-(2'-hydroxy ethoxy)-4'-nitrostilbene with terephthaloyl chloride, adipoyl chloride, and sebacoyl chloride, which possessed high thermal stability up to 260°C with a glass-transition temperature in the range 90-95°C and a high second harmonic generation (SHG) coefficient (d_{33}) of poled polymer films, hence was found to be acceptable for NLO device applications⁹⁷.

Angiolini et al. reported corona poling behaviour of optically active photochromic copolymers derived from methyl methacrylate (MMA) and the methacrylic ester of (S)-3-hydroxy pyrrolidine linked through the nitrogen atom to the highly conjugated photochromic 4'-(β -cyano- β -(methylsulfonyl) vinyl)-4-azobenzene moiety with the aim to evaluate the effect on the nonlinear optical properties originated by the presence of inactive side-chain MMA groups along the main chain. The corona poled polymeric films have d_{33} values in the range 10-86 pm/V. The temporal and thermal stability of the optimal SHG signals obtained after corona poling process of all the macromolecular materials has been investigated and compared. The results indicated that the maximum of these properties could be obtained at a molar percentage of photochromic units around 20-40%⁹⁸.

Lee et al. reported the synthesis of polyamides by using 2, 3-dioxynitrostilbenyl groups as NLO-chromophores and 2, 3-Bis-(3, 4-dicarboxy phenyl carboxy ethoxy)-4'-nitrostilbene dianhydride, which was obtained by the reaction with 4, 4'-oxydianiline and 4, 4'-diaminobenzanilide. Polymers showed thermal stability up to 300°C with T_g values in the range of 135-141°C. The material possessed high SHG coefficients (d_{33}) of poled polymer films (6.14×10^{-9}

esu). The dipole alignment of poled polymer films exhibited exceptionally high thermal stability even at 30°C higher than T_g and there was no SHG decay below 170-190°C due to the partial main chain character of polymer structure, which was acceptable for NLO device applications⁹⁹.

Yoon et al. had done a comparative study in between side chain and main chain polymers. They designed carbazole-based push-pull type nonlinear optical (NLO) polymers, P (Cz-CN), P(Cz-DR 19), and P(Cz-TCN). The structure of P (Cz-CN) was designed to contain di-acceptor-chromophores in the main chain and to have a two-dimensional (2D) charge transfer (CT) configuration. P (Cz-DR 19) and P(Cz-TCN) were designed to have NLO chromophores in the side chain. All the polymers synthesized were thermally stable approximately up to 250 °C. The glass transition temperatures (T_g) of P (Cz-DR 19) and P (Cz-TCN) appeared at 117 °C and 104 °C, respectively. The ratio of the second harmonic coefficients (d_{33}/d_{31}) was 1.5 in P (Cz-CN) and 3.3 in P(Cz-DR 19) and P(Cz-TCN). P (Cz-CN) showed enhanced off-diagonal tensor components due to 2D CT effects. The d_{33} values of P (Cz-DR 19) and P (Cz-TCN) were 61.6 pm/V and 41.7 pm/V, respectively. The electro-optic coefficients (r_{33}) of P (Cz-DR 19) and P (Cz-TCN) were 40.5 pm/V and 17.8 pm/V at 632.8 nm, respectively. P (Cz-DR 19) showed higher second-order optical nonlinearity than that of P (Cz-TCN) due to higher β -values of DR 19 moiety in the side chain. P (Cz-DR 19) and P (Cz-TCN) showed stable NLO coefficient up to 98 °C and 75 °C, respectively. The intensity of SHG of P (Cz-DR 19) was stable up to 20 days at room temperature.¹⁰⁰

Lee et al. developed novel Y-type polyurethanes containing 2,3-dioxy benzylidene malononitrile group as a nonlinear optical (NLO)-chromophore, which was obtained by the condensation of 2, 3-di-(2'-hydroxyethoxy) benzylidene malononitrile with 2, 4-toluene diisocyanate and 3, 3'-dimethoxy-4, 4'- biphenylene diisocyanate. The polyurethanes showed a thermal stability up to 270°C and the glass-transition temperatures (T_g) obtained were around 116-135°C. The second harmonic generation coefficients (d_{33}) of poled polymer films at 1064nm fundamental wavelength were around 2.72×10^{-9} esu. The dipole alignment exhibited high thermal stability up to 10°C higher than T_g , and there was no SHG signal decay below 145°C due to the partial main-chain character of

the polymer structure, which was acceptable for nonlinear optical device applications¹⁰¹.

Polymers containing azo group in the main chain showed that the presence of azo group in the main chain increased the second order NLO efficiency. This can be explained as the electron donating effect of azo group. The presence of azo group in the main chain increases the donor acceptor strength, polar order and efficiency to form higher molecular weight polyester, which increases the second order NLO response. Sreekumar et al. developed main chain chiral polymers by using the biphenolic azo diol chromophores, bis (4-hydroxy phenylazo)-2, 2'-dinitro diphenylmethane and bis (4-hydroxy phenylazo)-2, 2'-dinitrodiphenyl sulfone³⁸⁻⁴⁰ (Figure 1. 14).

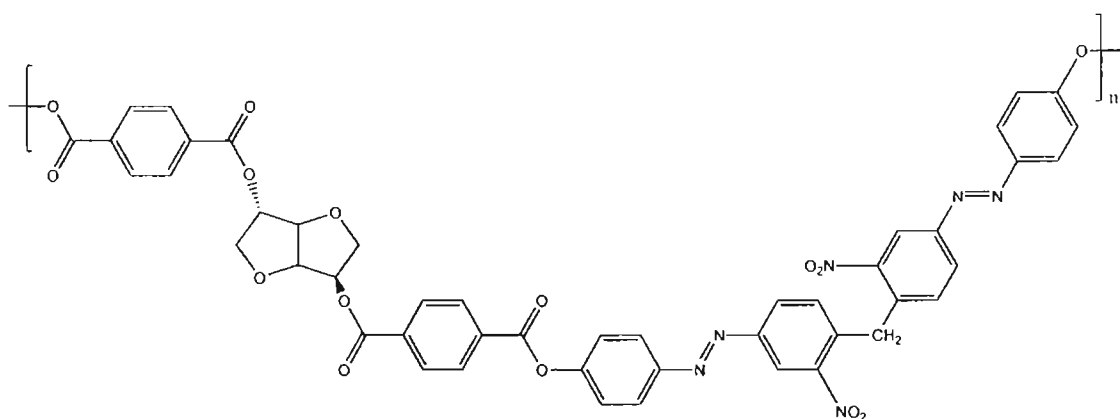


Figure 1. 14: Main chain polyester unit

1. 10. Crosslinked polymeric systems

Crosslinking is a natural strategy aimed at stabilizing the order of parameter relaxation in poled polymers⁶¹. The NLO chromophore is incorporated in a polymer backbone with high glass transition temperature. With high glass transition temperature with the exception of polyimides, crosslinked networks have provided the highest temporal stability. Thermally activated crosslinking and photochemically activated crosslinking were the methods used to prepare such systems⁶¹.

For thermal crosslinking, methods used were epoxy-amino coupling, radical-initiated thermal polymerization of multi-functional methacrylate monomers, epoxy-alcohol coupling, isocyanate-hydroxyl coupling, isocyanate-amino coupling, alcohol condensation of alkoxy silane and ethynyl thermal intramolecular reaction⁶¹. The most widely used are the epoxy and isocyanate

coupling chemistry and the diepoxide (bisphenol-A) was used for the early works on crosslinked materials for nonlinear optics⁹⁶ (Figure 1. 15).

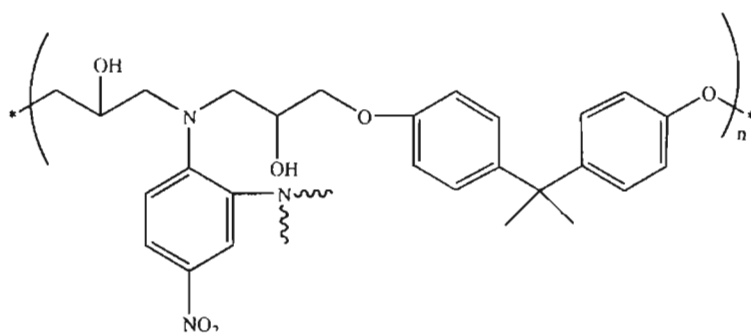


Figure 1. 15: Crosslinked epoxy polymer from 4-nitro-1, 2-phenylene diamine and bisphenol-A diglycidyl ether ⁹⁶

The reactive sites in side-chain polymer backbone may be crosslinked to improve temporal stability. An example was provided by the epoxy crosslinking of a polyhydroxy styrene copolymer¹⁰². Photocrosslinking was explored as an alternative route for crosslinked networks⁶⁷, which have advantages over thermal crosslinking. If a highly crosslinked network can be obtained under an electric field at low temperature, poling efficiency may be improved through both the Boltzmann factor and the possibility of a higher poling field. Also, under a poling electric field, the illuminated region of the polymer can be finely patterned, as in photolithography, creating not only a pattern in the refractive index, but also a pattern in the nonlinear optical susceptibility through the subsequent dipolar relaxation in the uncrosslinked regions.

Mandal et al.^{103, 104} have reported the doping of a bis cinnamoyloxy functionalized chromophore into a photo-crosslinkable polymer matrix, which is shown in Figure 1. 16. Photo-crosslinking with a few minutes of UV exposure under a poling field at its glass transition temperature resulted in both high nonlinearity and good temporal stability.

Polyimides possessing both high T_g and crosslinked networks seem to be a rational approach to enhance the NLO stability. Addition-type polyimides may be used to circumvent the need for thermal imidisation¹⁰⁵. Improved processability can be achieved without sacrificing properties such as excellent thermal stability and mechanical properties¹⁰⁶⁻¹¹⁰. Jeng et al.¹⁰⁵ have prepared a

series of maleimide based crosslinked organic and organic-inorganic materials, which showed large second order optical nonlinearity after poling and curing.

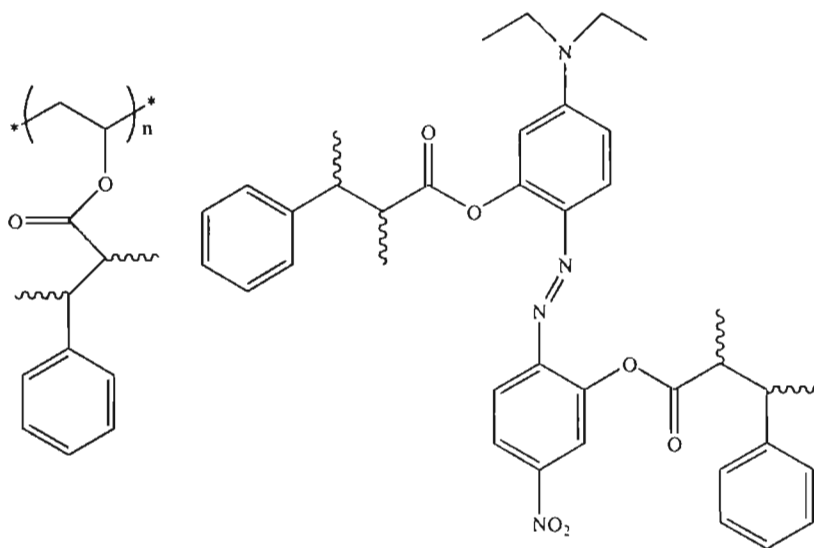


Figure 1. 16: Crosslinked polymer of polyvinylcinnamate doped with 3-cinnamoyloxy-4-[4-(N, N-diethylamino)-2-cinnamoyloxyphenyl azo] nitrobenzene^{103,104}

1. 11. Poling

To exhibit second-order nonlinear optical effects, the isotropic symmetry in amorphous polymers must be broken⁶¹. The noncentrosymmetric nonlinear optical molecules must be arranged in the materials in such a manner that the bulk material also does not have an effective centre of symmetry, for the polymer materials to exhibit bulk second order optical nonlinearities⁴⁶. To achieve the necessary noncentrosymmetry, the chromophores in the polymer matrix are poled¹¹¹. Poling is the procedure in which the chromophores are aligned electrically, thermally or by radiation⁵¹. For a poled polymer, acentricity is imparted with a poling electric field. If a polar alignment of the dipolar species in the polymer occurs during poling, this acentricity can be maintained, upon the removal of the poling field, for a time period determined by the orientation-relaxation time of the dipoles⁶¹.

Poling is carried out near the polymer glass-transition temperature where the dipolar orientation time is short, for attaining maximum alignment. The polar alignment is then dynamically "frozen" into the polymer by cooling under the poling field⁶¹. At reduced temperatures, the relaxation of the polar order

slows down considerably. If this relaxation can be reduced to an acceptable minimum, an amorphous material with quasi-permanent second order nonlinearity is obtained. The poled polymer approach offers more rational controls in the organization of molecular nonlinearity. On incorporation of chromophores into a polymer matrix, optically nonlinear thin films and fibers can be obtained easily, allowing for large area coverage as well as long interaction length. By linking the chromophores covalently into a polymer network, high number density and thus, high nonlinearity is possible. The optical quality of the polymer can also be optimized through compositional designs⁶¹. Electric field poling can be achieved in several ways and two common methods are corona-poling or (sandwich) contact electrode poling⁴⁷. Each method has its own advantages and disadvantages, contact electrode poling requires high quality polymer films and a careful electrode design. On the other hand, electrode poling is compatible with electro-optic and second harmonic device processing requirements. The most commonly used method in poling experiments is corona poling. Extremely high electric fields can be obtained and the quality of thin films is not so critical⁵¹. As alternatives to thermally activated corona or contact poling, other techniques have been reported including the use of a plasticizing gas¹¹², or photo induced cis-trans isomerization to assist orientational mobility^{113,114}.

1.12. Chiral polymers in second order nonlinear optics

Frequency conversion of lasers is a significant application of second order nonlinear optics¹¹⁵. For this, the nonlinear optical material should be noncentrosymmetric or otherwise it will not have a second-order nonlinear response. In most of the materials, macroscopic centrosymmetry has to be broken artificially by employing physical methods such as electric field poling of molecules embedded in polymers¹¹⁶ and Langmuir-Blodgett film fabrication¹¹⁷. These techniques result in polar order, the net alignment of molecular dipoles along an axis, the polar axis of the materials¹¹⁵. However, a major drawback is the decay of their nonlinear response with time. Host-guest complexation¹¹⁸ and intercalation, salt formation¹¹⁹, uses of molecules with negligible dipole moment¹²⁰ or octupolar molecules¹²¹ are some other approaches used. Introduction of special functionalities such as H-bonding groups¹²², optimally

long alkyl chains¹²³ and sterically bulky groups¹²⁴ have also proved useful in many cases. However none of these approaches guarantee a noncentrosymmetric lattice¹²⁵. When the fundamental frequency of the light source becomes sufficiently intense, two or three photon processes such as hyper-Rayleigh Scattering¹²⁶, Sum-frequency generation¹²⁷; second and third harmonic generation, the electro-optic effects etc. were observed¹²⁸. Only noncentrosymmetric systems will give a second harmonic response on the macroscopic level and so the polar order must be introduced.

Chiral materials provide a new approach to second order nonlinear optics. Chiral materials are inherently noncentrosymmetric and therefore possess an electric-dipole allowed^{127, 129, 130} second order and higher even-order nonlinearity¹³¹. Such nonlinear responses due to chirality do not require polar ordering and permits even in macroscopic samples with high symmetry. Chiral molecules may possess strong magnetic-dipole transitions, which allow second order nonlinearity in macroscopically centrosymmetric materials^{132, 133}. Amino acid family single crystals are gaining importance as highly feasible second order nonlinear optical materials. Efforts have been made to combine amino acids with interesting organic and inorganic matrices to produce materials¹³⁴ which are gaining prominence in view of their high laser damage threshold, wide transparency window, low UV cut-off and high NLO coefficients.

There are mainly two theories proposed to explain the large SHG efficiency of chiral films and materials.

Electric-dipole approximation: By this method, there are different number of chiral and achiral tensors of β and χ ⁽²⁾. Chiral tensor components arise due to the chirality of the medium and the contribution of these components will be higher in chiral media while it is negligible in achiral media.

Magnetic-dipole approximation: Chiral molecule may possess strong magnetic-dipole transitions, in addition to the electric-dipole transitions, which allow second-order nonlinearities in macroscopically centrosymmetric materials.

The strongest experimental evidence supporting the significance of magnetic -dipole contributions to chiro-optical effects in SHG was presented by Persoons et al.^{135, 136}. Despite the wide spread use of magnetic-dipole contributions in interpreting chiral SHG measurements, there is a significant

body of evidence suggesting that magnetic dipole contributions may be of only minor importance in oriented systems.¹³⁷

1.13. Chiral Polymers

The recent focus of the molecular material research has been on fabricating materials fine tuned for enhanced attributes such as electrical, magnetic, optical and nonlinear optical characteristics¹²⁵. Organic polymers, with combined functions of electric, magnetic and chiral properties are expected to be target molecules of current material chemistry¹³⁸. The important advantage of organic polymers is the manipulation of the molecular structure or molecular designing and the ease of processability. Helical and π -conjugated polymers would be potential candidates for such functional materials based on well defined chiral structures¹³⁸.

The simplest method of synthesizing optically active polymers involves the polymerization of optically active monomers. However, this is often less attractive from the view point of the polymerization reaction. Asymmetric polymerization which produces configurationally or conformationally specific optically active polymers starting from optically inactive monomers is much more attractive and challenging, and remarkable advances, particularly on helical polymers, have been made over the past two decades. Optically active polymers may be obtained in several ways including (a) polymerization with a chiral catalyst or initiator,^{139, 140} (b) chiral doping of achiral (racemic) polymers with enantiopure chiral ions,¹⁴¹ (c) separation of racemic mixture of enantiomeric helices using chiral stationary phase (CSP) chromatography (for nondynamic systems,¹⁴² (d) chiral complexation of achiral or racemic polymers with enantiopure chiral ligands/guests,¹⁴³ (e) post- polymerization functionalization with chiral moieties,¹⁴⁴ (f) polymerization of enantiopure chiral monomers,¹⁴⁵ (g) incorporation of enantiopure chiral end groups¹⁴⁶ and (h) copolymerization of enantiopure chiral monomers with achiral monomers or with an enantiomeric excess (ee) of one enantiomer over the other¹⁴⁷. In the last two cases, it is the presence of enantiopure chiral "seeds" which results in the adoption of a preferential helical screw sense; in even non-enantiopure-substituted backbone regions by the preferential stereo relationship between enantiopure chiral side chains and their nearest neighbours.

The chiro-optical properties exhibited by optically active polymers are very useful for understanding their configurational and conformational characteristics. Optical activity is a physical spectral property of a chiral material caused by asymmetric configurations and conformations, which have no plane or centre of symmetry. Chirality (optical activity) can be introduced in a macromolecule by attaching chiral centers in the lateral chains or in the main chain¹⁴⁸. The attachment of chiral groups in the polymer chain is observed to twist the main chain in predominantly one screw sense to generate helical structures^{149, 150}. Polymers with chirality in the main chain were also reported to have twisted helical crystal shape¹⁵¹. Polymers without any asymmetric center (carbon or hetero atom) can have chiral conformation links or steric hindrance, which direct such molecules into helical conformation and their mirror planes pass through bonds and not through atoms¹⁴⁸.

Helical polymers are representative chiral macromolecules and have precisely ordered structure. The chirality of helical polymers has attracted the interest of synthetic polymer scientists because their chirality leads to stereo regularity in the polymers and also provided much information about the polymer structures¹⁵². The chiro-optical activity of the helical polymers is based on the structural (or conformational) chirality of the helical polymers and whether or not the polymer involves a chiral unit in the monomeric moiety.

Self assembly based on chiral molecules is one approach in material development, which shows, how molecular engineering strategies can be used to develop new features in nonlinear optical systems¹⁵³. Helicenes, which are aromatic helical molecules composed of fused benzene and/or thiophene rings, have been synthesized because of their helical structure and very good nonlinear optical properties¹⁵⁴.

Verbiest¹⁵⁵ et al. have investigated the self-assembly of chiral molecules, in which chirality and supramolecular organisation play key roles. In the Langmuir-Blodgett films of a chiral helicenebisquinone^{156, 157} the molecules form supramolecular arrays that enhance the second-order nonlinear optical susceptibility about 30 times larger for the nonracemic material than for the racemic material with the same chemical structure. The susceptibility components that are allowed only by chirality dominate the second-order NLO response. The second harmonic generation for the highly symmetric thin films of

helicene and thiaheterohelicene have also been extensively studied¹⁵⁸⁻¹⁶⁰ and are shown in **Figure 1. 17**. The films were prepared by spin-coating, and no external force, such as electric field poling, was used to induce the noncentrosymmetry. The SHG susceptibility values were significantly high, which indicated the formation of highly symmetric thin films with considerable second-order nonlinearity.

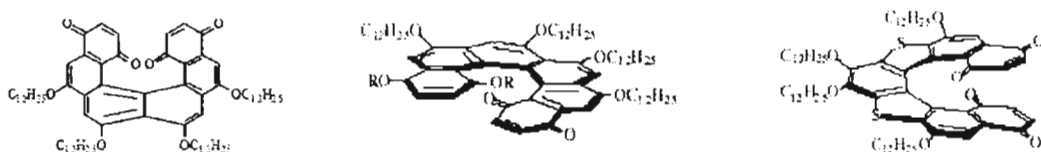


Figure 1. 17: Structure of chiral helicenebisquinone, helicene and thiaheterohelicene

Helicene structures have also been incorporated into metal phthalocyanines. The molecules are constructed by fusing copper and nickel octaazaphthalocyanines to four non racemic helices^{156, 157, 161}. These compounds tend to aggregate strongly in thin films and in appropriate solvents. Even though the molecules are symmetrical, their Langumir-Blodgett films gave very large second order nonlinear responses, dominated by the components of the susceptibility tensors that are allowed, only because the materials are chiral¹⁶².

Cooperative responses to chiral information and magnification effects can be extremely large in helical polymers^{148, 163}. Green et al.^{164,165} demonstrated that helical reversals along the chain are highly sensitive to chiral effects. Incorporation of a small number of units with pendant chiral groups in copolymers with hexylisocyanate, results in the control of helical reverses that force large number of polymer chain units to cooperate in directing the chirality of the polymer (**Figure 1. 18**). Green et al. formulated a majority rule and the so called "sergeants and soldiers" principle. A tiny majority of R over S monomers or a small amount of chiral units (sergeants) is incorporated within the achiral units (soldiers), can dictate the helical sense.

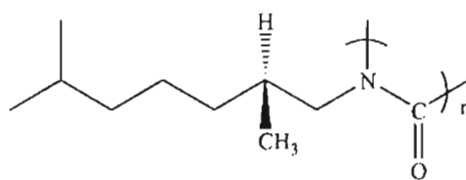


Figure 1. 18: Example for chiral polymers

Several interesting NLO phenomena in chiral media have been theoretically predicted¹⁶⁶⁻¹⁶⁸ and some of them have been verified experimentally in chiral, helical polymeric media¹⁶⁹⁻¹⁷⁴. Many reports have demonstrated the presence of chiral effects in second harmonic generation from monolayer of the chiral polymers and the chirality gave rise to a new electric-dipole-allowed component of the second order susceptibility tensor and to significant contributions to the nonlinearity. The results of the study also show that the overall nonlinear optical properties of chiral molecules can be significantly enhanced by optimizing the magnetic contributions to the nonlinearity and this is important in the field of electro-optics for the development of a material with high nonlinear optical response¹⁷⁴.

The occurrence of chirality at different levels of the polyisocyanide structure suggests that chiral and nonlinear optical properties of new materials can be optimized independently without losing the coupling between the properties¹⁷⁵. Persoons et al.^{176, 177} observed strong chiral effects in the second-order nonlinearity of poly (isocyanide)s (Figure 1. 19).

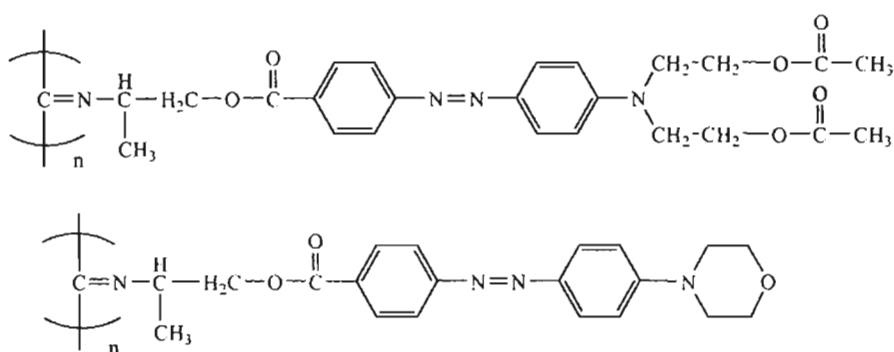


Figure 1. 19: Structure of chiral polyisocyanides

They showed that nonlinear optical chromophores could be organized in a fixed noncentrosymmetric arrangement as side groups of polymers with a rigid backbone. They investigated the second order response of chiral polyisocyanides¹⁷⁷ that contained nonlinear chromophore as side groups. The

chirality of the material was associated with the helical supramolecular configuration of the backbone. This resulted in a strong orientational correlation of side groups.

Evidence of high magnetic-dipole contributions to the nonlinearity was observed in Langmuir-Blodgett (L.B) films of a chiral poly (thiophene) (**Figure 1. 20**). The sample studied was a ten layer L.B film of the regioregular chiral poly (thiophene), poly [3-[2-((s)-2-methylbutoxy)- ethyl] thiophene]^{178,179} and the magnetic dipole contributions observed in these L.B films were of the same order of magnitude as the electric-dipole nonlinearities. The nonlinear response arises from properties of the $\pi \rightarrow \pi^*$ transition, which corresponds to displacement of electrons along the helical conjugate backbone. Spin coated thin films of a chiral poly (3-alkylthiophene) were investigated by Verbiest et al.¹⁸⁰. They found that the films showed a significant SHG and exhibited magnetic-dipole nonlinearities, in addition to the usual electric dipole contribution.

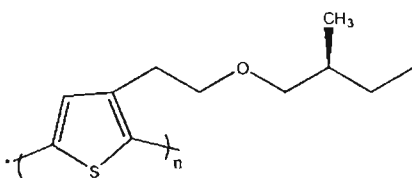


Figure 1. 20: Structure of chiral polythiophenes

Chen et al. reported the synthesis of novel optically active polyurethanes based on chiral 1, 1'-binaphthol via direct hydrogen transfer addition polymerization (**Figure 1. 21**). They found that the polymers showed better thermal stability and exceptionally good optical activity¹⁷¹.

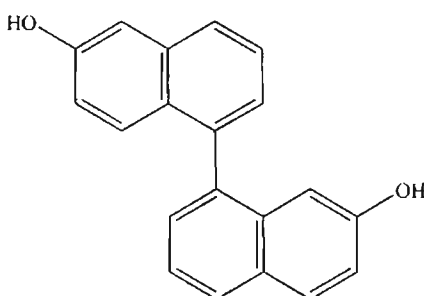


Figure 1. 21: Structure of 1, 1'-binaphthol

The incorporation of chiral binaphthyl units into polymer chains by Pu et al. led to a class of conjugated polymers with inherently chiral main chains

which are shown in **Figure 1. 22**. These polymers possessed a highly stable main chain chiral helical configuration, which made them potentially useful for nonlinear optics. The NLO chromophores can be organized in chiral binaphthyl polymer chains to construct non-centrosymmetric and multipolar materials^{181, 182}.

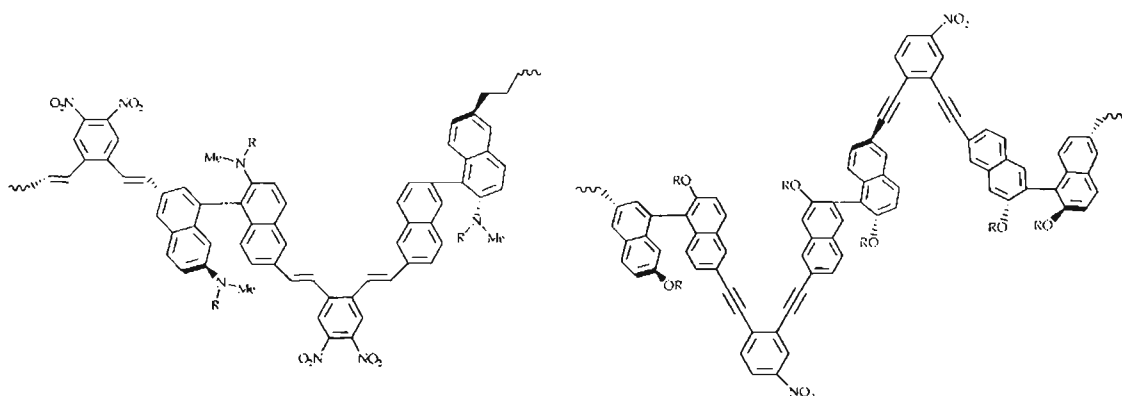


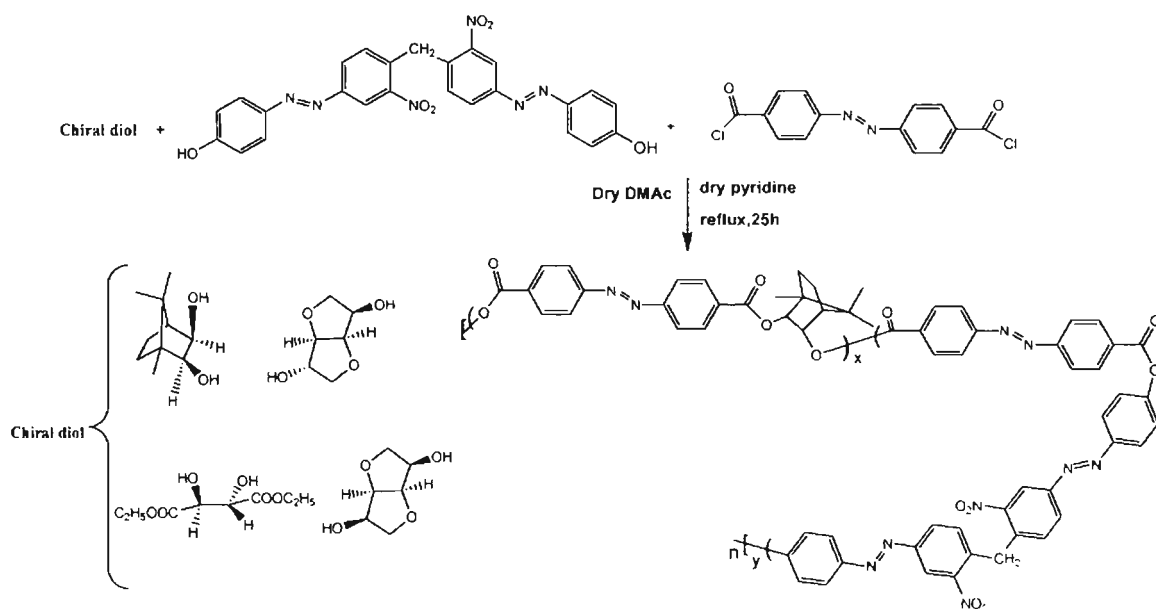
Figure 1. 22: Structure of chiral polymers based on binaphthyl unit

Pu et al. prepared a dipole oriented chiral binaphthyl based polymers containing different electron acceptors and conjugated dipole units which have large dipole moments since the dipole units are tilted in one direction along the polymer axis^[181]. Polymers of such organized geometry are very interesting since, orientation correlated NLO chromophore on a helical polymer have been observed to generate an enhanced second order NLO response¹⁸¹⁻¹⁸².

Sreekumar et al. developed several varieties of chiral polymers containing donor acceptor π -conjugated polar segments and chiral building block in the main chain (**Scheme 1. 1**). Chiral doping is made in a sense to attain noncentrosymmetric ordering of dipoles in macroscopic dimensions by chemical synthesis. Several polyesters containing push-pull electronic azobenzene mesogenic groups in the main chain were developed. The multifunctional polyesters were prepared by the polycondensation of terephthaloyl chloride, chiral diols (isosorbide, isomannide, camphane diol and diethyl (2R, 3R) tartrate) and Bis (4-hydroxyphenylazo)-2,2' dinitro-3, 5, 3', 5'-tetramethyl diphenyl methane as NLO chromophores, showed liquid crystalline behaviour with high glass transition temperatures, stable liquid crystalline mesophases and high second harmonic generation efficiency. The second order nonlinear optical

susceptibility values were also studied as a function of the percentages of the chiral building units ³⁸⁻⁴⁰.

A novel synthetic approach has been developed to incorporate donor-acceptor substituted π -conjugated segments and chiral centres in main chain polymeric systems. The polycondensation products obtained by using (2R, 3R)-(+)-diethyl tartarate, terephthaloyl chloride and the biphenolic chromophores bis(4-hydroxy phenylazo)-2, 2'-dinitrodiphenylmethane and bis(4-hydroxy phenylazo)-2, 2'-dinitrodiphenylsulfone were used for NLO measurement. The optical activity of the polymers showed that the introduction of a substantial amount of chiral groups in the polymer chain led to the formation of non-centric configurations. The polyesters showed glass transition temperatures in the range 100-190°C and were thermally stable (350°C)³⁸. By the condensation of azobenzene-4, 4'-dicarbonyl chloride with 1, 4: 3, 6- dianhydro-D-sorbitol and biphenolic chromophores, bis(4-hydroxy phenylazo)-2, 2'-dinitrodiphenylmethane and bis(4-hydroxy phenylazo)-2, 2'-dinitrodiphenylsulfone, the products which exhibited glass transition temperature in between 100 and 160°C were having high thermal stability(upto 400°C) ³⁸⁻⁴⁰.



Scheme 1. 1: Chiral polyester Synthesis

NLO active polyesters by varying the composition of the chiral diols were also developed (Scheme 1. 1). The polycondensation products of acid chloride of azobenzene-4, 4'-dicarboxylic acid with the chromophore, bis (4-hydroxyphenyl azo)-2, 2'-dinitro diphenylmethane and chiral diols, isosorbide, isomannide,

diethyl -L-tartarate and *exo,exo*-camphene diol were studied and concluded that the polymeric system which was having isomannide chiral moiety possessed more SHG efficiency³⁹. The polymer with isomannide chiral diol has more polar order and has shown higher T_g value which induced high SHG efficiency.¹⁸³

The second harmonic generation of the chiral polyesters synthesized was studied in thin films. The thin films of achiral polyesters were SHG inactive and chiral polyesters can provide an excellent noncentrosymmetric media and showed good second harmonic efficiency even in the absence of poling. The SHG in the thin films of chiral polymers also possessed temporal stability and indicated the thermal stability of the dipole orientation in the polymer¹⁸⁴. The hydrogen bonded liquid crystalline poly (ester-amides) (PEA)s were synthesized from 1, 4- terephthaloyl [bis- (3-nitro- N- anthranilic acid)] and 1, 4- terephthaloyl [bis- (N-anthranilic acid)] with and without nitro groups respectively through the separate condensation of each with hydroquinone or dihydroxy naphthalene. It was found that, the polymers were NLO active liquid crystalline polymers in which PEAs containing nitro groups exhibited polymorphism (smectic and nematic) where as those without nitro groups exhibited only one phase transition (nematic threaded texture).¹⁸⁵ This group reported the development of highly efficient NLO active side chain and main chain polyesters, poly (ester-amides), polyurethanes etc¹⁸⁶⁻¹⁹⁰.

Yashima et al. reported some chirality-responsive π -conjugated polymers¹⁹¹. The electrochemically polymerized emeraldine base form of polyaniline is known to show an induced circular dichroism (ICD) in the long absorption region in solution or in the film when doped with optically active strong acids, such as (R)-or (S)-camphorsulfonic acid (CSA)¹⁹². The (R)-CSA-dedoped polyaniline thin films¹⁹³ retained their optical activity which responded to the chirality of a pair of phenylalanine enantiomers and exhibited a different color change by responding to the chirality of the enantiomers. A partially hydrolyzed polythiophene (PT) derived from an optically active PT is sensitive to the chirality of the (R)- and (S)-2-amino-1-butanol and exhibited ICDs of almost mirror images to each other¹⁹⁴. Optically inactive π -conjugated copolymers with the C₂-symmetric carboxy biphenol units as the main chain component also exhibited an ICD in the copolymer backbone regions in the

presence of chiral amines¹⁹⁵. The chiral information of the amines is first transferred to the carboxybiphenol moieties with a dynamic axial chirality through noncovalent acid-base interactions, and subsequently the induced axial chirality with an excess single handed twist sense may be further amplified in the π -conjugated copolymer backbones as an excess of a single-handed helix.

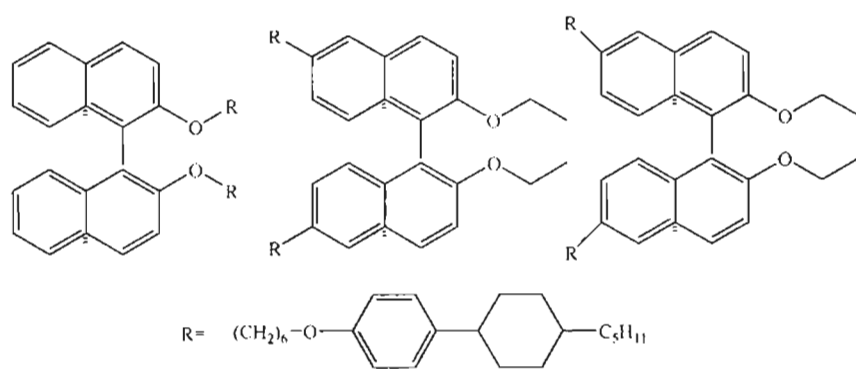


Figure 1. 23: The bridged and nonbridged binaphthyl derivatives

Akagi et al. developed chiral dopants with nonbridged and bridged type axially chiral biphenyl derivatives to prepare chiral nematic liquid crystals available for an asymmetric reaction field producing helical conjugated polymers (**Figure 1. 23**). The nonbridged binaphthyl derivatives exhibited transoid and cisoid conformations in isotropic and in liquid crystal solvents and bridged binaphthyl derivative formed cisoid conformation irrespective of solvents. The liquid crystals thus prepared were used as the asymmetric solvents for the synthesis of helical polyacetylene. The usage of the nonbridged and bridged binaphthyl derivatives, as chiral inducers having the same configuration but opposite helical sense, afforded a convenient way to construct the helicity controlled liquid crystal reaction field¹⁹⁶.

Koeckelberghs et al. reported the synthesis of a series of chiral 3, 6 substituted polythienothiophenes (PTTs) and the influence of the substituent on the chiroptical properties. 3, 6-dialkoxy substituted PTTs, 3, 6-dialkyl thio substituted PTTs and alternating copolymers of 3, 6-dialkoxythienothiophenes and 3, 6-dialkylthienothiophenes were used for the investigation, which are shown in **Figure 1. 24**. It is found that the substituent appeared to play a decisive role in the polymer's macromolecular structure and supramolecular organization¹⁹⁷. They also studied the chiroptical properties of

cyclopentadithiophene based conjugated polymers. They proved rigid and highly conjugated strands for the chiral substituted conjugated polymers containing the cyclopentadithiophene. Polycyclopentadithiophenes, polythienothiophene-alt-cyclopentadithiophenes and polythiophene-alt-cyclopentadithiophenes were the systems studied¹⁹⁸. (Figure 1. 24)

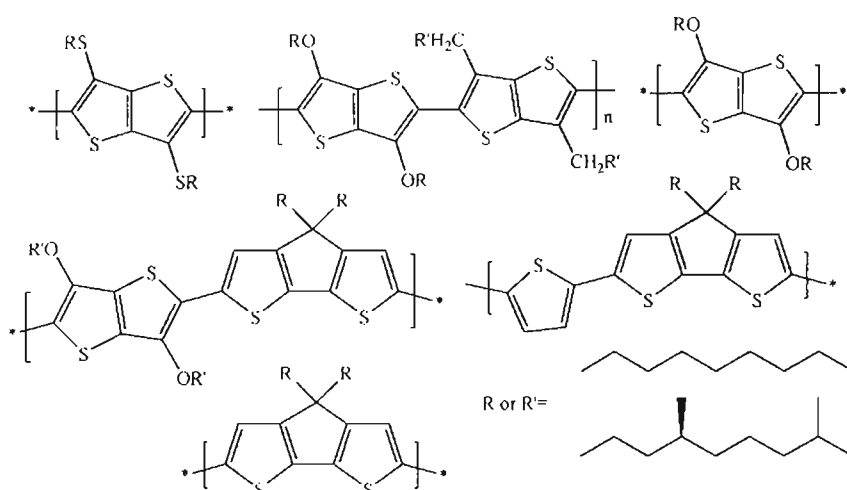


Figure 1. 24: Chiral 3, 6 substituted polythienothiophenes and conjugated polymers containing the cyclopentadithiophene

Tuuttila et al.¹⁹⁹ developed chiral donor π -acceptor azo benzene dyes in which the chiral moieties namely (S)-(+)-2-(6-methoxy-2-naphthyl) propionic acid (naproxen) and (S)-2-aminopropionic acid (L-alanine), were attached to either the donor end or the acceptor site of the azo compound using ester or amide bonds respectively. They reported that the developed chiral donor-acceptor azobenzene molecules are potential NLO materials because the donor-acceptor functionality of the azobenzene part supplemented with the chiral unit controlling the intermolecular interaction. Koeckelberghs²⁰⁰ reported the synthesis of a chiral 9, 10-dialkoxy functionalized poly (3, 6-phenanthrene) by using the Suzuki cross-coupling reaction. They demonstrated that 3, 6-polyphenanthrene systems adopted a random coil in a good solvent and a helical conformation in a nonsolvent rather than stacking in a supramolecular way.

In past decades, the NLO polymers were reported to be of various shapes such as Λ -shape, X-shape, Y-shape, U-shape, otupolar, dentron etc ^{48, 201-202}. The H-shape and AB-type second order nonlinear optical (NLO) polymers were

prepared for the first time by Zhong'an et al. The linkage positions of chromophores in the H-shape polymers were shoulder-to-shoulder, in which the chromophore moieties were part of the polymeric backbone. The subtle structure could be easily modified by the introduction of different isolation groups, to adjust the property of the resultant polymers. All the polymers exhibited good film-forming ability, thermal stability, large SHG coefficients of d_{33} values, and relatively good long-term temporal stability²⁰³.

No et al. recently reported the synthesis and nonlinear optical properties of novel Y-type polyurethane containing tricyanovinyl thiazole with enhanced thermal stability and second harmonic generation.⁴⁸ The Y-type polyurethane is shown in **Figure 1. 25**.

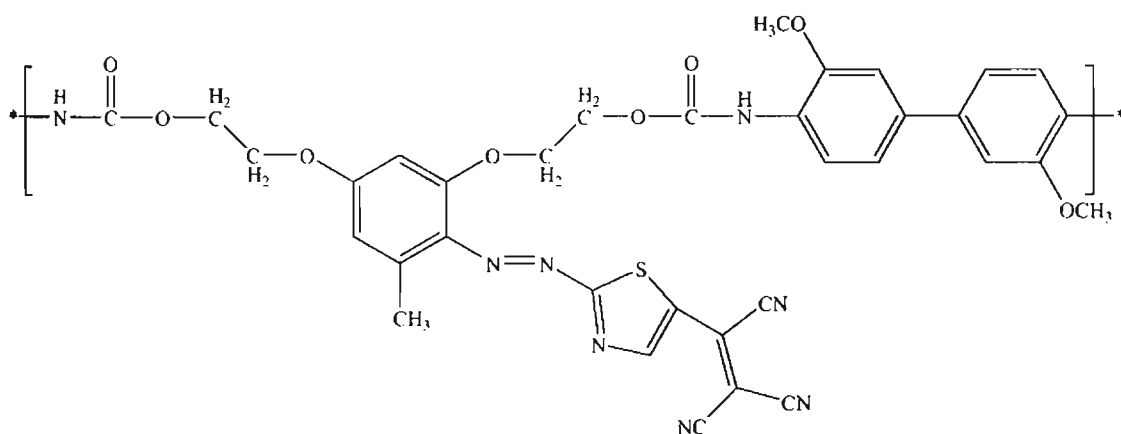


Figure 1. 25: Y-type polyurethane containing tricyanovinyl thiazole

Brasselet et al. developed two new classes of octupolar nonlinear optical chromophores, derived from 1, 3, 5-triazines and oligothiénylic crystal violet analogues which have been synthesized and their nonlinear optical properties investigated using the harmonic light scattering experiment. The easy preparation of these molecules made them attractive candidates for optical applications. Off-resonant measurements show high nonlinearities together with an excellent transparency, which made these compounds of promising interest for the emerging schemes of nonlinear optical applications whereby the multipolar character of the chromophores is of particular importance²⁰⁴.

1. 14. Spacer effects in second harmonic generation of polymers

The molecular second order NLO efficiency depends, on the strength of the donor and acceptor groups, on the extent of the π -conjugated path, on conjugating spacers based on aromatic systems and on the resonance stabilization energy of the aromatic system. Intensive studies regarding the NLO efficiencies of molecules containing π -conjugated spacers are seen in the literature^{205, 206}. Sreekumar et al. have studied the effect of alkyl spacers on the nonlinear optical properties. The polymer was designed as a condensation product of PNA derivatives with varying number of spacers and an azomesogen chromophore, azobenzene-4, 4'-dicarbonyl chloride. A series of polymers with varying number of CH₂ groups from 1-7 in the polymer chain were designed (Figure 1. 26).

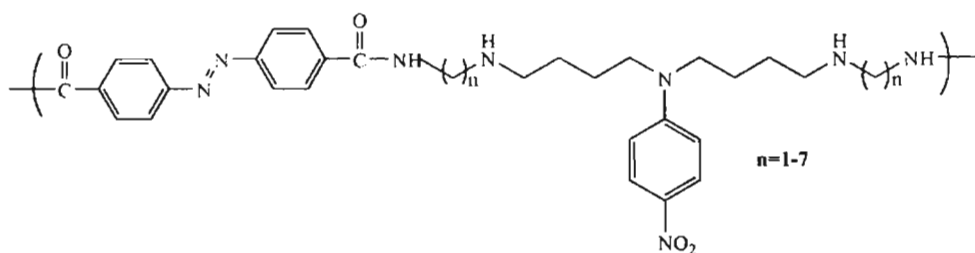


Figure 1. 26: Spacer effect in polymers

From measurements of SHG efficiency of polymers, it is found that the systems have shown increase in SHG efficiency with respect to increase in the number of alkyl spacer groups rather than showing an odd-even oscillation²⁰⁷. Sreekumar et al. recently reported the synthesis of nonconjugated amidodiols based chiral polyurethanes and its nonlinear optical activity.²⁰⁸⁻²⁰⁹

1. 15. Conclusion

The chapter has overviewed the recent and important developments in the field of organic chromophores and chiral polymers with nonlinear optical properties. The review gives a survey of NLO active polymeric materials with a brief introduction which comprises of principles and the origin of nonlinear optics and the various kinds of polymeric materials for nonlinear optics, including guest-host systems, side chain polymers, main chain polymers, crosslinked polymers and chiral polymers etc. It discusses the influence of

donor-acceptor chromophores and the influence of chirality for designing second order nonlinear optical materials.

One of the challenges in this century being faced by scientists is the commercialization of nonlinear optical devices, which are gaining greater interest in the field of communication technology and data storage. The introduction of the devices, however, is hampered by the limitations in achieving certain material properties. The materials should meet the requirements such as excellent thermal stability, processability, ease of fabrication, excellent mechanical and physical properties, high optical nonlinearity and at the same time should be commercially viable. In this respect, polymeric materials, which have the combination of all these properties, become important. Poled polymeric materials are potential candidates for nonlinear optics. They show greater promise due to their controlled nonlinearity, tailoring properties, ease of processing and fabrication to devices, fast response times, excellent mechanical and physical properties, low cost etc. However, problems such as the relaxation of poled order, thermal instability at operating temperatures etc faced by polymers are serious impediments to their development. Present study in nonlinear optics is therefore mostly concerned with improving the performance of NLO polymers for better thermal stability, orientational stability and processability. In this chapter many approaches have been discussed to achieve a long-term temporal stability of NLO properties and electro optic effects.

1. 16. Instrumentation used in this work

The UV-Visible spectra were recorded using Spectro UV-Visible Double beam UVD- 3500 instrument. FT-IR spectra of the powdered samples were recorded on JASCO 4100 FTIR spectrometer using KBr discs. The MALDI-MS analysis was carried out using Shimadzu Biotech Axima instrument. Optical rotations were measured using Atago AP100 automatic digital polarimeter. The fluorescence spectra were recorded using FluroMax-3 instrument. The refractive index measurements were carried out using ABBE Refractometer (ATAGO) using the wavelength of 589nm. NMR spectra were recorded using Bruker 300MHz instrument. The XRD analysis was carried out using Rigaku X-ray Photometer. The XRD pattern was taken 10° - 90° angles with an increment of

0.05° angle and with the rotation speed 5 degree per minute. TG/DTA measurements were performed using Perkin Elmer Pyrex diamond 6 instrument. The weight of the sample was plotted against temperature to get a thermogram. The analysis was done under nitrogen atmosphere using a heating rate of 10°C /min from room temperature to 800°C using platinum crucible. The second harmonic generation test for polymers was performed by Kurtz and Perry powder technique using Nd: YAG laser (1064 nm). The conductivity measurements were carried out using Keithley 2400 sourcemeter by 2 probe method. FTIR measurements were done at SAIF CUSAT Cochin, MALDI-MS analysis at NIIST Trivandrum and the NMR analysis at SAIF, IIT Chennai, NRC, IISc Bangalore. NLO measurements were done at IPC, IISc Bangalore.

1. 17. References

- 1 Bloembergen N, *IEEE Journal on Selected Topics in Quantum Electronics*, 2000, **6**, 876.
- 2 Hecht E, *Optics*, Addison Wesley, New York 1998.
- 3 Kuzyk M G, Disk C W, *Characterisation Techniques and Tabulations for Organic NLO Materials*, Marcell Dekker Inc., New York 1998.
- 4 Tingjian J, Zhiguo S, Yongguang Cheng, *Optics Communications*, 2010, **283**, 1110
- 5 Boyd R W, *Nonlinear Optics*, Academic Press, California, 1992.
- 6 Saleh B E A and Teich M C, *Fundamentals of Photonics*, Wiley, New York 1991
- 7 Long N J, *Angew Chem Int Ed Engl*, 1995, **34**, 21.
- 8 Khoo L C, *Liquid Crystals: Physical Properties and Nonlinear Optical Phenomena*, Wiley, New York, 1995.
- 9 Prasad P N, Williams D J, *Introduction to Nonlinear Optical Phenomena*, Wiley, New York, 1991.
- 10 Miller A, Eason R W (Eds), *Nonlinear Optics and Signal Processing*, Chapman and Hall, London, 1993.
- 11 Franken P A, Hill A E, Peters C W, Weinreich G, *Phys Rev Lett*, 1961, **7**, 118.
- 12 Maiman T H, *Nature*, 1960, **187**, 493.
- 13 Maker P D, Terhune R W, Nisenhoff M, Savage C M, *Phys Rev Lett*, 1962, **8**, 21.

- 14 Giordmaine J A, *Phys Rev Lett*, 1962, **8**, 19.
- 15 Zhongan L, Li W, Bi X, Cheng Y, Jingui Q, Zhen L, *Dyes and Pigments*, 2010, **84**, 134.
- 16 Fengxian Q, Wei Z, Dongya Y, Minijian Z, Guorong C, Pingping L, *J Appl Polym Sci*, 2010, **115**, 146.
- 17 Nalwa H S, Miyata S, *Nonlinear Optics of Organic Molecules and Polymers*; CRC Press: New York, 1997.
- 18 Davis D, Sreekumar K, Sajeev Y, Pal S, *J Phys Chem B*, 2005, **109**, 14093.
- 19 Chemla D S, Zyss J, *Nonlinear Optical Properties of Organic Molecules and Crystals*; Academic Press, Inc: New York, 1987.
- 20 Kanis D R, Ratner M A, Marks T J, *Chem Rev*, 1994, **94**, 195.
- 21 Sutherland R L, *Handbook of Nonlinear Optics*; Marcel Dekker, Inc: New York, 2003.
- 22 Louisell W H, Yariv A, Siegman A E, *Phys Rev*, 1961, **124**, 1646.
- 23 Munn R W, *J Mol Electron*, 1988, **4**, 31.
- 24 Onsager L, *J Am Chem Soc*, 1936, **58**, 1486.
- 25 Lorentz H A, *The Theory of Electric Polarization*; Elsevier: Amsterdam, 1952.
- 26 Kleinman D A, *Phy Rev*, 1962, **125**, 87.
- 27 Kleinman D A, *Phy Rev*, 1962, **128**, 1761.
- 28 Tasaganva R G, Kariduraganavar M Y, Inamdar S R, *Synth Met*, 2009, **159**, 1812.
- 29 Oudar J L, Chemla D S, *J Chem Phys*, 1977, **66**, 2664
- 30 Petsalakis I D, Georgiadou D G, Vasilopoulou M, Pistolis G, Dimotikali D, Argitis P, Theodorakopoulos G, *J Phys Chem A*, 2010, **114**, 5580.
- 31 Barzoukas M, Blanchard-Desce M, Josse D, Lehn J M, Zyss J, *Chem Phys*, 1989, **133**, 323.
- 32 Jürgen R, David V, Alberto B, Alex B, Alain F, Marcel M, *Euro J Org Chem*, 2010, **2010**, 1096
- 33 Uladzimir A H, Svetlana V S, Nelson V T, Landa H, Diane M S, Brian R K, *Optics Express*, 2010, **18**, 8697.
- 34 Verbiest T, Houbrechts S, Kauranen M, Clays K, Persoons A, *J Mater Chem*, 1997, **7**, 2175.
- 35 Schmidt K, Barlow S, Leclercq A, Zojer E, Jang S H, Marder S R, Jen A K Y, Bredas J L, *J Mater Chem*, 2007, **17**, 2944.

- 36 Rutkis M, Jurgis A, Kampars V, Vembris A, Tokmakovs A, Kokars V, *J Phys: Conf Series*, 2007, **93**, 012028.
- 37 Rezaeifard A, Jafarpour M, Rayati S, Shariati R, *Dyes and Pigments*, 2009, **80**, 80.
- 38 Philip B, Sreekumar K, *J Polym Sci : Part A: Polym Chem*, 2002, **40**, 2868.
- 39 Davis D, Sreekumar K, Pati S K, *Synth Met*, 2005, **155**, 384.
- 40 Bahulayan D, Sreekumar K, *J Mater Chem*, 1999, **9**, 1425.
- 41 Scarpaci A, Blart E, Montembault V, Fontaine L, Rodriguez V, Odobel F, *Appl Mater Interfaces*, 2009, **1**, 1799
- 42 Flory P J, *J Am Chem Soc*, 1952, **74**, 2718.
- 43 Xie J, Deng X, Cao Z, Shen Q, Zhang W, Shi W, *Polymer*, 2007, **48**, 5988.
- 44 Chang H L, Chao T Y, Yang C C, Dai S A, Jeng R J, *Eur Polym J*, 2007, **43**, 3988.
- 45 Samyn C, Verbiest T, Persoons A, *Macromol Rapid Commun*, 2000, **21**, 1.
- 46 Tambe S M, Tasaganva R G, Jogul J J, Castiglione, Kariduraganavar M Y, *J Appl Polym Sci*, 2009, **114**, 2291.
- 47 Aruna P, Rao B S, *Reactive and Functional Polymers*, 2009, **69**, 20.
- 48 Hyo J N, Hanna J, You J C, Ju- Yeon L, *J Polym Sci Part A, Polym Chem*, 2010, **48**, 1166.
- 49 Priimagi A, Shevchenko A, Kaivola M, Rodriguez F J, Kauranen M, Rochon P, *Opt Lett* 2010, **35**, 1813.
- 50 Philip B, Sreekumar K, *J Polym Mater*, 2001, **365**, 18.
- 51 Sandhya K Y, Pillai C K S, Tsutsumi N, *Prog Polym Sci*, 2004, **29**, 45.
- 52 Meredith G R, Van Dusen J G, Williams D J, *Macromolecules*, 1982, **15**, 1385.
- 53 Roberto Centore, Antonio Roviello, *Advances in Macromolecules*, M V Russo Ed, 2010, 79.
- 54 Wu J W, Binkley E S, Kenney J T, Garito A F, *Appl Phys Lett*, 1991, **69**, 7366.
- 55 Wu J W, Valley J F, Ermer S, Binkley E S, Kenney J T, Lipscomb G F, Lytel R, *Appl Phys Lett*, 1991, **58**, 225.
- 56 Petsalakis I D, Georgiadou D G, Vasilopoulou M, Pistolis G, Dimotikali D, Argitis P, Theodorakopoulos G, *J Phys Chem A*, 2010, **114**, 5580.
- 57 Lee S C, Kidoguchi A, Watanabe J, Yamamoto H, Hosomi T, Miyata S, *Polym J*, 1991, **23**, 1209
- 58 Boyd G T, Francis C V, Trend J E, Ender D A, *J Opt Soc Am*, 1991, **B8**, 887.

- 59 Stahelin M, Walsh C A, Burland D M, Miller R D, Twieg R J, Volksen W, *J Appl Phys*, 1993, **73**, 8471.
- 60 Twieg R J, Betterton K M, Burland D M, Lee V Y, Miller R D, Moylan C R, Volksen W, Walsh C A, *SPIE Proc*, 1993, **2025**, 94.
- 61 Cheng L T, *Handbook of Photonics*, M C Gupta (Ed), C R C Press LLC, 1997
- 62 Stahelin M, Walsh C, Burland D, Miller R, Twieg R, Volksen W, *J Appl Phys*, 1993, **73**, 8471
- 63 Sureshkumar M S, Goyal R K, Negi Y S, *Prog in Rub Plast Recycl Tech*, 2008, **24**, 53
- 64 Rau I, Armatys P, Chollet P A, Kajzar F, Andraud C, Bretonniere Y, *Nonlinear Opt Quantum Opt*, 2006, **35**, 57.
- 65 Jung G B, Akazawa T, Mutai T, Fujimura R, Ashihara S, Shimura T, Araki K, Kuroda K, *Jap J Appl Phys, Part 1: Regular Papers and Short Notes and Review Papers*, 2006, **45**, 102.
- 66 Zhang L, Allen S D, Woelfle C, Zhang F, *J Phys Chem C*, 2009, **113**, 13979.
- 67 Esselin S, Barny P L, Robin P, Broussoux D, Dubois J C, Raffy J, Pocholle J P, *SPIE Proc*, 1988, **971**, 120.
- 68 Georgi B H, Ivan L S, *Applied Optics*, 2010, **49**, 1876.
- 69 Kajzar F, Krupka O, Pawlik G, Mitus A, Rau I, *Molecular Crystals and Liquid Crystals*, 2010, **522**, 180.
- 70 Pawlik G, Rau I, Kajzar F, Mitus A C, *Optics Express*, 2010, **18**, 18793.
- 71 Hayashi A, Goto Y, Nakayama M, Kaluzynski K, Sato H, Watanabe T, Miyata S, *Chem Mater*, 1991, **3**, 6.
- 72 Ye C, Marks T J, Yang J, Wong G K, *Macromolecules*, 1987, **20**, 2322.
- 73 Lu J, Yin J, Deng X, Shen Q, Cao Z, *Opt Mater*, 2004, **25**, 17.
- 74 Peng Z, Yu L, *Macromolecules*, 1994, **27**, 2638.
- 75 Yang S, Peng Z, Yu L, *Macromolecules*, 1994, **27**, 5858.
- 76 Yu D, Yu L, *Macromolecules*, 1994, **27**, 6718.
- 77 Yu D, Gharavi A, Yu L, *Macromolecules*, 1996, **29**, 6139.
- 78 Caruso U, Casalboni M, Fort A, Fusco M, Panunzi B, Quatela A, Roviello A, Sarcinelli F, *Opt Mater*, 2005, **27**, 1800
- 79 Pan Y, Tang X, *Eur Polym J*, 2008, **44**, 408
- 80 Shalini Rosalyn P D, Senthil S, Kannan P, Vinitha G, Ramalingam A, *J Phys Chem Solids*, 2007, **68**, 1812.

- 81 Ju H K, Lim J S, Yoon S C, Lee C, Choi D H, Park S K, Kim D W, *Macromol Symp*, 2007, **249**, 21.
- 82 Chen X, Zhang J, Zhang H, Jiang Z, Shi G, Li Y, Song Y, *Dyes and Pigments*, 2008, **77**, 223.
- 83 Zhao W K, Wang Z P, Chen Z, Xu G M, Han X, Qiu L, Zhen Z, Liu X H, *Photographic Science and Photochemistry*, 2007, **25**, 452.
- 84 Li. H, Termine R, Angiolini L, Giorgini L, Mauriello F, Golemme A, *Chem Mater*, 2009, **21**, 2403.
- 85 Li .N, Lu. J, Xia X, Xu Q, Wang L, *Dyes and Pigments*, 2009, **80**, 73.
- 86 Shi Z, Luo J, Huang S, Cheng Y J, Kim T D, Polishak B M, Zhou X H, Tian Y, Jang S H, Knorr D B, Overney R M, Younkin T R, Jen A K Y, *Macromolecules*, 2009, **42**, 2438.
- 87 Mitchell M, Mulvaney J, Hall Jr H K, Willand C, Hampsch H, Williams D J, *Polym Bull*, 1992, **28**, 381.
- 88 Fuso F, Padias A B , Hall Jr H K, *Macromolecules*, 1991, **24**, 1710.
- 89 Green G D, Hall Jr H K, Mulvaney J E, Noonan J, Williams D J, *Macromolecules*, 1987, **20**, 716.
- 90 Green G, Weinschenk J I, Mulvaney J, Hall Jr H K, *Macromolecules*, 1987, **20**, 722.
- 91 Hall Jr H K, *J Macromol Sci Chem*, 1998, **25**, 729.
- 92 Lindsay G A, Stenger Smith J D, Henry R A, Hoover J M, Nissan R A, Wynne K T, *Macromolecules*, 1992, **25**, 6075.
- 93 Wang C H, Guan H W, *SPIE Proc*, 1992, **1775**, 318.
- 94 Xu C, Wu B, Dalton L R, Ranon P M, Shi Y, Steier W H, *Macromolecules*, 1992, **25**, 6716.
- 95 Xu C, Wu B, Dalton L R, Ranon P M, Shi Y, Steier W H, *SPIE Proc*, 1993, **1852**, 198.
- 96 Eich M, Reck B, Yoon D Y, Willson C G, Bjorklund G C, *J Appl Phys*, 1989, **66**, 3241.
- 97 Kim J H, Won D S, Lee J Y, *Bull Korean Chem Soc*, 2008, **29**, 181.
- 98 Angiolini L, Benelli T, Bozio R, Cozzuol M, Giorgini L, Pedron D, Salatelli E, *E-Polymers*, 2008, 13.
- 99 Lee J Y, Baek C S, Bang H B, *Mol Cryst and Liq Cryst*, 2006, **445**, 239.
- 100 Yoon K R, Byun N M, Lee H, *Synth Met*, 2007, **157**, 603.

- 101 Lee J Y, Kim J H, Jung W T, Park Y K, *J Mater Sci*, 2007, **42**, 3936.
- 102 Park J, Marks T J, Yang J, Wong G K, *Chem Mater*, 1990, **2**, 229.
- 103 Mandal B K, Chen Y M, Lee J Y, Kumar J, Tripathy S K, *Appl Phys Lett*, 1991, **58**, 2459.
- 104 Mandal B K, Lee J Y, Zhu X F, Chen Y M, Prakeenavincha E, Kumar J, Tripathy S K, *Synth Met*, 1991, **43**, 3143.
- 105 Jeng R J, Chang C C, Chen C P, Chen C T, Su W C, *Polymer*, 2003, **44**, 143.
- 106 Lin J T, Hubbard M A, Marks T J, Lin W, Wong G K, *Chem Mater*, 1992, **4**, 1148.
- 107 Wu W, Wang D, Zhu P, Wang P, Ye C, *J Polym Sci Polym Chem*, 1999, **37**, 3598.
- 108 Lue J, Zhan C, Qin J, *React Funct Polym*, 2000, **44**, 219.
- 109 Wang C, Zhang C, Wang P, Zhu P, Wu W, Ye C, Dalton L R, *Polymer*, 2000, **41**, 2583.
- 110 Samyn C, Ballet W, Verbiest T, Van Beylen M, Persoons A, *Polymer*, 2001, **42**, 8511.
- 111 Kishore V C, Dhanya R, Sreekumar K, Joseph R, Kartha C S, *Spectrochimica Acta Part A*, 2008, **70**, 1227.
- 112 Barry S E, Soane D S, *Appl Phys Lett*, 1991, **58**, 1134.
- 113 Blanchard P M, Mitchell G R, *Appl Phys Lett*, 1993, **63**, 2038.
- 114 Sekkat Z, Dumont M, *Appl Phys B*, 1992, **54**, 486.
- 115 Busson B, Kauranen M, Nuckolls C, Katz T J, Persoons A, *Phys Rev Lett*, 2000, **84**, 79.
- 116 Miyata S, Sasabe H (Eds), *Poled Polymers and their Applications to SHG and EO Devices*, Gordon and Breach, Amsterdam, 1997.
- 117 Ashwell G J, Jefferies G, Hamilton D G, Lynch D E, Roberts M P S, Bahra G S, Brown C R, *Nature*, 1995, **375**, 385.
- 118 Hoss R, Konig O, Kramer-Hoss V, Berger U, Rogin P, Hulliger J, *Angew Chem Int Ed Engl*, 1996, **35**, 1664.
- 119 Marder S R, Perry J W, Schaefer W P, *Science*, 1989, **245**, 626.
- 120 Zyss J, Chemla D S, Nicoud J F, *J Chem Phys*, 1981, **74**, 4800.
- 121 Wolff J J, Siegler F, Matschiner R, Wortmann R, *Angew Chem Int Ed Engl*, 2000, **39**, 1436.
- 122 Huang K, Britton D, Etter M C, Byrn S R, *J Mater Chem*, 1995, **5**, 379.
- 123 Gangopadhyay P, Radhakrishnan T P, *Chem Mater*, 2000, **12**, 3362.

- 124 Levine B F, Bethea C G, Thurmond C D, Lynch R T, Bernstein J L, *J Appl Phys*, 1979, **50**, 2523.
- 125 Gangopadhyay P, Rao D N, Agranat I, Radhakrishnan T P, *Enantiomer*, 2002, **7**, 119.
- 126 Clays K, Persoons A, *Phys Rev Lett*, 1991, **66**, 2980.
- 127 Rentzepis P M, Giordmaine J A, Wecht K W, *Phys Rev Lett*, 1966, **16**, 792.
- 128 Sioncke S, Verbiest T, Persoons A, *Mater Sci Eng*, 2003, **42**, 115.
- 129 Philip B, Sreekumar K, *Designed Monomers and Polymers*, 2002, **5**, 115.
- 130 Giordmaine J A, *Phys Rev*, 1965, **138**, 1599.
- 131 Duangporn W, Victoria J H, Nathan J B, James G G, Garth J S, *Chem Phys Chem*, 2009, **10**, 2674.
- 132 Meijer E W, Havinga E E, Rikken G L J A, *Phys Rev Lett*, 1990, **65**, 37.
- 133 Meijer E W, Havinga E E, *Synth Metals*, 1993, **57**, 4010.
- 134 Vasantha K, Dhanuskodi S, *J Crystal Growth*, 2004, **263**, 466.
- 135 Kauranen M, Verbiest T, Maki J J, Persoons A, *J Chem Phys*, 1994, **101**, 8193.
- 136 Elshocht S V, Verbiest T, Kauranen M, Persoons A, Langeveld-Voss B M W, Meijer E W, *J Chem Phys*, 1997, **107**, 8201.
- 137 Simpson G J, *Chem Phys Chem*, 2004, **5**, 1301.
- 138 Shinichi I, Devproshad K P, Salam M A, Naoki H, *J Am Chem Soc*, 2010, **132**, 2864.
- 139 Deming T J, Novak B J, *J Am Chem Soc*, 1992, **114**, 7926.
- 140 Takei F, Koichi Y, Onitsuka K, Takahashi S, *Angew Chem Int Ed Engl*, 1996, **35**, 1554.
- 141 Majidi M R, Kane-Maguire A P, Wallace G G, *Polymer*, 1996, **37**, 359.
- 142 Nolte R J M, van Beijnen A J M, Drenth W, *J Am Chem Soc*, 1974, **96**, 5932.
- 143 Yashima E, Maeda Y, Okamoto Y, *Nature*, 1999, **399**, 449.
- 144 Terunuma D, Nagumo K, Kamata N, Matsuoka K, Kuzuhara H, *Chem Lett*, 1998, **31**, 4666 .
- 145 Shinihara K, Aoki T, Kaneko T, Olikawa E, *Chem Lett*, 1997, **6**, 361.
- 146 Obata K, Kira M, *Macromolecules*, 1998, **31**, 4666.
- 147 Jha S K, Cheon K S, Green M M, Selinger J V, *J Am Chem Soc*, 1991, **121**, 1665.
- 148 Selegny E, *Optically Active Polymers*; D Reidel Publishing Company: Holland, 1979.
- 149 Nakako H, Mayahara Y, Nomura R, Tabata M, Masuda T, *Macromolecules*, 2000, **33**, 3978.

- 150 Koe J R, Fujiki M, Motonaga M, Najashima H, *Macromolecules*, 2001, **34**, 1082.
- 151 Li C Y, Yan D, Cheng S Z D, Bai F, He T, Chein L, Harris F W, Lotz B, *Macromolecules*, 1999, **32**, 524.
- 152 Iwasaki T, Nishide H, *Curr Trends Org Chem*, 2005, **9**, 1665.
- 153 Gubler U, Bosshard C, *Nat Mater*, 2002, **1**, 209.
- 154 Zhihua W, Jianwu S, Jiange W, Chunli L, Xinyong T, Yanxiang C, Hua W, *Org Lett*, 2010, **12**, 456.
- 155 Verbiest T, Van Elshocht S, Kauranen M, Hellemans L, Snauwaert J, Nuckolls C, Katz T J, Persoons A, *Science*, 1998, **282**, 913.
- 156 Nuckolls C, Katz T J, Castellanos L, *J Am Chem Soc*, 1996, **118**, 3767.
- 157 Lovinger A J, Nuckolls C, Katz T J, *J Am Chem Soc*, 1998, **120**, 264.
- 158 Verbiest T, Elshocht S V, Persoons A, Nuckolls C, Philips K E, Katz T J, *Langmuir*, 2001, **17**, 4685.
- 159 Siltanen M, Cattaneo S, Vuorimaa E, Lemmetyinen H, Katz T J, Philips K E S, Kauranen M, *J Chem Phys*, 2004, **121**, 1.
- 160 Verbiest T, Sioncke S, Persoons A, Vyklicky L, Katz T J, *Angew Chem Int Ed*, 2002, **41**, 3882.
- 161 Nuckolls C, Katz T J, *J Am Chem Soc*, 1998, **120**, 9541.
- 162 Fox J M, Katz T J, Elshocht S V, Verbiest T, Kauranen M, Persoons A, Thongpanchang T, Krauss T, Brus L, *J Am Chem Soc*, 1993, **121**, 3453.
- 163 Morawetz H, *Macromolecules in Solution*, 2nd Ed., Wiley-Interscience, New York, 1975.
- 164 Green M M, Reidy M P, Johnson R J, Darling G, O'Leony D J, Wilson G, *J Am Chem Soc*, 1989, **111**, 6452.
- 165 Green M M, Peterson N C, Sato T, Teramoto A, Cook R, Lifson S, *Science*, 1995, **268**, 1860 .
- 166 Verbiest T, Kauranen M, Persoons A, *J Mater Chem*, 1999, **9**, 2005.
- 167 Kauranen M, Verbiest T, Persoons A, *J Nonlinear Opt Phys*, 1999, **8**, 171.
- 168 Beljonne D, Shuai Z, Bredas J L, Kauranen M, Verbiest T, Persoons A, *J Chem Phys*, 1998, **108**, 1301.
- 169 Philip B and Sreekumar K, *Polym Int*, 2001, **50**, 1318.
- 170 Verbiest T, Samyn C, Boutton C, Houbrechts S, Kauranen M, Persoons A, *Adv Mater*, 1996, **8**, 756.
- 171 Jing C, Qiuli N, Lingxiang G, Yuming Z, *J Appl Polym Sci*, 2010, **115**, 2190.

- 172 Terrenstra M N, Hagting J G, Oostergetel G T, Schouten A J, Devillers M A C, Nolte R J M, *Thin Solid Films*, 1994, **248**, 110.
- 173 Koeckelberghs G, Van Beylen M, Samyn C, *Eur Polym J*, 2001, **37**, 1991.
- 174 Philip B, Sreekumar K, *J Mater Sci*, 2003, **38**, 1573.
- 175 Valev V K, Silhanek A V, Smisdorn N, De-Clercq B, Gillijns W, Aktsipetrov O A, Ameloot M, Moshchalkov V V, Verbiest T, *Optics Express*, 2010, **18**, 8286.
- 176 Kauranen M, Verbiest T, Boutton C, Teernstra M N, Schouten A J, Nolte R J M, Clays K, Persoons A, *Science*, 1995, **270**, 966.
- 177 Kauranen M, Verbiest T, Meijer E W, Havinga E E, Teernstra M N, Schouten A J, Nolte R J M, Persoons A, *Adv Mater*, 1995, **7**, 641.
- 178 Jusroop S M, Gary W L, *J Am Chem Soc*, 2010, **132**, 3204.
- 179 Fernando T, Reyna-González J M, Huerta G, Almeida S Rivera E, *Polymer Bulletin*, 2010, **64**, 581.
- 180 Verbiest T, Sioncke S, Koeckelberghs G, Samyn C, Persoons A, Botek E, Andre J M, Champagne B, *Chem Phys Lett*, 2005, **404**, 112.
- 181 Pu L, *Chem Rev*, 1998, **98**, 2405.
- 182 Pu L, *Macromol Rap Commun*, 2000, **21**, 795.
- 183 Maniram K A, Sreekumar K, *Proc SPIE, Smart Mater, Struct. MEMS*, 1998, **67**, 3321.
- 184 Philip B, Sreekumar K, *Colloid Polym Sci*, 2003, **281**, 485.
- 185 Sandhya K Y, Pillai C K S, Sreekumar K, *J Polym Sci: Part B: Polym Phys*, 2004, **42**, 1289.
- 186 Elizabeth C V, Sreekumar K, *Proc Polychar 16*, Lucknow, India, 2008.
- 187 Elizabeth C V, Sreekumar K, *Proc SAMPADA 2008*, NCL Pune, India, 2008.
- 188 Elizabeth C V, Sreekumar K, *Proc MACRO 2009*, IIT Chennai, India, 2009.
- 189 Elizabeth C V, Sreekumar K, *Proc MATCON 2010*, CUSAT, Kerala, India, 2010.
- 190 Elizabeth C V, Sreekumar K, *Proc I2CAM, 2010*, JNCASR, Bangalore, India, 2010.
- 191 Yashima E, Maeda K, *Macromolecules*, 2008, **41**, 3.
- 192 Majidi M R, Kanemaguire L A P, Wallace G G, *Polymer*, 1995, **36**, 3597.
- 193 Guo H, Knobler C M, Kaner R B, *Synth Met*, 1999, **101**, 44.
- 194 Yashima E, Goto H, Okamoto Y, *Macromolecules*, 1999, **32**, 7942.

- 195 Maeda K, Morioka K, Yashima E, *Macromolecules*, 2007, **40**, 1349.
- 196 Mori T, Kyotani M, Akagi K, *Macromolecules*, 2008, **41**, 607.
- 197 Cremer L D, Verbiest T, Koeckelberghs G, *Macromolecules*, 2008, **41**, 568.
- 198 Cremer L D, Vandeleene S, Maesen M, Verbiest T, Koeckelberghs G, *Macromolecules*, 2008, **41**, 591.
- 199 Tuuttila T, Lipsonen J, Huuskonen J, Rissanen K, *Dyes and Pigments*, 2009, **80**, 34.
- 200 Vanormelingen W, Smeets A, Franz E, Asselberghs I, Clays K, Verbiest T, Koeckelberghs G, *Macromolecules*, 2009, **42**, 4282.
- 201 Zhongan L, Wenbo W, Gui Y, Yunqi L, Cheng Y, Jingui Q, Zhen L, *Appl Mater and Interfaces*, 2009, **4**, 856
- 202 Qianqian L, Gui Y, Jing H, Haijie L, Zhen L, Cheng Y, Yunqi L, Jingui Q, *Macromol Rapid Commun*, 2008, **29**, 798.
- 203 Li Z, Hu P, Yu G, Zhang W, Jiang Z, Liu Y, Ye C, Qin J, Li Z, *Phys Chem Chem Phys*, 2009, **11**, 1220.
- 204 Brasselet S, Cherioux F, Audebert P, Zyss J, *Chem Mater*, 1999, **11**, 1915.
- 205 Datta A, Pati S K, *Chem Soc Rev*, 2006, **35**, 1305.
- 206 Datta A, Pati S. K., Davis D, Sreekumar K, *J Phys Chem A*, 2005, **109**, 4112.
- 207 Davis D, Ph. D thesis, Department of Applied Chemistry, Cochin University of science And Technology, 2005.
- 208 Elizabeth C V, Sreekumar K, *J Mater Sci*, 2010, **45**, 1912.
- 209 Elizabeth C V, Sreekumar K, *J Appl Polym Sci*, 2010, **xx**, **xx**.

Chapter 2

COMPUTATIONAL STUDIES ON THE STABILITY AND SPECTROSCOPIC PROPERTIES OF PORPHYRIN, CHLORIN, BACTERIOCHLORIN AND THEIR FEW METAL COMPLEXES**2.1. Introduction**

In nature, there exist a wide variety of tetrapyrroles, including porphyrins, chlorin, bacteriochlorins, isobacteriochlorins, oxygenated hydroporphyrins and tetrapyrroles with interrupted conjugation¹⁻³. Porphyrins, chlorins and bacteriochlorins share a common macrocyclic skeleton containing 20 carbons and four inner nitrogens which differ in the degree of saturation of the π -conjugated system. The porphyrin is fully unsaturated, the chlorin is a dihydroporphyrin wherein one β , β' -bond is saturated and the bacteriochlorin is a tetrahydro-porphyrin wherein a β , β' -bond in each of the two ring positions trans to each other is saturated⁴. The tetrapyrrole systems have been widely studied in recent years, due to their structural variety as a π -conjugated macrocycle, their high thermal and chemical stability and as they possess a large number of unique properties⁵. Their potential applications have been investigated, such as chemical sensors, photodynamic reagents for cancer therapy, photovoltaic, optical discs, nonlinear optics, electrocatalysis, liquid crystals and Langmuir-Blodgett films. These applications are mainly concerned with the π -conjugated macrocycle, as well as the type of metal encapsulated in the core tetrapyrroles⁶⁻¹⁰. The ability of tetrapyrrole compounds either to accept or to donate electronic charges plays a key role in biological processes, such as photosynthesis, oxygen transport and enzymatic reactions¹¹⁻¹². Therefore, exploring the novel features of the tetrapyrrole complexes is expected to be an interesting topic for the photochemists, photophysicists and photobiologists. The studies related to excited state structure and properties of tetrapyrrole compounds are found to be very important for understanding the biologically important processes such as energy transfer in photosynthesis, photodynamic therapy of cancers, and chromophore-protein interaction in heme proteins¹³⁻¹⁶.

The tetrapyrroles are highly conjugated and as a consequence, have very intense absorption in the visible region. The optical spectra of all tetrapyrroles

are generally quite similar which are being characterized by a number of weak bands in the visible region (Q band) and a relatively strong band in the UV region (B band). The interpretation of absorption spectra of tetrapyrroles is given by the Gouterman four-orbital model, which involves excitations from the two highest occupied molecular orbitals (HOMOs) to two lowest unoccupied molecular orbitals (LUMOs)¹⁷⁻²³. The time dependent density functional theory (TD-DFT) calculations have been carried out in order to characterize the electronic and optical properties of the tetrapyrroles and their metal complexes.

The presence of large π electron delocalization and the novel structural features are the key elements in the design of organic materials for potential applications in nonlinear optics. Recently, a major attention has been imposed for tetrapyrroles and metal encapsulated tetrapyrroles in the field of nonlinear optics by virtue of their exceptional stability and the π conjugated electrons in the aromatic pathway. Because of these special characteristics, these systems are popular for electronic communication, data storage, optical switching and opto electronics. Due to the strong dependence of the utility of macrocycles for optical applications based on a permanent dipole moment, the asymmetric tetrapyrroles have more potential for NLO applications than the symmetric ones^{24- 28}.

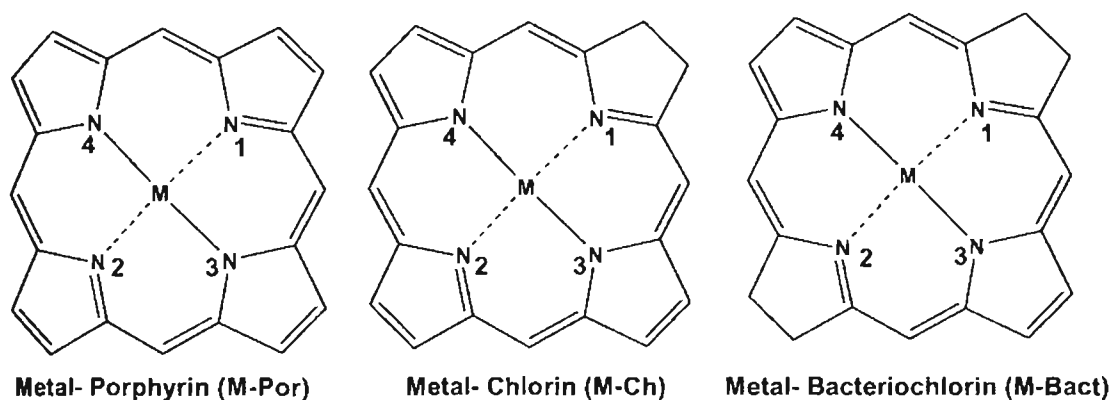
The study provides a comparative analysis on the structural stability, electronic, and various spectroscopic properties of porphyrin, chlorin and bacteriochlorin with its metal encapsulated complexes (M-porphyrin, M-chlorin and M- Bacterichlorin) within the frame work of DFT and TD-DFT computations. We have selectively chosen two different types of metal tetrapyrroles in the present study. The first category is alkaline earth metals (M=Be, Mg, Ca, Sr, Ba) encapsulated in the delocalized tetrapyrroles and the second category is few selected fully filled d block elements (Zn and Cd) incorporated tetrapyrroles. The major role played by the metal ions on the electronic structure and several spectroscopic properties of the macrocycles are also discussed.

2. 2. Computational methods

All the tetrapyrrole macrocyclic ring systems and their metal encapsulated analogues have been fully optimized within DFT/B3LYP with 6-31G (d, p) and LANL2DZ basis sets, respectively using the Gaussian 03 suit of programs²⁹⁻³³. The optimized geometries are used as the input for single point

property calculations. The various spectroscopic properties (IR and Raman) are explored using DFT/LANL2DZ. The excitation energy together with oscillator strength has been computed using TD-DFT response theory as implemented in Gaussian 03. The nuclear magnetic shielding has been calculated at the B3LYP/LANL2DZ level. Natural Bond Orbital (NBO) analysis has been carried out to evaluate the bond order and their absolute NICS values using the gauge-including atomic orbital (GIAO) approach at B3LYP/LANL2DZ level^{10, 34-36}. The static polarizability and hyperpolarizability values are obtained by frequency calculations using DFT at LANL2DZ level.

2.3. Results and discussion



Where M=Alkaline earth metals(Be^{2+} , Mg^{2+} , Ca^{2+} , Sr^{2+} , Ba^{2+}), d-block elements (Zn^{2+} , Cd^{2+})

Figure 2. 1: Metal incorporated porphyrin, chlorin and bacteriochlorin

The metal free cyclic tetrapyrroles, porphyrin, chlorin and bacteriochlorin and their metal complexes (beryllium, magnesium, calcium, strontium, barium, zinc, cadmium) were selected for the present study. The structures of metal incorporated porphyrin, chlorin and bacteriochlorin studied are shown in **Figure 2. 1**. Both the metal free and metal incorporated structures have been optimized by DFT/B3LYP method. The optimized structure of porphyrin possesses a planar geometry, whereas its Ba metallic analogue gives a puckered geometry.

In Chlorin, the Sr and Ba alkaline earth metals move upwards from the conjugated macrocyclic system. Sr-Bacteriochlorin and Ba-Bacteriochlorin also show some distortion in geometry (upward shifting of metal) from its base macrocycle. But in the case of Be-bacteriochlorin slight folding of macrocyclic geometry is observed.

Table 2. 1: Ground state dipole moment in Debye of M-Porphyrin, M-Chlorin and M-Bacteriochlorin

System	M-Porphyrin	M-Chlorin	M-Bacteriochlorin
M- free	0.0004	1.9966	0.0035
Be	0.0117	1.7489	0.4461
Mg	0.0001	2.3147	0.0027
Ca	0.0006	3.4961	0.009
Sr	0.0012	5.4628	0.1874
Ba	7.2146	7.5430	7.1927
Zn	0.0020	2.3146	0.0037
Cd	0.0016	2.3652	0.0083

The ground state dipole moment obtained for the energy minimized form of the metal free and metal incorporated tetrapyrroles are shown in the Table 2.

1.

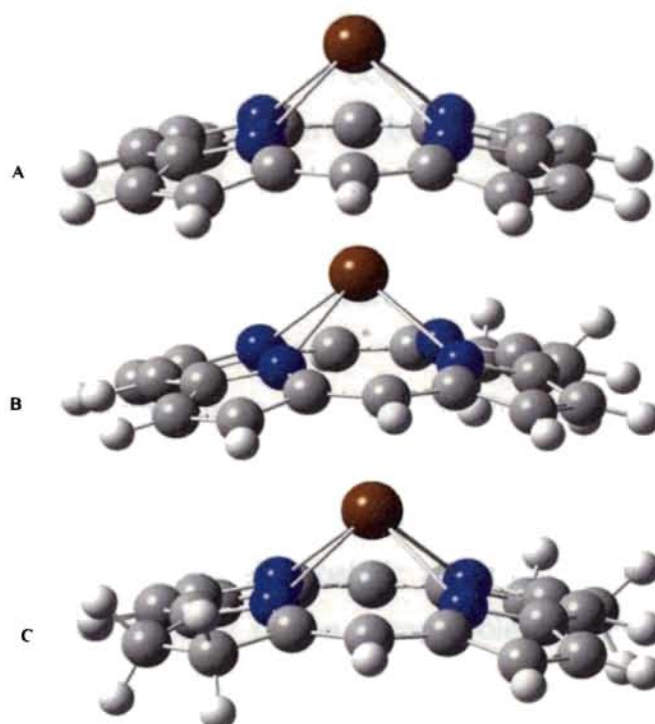


Figure 2. 2: Optimized geometry of Ba-Porphyrin (A), Ba-Chlorin (B) and Ba-Bacteriochlorin (C)

Since Barium atom possesses larger radius, the Ba attached to pyrrole ring leads to a distortion in geometry, where the dipole moments of the pyrrole rings no longer cancel each other completely. Hence among alkaline earth metals, except Ba porphyrin, all other systems are planar and possess very small or even negligible ground state dipole moment. Ba-porphyrin possesses a high dipole moment which possesses a puckered geometry in which Ba metal is pulled out from the planar porphyrin rings. The optimized geometry of Ba incorporated Porphyrin (A), Chlorin (B) and Bacteriochlorin (C) are shown in **Figure 2. 2**.

2. 3. 1. Bond orders and bond lengths

In order to elucidate the stability of metal tetrapyrroles, the strength of M-N bond is analysed from the calculated bond orders (Wiberg bond index). The other characteristics of optimized structures of tetrapyrroles and metal tetrapyrroles are reported in the **Table 2. 2** with respect to their corresponding bond lengths and bond orders (M-N). The metal-nitrogen bond lengths and bond orders are reported in the **Table 2. 2**. Since the bond order is less than 0.5, the system possesses only ionic interaction with the metals. From the concept of bond orders, the stability of the tetrapyrrole complexes is found to be as follows $\text{Be} > \text{Mg} > \text{Ca} > \text{Sr} > \text{Ba}$ and $\text{Zn} < \text{Cd}$, since the bond order and bond lengths follow the same sequence. This stability criterion can be explained by means of the size of metals considered. In general, the metal ion with smaller size can form more stable complexes. A smaller metal permits a closer approach to the ligands and hence induce a larger electrostatic attraction and gives a more stable tetrapyrrole complex.

On proceeding downwards in a group, the electrons are added to the higher main energy levels which are very farther from the nucleus. This effect causes a decrease in electrostatic attraction between the nucleus and the valence shell electrons and this decreased electrostatic attraction increases the atomic and ionic radii. The extra stability of the tetrapyrrole complexes can also be explained by means of the decreased electrostatic attraction which is caused by the effect of the extra shell being added in the configuration of the elements.

Table 2. 2: Bond orders and Bond lengths of M-N for M-Porphyrin, M-chlorin and M-Bacteriochlorin

Metal	M-Chlorin			M-Bacteriochlorin		
	Bond Order (M-N)	Bond Length (M-N)	Bond Order (M-N)	Bond Length (M-N)	Bond Order (M-N)	Bond Length (M-N)
Be	0.125	1.95	0.043 (N1)	2.58 (M-N1)	0.115(N1, N2)	2.51 (M-N1, M-N2)
			0.130 (N2)	1.74 (M-N2)	0.167(N3, N4)	1.80 (M-N3, M-N4)
Mg	0.091	2.06	0.162 (N3, N4)	1.83(M-N3, M-N4)		
			0.080 (N1)	2.12 (M-N1)	0.078(N1,N2)	2.04 (M-N1, M-N2)
Ca	0.060	2.22	0.091 (N2)	2.07(M-N2)	0.102(N3, N4)	2.13 (M-N3, M-N4)
			0.096 (N3, N4)	2.05(M-N3, M-N4)		
Sr	0.051	2.30	0.053 (N1)	2.35 (M-N1)	0.053(N1,N2)	2.22 (M-N1, M-N2)
			0.061 (N2)	2.32 (M-N2)	0.064(N3, N4)	2.27 (M-N3, M-N4)
Ba	0.047	2.64	0.063 (N3, N4)	2.30(M-N3, M-N4)		
			0.046 (N1)	2.51 (M-N1)	0.046(N1,N2)	2.45 (M-N1, M-N2)
Zn	0.124	2.07	0.056 (N2)	2.47 (M-N2)	0.060(N3, N4)	2.51 (M-N3, M-N4)
			0.057 (N3, N4)	2.46(M-N3, M-N4)		
Cd	0.128	2.16	0.039 (N1)	2.68 (M-N1)	0.040(N1,N2)	2.62 (M-N1, M-N2)
			0.048 (N2)	2.64 (M-N2)	0.053(N3, N4)	2.68 (M-N3, M-N4)
			0.049 (N3, N4)	2.63(M-N3, M-N4)		
			0.108 (N1)	2.14 (M-N1)	0.102(N1,N2)	2.04 (M-N1, M-N2)
			0.123 (N2)	2.08 (M-N2)	0.149(N3, N4)	2.15 (M-N3, M-N4)
			0.137 (N3, N4)	2.06(M-N3, M-N4)		
			0.111 (N1)	2.20 (M-N1)	0.105(N1,N2)	2.14 (M-N1, M-N2)
			0.124 (N2)	2.17 (M-N2)	0.151(N3, N4)	2.22 (M-N3, M-N4)
			0.138 (N3, N4)	2.15(M-N3, M-N4)		

The size of the central metal ions along alkaline earth metal series is as follows Be (0.31 Å) < Mg (0.65 Å) < Ca (0.99 Å) < Sr (1.13 Å) < Ba (1.35 Å). Hence the stability of the complexes formed by these metals normally follows the order Be>Mg> Ca> Sr> Ba. The extra stability of Be tetrapyrrole complexes can also be explained by means of electron penetration effects and shielding effects. Since the s-electron will approach the nucleus more closely than a p-electron, the penetration of electron will increase for s than p electrons. Hence Be (1s² 2s²) possesses a high ionization potential due to the presence of mere s-electrons. Another factor contributing to the stabilization is the screening effect which is the combined effect of the attractive and repulsive forces acting on the valence electron (valence electron experiences less attraction from the nucleus). Thus, larger the number of electrons in the inner shell, lesser is the attractive force holding the valence electron to the nucleus and consequently the lower will be the value of ionization potential. Since the number of inner shells for Ba and Sr are high (5 and 4), they possess very less ionization potential. Hence a decrease in stability for the complexes is observed while going down the group. Similarly the ionic radius of Zn is 0.74 Å and Cd is 0.97 Å. Even if the bond orders of Zn and Cd complexes show approximately same values from the Wiberg bond index analysis, Zn is expected to be more stable than Cd due to its smaller size compared to Cd.

2.3.2. Formation energy

As far as the stability of tetrapyrrole complexes are concerned, the formation energy has a significant effect on the studied compounds. The heat of formation for the following reaction is determined based on the equation (1).

$L-H_2 + M \rightarrow M-L + H_2$, where M=metal, L=tetrapyrrole ligand.

$$\text{Heat of formation (Formation energy)} = E(M-L) + E(H_2) - \{E(L-H_2) + E(M)\} \quad (1)$$

The stability of the metal-ligand complexes can be explained by making use of the formation energy values. All the energy values are reported in au and KCal/Mol in Table 2.3. The formation energy of metal complexes presented in the table leads to the choice of highly stable tetrapyrrole complexes. The formation energy for Be and Mg are found to be much higher than those for Ba and Sr among the alkaline earth metal group. Similarly the formation energy for Zn tetrapyrroles is found to be higher than the Cd tetrapyrroles. These results indicate that the formation energy of metal-porphyrin, metal-chlorin and metal-

bacteriochlorin follows the order of stability as, Be >Mg >Ca> Sr> Ba and Zn >Cd.

Table 2. 3: Formation energy for M-Porphyrin, M-chlorin and M-Bacteriochlorin

Metal	M-Porphyrin (kcal/mol)	M-Chlorin (kcal/mol)	M-Bacteriochlorin (kcal/mol)
Be	-119.026	-108.384	-101.287
Mg	-111.929	-100.013	-94.095
Ca	-58.697	-60.398	-48.871
Sr	-49.319	-42.771	-38.887
Ba	-46.417	-36.069	-32.232
Zn	-57.342	-45.877	-40.640
Cd	-55.876	-44.102	-39.967

2.3.3. NICS values

The aromatic pathways of the tetrapyrroles and the metal-tetrapyrroles have been studied by calculating the nuclear magnetic shielding in the systems. The strength of the induced ring currents for a given magnetic field has been obtained by using GIAO method which gives the overall current strength and the NICS calculations give the additional information about the current routes in the multiple ring systems. Aromaticity of all the systems has been studied by using the nucleus independent chemical shift (NICS), a method developed by Schleyer and coworkers³¹, which is a magnetic criterion that mirrors the ring current. In this method, the nuclear magnetic resonance (NMR) parameters are calculated for a ghost atom, usually placed at the centre of the ring, and the negative of the isotropic magnetic shielding constant at the ghost atom is taken as the NICS value. Systems with negative NICS values are aromatic, since negative values arise from when diatropic ring current (shielding) dominates, whereas systems with positive values are antiaromatic because positive values arise when paratropic current (deshielding) dominates. Since the NICS (0 Å) values calculated at the centre of the ring is influenced by σ bonds, whereas the NICS values calculated 1 Å out of the plane are more affected by the π -system, hence we have chosen the NICS values at 1 Å distance. The aromaticities of metal tetrapyrroles are discussed in detail with the NICS values as shown in Table 2. 4.

Table 2. 4: NICS for M-Porphyrin, M-chlorin and M-Bacteriochlorin

System	M-Porphyrin	M-Chlorin	M-Bacteriochlorin
M-free	-29.882	-28.549	-28.014
Be	-30.522	-29.053	-28.940
Mg	-30.116	-28.990	-28.368
Ca	-19.968	-18.704	-17.005
Sr	-17.404	----	----
Ba	----	----	----
Zn	-30.548	-29.261	-29.326
Cd	-9.026	-8.983	-8.755

From the **Table 2. 4**, it is clear that all the tetrapyrroles and metal tetrapyrroles species exhibit characteristics of aromaticity or in other words it retains its aromaticity even after incorporating metals. The strength of aromaticity is found to vary according to the characteristics of the encapsulated metal. According to Schleyer et al. the aromatic compounds stabilize the structures by means of high -ve value of NICS. We have computed the NICS value for all the metal free and metal tetrapyrroles at GIAO-B3LYP/LANL2DZ to quantify the aromaticity. The NICS values are reported in **Table 2. 4**, showing that all complexes are aromatic. The NICS value of Be complexes are more negative than other complexes. This indicates that Be complex is the most stable among the studied metal tetrapyrrole complexes. Ba and Sr elements of alkaline earth series form complexes of weaker aromaticity compared to Be and Mg complexes. Since the aromaticity of metal tetrapyrroles follows the order Be >Mg >Ca> Sr> Ba and Zn >Cd, the stability of metal tetrapyrroles also shows the similar order. In free porphyrin, the macrocycle is highly conjugated and a number of resonance forms can be possible. The porphyrin system is nominally of 22 π -electrons, but only 18 of them are included in any one delocalization pathway. These 18 π -electrons are common for chlorine and bacteriochlorin systems. The pyrrole rings with NH groups are much more aromatic than the other five membered rings with N< groups. This indicates that the NH groups in the five membered rings are involved in the π -electron delocalization, which follows the path of 18 π delocalization (N3 and N4 rings of the ring involved for the resonance). While doing the energy minimization, Ba and Sr elements of

alkaline earth series form a puckered geometry and hence reduce its stability. Since planarity is one of the basic requirements for aromaticity, there is no need to work with Ba-porphyrin, Sr-chlorin, Ba-chlorin, Sr-bacteriochlorin and Ba-bacteriochlorin.

2.3.4. Natural electronic configuration

The natural electronic configuration of metals and metal complexes are reported in the Table 2.5. The total electronic configurations on nitrogen and metal in metal tetrapyrroles are given in which configurations involve [core] 2s 2p 3p for N, and [core] ns np. The net electronic configuration of metals and metal tetrapyrroles are given in the Table 2.5. The electronic configuration in metal is found to be reduced and in nitrogen it is increased when encapsulated in the macrocycle. This indicates that there occurs a transfer of charge from the metal to the nitrogens of tetrapyrrole ring. From the NBO analysis the observation suggest that the charge transfer is occurring from M→L (macrocycle) for all the metal complexes.

Table 2.5: Natural electronic configuration of tetrapyrrole complexes

System	Metal		M-Porphyrin		M-Chlorin		M-Bacteriochlorin	
	Metal	Nitrogen	Metal	Nitrogen	Metal	Nitrogen	Metal	Nitrogen
M-free	-	-	-	5.60	-	5.59	-	5.58
Be	2	-	0.32	5.8	0.31	5.8	0.31	5.79
Mg	2	-	0.23	5.79	0.23	5.79	0.23	5.78
Ca	2	-	0.14	5.78	0.15	5.77	0.14	5.78
Sr	2	-	0.11	5.78	0.13	5.75	0.12	5.75
Ba	2	-	0.11	5.74	0.11	5.74	0.11	5.74
Zn	12	-	10.3	5.79	10.30	5.78	10.31	5.78
Cd	12	-	10.32	5.77	10.32	5.77	10.32	5.76

2.3.5. Mulliken charges

For all the metal tetrapyrroles, as we go down through the alkaline earth series it is obvious that there occurs a sequential increase of charge on the metal atoms. The calculated Mulliken charges of selected metals and N are listed in the Table 2.6.

Table 2. 6: Mulliken charges on metal and nitrogen

System	M-Porphyrin		M-Chlorin		M-Bacteriochlorin	
	Metal	Nitrogen	Metal	Nitrogen	Metal	Nitrogen
M-free	-	-0.673		-0.5881 (N1)	-	-0.588(N)
		-0.655	---	-0.6782 (N2)		-0.1665(NH)
				-0.6600 (N3, N4)		
Be	0.543	-0.369	0.489	-0.195 (N1)	0.482	-0.420
				-0.428 (N2)		-0.372
				-0.406 (N3, N4)		-0.196
Mg	1.011	-0.498	1.015	-0.439 (N1)	1.019	-0.423
				-0.494 (N2)		-0.539
				-0.517 (N3, N4)		
Ca	1.596	-0.597	1.624	-0.483 (N1)	1.573	-0.519
				-0.529 (N2)		-0.626
				-0.551 (N3, N4)		
Sr	1.697	-0.602	1.714	-0.441 (N1)	1.700	-0.429
				-0.484 (N2)		-0.528
				-0.505 (N3, N4)		
Ba	1.725	-0.435	1.720	-0.392 (N1)	1.723	-0.379
		-0.433		-0.434 (N2)		-0.474
				-0.454 (N3, N4)		
Zn	1.097	-0.49	1.078	-0.415 (N1)	1.060	-0.395
				-0.482 (N2)		-0.398
				-0.510 (N3, N4)		-0.534
Cd	0.964	-0.45	0.959	-0.394 (N1)	0.953	-0.375
				-0.444 (N2)		-0.378
				-0.465 (N3, N4)		-0.481

The effective charge of each metal atom corresponding to the alkaline earth metal series lies in the range of +0.5 to 1.8 and for Zn and Cd between 0.9 to 1.1. The Mulliken charges on the N atom of the pyrrole ring is also found to be changing with the metals. From berilium to barium, in the alkaline earth metal series, the charges on metal atom is increased. The negative charge in nitrogen atom increases upto Sr. The metal nitrogen bond length is found to be increasing

along the group II. Cd possesses less charge compared to Zn. The M-N bond length is more for Cd.

2.3.6. Polarizability and hyperpolarizability

Response properties of molecular system in general involves energy derivatives namely, polarizabilities and hyperpolarizabilities. The polarizability and hyperpolarizability of the metal free and metal encapsulated tetrapyrroles have been calculated using DFT level at LANL2DZ basis set. The electronic polarizability is defined as the ratio of the induced dipole moment of a system to the applied electric field that produces the dipole moment. For systems where the electric field induced polarization is not constrained only to the direction of applied field, polarizability is a tensor of rank 2. Kleinman's symmetry relations allow us to simplify the calculations of the tumbling average of the polarizability from the tensors as follows ³⁷.

$$\alpha = \frac{1}{3}(\alpha_{xx} + \alpha_{yy} + \alpha_{zz}) \quad (2)$$

The polarizability of the tetrapyrroles and metal incorporated tetrapyrroles remains almost constant in the range 310-360 au. Among the tetrapyrroles, the polarizability increases in the order Porphyrin < Chlorin < Bacteriochlorin, even if there is much variation in ground state dipole moment observed among the three. Even though the dipole moments for porphyrin system are very less, it reports a reasonable polarizability by DFT/B3LYP calculation. The polarizability of metal porphyrins follows the order M-free por < Be-por < Mg-por < Ca-por < Sr-por > Ba-por, Zn-por < Cd-por. There occurs a decrease in polarizability for Ba-porphyrin which is mainly due to the puckered structure of Ba por and also because of the higher ground state dipole moment (μ_g) in **Table 2. 1**. A sequential increase in polarizability is observed for metal chlorins as M-free chlorins < Be-ch < Mg-ch < Ca-ch < Sr-ch < Ba-ch, Zn-ch < Cd-ch, which is also observed for μ_g . Because of the geometric distortions, the metal bacteriochlorins show the polarizability variation in a zig-zag manner which is caused due to the ground state dipole moment.

The first hyperpolarizability (β) is the second order electric susceptibility of the system which is a 3rd rank tensor, it has 27 tensor components. But in the general case of a molecule with no symmetry, these 27 elements are reduced to 10 according to Kleinman symmetry for second harmonic generation $\beta(2\omega; \omega,$

ω). Due to independent interchange of Cartesian coordinates, $\beta_{ijk} = \beta_{ikj}$, these irreducible 10 tensor components are β_{xxx} , β_{xxy} , β_{xyy} , β_{yyy} , β_{xxz} , β_{xyz} , β_{yyz} , β_{xzz} , β_{yzz} , and β_{zzz} . By taking the tensor product of these 10 tensor components, orientationally averaged hyperpolarizabilities can be calculated from the equations given below³⁸⁻⁴¹.

$$\beta_{vec}(-2\omega; \omega, \omega) = \sqrt{\beta_x^2 + \beta_y^2 + \beta_z^2} \quad (3)$$

$$\text{where } \beta_i = \sum_{j=x,y,z} \frac{\beta_{ijj} + \beta_{jij} + \beta_{jji}}{3} \quad ; \quad i = x, y, z \quad (4)$$

The hyperpolarizability of tetrapyrroles purely depends on the ground state dipole moments. The porphyrin has four dipoles (the pyrrole rings) pointing to the central cavity. In the free base porphyrin, two trans pyrrole rings each have a proton attached to them, whereas the other two do not. If the porphyrin chelates to a divalent metal, all pyrrole rings become identical, and the most stable structure has D_{4h} symmetry. The metal porphyrin system may be considered as a system where four dipoles are situated on the vertices of a square. The overall dipole moments of both the H₂-Por and M-Por are zero because, in either case, all the in plane dipole moments of the pyrrole rings cancel each other. Among the three tetrapyrroles, chlorin possesses the highest value of hyperpolarizability due to the less cancellation of dipole moments. Some of the metal encapsulated Bacteriochlorin systems also show good hyperpolarizability. The polarizabilities and hyperpolarizabilities of metal free and metal tetrapyrroles are shown in Table 2. 7 and the ground state dipole moment is reported in Table 2. 1.

Among the various classes of NLO active tetrapyrroles, chlorins appear to have unique characteristics that render them superior to other compounds as nonlinear optical materials. Their nonlinear optical properties can be modulated by changing the metal centre in the macrocycle. It has now been realized that significant changes in the physical and chemical properties are possible by using conformationally designed systems. The hyperpolarizability studies are based on the realization that conformational distortion imparts significant alterations in the physicochemical properties of the aromatic macrocycle.

Table 2. 7: The polarizability and hyperpolarizability of tetrapyrroles

System	M-Porphyrin		M-Chlorin		M-Bacteriochlorin	
	α (au)	β (au)	α (au)	β (au)	α (au)	β (au)
M- free	318.44	0.20	325.51	927.38	333.09	6.62
Be	322.86	2.97	325.93	602.69	330.61	328.94
Mg	332.44	0.01	332.17	787.64	345.05	2.97
Ca	347.71	0.04	342.00	796.31	359.82	1.68
Sr	355.99	0.14	343.79	1105.29	356.98	46.62
Ba	346.24	1143.58	346.31	1306.51	359.11	665.72
Zn	332.79	0.22	332.67	760.80	344.66	3.60
Cd	340.38	0.32	340.29	825.38	352.19	12.91

2. 3. 7. Excitation energy and oscillator strength

The excitation energies (E) and oscillator strength (f) are reported in Table 2. 8.

Table 2. 8: The ground state dipole moment (μ_g) in Debye, transition dipole moment (μ_t) in Debye, oscillator strength (f) and excitation energies (E) in eV of metal free and metal tetrapyrrole complexes

System	M-Porphyrin		M-Chlorin		M-Bacteriochlorin	
	f	E (eV)	f	E (eV)	f	ΔE (eV)
M- free	0.796	3.886	0.989	3.654	1.087	4.077
Be	0.963	3.586	1.105	3.638	0.937	3.808
Mg	0.894	3.500	0.489	3.503	1.058	3.791
Ca	0.742	3.354	0.401	3.792	1.089	3.773
Sr	0.667	3.274	0.513	3.454	1.086	3.844
Ba	0.002	2.563	0.569	3.446	0.771	3.709
Zn	0.891	3.495	0.626	3.514	0.014	3.786
Cd	0.826	3.437	0.537	3.453	1.001	3.783

As one goes through the group of periodic table from top to bottom, a decrease in energy for absorption (E) and oscillator strength (f) is observed for porphyrin system as Be>Mg>Ca>Sr>Ba porphyrin, and Zn>Cd porphyrin. Among the metal porphyrins, Be- porphyrin possesses the highest excitation

energy. Ca-chlorin and Sr- bacteriochlorin gives intense bands for chlorin and Bacteriochlorin systems (Table 2. 8).

2.3.8. Molecular orbital studies

The major applications of tetrapyrroles are mainly due to the special spectroscopic features, which are used for sensor applications. The absorption spectrum of tetrapyrroles show Soret intensive absorption band at around 400nm in near UV region, followed by several weaker absorptions (lesser intensity) at higher wave lengths from 450-700nm named as Q bands and these spectroscopic features have been described successfully by Gouterman's four orbital model. According to this theory, the absorption bands in porphyrin systems arise from transitions between two HOMOs and two LUMOs. The electronic transitions studied are illustrated in Figure 2. 3. The probable transitions are HOMO to LUMO, HOMO to LUMO+1, HOMO-1 to LUMO and HOMO-1 to LUMO+1.

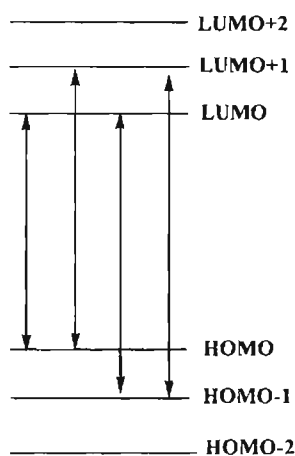


Figure 2. 3: Probable electronic transitions studied

The relative energies of these transitions may be affected by the metal centre and the substituents on the ring (macrocycle). On transition from the metal free tetrapyrrole to metal tetrapyrroles, considerable changes take place in their absorption spectra. The variations in metal and tetrapyrrole rings cause some effects on the intensity and wavelength of the absorptions. The metal ions are found to influence the absorption bands of the tetrapyrroles by interaction with the molecular orbitals.

The various energy levels of molecular orbitals HOMO-1 (H-1), HOMO (H), LUMO (L), LUMO+1 (L+1) and the corresponding electronic transitions from H-1→L, H→L+1, H→L, H-1→L+1 are reported in Tables 2. 9 and 2. 10.

For the porphyrin systems, it is observed that the LUMO energy levels (L and L+1) are degenerate. Hence only two major transitions are reported as ΔE_1 and ΔE_2 , which are shown in Table 2. 9. The most intense peak observed in the excitation spectra which is contributed by ΔE_2 which is the transition from HOMO-1 to LUMO (LUMO+1) energy level. For all the porphyrin systems and metal porphyrin systems, the B band (Soret band) formation is due to the electronic transition from H-1 to L (or LUMO+1). For the porphyrin systems, a special splitting pattern of B bands were observed as a form of shoulder peaks with near oscillator strengths. These results indicate that the splitting of Soret band increases with the increase of π -conjugation in the macrocycle system. The molecular orbital energies and the energy gaps of Porphyrin and metal-Porphyrins are reported in Table 2. 9.

Table 2. 9: Molecular orbital energies and the energy gaps of Porphyrin tetrapyrroles and their metal containing analogues

Systems	ΔE_1	ΔE_2
Metal free	2.913	3.054
Be-Por	2.961	3.105
Mg-Por	2.919	3.060
Ca-Por	2.688	3.034
Sr-Por	2.577	3.014
Ba-Por	2.789	3.058
Zn-Por	2.942	3.075
Cd-Por	2.862	3.077

$\Delta E_1 = \text{HOMO-LUMO (in eV)}$,
 $\Delta E_2 = \text{HOMO-1-LUMO (in eV)}$

For the metal chlorin system, many bands are observed in the excitation spectra. Among these the B bands arise due to the transition energies ΔE_2 (H-1→L+1) or ΔE_4 (H→L+1), and Q bands arise due to ΔE_1 (H-1→L) and ΔE_3 (H→L).

For the bacteriochlorin complex, ΔE_4 transition (H→L+1), is regarded as the main configuration of B-bands and the ΔE_1 (H-1→L) and ΔE_3 (H→L) are

considered as the origin for Q bands. For all the tetrapyrrole systems, in addition to the B bands and Q bands, other bands of various oscillator strengths named, N and L bands are also observed in between the B and Q bands. The various molecular orbital energies and energy transitions of Chlorin and Bacteriochlorin are shown in Table 2. 10. The shoulder of B bands (B band splitting) is not prominent among Chlorin and Bacteriochlorin systems. The shoulders that are observed show less oscillator strength compared to B band oscillator strength.

Table 2. 10: Molecular orbital energies and the energy gaps of chlorin, bacteriochlorin tetrapyrroles and their metal containing analogues

Metal	ΔE_1	ΔE_2	ΔE_3	ΔE_4
Chlorin	2.881	3.411	2.668	3.199
Be-Ch	3.030	3.463	2.745	3.153
Mg-Ch	2.989	3.350	2.690	3.169
Ca-Ch	2.747	3.318	2.625	3.196
Sr-Ch	2.755	3.316	2.641	3.207
Ba-Ch	2.753	3.131	2.655	3.033
Zn-Ch	2.908	3.487	2.641	3.221
Cd-Ch	2.832	3.395	2.663	3.226
Bact-chlorin	2.795	4.082	2.221	3.508
Be-Bact	2.908	4.355	2.094	3.541
Mg-Bact	2.764	4.249	2.043	3.528
Ca-Bact	2.551	3.982	2.094	3.525
Sr-Bact	2.606	4.096	2.086	3.577
Ba-Bact	2.634	3.061	2.116	3.544
Zn-Bact	2.793	4.260	2.081	3.547
Cd-Bact	2.725	4.167	2.122	3.563

$$\Delta E_1 = \text{HOMO-1} - \text{LUMO (in eV)}, \Delta E_2 = \text{HOMO-1} - \text{LUMO+1 (in eV)}$$

$$\Delta E_3 = \text{HOMO} - \text{LUMO (in eV)}, \Delta E_4 = \text{HOMO} - \text{LUMO+1 (in eV)}$$

The TD-DFT formalism at B3LYP level is employed to calculate the electronic absorption spectra of the whole set of metal porphyrin, chlorin and bacteriochlorin complexes. The molecular orbital calculations are used to interpret the electronic spectroscopic properties and the electronic spectral data are shown in the Table 2. 11. The B and Q bands of all metal free and metal

incorporated tetrapyrroles are also reported in the Table 2. 11. Significant changes in the intensity of absorption bands can be observed for all the tetrapyrrole systems.

Table 2. 11: UV spectra of metal free and metal encapsulated tetrapyrroles. The corresponding oscillator strength (f) and Band names (Q, B) are mentioned for the excitation energies (E)

System	M-Porphyrin			M-Chlorin			M-Bacteriochlorin		
	E eV (eV)	Osc. Str. (f)	Band	E (eV)	Osc. Str. (f)	Band	E (eV)	Osc. Str. (f)	Band
No	2.299	0.0026	Q	2.291	0.0769	Q	2.128	0.2218	Q
metal	2.477	0.0005	Q	2.491	0.0041	Q	2.532	0.0415	Q
	3.886	0.7962	B	3.654	0.9892	B	3.805	1.0868	B
Be	2.454	0.0025	Q	2.354	0.0674	Q	2.022	0.2157	Q
	2.455	0.0025	Q	2.359	0.0675	Q	2.595	0.0394	Q
	3.586	0.9625	B	3.638	1.1046	B	3.808	0.9374	B
Mg	2.211	0.0015	Q	2.323	0.1084	Q	2.042	0.2660	Q
	2.378	0.0015	Q	2.454	0.0071	Q	2.473	0.0512	Q
	3.500	0.8943	B	3.503	0.4892	B	3.791	1.0582	B
Ca	2.246	0.0036	Q	2.291	0.0865	Q	2.077	0.2625	Q
	2.246	0.0036	Q	2.368	0.0155	Q	2.314	0.0716	Q
	3.354	0.7423	B	3.792	0.4012	B	3.773	1.0890	B
Sr	2.177	0.0071	Q	2.298	0.0848	Q	2.075	0.2577	Q
	2.177	0.0070	Q	2.370	0.0162	Q	2.321	0.0670	Q
	3.274	0.6673	B	3.454	0.5132	B	3.844	1.0860	B
Ba	2.303	0.0013	Q	2.308	0.0834	Q	2.370	0.0651	Q
	2.563	0.0019	Q	2.375	0.0167	Q	2.435	0.0016	Q
	3.456	0.5020	B	3.446	0.5686	B	3.709	0.7712	B
Zn	2.438	0.0016	Q	2.339	0.1077	Q	2.061	0.2598	Q
	2.439	0.0016	Q	2.475	0.0063	Q	2.501	0.0505	Q
	3.495	0.8914	B	3.514	0.6259	B	3.786	1.0141	B
Cd	2.357	0.0004	Q	2.338	0.0962	Q	2.094	0.2632	Q
	2.358	0.0004	Q	2.437	0.0115	Q	2.459	0.0605	Q
	3.437	0.8264	B	3.453	0.5372	B	3.783	1.0012	B

By making use of the exceptionally large π -electron delocalization properties and the absorption characteristics, these tetrapyrroles can be suitably used as molecular wires and optical nanosystems.

2.3.9. IR spectra of metal tetrapyrroles

The IR spectra of metal free porphyrin, chlorin and bacteriochlorin are evaluated using B3LYP/LANL2DZ method (Figure 2.4-Figure 2.6). For all the three metal free tetrapyrroles, a common medium IR band is observed in the region $3450\text{-}3550\text{ cm}^{-1}$ which is due to the N-H vibrations of pyrrole rings. For all the systems, the aromatic C-H stretching of pyrrole systems is reported in between $3200\text{-}3300\text{ cm}^{-1}$ range in which a slight variation in infrared intensity occurs. The IR bands reported in between $1500\text{-}1700\text{ cm}^{-1}$ is due to the stretching vibrations of C=C and C=N double bonds. The C-C and C-N single bonds in pyrrole rings vibrate in the $1000\text{-}1200\text{ cm}^{-1}$ region. The vinyl C-H in plane bend vibrations is observed in the $1400\text{-}1450\text{ cm}^{-1}$ region. The out of plane pyrrole C-H deformation vibrations were observed in between $650\text{-}900\text{ cm}^{-1}$ range in which the number of bands and the positions of the bands are dependent on the number of neighbouring hydrogen atoms in the pyrrole ring. For the metal tetrapyrrole systems, the bands in between $350\text{-}500\text{ cm}^{-1}$ are mainly due to the contribution of M-N vibrations (metal sensitive bands). This is interpreted as indicative of a significant degree of M \rightarrow L electronic transitions involving the lone pair of electrons on N and vacant orbitals on the M and is responsible for the M-N vibrations. The IR spectra of Porphyrin and Mg incorporated Porphyrin are shown in Figure 2.4.

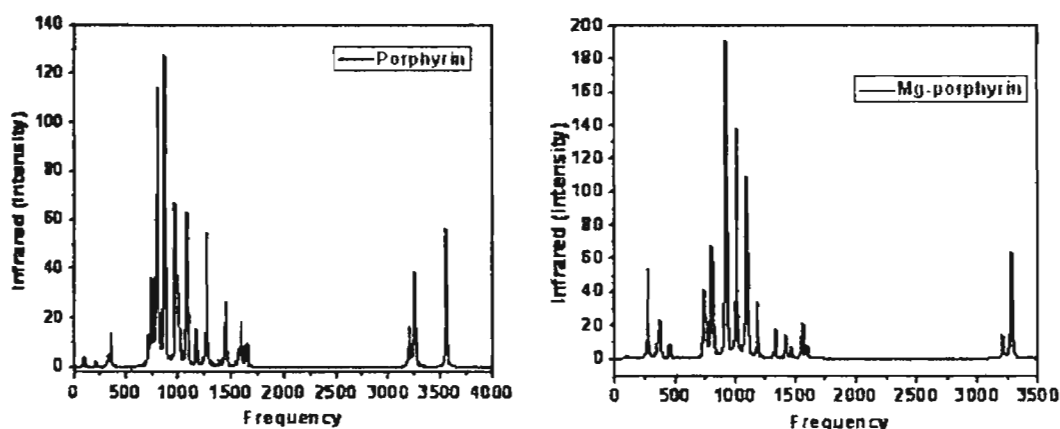


Figure 2.4: IR spectra of metal free Porphyrin and Mg-Porphyrin

The most important set of bands are the aromatic ring vibrations centered around $1500\text{-}1700\text{ cm}^{-1}$, which are found to appear as a pair of bands with some splitting. The IR spectra of free base chlorin and its Mg analogue are shown in Figure 2. 5. The vibrations in the range $3000\text{-}3100$ is observed due to the -C-H stretching of -CH_2 groups present in Chlorin and Bacteriochlorin. The CH -bending vibration of -CH_2 is observed in the $1400\text{-}1500\text{ cm}^{-1}$ range.

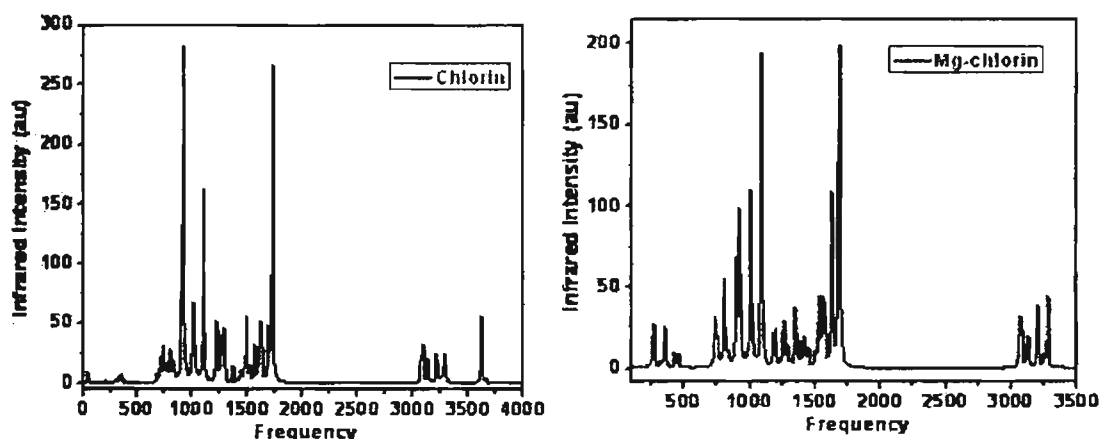


Figure 2. 5: IR spectra of metal free Chlorin and Mg-Chlorin

The vibrational frequency at $3500\text{-}3600\text{ cm}^{-1}$ of free base Chlorin and Bacteriochlorin represents the characteristic -NH stretching vibration of heterocyclic amine. IR spectra of metal free Bacteriochlorin and Mg-Bacteriochlorin complex are shown in Figure 2. 6.

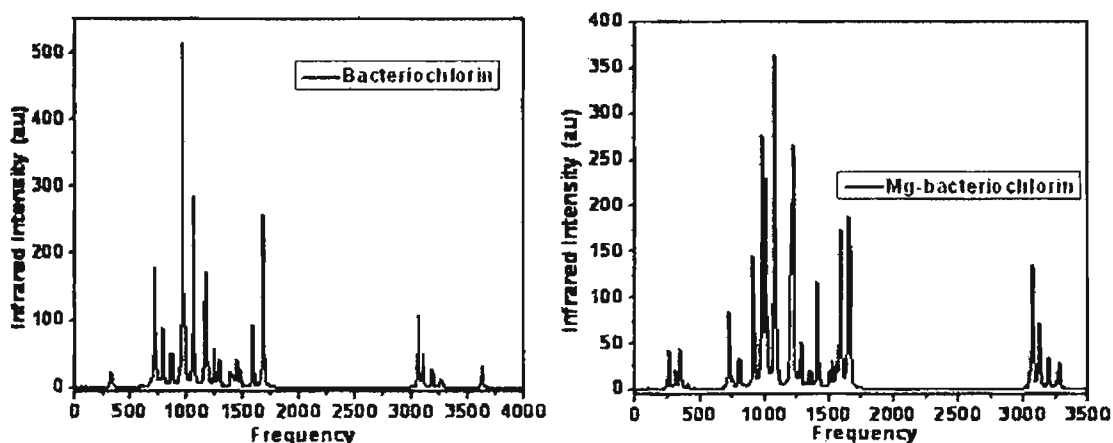


Figure 2. 6: IR spectra of metal free Bacteriochlorin and Mg-Bacteriochlorin

The vibrational bands observed between $3000\text{-}3150\text{ cm}^{-1}$ are exclusively indicative of unsaturation C=C-H groups. The IR spectra show all the vibrations

corresponding to the tetrapyrroles and their metallic analogues. Only Mg incorporated tetrapyrroles are shown in the figures.

2.3.10. Raman spectra of metal tetrapyrroles

The Raman spectra of metal free porphyrin, chlorin, bacteriochlorin and metal encapsulated tetrapyrroles are shown in the **Figure 2.7-Figure 2.9**. For all the tetrapyrrole systems a solet resonance band (B band) is observed below 500 cm^{-1} which is found to be a characteristic band of tetrapyrroles. This solet band is more intense in electronic spectra rather than in Raman spectra, which is already discussed earlier in the molecular orbital studies. The Raman peak of sp^3 hybridized carbons show a medium band in the range 1000-1300 cm^{-1} region which is otherwise known as D band. The bands in the range 1450-1700 cm^{-1} is observed in all the M-tetrapyrroles which is commonly considered as G bands that are characteristic of sp^2 hybridised carbon systems. The intense band in between 3200-3300 cm^{-1} is due to the aromatic -C-H vibrations. This most intense Raman peak arises due to the coupling of the phonons with peripheral ring current which gives rise to strong electron-phonon coupling and hence produce, an intense Raman band. The Raman spectra of metal free Porphyrin and Mg incorporated Porphyrin complexes are shown in **Figure 2.7**.

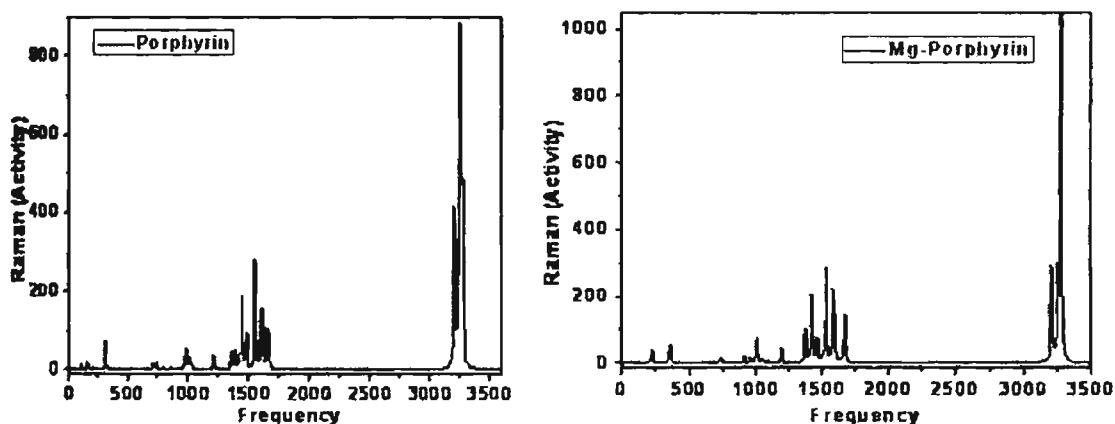


Figure 2.7: Raman spectra of metal free Porphyrin and Mg-Porphyrin

The well-pronounced band in the Raman spectrum is observed in the range 1450-1700 cm^{-1} and is associated with the planar deformation vibrations of porphyrin macrocycle. The Raman spectra of metal free Chlorin and Mg incorporated Chlorin complexes are shown in **Figure 2.8**.

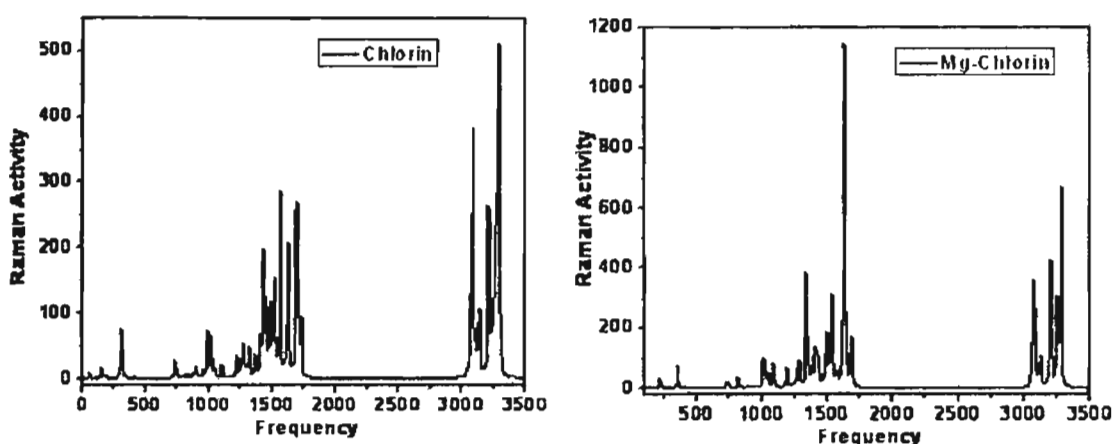


Figure 2. 8: Raman spectra of metal free Chlorin and Mg-Chlorin

The Raman spectra of free base Bacteriochlorin and Mg incorporated Bacteriochlorin complexes are shown in Figure 2. 9.

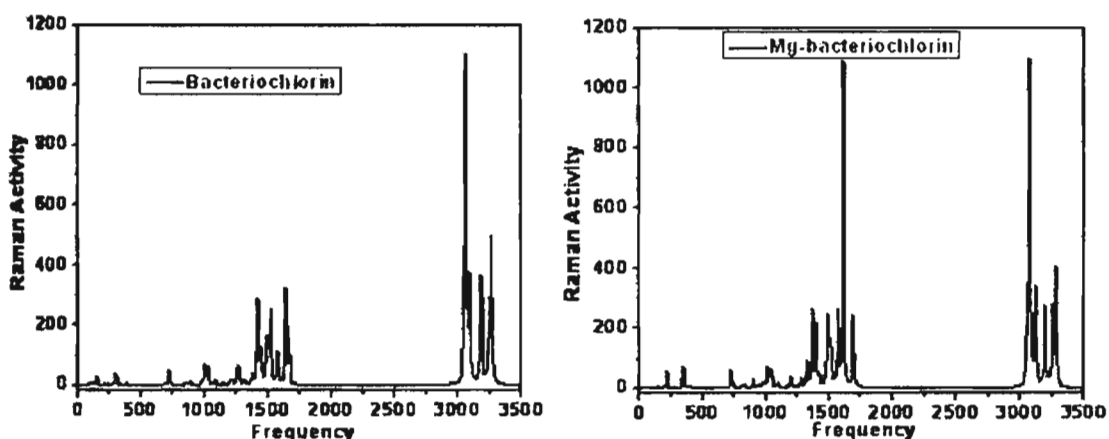


Figure 2. 9: Raman spectra of metal free bacteriochlorin and Mg-bacteriochlorin

The Raman spectra show all the vibrations corresponding to the tetrapyrroles and their metallic analogues. The intensity of Raman activity is found to vary with tetrapyrroles and metals. The spectroscopic study of all the metal tetrapyrroles was done. The IR and Raman spectra of Mg incorporated tetrapyrroles are shown in the figures, because the other metallic analogues also showed similar spectra.

2.4. Conclusions

The electronic structure, stability, aromaticity, several spectroscopic and NLO properties of the various tetrapyrroles and metal-encapsulated tetrapyrroles have been explored by first principle DFT and TD-DFT methods. The stability of the complexes are mainly explained based on the size of the

metal, bond order between metal and nitrogen, formation energy and the π -electron delocalization of the macrocycle. It is found that the higher formation energy and stronger aromatic character stabilize the complexes in the order, Be > Mg > Ca > Sr > Ba and Zn > Cd. Our calculations predict that among all the metals, Be binds strongly on Porphyrin, Chlorin and Bacteriochlorin as its size matches unambiguously with the pore size of the macrocycle. The computational findings suggest that the incorporation of metal moieties of +2-oxidation state into the tetrapyrrole system with careful consideration of steric and electronic factors can allow for significant enhancement of NLO properties in comparison with the metal free tetrapyrrole analogues. The absorption spectral studies are performed by making use of the TD-DFT methodology, that explains the Gouterman model, in which the HOMO, HOMO-1, LUMO and LUMO+1 are the major energy levels involved for the observed Q and B bands. Moreover, the Infrared and Raman spectra of the metal free and metal encapsulated tetrapyrroles have also been thoroughly analyzed in detail.

2.5. References

1. Petit L, Quartarolo A, Adamo C, Russo N, *J Phys Chem B*, 2006, **110**, 2398.
2. Parusel A B J, Ghosh A, *J Phys Chem A*, 2000, **104**, 2504.
3. Ghosh A, *J Phys Chem B*, 1997, **101**, 3290.
4. Muthiah C, Taniguchi M, Kim H J, Schmidt I, Kee H L, Holten D, Bocian D F, Lindsey J S, *Photochemistry and Photobiology*, 2007, **83**, 1513.
5. Misra R, Kumar R, Chandrashekar T K, Suresh C H, Nag A, Goswami D, *J Am Chem Soc*, 2006, **128**, 16083.
6. Gokulnath S, Prabhuraja V, Suresh C H, Chandrashekar T K, *Chem Asian J*, 2009, **4**, 861.
7. Liu Y, Guo X, Xiang N, Zhao B, Huang H, Li H, Shen P, Tan S, *J Mater Chem*, 2010, **20**, 1140.
8. Lee C Y, Hupp J T, *Langmuir*, 2010, **26**, 3760.
9. Velusamy M, Shen J Y, Lin J T, Lin Y C, Hsieh C C, Lai C H, Lai C W, Ho M L, Chen Y C, Chou P T, Hsiao J K, *Adv Funct Mater*, 2009, **19**, 1.
10. Yang Y J, Su Z M, *International J Quant Chem*, 2005, **103**, 54.
11. Fredj A B, Lakhdar Z B, Lopez M F R, *Chemical Phys Lett*, 2009, **472**, 243.
12. Kang Y, Chen H, Jeong Y J, Lai W, Bae E H, Shaik S, Nam W, *Chem Eur J*, 2009, **15**, 10039.

13. An W, Jiao Y, Dong C, Yang C, Inoue Y, Shuang S, *Dyes and Pigments*, 2009, **81**, 1.
14. Pushpan S K, Chandrashekar T K, *Pure Appl Chem*, 2002, **74**, 2045.
15. Poon C T, Chan P S, Manc C, Jiang F L, Wongb R N S, Mak N K, Kwong D W J, Tsao S W, Wonga W K, *J Inorg Biochem*, 2010, **104**, 62.
16. Rath H, Sankar J, Prabhuraja V, Chandrashekar T K, Joshi B S, *Org lett*, 2005, **7**, 5445.
17. Yurenev P V, Shcherbinin A V, Stepanov N F, *Russ J Phys Chem A*, 2010, **84**, 39.
18. Ohira S, Bredas J L, *J Mater Chem*, 2009, **19**, 7545.
19. Gouterman M, *J Chem Phys*, 1960, **33**, 1523.
20. Gouterman M, Wagniere G H, *J Molec Spectr*, 1963, **11**, 108.
21. Liao M S, Bonifassi P, Leszczynski J, Huang M J, *Molecular Phys*, 2008, **106**, 147.
22. Palummo M, Hogan C, Sottile F, Bagala P, Rubio A, *J Chem Phys*, 2009, **131**, 084102.
23. Gokulnath S, Chandrashekar T K, *J Chem Sci*, 2008, **120**, 137.
24. Yan L K, Pomogaeva A, Gu F L, Aoki Y, *Theor Chem Acc*, 2010, **125**, 511.
25. Kruk N N, *Journal of Appl Spectr*, 2008, **75**, 4.
26. Senge M O, Fazekas M, Notaras E G A, Blau W J, Zawadzka M, Locos O B, Mhuircheartaigh E M, *Adv Mater*, 2007, **19**, 2737.
27. Davis D, Sreekumar K, Pati S K, *Syn Met*, 2005, **155**, 384.
28. Datta A, Pati S K, Davis D, Sreekumar K, *J Phys Chem A*, 2005, **109**, 4112.
29. Gaussian 03 Revision B.05 Gaussian Inc Pittsburgh P A 2003.
Gaussian 03, Revision C.02, Frisch M J, Trucks G W, Schlegel H B, Scuseria G E, Robb M A, Cheeseman J R, Montgomery J A, Vreven T, Kudin K N, Burant J C, Millam J M, Iyengar S S, Tomasi J, Barone V, Mennucci B, Cossi M, Scalmani G, Rega N, Petersson G A, Nakatsuji H, Hada M, Ehara M, Toyota K, Fukuda R, Hasegawa J, Ishida M, Nakajima T, Honda Y, Kitao O, Nakai H, Klene M, Li X, Knox J E, Hratchian H P, Cross J B, Bakken V, Adamo C, Jaramillo J, Gomperts R, Stratmann R E, Yazyev O, Austin A J, Cammi R, Pomelli C, Ochterski J W, Ayala P Y, Morokuma K, Voth G A, Salvador P, Dannenberg J J, Zakrzewski V G, Dapprich S, Daniels A D, Strain M C, Farkas O, Malick D K, Rabuck A D, Raghavachari K, Foresman J B, Ortiz J V, Cui Q, Baboul A G, Clifford S, Cioslowski J, Stefanov B B, Liu G, Liashenko

- A, Piskorz P, Komaromi I, Martin R L, Fox D J, Keith T, Al-Laham M A, Peng C Y, Nanayakkara A, Challacombe M, Gill P M W, Johnson B, Chen W, Wong M W, Gonzalez C, Pople J A, Gaussian, Inc., Wallingford CT, 2004.
30. Becke A D, *J Chem Phys*, 1993, **98**, 5648.
 31. Hehre W J, Radom L, Schleyer P V R, Pople J A, *Ab Initio Molecular Orbital Theory*, Wiley, 1986, New York.
 32. Check C E, Faust T O, Bailey J M, Wright B J, Gilbert T M, Sunderlin L S, *J Phys Chem A*, 2001, **105**, 8111.
 33. Yang Y, Weaver M N, Merz K M Jr, *J Phys Chem A*, 2009, **113**, 9843.
 34. Hameka H, *Mol Phys*, 1958, **1**, 203.
 35. Wolinski K, Hilton J F, Pulay P, *J Am Chem Soc*, 1990, **112**, 8251.
 36. Schleyer P V R, Maerker C, Dransfield A, Jiao H, Hommes N J R E, *J Am Chem Soc*, 1996, **118**, 6317.
 37. Pal S, Manna A K, Pati S K, *J Chem Phys*, 2008, **129**, 204301.
 38. Bishop D M, *Adv Chem Phys*, 1998, **104**, 1.
 39. Ouder J L, Chemla D S, *J Chem Phys*, 1977, **66**, 2664.
 40. Ouder J L, Zyss J, *Phys Rev A*, 1982, **26**, 2016.
 41. Simpson G J, *Chem Phys Chem*, 2004, **5**, 1301.

Chapter 3

NONLINEAR OPTICAL PROPERTIES OF ORGANIC MOLECULES: THEORETICAL INVESTIGATIONS**3.1. Introduction**

In recent years there has been a growing interest in nonlinear optical properties of molecules. Conjugated organic molecules have a lot of potential to be used as good nonlinear optical materials¹. These molecules have delocalized π -electrons over a large length scale of the molecule, which can be very easily manipulated by substitution of electron donating (push) and electron withdrawing (pull) groups around the aromatic moieties². Apart from structural flexibility, which allows fine-tuning of chemical structures for the desired nonlinear optical properties, organic materials are of great technological interest because of their low cost, ease of fabrication, and integration into devices³. For a molecule to show nonlinear optical properties, the basic requirements are polarizability (electrons need to be greatly perturbed from their equilibrium positions), asymmetric charge distribution (incorporation of donor and acceptor molecules) and acentric crystal packing⁴. On a molecular level, the parameters that can be changed are the relative electron affinities of the donor and acceptor groups and the length and nature of the conjugated segment connecting the donor to the acceptor⁵. The π -conjugated organic molecules comprise one of the most promising materials at the molecular scale because of the delocalized π -electrons over a large area of the molecule that allows easy polarization due to shining of light⁶. Devices made up of these materials find a large number of applications in various disciplines, from lasers to optical switches and electronics. Theory can play a leading role in finding suitable NLO materials if a reliable and efficient approach is adopted.

3.2. Theoretical background

Nonlinear optics deals with the interaction of electromagnetic fields in various media to produce new fields altered in phase, frequency, amplitude or other propagation characteristics from the incident fields. When a beam of light

is impinged on a molecule it causes the charges of the atom to oscillate. In a linear molecule the amount of charge displacement is proportional to the instantaneous magnitude of the electric field. The charges oscillate at the same frequency as the frequency of the incident light. The oscillating charges either radiate light at that frequency or the energy is transferred into non-radiative modes that result in material heating or other energy transfer mechanisms. With small fields the displacement of charge from the equilibrium position, polarization (P), will be proportional to the applied field E.

$$\text{Polarization, } P = \alpha E \quad (1)$$

where, α -is the linear polarizability

In a nonlinear optical material, the displacement of charge from its equilibrium value is a nonlinear function of the electric field. All materials when exposed to laser light, i.e. very high intensity electric field, its polarizability can be drawn beyond a linear regime⁷⁻⁸.

$$\text{Nonlinear polarization, } P = P_0 + \chi^{(1)}E + \chi^{(2)}E^2 + \chi^{(3)}E^3 + \dots \quad (2)$$

Response properties of molecular system in general involves energy derivatives namely, polarizabilities and hyperpolarizabilities. To understand the nonlinear optical properties, the polarizability and hyperpolarizability of the chromophores are calculated. The electronic polarizability is defined as the ratio of the induced dipole moment of a system to the applied electric field that produces the dipole moment. For systems where the electric field induced polarization is not constrained only to the direction of applied field, polarizability is a tensor of rank 2. Kleinman's symmetry relations allow us to simplify the calculations of the tumbling average of the polarizability from the tensors as follows⁹

$$\alpha = \frac{1}{3}(\alpha_{xx} + \alpha_{yy} + \alpha_{zz}) \quad (3)$$

The first hyperpolarizability (β) is the second order electric susceptibility of the system which is a 3rd rank tensor, it has 27 tensor components. But in the general case of a molecule with no symmetry, these 27 elements are reduced to 10 according to Kleinman symmetry for second harmonic generation $\beta(2\omega; \omega, \omega)$. Due to independent interchange of Cartesian coordinates, $\beta_{ijk} = \beta_{ikj}$. These irreducible 10 tensor components are $\beta_{xxx}, \beta_{xyy}, \beta_{yyy}, \beta_{yyy}, \beta_{xxz}, \beta_{yyz}, \beta_{yyz}, \beta_{zzz}, \beta_{zzz}$ and β_{zzz} . By taking the tensor product of these 10 tensor components,

orientationally averaged hyperpolarizabilities can be calculated from the equations given below¹⁰⁻¹³

$$\beta_{\text{vec}}(-2\omega; \omega, \omega) = \sqrt{\beta_x^2 + \beta_y^2 + \beta_z^2} \quad (4)$$

$$\text{where } \beta_i = \sum_{j=x,y,z} \frac{\beta_{ij} + \beta_{ji} + \beta_{ii}}{3} \quad ; \quad i = x, y, z \quad (5)$$

Ouder and Chemla established a link between β and the details of a low-lying charge-transfer transition through the two-level model. NLO properties of organic charge transfer complexes like D- π -A can be captured very nicely by this model¹⁴⁻¹⁵. This model assumes that the electronic properties of the molecules are determined by the ground state and a low energy charge transfer excited state. Polarization results primarily from the mixing of charge transfer state with the ground state through the interaction of the molecule with the electric field. The Sum Over States (SOS) formalism lies within the limit of two level model, when the contribution from higher excited states are negligible compared to the first excited state¹⁶. From the two-level model, using electric dipole approximation, the second harmonic generation response (SHG) can be written as¹⁴

$$\beta_{\text{two-level}} = \frac{3e^2}{2\hbar} \frac{\omega_{12} f \Delta\mu}{(\omega_{12}^2 - \omega^2)(\omega_{12}^2 - 4\omega^2)} \quad (6)$$

where $\eta\omega_{12}$ is the excitation energy, f is the oscillator strength, $\Delta\mu$ is the difference between the dipole moments of the ground and the excited state, and ω specifies the excitation frequency of the oscillating electric field. The most important factor in the above simple expression is that the SHG coefficient is directly proportional to the oscillator strength and the dipole moment difference and is inversely proportional to the optical gap. Thus, any phenomenon that decreases the gap or increases the dipole moment difference between the ground and the excited state or increases the oscillator strength will enhance β ¹⁷⁻¹⁹.

3. 3. THEORETICAL STUDIES OF NLO PROPERTIES OF CONJUGATED-BICHROMOPHORES WITH ALKYL SPACER

NLO chromophores are molecules with electron donor and acceptor conjugated π -systems²⁰. A molecular design often used to make molecules with large β values is *D- π -conjugation-A*. A molecular unit involving π -conjugation is connected to an electron donor, D, at one end and to an electron acceptor group, A, at the other end. The donor-acceptor systems show charge transfer between electron donating and electron withdrawing groups.

Derivatives of azo benzene compounds containing donor-acceptor groups have been widely used as NLO chromophores in polymeric systems²¹⁻²². The synthesis of these compounds can be easily accomplished by a diazo coupling reaction. Diazo coupling reaction is the first reported reaction for the synthesis of azo benzene compounds and it is the single most used reaction for the synthesis of azo dyes till date. This electrophilic substitution reaction leads to regioselectivity and usually a high yield of the product. The reaction involves coupling between a diazotized aromatic amine and a coupling component such as phenol, naphthols, aromatic amines and active methylene compounds²³. The regioselectivity of diazo coupling reaction leads to the preferential formation of the para isomers. There are two geometrical isomers known for azobenzene derivatives named cis and trans. Among these conformers the trans form is more stable²⁴.

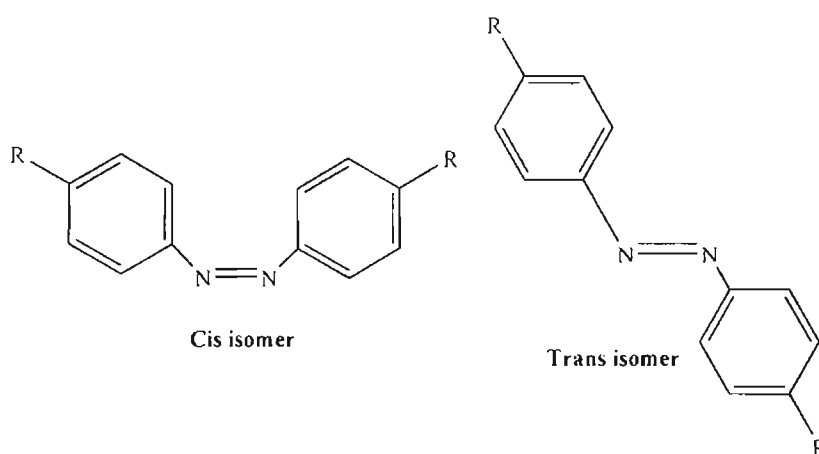


Figure 3. 1: Cis and Trans forms of azo benzene system

In the present studies extensive calculations on donor-acceptor systems have been performed and studied the role of the bridge for the charge transfer as

well as second harmonic generation efficiency of the donor-acceptor groups. The bridge energetics have been found to influence the strength of the donor acceptor coupling because of strong mixing between donor and acceptor and bridge orbitals²⁵. In this chapter, the bichromophoric molecules selected having two azobenzene based mesogens linked with a methylene spacer have been studied and their SHG efficiencies were investigated. The bifunctional azo chromophores selected for the study were bis(4-hydroxy phenylazo)-2, 2'-dinitrodiphenyl methane²⁶ and bis (8-hydroxy quinolinazo) -2, 2'-dinitrodiphenyl methane, shown in **Figure 3. 2**. The introduction of strong electron donors and acceptors in the 4 and 4' positions of many of the typical mesogens, like azobenzene, stilbene, biphenyl etc., makes them potential candidates for observation of NLO activity.

The chapter deals with the results of DFT and semiempirical calculations on the bichromophoric and chromophoric π -conjugated systems. The calculations were performed for evaluating the structural and nonlinear optical characteristics. Apart from the structural and electronic properties, the polarizability, and hyperpolarizability properties were investigated. The chromophore and bichromophore systems under consideration consist of -OH as donor and -NO₂ as acceptor with π -conjugation. Significantly high value of the first-order NLO coefficient has been observed in the case of bichromophoric molecules bridged by a methylene spacer.

The theoretical analysis begins with the optimization of the four azo systems. It is followed by studying the molecular orbital properties like the highest occupied molecular orbital (HOMO) energies, lowest unoccupied molecular orbital (LUMO) energies and HOMO-LUMO gap. Discussion of the optical properties like oscillator strength, optical gap, polarizability and hyperpolarizability parameters follows. The calculation of the nonlinear optical properties of the chromophores is done by using the established ZINDO/CV quantum chemical formalism.

3.3.1. Methodology

The calculation begins by optimizing the geometries of the D- π -A chromophores and D- π -A---A- π -D systems using the density functional theory available in the Gaussian-03 set of codes²⁷. For the optimization, electron correlation was included using the Becke's three parameter hybrid method and

the Lee–Yang–Parr correlation functional (B3LYP) at the 6-31G basis set²⁸. The B3LYP has been known in literature for being quite efficient in terms of accuracy and computational time²⁹. However, for large systems, the accurate determination of the excitation characteristics for dynamic spectroscopic applications still relies on semiempirical methods with configuration interaction. The geometry optimized structures were used for configuration interaction (CI) calculations to obtain energies and the dipole moments in the CI basis using the Zerner's Intermediate Neglect of Differential Overlap (ZINDO) method. The CI approach adopted here has been extensively used in earlier works, and was found to provide excitation energies and dipole matrix elements in good agreement with experiments⁶. Reference determinants which are dominant in the description of the ground state and the lowest one-photon excited state were chosen. For the Hartree-Fock determinant, varying number of occupied and unoccupied molecular orbital has been used to construct the SCI space until a proper convergence is obtained. The singles CI (CIS) was used, because the first nonlinear optical coefficients are derived from second-order perturbation theory involving one-electron excitations. For each reference determinant, 8 occupied and 8 unoccupied molecular orbitals were used to construct a CI space with configuration dimension of 65. To calculate NLO properties, the correction vector method was used which implicitly assumed all the excitations to be approximated by a correction vector^{18, 30}. For the calculation of the optical coefficients, an excitation frequency of 1064nm (1.17eV) which corresponded to the frequency of the Nd-YAG laser was used. Given the Hamiltonian matrix, the ground state wave function, and the dipole matrix, all in CI basis, it is straightforward to compute the dynamic nonlinear optic coefficients using either the first-order or the second-order correction vectors. Details of this method have been published in a number of papers^{14, 31-33}.

The geometry optimization and the calculation of nonlinear optical properties were done by using the above mentioned computational procedures. For the structure optimizations, two bichromophores (D- π -A---A- π -D) were used with methyl spacer and the corresponding cis and trans forms of D- π -A systems with -OH and -NO₂ as donor and acceptor. From the energy minimization, the stable trans geometry was used for further property studies. The azo benzene derivatives, Azo1, Azo 2, Azo 3 and Azo 4 were considered for the detailed property calculations. The trans D- π -A system was found to be planar due to the

strong π -electron delocalization. The bichromophoric systems (D- π -A---A- π -D) separated by alkyl bridge possessed an angle of 115° for azo 1 and azo 3 systems with the corresponding two dipoles. In azo 1 and azo 3 systems, the dipolar planes were found to be perpendicular with each other.

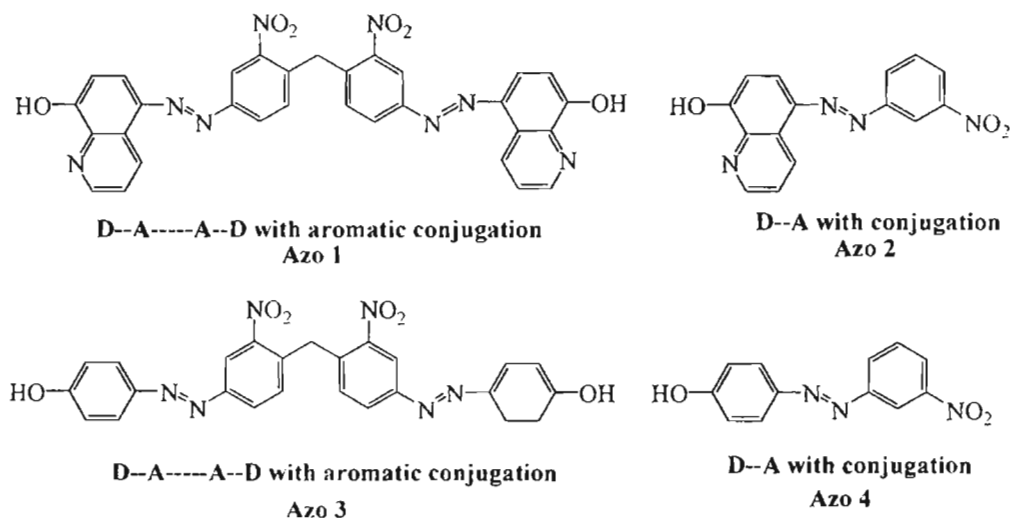


Figure 3. 2: The chromophores and bichromophores used for NLO study

To obtain large SHG efficiency, at the molecular level, the molecule must possess a) excited states close in energy to the ground state, b) large oscillator strength for electronic transitions from ground to optically excited state and c) a large difference between ground and excited state dipole moments. Such requirements are best met by the highly polarizable donor- π -acceptor (D- π -A) system, showing charge transfer between electron donating and electron withdrawing groups²⁶. The HOMO-LUMO gap in the molecular orbital picture plays a vital role in the charge transfer. If the gap is so small, it is very easy for the charge transfer to occur. Thus, the HOMO largely dictates the source of charge transfer and the details of the molecular LUMO govern the acceptor portion of the excitation. The energies of HOMO and LUMO and HOMO-LUMO gap are determined by making use of Density Functional Theory and the values are reported in **Table 3. 1** and the Molecular orbitals are shown in **Figure 3. 3**. Based on the corresponding HOMO- LUMO gaps, several important conclusions about the molecular orbital characteristics can be drawn. The characteristic energies are often referred to as ionization potential (IP) and electron affinity (EA). According to Koopman's theorem, the ionization potential is approximately determined as minus the HOMO energy and electron affinity is

minus the LUMO energy. The absolute hardness (η) is equal to half the difference between IP and EA, and chemical potential (μ) is half the sum of IP and EA. The global electrophilicity index (ω) was calculated using the chemical potential (μ) and the chemical hardness (η) which is shown in the equation (7)³⁴⁻³⁵. These two latter parameters can be approximated in terms of the one-electron energies of the HOMO and the LUMO as in the equations.

$$\omega = \mu^2/2\eta \quad (7)$$

Table 3. 1: Reports the parameters such as energies of HOMO and LUMO, HOMO-LUMO energy gaps (ΔE), ionization potential (IP), electron affinity (EA), chemical potential (μ), absolute hardness (η) and electrophilicity index (ω) from the Density Functional Theory (B3LYP/6-31G basis set). All the energies are reported in au.

Chromophores	Azo 1	Azo 2	Azo 3	Azo 4
HOMO	-0.221	-0.225	-0.228	-0.234
LUMO	-0.113	-0.108	-0.109	-0.105
ΔE	0.108	0.117	0.120	0.129
IP	0.221	0.225	0.228	0.234
EA	0.113	0.108	0.109	0.105
μ	0.167	0.167	0.168	0.169
η	0.054	0.058	0.060	0.064
ω	0.259	0.238	0.237	0.223

It was observed that compared to the simple chromophores, the bichromophores possessed smaller HOMO- LUMO gap even if they carry an alkyl bridge in between the two D-A systems. The bridge energetics has been found to influence the strength of the donor-acceptor coupling because of strong mixing between donor and acceptor and bridge orbitals³⁶. The spacer group should serve as a tunneling barrier that allows electron transfer mediated by super exchange coupling. The alkyl chain is not an ideal spacer because of its molecular flexibility which is drawn as a synonym for related unsaturated molecular segments.

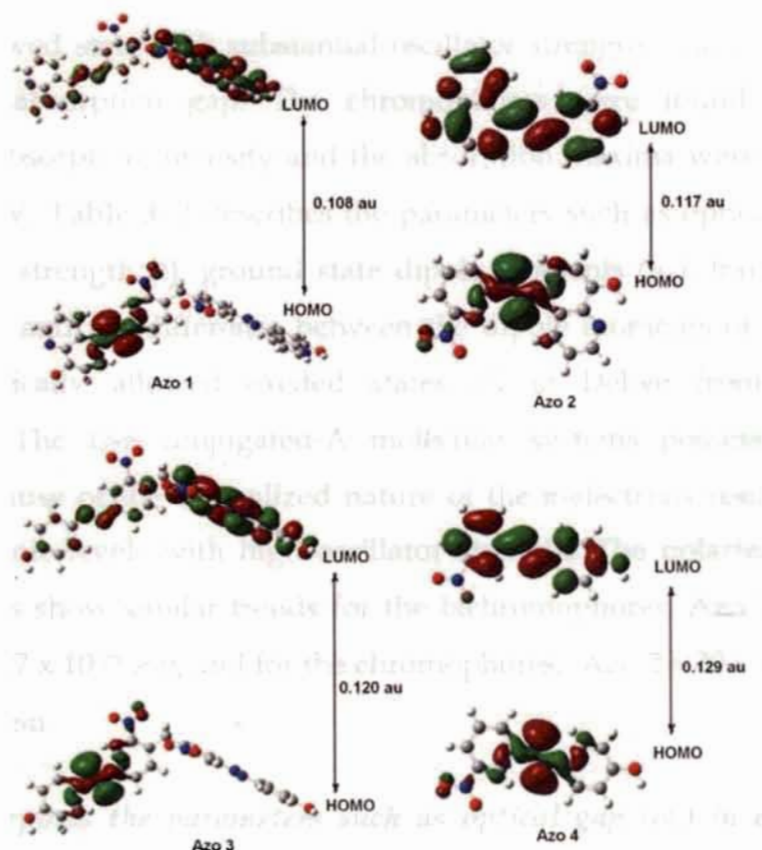


Figure 3. 3: The HOMO and LUMO and their energy differences for of Azo1, Azo 2, Azo 3 and Azo 4

The variation of the dipole moment difference between the ground state and the excited state (with large oscillator strength) was calculated by ZINDO/CI calculations. The excited state dipole moment shows the extent of charge transfer taking place after excitation by radiation of sufficient energy. If the difference between the ground and excited state dipole moments is large, the charge transfer is also large, provided the bond length remains unaltered upon excitation. Thus, any phenomena that decreases the band gap or increases the dipole moment difference between the ground and the excited state or increases the oscillator strength will enhance β . The dipole moment difference $\Delta\mu$ between the ground and excited state is the major contributing factor in determining the value of β vector^{37, 38}.

In quantum mechanics, oscillator strength is used as a measure of the relative strength of the electronic transitions within atomic and molecular systems. The easy charge transfer is determined by higher value of oscillator

strength and lower value of optical gap. The optical gap is calculated as the energy difference between the geometry relaxed ground state and the lowest optically allowed state with substantial oscillator strength. This corresponds to the vertical absorption gap. The chromophores were found to have an appreciable absorption intensity and the absorption maxima were found in the range of 3-4eV. **Table 3. 2** describes the parameters such as optical gap (δE) in eV, oscillator strength (f), ground state dipole moments (μ_g), transition dipole moments (μ_t) and the difference between the dipole moments of ground state and the optically allowed excited states all in Debye from ZINDO/CI calculations. The D- π conjugated-A molecular systems possess large NLO response because of the delocalized nature of the π -electrons resulting in low-energy excitonic levels with high oscillator strength. The polarizability of the chromophores show similar trends for the bichromophores, Azo 1 $\approx 25 \times 10^{-23}$ esu, Azo 3 $\approx 27 \times 10^{-23}$ esu, and for the chromophores, Azo 2 $\approx 20 \times 10^{-23}$ esu, Azo 4 $\approx 20 \times 10^{-23}$ esu.

Table 3. 2 Reports the parameters such as optical gap (δE) in eV, oscillator strength (f), ground state dipole moments (μ_g), transition dipole moments (μ_t), change in dipolemoment ($\Delta\mu$), the linear polarizability (α in 10^{-23} esu) and first hyperpolarizability (β in 10^{-30} esu), from the dynamic ZINDO/SOS calculation.

System	Azo 1	Azo 2	Azo 3	Azo 4
δE	3.920	3.792	3.818	3.816
f	1.437	0.900	1.839	0.887
μ_g	6.436	5.552	8.821	5.591
μ_t	9.826	7.903	11.260	7.822
$\Delta\mu$	3.390	2.351	2.438	2.231
α	25.932	20.069	27.440	19.951
β	17.929	15.954	17.828	15.541

As seen from **Table 3. 2**, the optical gap (δE) remains almost constant for all the chromophores. The significantly higher SHG efficiencies for the D- π -A---A- π -D systems imply that there is a less effective cancellation of dipoles, associated with the chromophores. However, the bichromophores with methyl spacer appear to crystallize in a noncentrosymmetric arrangement, and hence

exhibit significantly higher second harmonic generation efficiencies. Significantly high value of the SHG efficiencies was observed in the case of bichromophoric molecules, bridged by a methylene spacer.

The NLO properties of the chromophoric molecules were studied by using the semiempirical calculations (ZINDO/CV). From the Dynamic SOS calculation, it can be observed that the chromophores have good hyperpolarizability coefficient with high oscillator strength and low optical gap which can be used as good NLO active materials for polymer synthesis and for laser applications. The β values of bichromophores are comparable with the chromophores even if there is a presence of CH_2 unit being π -NLO inactive. It was found that the alkyl spacer connecting the donor to the acceptor moiety has a major effect in β value. The β has a strong dependence on the geometry of the system through the dipole moment difference between the ground state and the excited state. Determination of the ground and excited state dipole moment showed that the excited state has a high value for the dipole moment which indicated a higher degree of charge transfer from the donor to the acceptor groups on the excitation using light. It is found that the ground-state dipole moment and the hyperpolarizability are governed by the extent of π -electron delocalization, which in turn depends on the structural details of the molecules. Since charge transfer plays an important role in nonlinear optical process, the systems having more favourable features for a charge transfer give higher NLO coefficients. Hence the strength and the number of donors and acceptors, asymmetry and geometry of the systems and positions of the substituents play an important role in determining the NLO responses.

3.4. HYPERPOLARIZABILITY STUDIES OF SOME NONCONJUGATED TWIN DONOR-ACCEPTOR MOLECULES

In this section, a theoretical analysis of the nonlinear optical properties of twin donor acceptor systems is presented using the established ZINDO (SOS)/CV quantum chemical formalism. Even though, *ab initio*-CPHF computations are numerically more accurate and precise, the results are not easily amenable to chemical interpretation. Since they are based on derivative rather than SOS formalism, the interpretation of computed response is difficult, albeit of their accuracy in predicting trends. Also, in experimental measurements, electrons will go to the higher excited states and the higher level

contribution may not be too small to neglect. Almost all the semiempirical SOS procedures provide second order responses in reasonable agreement with experiments. Moreover, they permit a basic understanding of the origin of the NLO response in a chemical sense, by identifying the molecular excited states primarily responsible for an NLO response within the SOS formalism¹⁶.

Extensive theoretical calculation on the effects of spacer length enhancement on the second-order NLO properties of twin donor acceptor molecules having two amide units bridged by CH₂ spacers has been performed. The role of such aliphatic bridges on the Donor-Acceptor groups was computed by ZINDO/CV quantum chemical formalism. The odd-even effects were observed in twin donor acceptor systems (with two aliphatic units) linked by an alkyl spacer of varying length from $n=1$ to $n=12$. The system considered for the present study were N, N'-alkane-(1, n) diyl bis-4-hydroxy hexanamides. It was found that for an odd number of CH₂ spacers, the β value was an order of magnitude higher than that for the even number of CH₂ spacers. The origin for such oscillation is attributed to the similar oscillations in the dipole moment difference between the ground state and the dipole allowed state and to some extent on the variation in the oscillator strength.

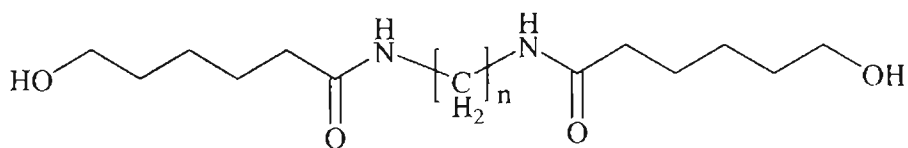
3.4.1. Methodology

All the geometries have been optimized using the AM1 parametrized Hamiltonian available in the Gaussian 03 set of codes²⁷. Some of the molecules (with smaller alkyl units) have already been synthesized in good yields and well characterized³⁹. The geometries obtained by the AM1 calculations have been compared with geometries obtained using the HF based methods for the smaller chromophore with $n=2$. It was found that the geometries obtained by the HF and AM1 methods have similar bond lengths and bond angles. Therefore, it is believed that the AM1 Hamiltonian is quite reliable for these systems and thus have proceeded with it for bigger systems with size up to $n=12$. These optimized geometries were used to compute the NLO properties using the Zerner's INDO method^{25, 26}. The level of CI calculations, were taken with singles (SCI) to obtain a reliable estimate of the second order optical response. The reference determinants have been chosen which are dominant in the description of the ground state and the lowest one-photon excited states. For each reference determinant, 8 occupied and 8 unoccupied molecular orbitals were used to

construct a CI space with configuration dimension of 900. To calculate NLO properties, the correction vector method was used, which implicitly assumes all the excitations to be approximated by a correction vector^{17, 19}. The CI approach adopted here has been extensively used in earlier works and was found to provide excitation energies and dipole matrix elements in good agreement with experiment. The polarizabilities were also computed using the sum-over-states (SOS) formalism, and values similar to those provided by the CV method were obtained³⁰⁻³³. All the calculations have been performed at a frequency of 1064nm (1.17 eV) corresponding to the Nd: YAG laser.

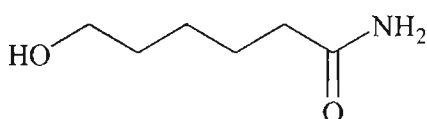
3. 4. 2. Twin D-A system for NLO study

The molecular systems considered for the NLO study were the amidodiols which were experimentally synthesized by the aminolysis of ϵ -Caprolactone by using the diamino alkanes⁴⁰.



Where $n=1$ to 12

**D--A-----A--D with aliphatic groups
(CD1 to CD12)**



D--A without conjugation (DA)

Figure 3. 4: Donor-acceptor systems studied

The electron acceptor groups and donor groups were attached to a non conjugated system and the donor-acceptor systems show charge transfer between electron donating and electron withdrawing groups and hence develop the polarization in the system. By designing the effective NLO chromophores (highly active chromophore molecules which have a large molecular hyperpolarizability β), which can be incorporated into a polymer chain either in the main chain or side chain by covalent linkages. The twin donor-acceptor

system(D-A--A-D) and single donor-acceptor system (D-A) selected for the NLO study are shown in the **Figure 3. 4**.

In this system we have tried to examine the dipole moment, polarizability, hyperpolarizability, oscillator strength and optical gaps of the twin donor acceptor systems by varying the number of alkyl groups between D-A and A-D chromophores. The change in dipole moment ($\Delta\mu$) (the difference in dipole moments between the ground state (μ_g) and the lowest energy dipole allowed state (μ_i)), oscillator strength (f), polarizability (α), hyperpolarizability (β), and the optical gap(δE) (the energy difference between the ground state and the lowest energy dipole allowed state) were calculated for the molecules of spacer length from $n=1$ to $n=12$. The corresponding values obtained by the dynamic SOS and Correction Vector method are shown in the **Table 3. 3**.

Table 3. 3: *The ground state dipole moment (μ_g in debye), the change in dipole moment ($\Delta\mu$ in debye), polarizability (α in 10^{-24} esu), hyperpolarizability (β in 10^{-32} esu), EFISH β ($\mu\beta$ in 10^{-32} esu), Oscillator strength (f), the optical gap (δE in eV) (the difference between the ground state and the lowest energy dipole allowed state) and the distance between the dipoles (d in Å)*

System	μ_g	$\Delta\mu$	α	β	$\mu\beta$	f	δE	d
CD1	12.016	8.859	18.626	76.720	903.272	0.255	6.729	2.361
CD2	3.491	1.054	18.111	3.293	6.267	0.519	6.619	3.732
CD3	12.311	8.917	17.778	89.102	1065.300	0.291	6.653	4.965
CD4	3.487	1.081	17.842	2.507	4.663	0.525	6.622	6.264
CD5	12.334	8.895	17.788	94.127	1134.672	0.298	6.628	7.534
CD6	3.479	1.112	18.211	2.342	6.869	0.530	6.622	8.814
CD7	12.343	8.895	18.499	95.840	1136.173	0.299	6.618	10.105
CD8	3.517	0.531	18.570	14.354	28.143	0.411	6.605	11.393
CD9	12.314	8.900	18.611	98.168	1142.608	0.293	6.614	12.666
CD10	3.523	0.220	18.583	16.109	30.510	0.274	6.610	13.962
CD11	12.308	8.927	18.623	99.083	1149.103	0.287	6.612	15.230
CD12	3.523	0.216	18.641	17.705	33.058	0.275	6.610	16.528
DA	7.3013	4.090	16.021	16.549	33.530	0.275	7.017	6.484

For the twin donor-acceptor system, the even chains have very little dipole moment (≈ 3 D) while the odd ones have much higher dipole moment (≈ 12 D). The dipole moment for the single D-A molecule, is calculated as, $\mu_G \approx 7.3$ D. For a perfect parallel arrangement of the dipoles, the classical non-interacting picture predicts the total dipole moment as twice the single D-A molecule value for parallel arrangement and 0 for a perfect anti-parallel arrangement. While, for the even spacers the dipole moments are nearer to zero, the odd-spacers show much smaller value from the classical result of twice the single D-A system value. Such a trend can be easily understood: for the even chains, the dipoles are staggered and almost perfectly anti-parallel, however, for the odd chains, even though the orientations are eclipsed, the dipoles are not exactly parallel because of the sp^3 hybridization along the alkyl principle axis¹⁹. The even chains have very little change in dipole moment ($\Delta\mu \approx 1$ D) while the odd ones have much higher change in dipole moment ($\Delta\mu \approx 8$ D). The change in dipole moment for the single D-A molecule, is calculated as, $\Delta\mu \approx 4$ D. Hence for the twin donor-acceptor system a strong odd even effect was observed in the case of dipole moments and change in dipole moments.

To understand the linear and nonlinear optical properties, the polarizability, α and first frequency dependent hyperpolarizability, β was calculated with varying chain lengths for the D-A---A-D systems. In the case of the twin donor-acceptor system the polarizability (α) value was found to be constant in all the odd-even series ($\approx 18 \times 10^{-24}$), while the single donor acceptor system possesses the polarizability value slightly lesser than the twin donor acceptor system. No odd-even effects were observed on the polarizability parameters of the twin donor acceptor systems. The hyperpolarizability factor shows similar trends as the dipole moment for D-A-(CH₂)_n-A-D system from $n=1$ to $n=12$. Odd numbered -CH₂- systems were found to be having high hyperpolarizability value ($76-100 \times 10^{-32}$ esu) and even numbered -CH₂- system possess low hyperpolarizability ($2-17 \times 10^{-32}$ esu). The D-A system with aliphatic groups is also having D-(CH₂)₅-A, an odd number spacer, it possesses a low value of β (16.5×10^{-32} esu) compared to the other odd numbered species. But it possesses a higher value than the even numbered species. The EFISH β values also show strong odd-even oscillation phenomena.

The oscillator strength shows remarkable features in which f increases for even numbered spacers and decreases for odd numbered spacers. A uniform increase is observed in the case of even numbered spacers and decrease is observed in the case of odd numbered spacers upto the spacer length of $n=8$. But after the spacer $n=8$ the odd-even oscillations were found to be not that much pronounced compared to the spacer less than eight. This indicates that the spacer above $n=8$ had little influence for the electronic transitions. Hence it was found that the charge transfer is predominant only upto spacer= 7 . The optical gap is calculated as the energy difference between the geometry relaxed ground state and the lowest optically allowed state with substantial oscillator strength¹³. The optical gap of the systems were found to be very high in a range of 6-7eV. A high optical gap was observed in the D-A system which prevented any coupling between donor and acceptor groups and resulted in the reduction of polarization effects.

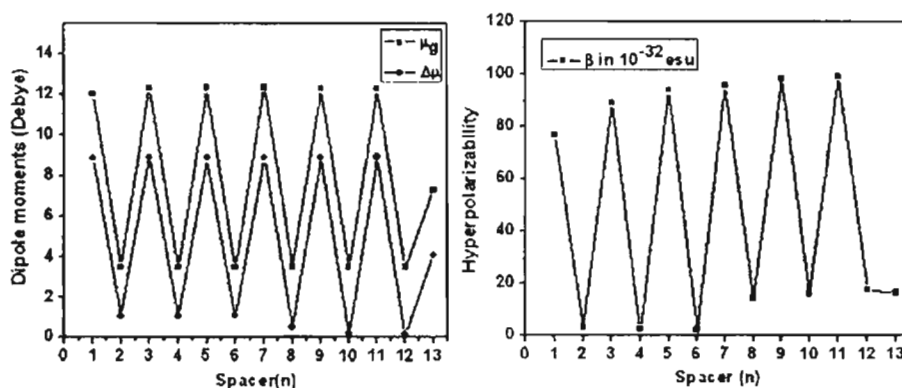


Figure 3. 5: Pictorial representation of odd-even effects observed in ground state dipole moment (μ_g in debye), the change in dipole moment ($\Delta\mu$ in debye) and hyperpolarizability (β in 10^{-32} esu)

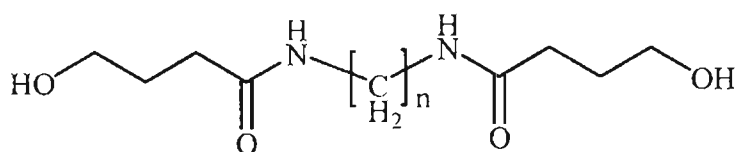
The distance between the dipoles increases as the number of alkyl units increases. The distance between the dipoles also exhibit an influence on the odd-even phenomena. The distance between the even dipoles is more than their odd counterparts as the even ones have a centrosymmetric arrangement which increases their interchromophoric distances¹⁹. For each even spacer distance, β is smaller and for each odd spacer distance β is larger.

It can be seen from **Table 3. 3**, the optical gap (δE) remains almost constant along the series and shows no such odd-even oscillations. In fact, the oscillator strength for the even chromophores is slightly larger than that for the

odd ones. Thus, the only factor that governs such an odd-even oscillation is $\Delta\mu$. **Figure 3. 5** shows the variation of $\Delta\mu$ with increase in the spacer length. One can clearly see the odd-even variation in $\Delta\mu$ similar to that observed for β . This suggests that the excited state polarization has a strong dependence on the interchromophoric arrangements¹⁷⁻¹⁹.

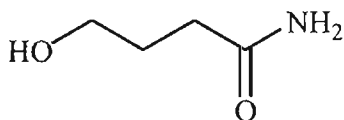
3. 5. ODD-EVEN EFFECTS IN TWIN DONOR-ACCEPTOR SYSTEMS FROM γ - BUTYROLACTONE

Similar trend was also observed for the twin donor-acceptor system obtained by the aminolysis of γ - Butyrolactone (**Figure 3. 6**)



Where $n=1$ to 12

**D--A-----A--D with aliphatic groups
(BD1 to BD12)**



D--A without conjugation (DA)

Figure 3. 6: Donor-acceptor systems from γ - Butyrolactone

We have examined the dipole moment, polarizability, hyperpolarizability, oscillator strength and optical gaps of the twin donor acceptor systems by varying the number of alkyl groups between D-A and A-D chromophores. The amidodiols from γ -Butyrolactone with $n=1$ to $n=12$ possess high μ_g , $\Delta\mu$ and β values for odd number of spacers as in the case of twin donor-acceptor molecule from ϵ -Caprolactone.

Semiempirical calculations were performed to understand the NLO efficiency of donor-acceptor systems with saturated spacers ($n=1$ to $n=12$) and the odd-even oscillation was observed. The NLO responses of the chromophores are mainly due to the electrostatic interaction on the strengths of the donor (D) and acceptor (A). For the saturated bridged molecules, electrons are localized at the respective sites and thus the electron transfer has a much shorter range.

Hence the hyperpolarizability of saturated D-A systems were found to be low compared to the conjugated NLO chromophores. The single D-A system behaves independent of each other, and there was no possibility for intermixing between the chromophores. It was observed that while the linear polarizability remained almost constant throughout the series, the ground state dipole moment, change in dipole moment, EFISH β and the first hyperpolarizability (β) showed strong odd-even oscillations. The hyperpolarizability value (β) showed an order of magnitude increase for odd spacers compared to the even spacers.

Table 3. 4: *The ground state dipole moment (μ_g in debye), the change in dipole moment ($\Delta\mu$ in debye), polarizability(α in 10^{-24} esu), hyperpolarizability(β in 10^{-32} esu), Oscillator strength (f) and the optical gap (δE in eV) (the difference between the ground state and the lowest energy dipole allowed state).*

System	μ_g	$\Delta\mu$	α	β	f	δE
BD1	14.896	10.856	18.826	96.720	0.5547	6.6826
BD2	3.654	1.054	18.165	10.2928	0.2194	6.6185
BD3	14.346	10.946	18.746	99.1017	0.5911	6.6532
BD4	3.346	1.081	18.842	11.5068	0.2249	6.6273
BD5	14.334	10.898	18.988	94.1268	0.5967	6.6259
BD6	3.418	1.112	18.211	11.3422	0.2356	6.6283
BD7	14.356	10.856	18.500	95.8396	0.5969	6.6295
BD8	3.518	1.577	18.670	12.3541	0.2111	6.6037
BD9	14.314	10.906	18.679	98.1683	0.5968	6.6149
BD10	3.623	1.268	18.788	12.8610	0.2739	6.6046
BD11	14.308	10.457	18.593	99.0828	0.5845	6.6193
BD12	3.598	1.257	18.645	13.7570	0.2746	6.6165
DA	6.368	3.186	17.624	19.5467	0.2893	6.8560

The significantly higher SHG efficiencies for the twin D-A systems of odd series implies that there is a less effective cancellation of dipoles associated with the chromophores of the odd numbered molecule compared to the even ones. In the even cases, the all trans arrangement of the alkyl spacer of the twin molecule will lead to conformers that possess a centre of symmetry, while in the odd cases

it could lead to structures which may possess a mirror plane. The odd and even spacer series separately shows the values to be almost constant with the increase of odd $-CH_2$ spacers and even $-CH_2$ spacers. The origin for such oscillation is attributed to the similar oscillations in the ground state dipole moment, dipole moment difference between the ground state and the dipole allowed excited state and to some extent on the variation in the oscillator strength. This arises due to the change in the dipolar orientations between the staggered and eclipsed form for the even and odd chains, respectively. The more NLO activity (high β) was observed for odd spacers of amidodiols from γ - Butyrolactone than ϵ -caprolactone.

3. 5. THEORETICAL INVESTIGATION ON THE DIELS-ALDER REACTION OF FULGIDES WITH MALEIC ANHYDRIDE

Photochromic compounds have attracted much attention because of their potential ability for optical memory, photooptical switching and display devices. Among them fulgides, which were discovered by Stobbe et al are the most promising candidates for the applications because of their fatigue resistant and thermally irreversible photochromic performance⁴¹⁻⁴³. On exposure to ultra violet radiation they undergo a transformation to a highly coloured form which can be returned to the original, colourless form by irradiation with visible light⁴⁴.

The spectroscopic properties of fulgides obtained by the Stobbe condensation⁴¹ of acetone, acetophenone and benzophenone with diethyl succinate and the theoretical studies regarding their Diels-Alder reaction with maleic anhydride were conducted. The studies were performed using Density Functional Theory with B3LYP functional combined with the split valence 6-31G (d, p) basis set. In this study the probability of Diels-Alder reaction for the less hindered and more hindered fulgides and the possibility of conservation of orbital symmetry were analyzed. The B3LYP method is capable for the prediction of the geometrical parameters of the dienes taking part in the Diels-Alder reaction. The reactivity of the (4+2) reaction is explained on the basis of geometrical analysis, FMO theory, global properties and activation energy studies. The various structural and spectroscopic studies were carried out in order to predict the reactivity of fulgide systems.

In the present study, the feasibility of Diels-Alder reaction for the less hindered and more hindered fulgide systems (obtained by the Stobbe condensation of acetone, acetophenone and benzophenone with diethyl succinate) with maleic anhydride were analyzed using Density functional theory. The possibility of conservation of orbital symmetry and the stability of the products were also predicted. The results are explained on the basis of HOMO energy of dienes⁴⁵⁻⁴⁷, HOMO-LUMO gap between dienes and dienophile, the global properties of the reactants⁴⁸⁻⁵² and transition state energy levels. The Diels-Alder reaction depends on the interaction between the HOMO of diene and the LUMO of dienophile. According to FMO theory, Diels-Alder reaction rates should correlate with the HOMO (Diene)-LUMO (Dienophile) energy gap⁴⁵⁻⁴⁷. When the gap is small the charge transfer increases and a stronger diene-dienophile bond should form in the transition state. The stronger bond will stabilize the transition state and lead to a faster reaction. The global values for the dienes are also calculated on the basis of the molecular orbital theory using the B3LYP/6-31G (d, p) calculations. They are also efficient in predicting the reactivity in a chemical reaction. The main global properties under focus in the present study are the electrophilicity index (ω), chemical potential (μ) and chemical hardness (η) (nuclear response). Parr's electrophilicity index (ω) is the square of the chemical potential divided by twice the chemical hardness. High value of the chemical potential and electrophilicity indicates the high stability and low reactivity of the reactants. According to chemical hardness, the molecules which are soft, are found to be more reactive than hard molecules⁴⁸⁻⁵².

Chemical potential (μ) is the partial derivative of the energy of the system E with respect to the number of electrons N at the fixed external potential $v(r)$,

$$\mu = - (\partial E / \partial N)_{v(r)} \quad (8)$$

which characterizes the escaping tendency of electrons from equilibrium^{50, 53}.

The global chemical hardness (η) is the resistance of a system to change the electron distribution in a collection of nuclei and electrons^{50, 54}

$$\eta = 1/2 (\partial^2 E / \partial^2 N)_{v(r)} \quad (9)$$

Recently, Parr et al⁵⁵ proposed a new DFT concept called electrophilicity index ω , in terms of the above two global activity indices, μ and η ,

$$\omega = \mu^2/2\eta \quad (10)$$

which measures the capacity of an electrophile to accept the maximal number of electrons in the neighbouring reservoir of electron sea⁵⁶.

The fulgides (dienes) and dienophile considered for the study of Diels Alder reaction are given in the **Figure 3. 7**.

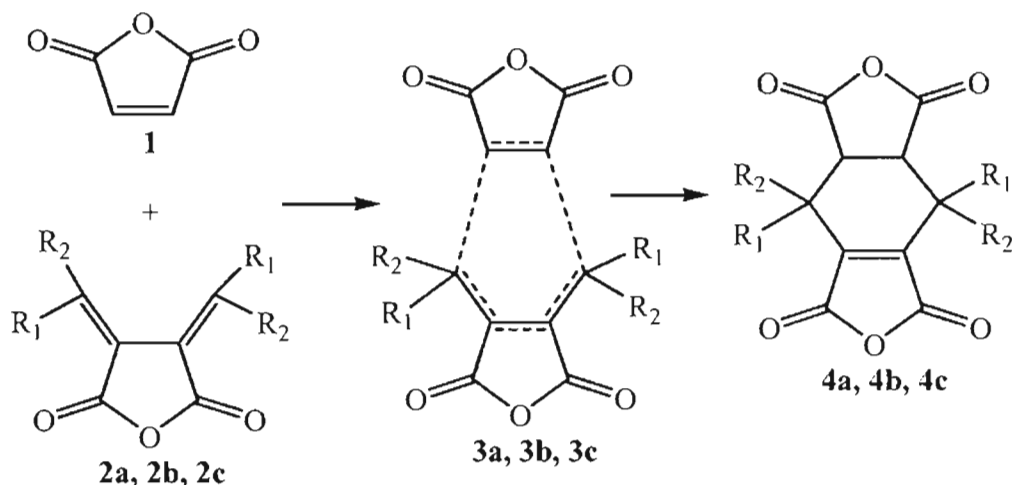


Figure 3. 7: Diels Alder reaction of fulgides 2a, 2b, 2c with maleic anhydride 1, transition states 3a, 3b, 3c and cyclic adducts 4a, 4b, 4c

R₁=R₂=CH₃ for 2a, 3a, 4a;

R₁=CH₃, R₂=C₆H₅ for 2b, 3b, 4b

R₁=R₂=C₆H₅ for 2c, 3c, 4c

The reactants are fulgides obtained from acetone (2a; R₁=R₂=CH₃), acetophenone (2b; R₁=CH₃, R₂=C₆H₅), benzophenone (2c; R₁=R₂=C₆H₅) as dienes and maleic anhydride (1) as dienophile. 3a, 3b, 3c are the corresponding transition states of the Diels-alder reaction. 4a, 4b, 4c are the corresponding cyclic adducts formed. In addition to these reactants, butadiene (diene) and maleic anhydride (dienophile) were also used as a reference to explain the reactivity.

3. 5. 1. Computational methods

The DFT methods are now mostly used for studying structures and reactivity of chemical systems instead of traditional Hartree-Fock calculations, which are more difficult to perform. All the calculations were performed with Gaussian 98⁵⁷ and 03²⁷ programmes. The visualization of the molecules was

done with Gauss View⁵⁸. In the present study the gradient corrected exchange and correlation functional Becke, Lee, Yang and Parr (B3LYP)²⁸ was used with the standard 6-31G (d, p) basis set. The geometrical and molecular orbital studies of the reactants have been done and their structures were completely optimized with the Bery analytical gradient optimization method. The global electrophilicity index was calculated by knowing the chemical potential and chemical hardness values. The chemical potential and chemical hardness are approximated in terms of the one electron energies of the highest occupied molecular orbital and lowest unoccupied molecular orbital. Static property calculations give the polarizability and hyperpolarizability of the fulgide molecules. All the optimized transition state structures have one and only one imaginary frequency whose motion is along the formation of the new C-C bonds.

The various geometrical parameters were studied by the DFT method. **Figure 3. 8** describes the optimized geometry of fulgide 1 (2a), which possesses a dihedral angle $\Phi=0$. This infers that the butadiene (C1=C2-C3=C4) skeleton in fulgide 1 shows planarity after energy minimization

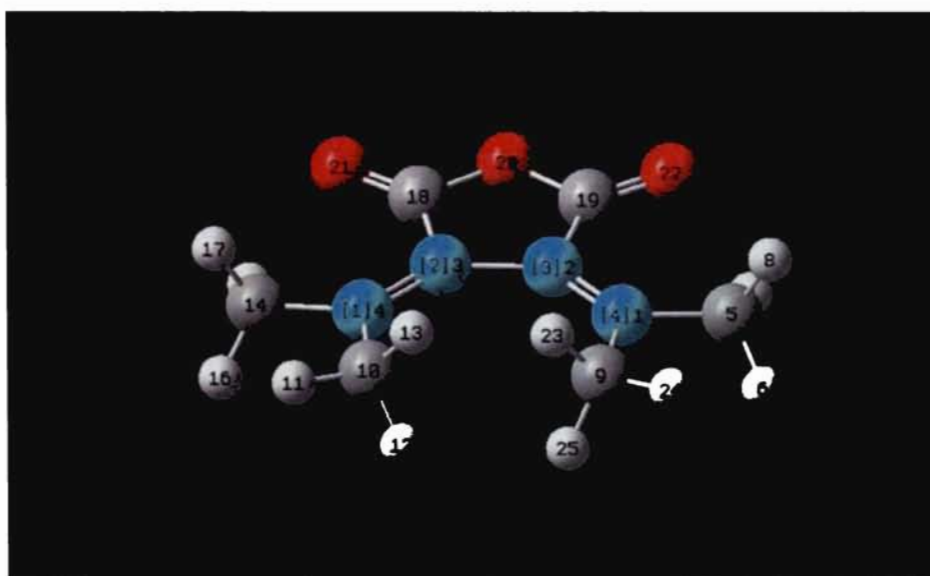
5/12
;

Figure 3. 8: Optimized structure of fulgide 1(2a)

In the case of fulgide 2(2b), the diene carbons lie in one plane, which confirms the planar characteristics of the acetophenone substituted dienes. The optimized geometry of 2b is shown in **Figure 3. 9**, which represents the dihedral angle $\Phi=0$ (C1=C2-C3=C4).

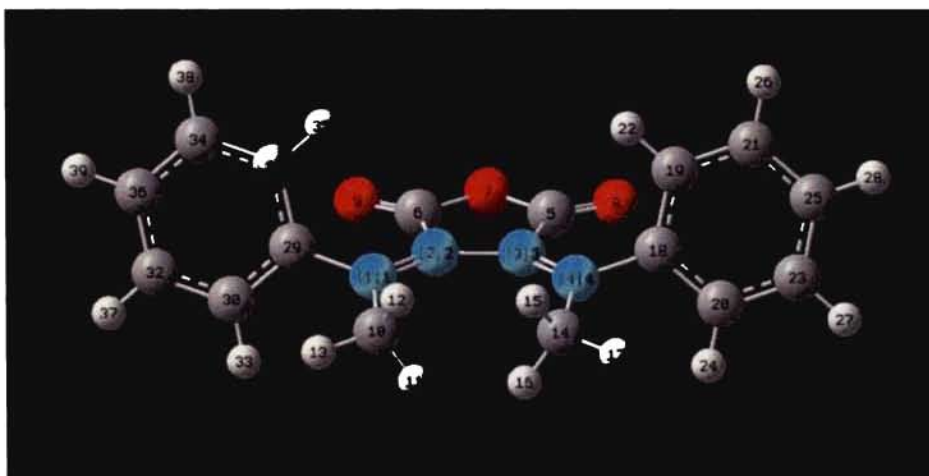


Figure 3. 9: The optimized geometry of fulgide 2 (2b), shows dihedral angle, C1-C2-C3-C4, $\Phi=0$

The optimized structure of fulgide 3 (2c) with benzophenone substitution is shown in **Figure 3. 10** which describes the nonplanar geometrical orientation of diene skeleton (C1=C2-C3=C4). The diene lost its planarity due to the steric hindrance of phenyl substitution. The dihedral angle of the diene is found to be $\Phi=40.67$. From the initial observation itself the 2c can be predicted to have less importance in Diels-Alder reaction. This is because the planarity of diene system is one of the prerequisites for Diels Alder cycloaddition.

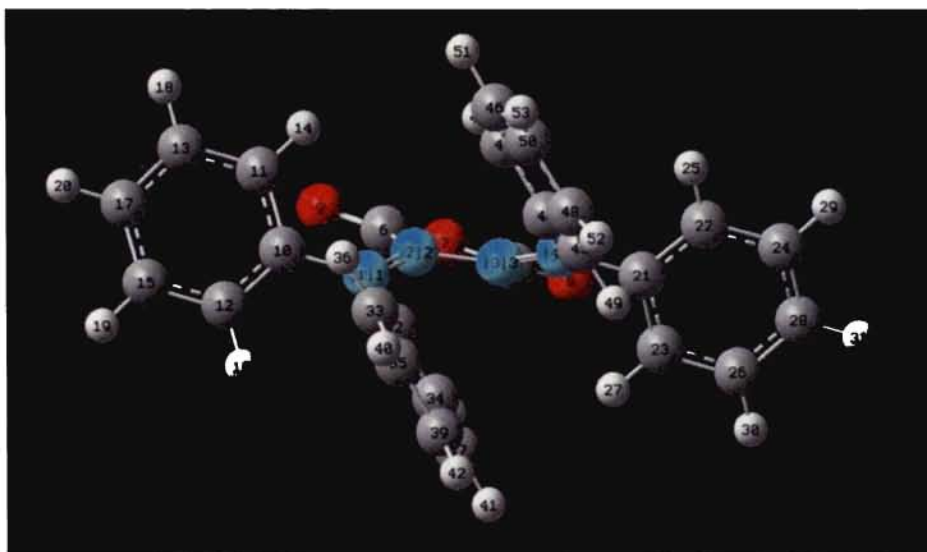


Figure 3. 10: The nonplanarity of fulgide (2c) due to steric hindrance

The static method was adopted for finding the polarizability and hyperpolarizability of dienes. The static polarizability and hyperpolarizability values are reported in the Table 3. 5 (au). The α and β values for fulgide shows an order of $2c > 2b > 2a$. But butadiene shows a very less α and β values compared to fulgides. The high β value for 2c is due to the structural distortions observed in the optimized geometry (nonplanarity). Butadiene possess zero dipole moment, hence exhibits a very low β value.

Table 3. 5: The polarizability (α) and hyperpolarizability (β) of dienes

Diene	α_{xx}	α_{yy}	α_{zz}	α	β
2a	150.557	63.283	140.385	118.075	98.099
2b	311.340	132.787	258.685	234.271	577.857
2c	358.458	159.736	340.946	286.380	1082.322
Butadiene	46.248	15.960	62.819	41.676	18.543

According to molecular orbital concept, the Diels alder reaction occurs by the effective interaction between the HOMO and LUMO of the reactants. The more predominant interaction is in between the HOMO of diene and the LUMO of dienophile⁴⁵⁻⁴⁷. Since maleic anhydride is the only dienophile used, the feasibility reaction will be fully concentrated on the properties of fulgides. As the LUMO of dienophile remains the same, we consider only the HOMO energy of the dienes.

Table 3. 6: HOMO energies (au), LUMO energies (au) for the dienophile (1), dienes (2a, 2b, 2c) B3LYP/6-31G (d, p) theoretical level

Reactant	HOMO (au)	LUMO (au)
1	-0.321	-0.147
2a	-0.238	-0.075
2b	-0.224	-0.085
2c	-0.209	-0.091
Butadiene	-0.229	-0.032

As the HOMO energy of diene increases, the HOMO will come more close to the LUMO of dienophile and the electronic excitation will become easier.

The HOMO and LUMO of the reactants are given in the **Table 3. 6**. Considering the molecular orbital calculations for **2a**, **2b** and **2c** it was found that HOMO of **2c** is more than **2b** and **2a**. HOMO of **2c** is -0.2091au which is more close to the LUMO energy of **1** with -0.1467au .

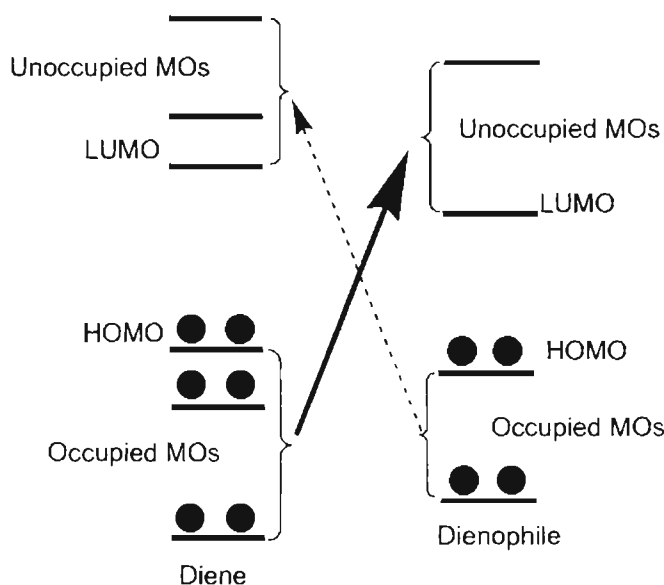


Figure 3. 11: Molecular orbital transition and possibility of electron transfer from HOMO of diene to LUMO of dienophile and from HOMO of dienophile to LUMO of diene. The predominant transition is bold lined

In quantum theory, changes in the electron density of a chemical system result from the mixing of suitable excited state wave functions with ground state wave functions. The mixing coefficient is inversely proportional to the excited energy between the ground and the excited state. A small HOMO-LUMO gap automatically indicates small excitation energies to the manifold of excited state⁵⁰.

The mechanism of the reaction could be explained with the molecular orbital diagram shown in **Figure 3. 11**. The FMO approach can be used to determine the relative reactivity of the dienes and which will help to select the best candidate material for the reaction. **Table 3. 7** list the HOMO energies of dienes, LUMO energies of dienophile together with the FMO gaps (eV). The Diels-Alder reaction occurs by the effective interaction between the HOMO and LUMO of the reactants⁴⁵⁻⁴⁷. By the symmetry conservation of molecular orbitals shown in the above **Figure 3.11** it becomes clear that the more predominant interaction is in between the HOMO of diene and the LUMO of dienophile,

rather than LUMO of diene and HOMO of dienophile. This is because the gap between the HOMO of diene and the LUMO of dienophile is smaller than the other. The electronic transition occurs more in the case of the smaller gap interaction. Here the gap between HOMO of **2a**, **2b**, **2c**, butadiene and LUMO of **1** were calculated

Table 3. 7: HOMO energies (au) of dienes (2a, 2b, 2c), LUMO energy (au) for the dienophile (1) and HOMO- LUMO gap (eV) for Diels Alder reaction at B3LYP/6-31G theoretical level

Dienes	HOMO of Diene (au)	LUMO of Dienophile(au)	HOMO-LUMO Gap (eV)
2a	-0.2381	-0.1467	2.4861
2b	-0.2244	-0.1467	2.1134
2c	-0.2091	-0.1467	1.6973
Butadiene	-0.2285	-0.1467	2.2250

For the formation of a stronger diene–dienophile bond in the transition state the HOMO-LUMO Gap must be smaller. The HOMO-LUMO Gap of the reactants obtained in **Table 3. 7** showed that the **2a** diene is having 2.4861 eV, **2b** having 2.1134 eV and **2c** having 1.6973 eV, in which the standard butadiene possess 2.2250 eV. It is clear from the data that the **2c** diene with lower HOMO-LUMO gap will more readily form the stronger bond with **1** than **2a** and **2b**. Shrinkage of the energy gap between HOMO and LUMO will strengthen the bonding interaction between these orbitals. The reaction goes on more readily when the energy difference between the two orbitals is small. But the **2c** molecule lost its planarity while doing energy minimization. Hence the concept of FMO is not enough to explain the reactivity of fulgides.

Global properties such as chemical hardness (η), chemical potential (μ) and electrophilicity index (ω) are also useful for understanding the behaviour of a chemical system⁵⁹. It is important that μ and η be put into a molecular orbital framework⁵⁰. The higher the FMO gap the greater will be the hardness. In terms of chemical reactivity it is concluded that soft molecules will be more reactive than hard molecules. A good electrophile is characterized by the high value of μ (chemical potential) and low value of η (chemical hardness). The good

electrophile will induce higher electrophilicity index and which possess higher reactivity⁴⁸⁻⁵². The evaluation of ionization potentials and electron affinities must be crucial for getting a reliable estimation of chemical potential, chemical hardness and electrophilicity index. These properties are quite sensitive to the exchange and correlation functional used in DFT calculations. The global properties are listed in **Table 3. 8**.

Table 3. 8: Global properties such as chemical potential (μ), chemical hardness (η) and electrophilicity index (ω) for the reactants 1, 2a, 2b, 2c at B3LYP/6-31G (d, p) basis set

Reactants	Global properties		
	μ (au)	η (au)	ω eV
1	0.2338	0.0871	8.5351
2a	0.1567	0.0814	4.1025
2b	0.1547	0.0698	4.6630
2c	0.1501	0.0591	5.1846
Butadiene	0.1301	0.0984	2.3394

In a Diels-Alder reaction, the dienophile is electrophilic and the diene is nucleophilic in nature. The μ value of **2c** is 0.1501au which is the lower value compared to **2b** and **2a** as shown in **Table 3. 8**. The chemical hardness η is found to be too small for **2c** which is about 0.0591 au where as **2a** having 0.0814 and **2b** having 0.0698 au. The electrophilicity index of the dienes shows that ω for **2c** is higher as 5.1846eV while for **2a** it is 4.1025eV and **2b** is 4.663eV. The global properties showed that fulgides from benzophenone **2c** is found to be a soft molecule with lower chemical potential. The molecular orbital properties failed to explain the nonplanarity of **2c** and showed contradictory results for Diels-Alder reaction. So it cannot be concluded, say the **2c** is more reactive than **2b** and **2a**.

Some contradictions in global properties were observed for the dienes. Hence the reactivity of the dienes were analysed by means of energetic studies. The activation energy studies were done on the reactant molecules and there existed single imaginary frequency for all the transition states studied. **Figure 3. 12** shows transition state of **2b** and **1**, with its displacement vector. Using

computational tools the exact saddle points of the reactants were found, thereby the activation energy for the reaction is predicted. The difference between the energy of the transition state compared to the energy of reactants is called the activation energy.

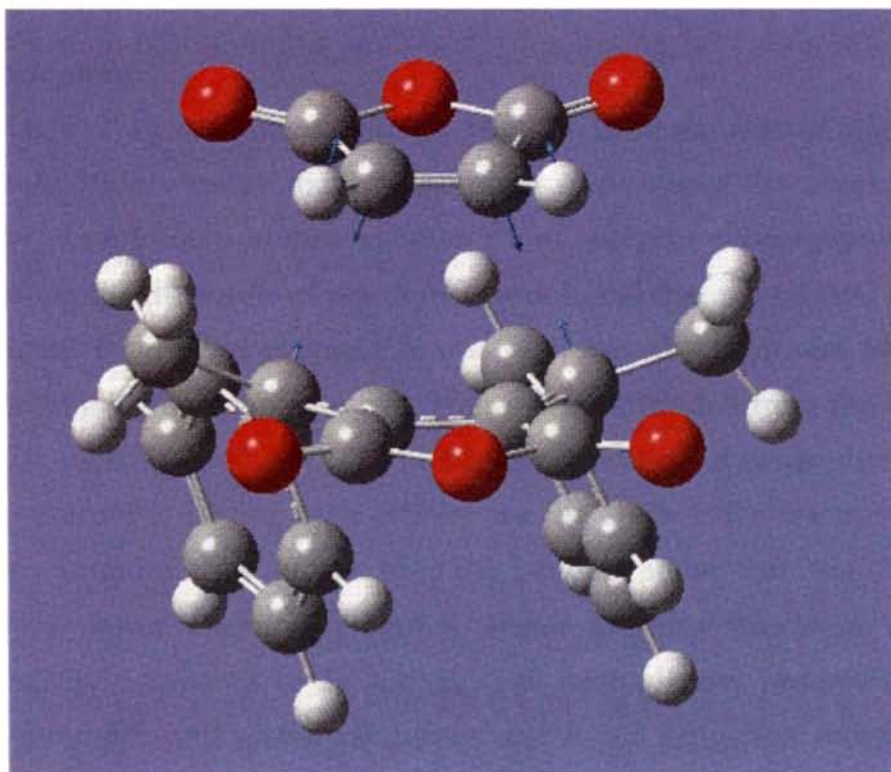


Figure 3. 12: Transition state of **2b** and **1** with displacement vector

The transition state for the Diels-Alder reaction of fulgides with maleic anhydride was located and the activation energies estimated. Each transition structure afforded only one imaginary frequency that corresponded to the formation of the new C-C bonds. The activation energies were estimated from the density functional theory with 6-31 G (d, p) calculation using Gaussian. The DFT computational results suggest that the ground state geometry of the diene moiety in **2c** is not planar. The computed dihedral angle C1-C2-C3-C4 in **2c** deviates from planarity by 40.67°. The geometric perturbation in **2c** associated with non planarity of the diene system will raise questions regarding the practicability of Diels-Alder reaction. The activation energy determined for **2a** system is 19.58 kcal/mol lower than that of **2b** with E_a 29.679 kcal/mol, whereas, the reference reactant butadiene possesses an E_a of 26.198 kcal/mol. There is no point in doing the transition state studies in **2c** due to the lack of planarity. The steric effects could be important and which prevent the

dienophile to approach the diene **2c**. Calculations indicate that the reaction of **2a** fulgide with maleic anhydride is more favourable than the **2b** due to the less hindrance in **2a**. The steric factor dominates on the selectivity of dienes in the DA reaction of fulgides. The activation energy factors negate the molecular orbital concepts (FMO).

3.6. Conclusions

The (4+2) cycloaddition reactions between three varieties of fulgides with maleic anhydride were studied. A thorough study about the conservation of symmetry of molecular orbitals, geometric and energetic properties were done. By analyzing the three sets of reactions it was found that the HOMO energy of fulgide diene from benzophenone **2c** was high and FMO gap was low for the corresponding diene-dienophile pair. Hence it is concluded from the FMO that the fulgide diene formed from the Stobbe condensation of benzophenone with diethyl succinate is having high affinity for the Diels-Alder reaction than the other two fulgides. The global property studies show that the **2c** fulgide possesses a lower chemical potential, lower chemical hardness and high electrophilicity compared to **2a** and **2b**. The contradictory observations were seen in geometric and global properties and hence activation energy studies were performed. From the transition state studies it is concluded that fulgide **2a** is much favoured against fulgide **2b**, with lower values of activation energy.

3.7. References

1. Tuuttila T, Lipsonen J, Huuskonen J, Rissanen K, *Dyes and Pigments* 2009, **80**, 34.
2. Tambe S M, Kittur A A, Inamdar S R, Mitchell G R, Kariduraganavar M Y, *Opt Mat*, 2008, **31**, 817.
3. Li N, Lu J, Xia X, Xu Q, Wang L, *Dyes and Pigments*, 2009, **80**, 73.
4. Yesoda S K, Pillai C K S, Tsutsumi N, *Prog Polym Sci*, 2004, **29**, 45.
5. Schmidt K, Barlow S, Leclercq A, Zojer E, Jang S, Marder S R, Jen A K Y, Bredas J L, *J Mater Chem*, 2007, **17**, 2944.
6. Datta A, Pati S K, *Journal of Molecular Structure, Theochem*, 2005, **756**, 97.
7. Gunter P, *Nonlinear Optical Effects and Materials*, 2000, **72**, 11.
8. Robert W, Boyd J, *Bioned Opt*, 2009, **14**, 29902.
9. Pal S, Manna A K, Pati S K, *J Chem Phys*, 2008, **129**, 204301.

10. Bishop D M, *Adv. Chem Phys*, 1998, **104**, 1.
11. Ouder J L, Chemla D S, *J Chem Phys*, 1977, **66**, 2664.
12. Ouder J L, Zyss J, *Phys Rev A*, 1982, **26**, 2016.
13. Simpson G J, *Chem Phys Chem*, 2004, **5**, 1301.
14. Pati S K, Marks T J, Ratner M A, *J Am Chem Soc*, 2001, **123**, 7287.
15. Bishop D M, *Adv Chem Phys*, 1998, **104**, 1.
16. Kanis D R, Ratner M A, Marks T J, *Chem Rev*, 1994, **94**, 195.
17. Dewar M J S, Zoebisch E G, Healy E F, Stewart J J P, *J Am Chem Soc*, 1985, **107**, 3902.
18. Datta A, Pati S K, *J Phys Chem A*, 2004, **108**, 320.
19. Datta A, Pati S K, Davis D, Sreekumar K, *J Phys Chem A*, 2005, **109**, 4112.
20. Zyss J, Oudar J L, *Phys Rev A*, 1982, **26**, 2028.
21. Li Z, Zhao Y, Zhou J, Shen Y, *Eur Polym J*, 2000, **36**, 2417.
22. Beltrania T, Boschb M B, Centorea R, Concilio S C, *Polymer*, 2001, **42**, 4025.
23. Tedder J M, Venkataraman K, *The Chemistry of Synthetic Dyes*, Academic Press, New York 1970.
24. Kumar S, Neckers D C, *Chem Rev*, 1989, **89**, 1915.
25. Datta A, Pati S K, *Chemical Society Reviews*, 2006, **35**, 1305.
26. Davis D, Sreekumar K, Pati S K, *Syn Metals*, 2005, **155**, 384.
27. Gaussian 03 Revision B.05 Gaussian Inc. Pittsburgh P A, 2003.
28. Becke A D, *J Chem Phys*, 1993, **98**, 5648.
29. Hehre W J, Radom L, Schleyer P V R, Pople J A, *Ab Initio Molecular Orbital Theory*, Wiley, New York, 1986.
30. Ramasesha S, Shuai Z, Bredas J L, *Chem Phys Lett*, 1995, **245**, 224.
31. Albert I D L, Ramasesha S, *J Phys Chem*, 1990, **94**, 6540.
32. Ramasesha S, Albert I D L, *Phys Rev B*, 1990, **42**, 8587.
33. Pati S K, Ramasesha S, Shuai Z, Bredas J L, *Phys Rev B*, 1999, **59**, 14827.
34. Zhu Z, Wu S, Zhang Y, *Russ J Phys Chem A*, 2008, **82**, 2293.
35. Zhan C G, Nichols J A, Dixon D A, *J Phys Chem A*, 2003, **107**, 4184.
36. Lakshmi S, Datta A, Pati S K, *Phys Rev B*, 2005, **72**, 45131.
37. Vannikov A V, Girishina A D, *Russ Chem Rev*, 2003, **72**, 471.
38. Kishore V C, Dhanya R, Sreekumar K, Joseph R, Kartha C S, *Spectrochimica Acta Part A.*, 2008, **70**, 1227.
39. Elizabeth C V, Sreekumar K, *J Mater Sci*, 2010, **45**, 1912.
40. Guass J, *Modern Methods and Algorithms of Quantum Chemistry, Proceedings*,

Second Edn, 2000, **3**, 541.

- 41 Stobbe H, Eckert R, *Chem Ber*, 1905, **38**, 4075
42. Takami S, Irie M, *Tetrahedron*, 2004, **60**, 6155
43. El-Nahass M M, Zeyada H M, Hendi A A, *Optical Materials*, 2004, **25**, 43
44. Price D M, Church S P, Sambrook- Smith C P, *Thermochimica Acta*, 1999, **332**, 197
45. Fukui K, *Accounts Chem Research*, 1971, **4**, 57
46. Goldstein E, Beno B, Houk K N, *J Am Chem Soc*, 1996, **118**, 6036
47. Zhang Q, Bell R, Truong N, *J Phys Chem*, 1995, **99**, 592
48. Della Rosa C, Paredes E, Kneeteman M, Mancini P, *Lett Org Chem*, 2004, **1** 369
49. Della Rosa C, Kneeteman M, Mancini P, *Tetrahedron Lett*, 2005, **46**, 8711
50. Ralph G P, *J Chem Sci*, 2005, **117**, 369
51. Domingo L R, Aurell M, Contreras M, Perez P, *Tetrahedron*, 2002, **58**, 4417
52. Chattaraj P K, Maiti B, Sarkar U, *J Chem Phys A*, 2003, **107**, 4973
53. Shubin L, *J Chem Sci*, 2005, **117** 477
54. Jorge G R, Vargas N A, Sen K D, *J Chem Sci*, 2005, **117**, 379
55. Parr R G, Von Szentpaly L, Liu S, *J .Am Chem Soc*, 1999, **121**, 1922
56. Nagy A, *J Chem Sci*, 2005, **117**, 437.
57. Gaussian 98 Revision A11.4 Gaussian Inc. Pittsburgh PA 2002.
58. Gauss View 03 Gaussian Inc Pittsburgh PA 2003.
59. Paul C, Hu P, *J Phys Chem B*, 2006, **110**, 4157.

Chapter 4

NONLINEAR OPTICAL POLYMERS FROM NATURAL RESOURCES: THEORETICAL AND EXPERIMENTAL STUDIES ON CARDANOL-BASED POLYURETHANES

4.1. Introduction

Most of the industrial demands for the manufacture of polymeric products depend upon petroleum feedstock. The need to reduce the use of fossil fuel derived monomers in the manufacture of polymers is evident as a result of the spiralling cost and the high rate of depletion of the petrochemical-derived stocks. This requires the investigation and use of natural and renewable sources which can serve as alternative feedstock of monomers for the polymer industry¹. Cashew nut shell liquid (CNSL) is a renewable natural resource obtained from the cashew nut (*Anacardium occidentale* L.) as a by-product during the process of removing the cashew kernel from the nut and its total production approaches one million tons annually^{2,4}. In its natural form, the crude CNSL is essentially a mixture of different unsaturated long-chain phenols and represents a good natural alternative to petrochemically derived phenols⁵⁻⁷. CNSL constitutes nearly 25% of the total weight of the nut and is composed of anacardic acid (3-n-pentadecylsalicylic acid) and smaller amounts of cardanol (3-n-pentadecylphenol), cardol (5-n-pentadecyl resorcinol), and methylcardol (2-methyl-5-n-pentadecyl resorcinol), the long aliphatic side-chain being saturated⁸, mono-olefinic, di-olefinic, and tri-olefinic (**Figure 4. 1**). The thermal treatment of cashew nut and CNSL induces the partial decarboxylation of anacardic acid, which is completed by the distillation. The result is an industrial grade cardanol, in the form of a yellow oil containing cardanol (about 90%), with a smaller percentage of cardol and methyl cardol⁹⁻¹¹. Because of their natural origin and structure, anacardic acid and cardanol are likely candidates for preparing "green" surfactant species like cardanol sulfonates, cardanol ethoxylates and cardanol-formaldehyde polymers.

The work on polymeric materials derived from CNSL or Bis (3-pentadecyl phenol) has attracted attention recently due to their use in the preparation of NLO active polymer. Cardanol-formaldehyde oligomers are special phenolic

materials having attractive properties such as high-temperature resistance, quick drying after baking, high electrical insulation, and good thermal stability, modulus retention at elevated temperatures, resistance to chemicals and detergents, high surface hardness, and low cost.¹²⁻¹⁴ The reactivity of hydroxyl group of cardanol has been utilised in modifying and synthesizing varieties of polymers. In the present study, we have explored the phenoxy group of the cardanol by reacting it with 2,4-toluene diisocyanate.

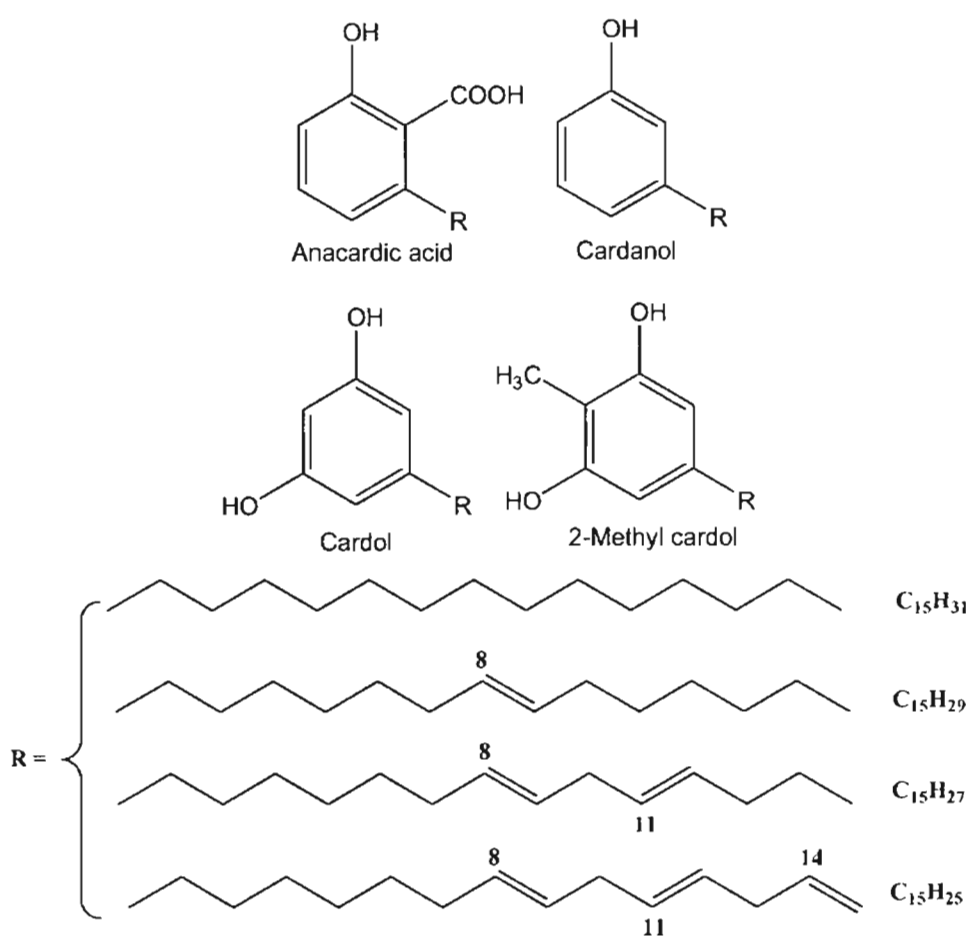
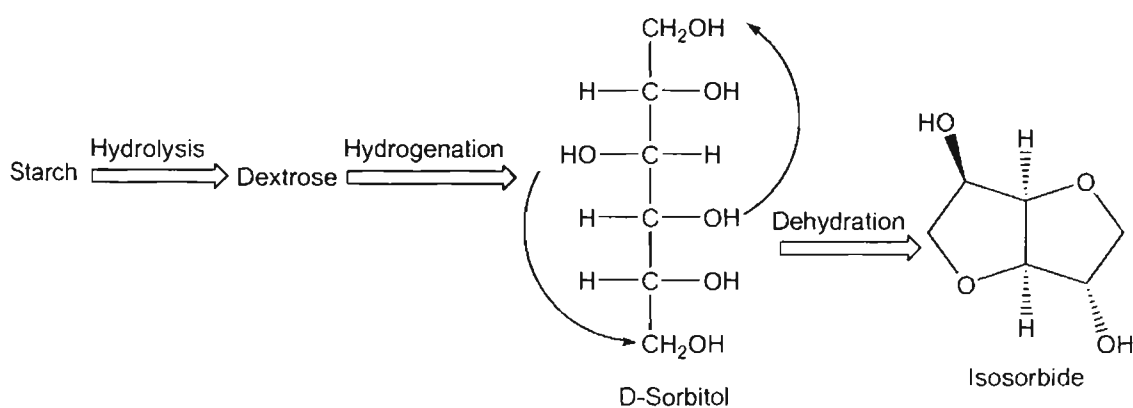


Figure 4. 1: Components of CNSL

A growing interest currently exists for chemicals derived from renewable resources as an alternative method to oil-based monomers for the production of well established industrial polymers¹⁵. Among the natural resources, carbohydrate- based polymer synthesis has attracted much attention due to the degradable and biocompatible behavior of the polymers. Carbohydrates are also considered to be acceptable because they are inexpensive, readily available, and provide great functional diversity. A highly promising carbohydrate derivative for the synthesis of sustainable polymers is the bicyclic compounds coming

under the dianhydrohexitol category. Several notable examples have been reported in the literature, for the synthesis of polyesters, poly (ester-amide)s, polycarbonates based on dianhydrohexitols¹⁶. Among the dianhydrohexitols, the use of the bicyclic diols, isosorbide and isomannide from sugars as monomers for the synthesis of polymers has been widely explored^{17,18}. The cyclic dianhydride was prepared from corn starch following the route depicted in **Scheme 4.1**. Similarly isomannide can also be obtained from D-mannitol.



Scheme 4.1: Synthesis of isosorbide from corn starch

Several optically active polymers derived from (2R, 3R)-diethyl tartrate has been reported in literature. (2R, 3R)-diethyl tartrate, obtained from tartaric acid core (occurs naturally in many plants, particularly grapes, bananas, tamarinds, and is one of the main acids found in wine) is especially appealing for the design of chiral polymers (which will induce intrinsic chirality) because of its easy availability from the chiral pool and renewable resources, biocompatibility, low toxicity and C_2 - symmetry as well as natural polyfunctionality¹⁹.

4.2. METHODOLOGY

4.2.1. Computational methods

4.2.1.1. Monomers

All the chiral monomers have been optimized using restricted B3LYP formalism in density functional theory (DFT) using 6-31+G(d,p) basis set available in the Gaussian algorithm.²⁰⁻²³ Since DFT methods give more accurate results (with electron correlation) than semiempirical calculations, which are done at extremely minimal (Slater type orbitals) basis set; (electron correlation is

only included implicitly by the parameters), and less computationally demanding for geometry optimization compared to *ab initio* methods (with high electron correlation), all the geometry optimizations of monomers have been done using DFT methods. The optimized geometries were used to compute the SCF MO energies. The *static* spectroscopic properties of monomers have been calculated using Coupled Perturbed Hartree-Fock (CPHF) method at RHF 6-31++G(d,p) level available in the Gaussian codes.²⁴ The *dynamic* spectroscopic properties have been calculated using the Zerner's INDO SOS method with sum over 82 states.²⁵ Theoretical value of optical rotation have been calculated using frequency dependent, *ab initio*, Hartree-Fock/6-31G(d) level of theory at a wavelength of 500 nm using Gaussian algorithm²⁶⁻²⁷.

4.2.1.2. Polymer

The number of atoms present in polyurethanes is very high, therefore, the cost of computation will be higher. Hence 2 repeating units of polyurethanes were used for the optimization of multifunctional polymers. The AM1 parameterized Hamiltonian available in the Gaussian 03 set of codes was used for the energy minimization. However, for large systems, the accurate determination of the excitation characteristics for dynamic spectroscopic applications still relies on semiempirical methods with configuration interactions. The geometry optimized structures were used for configuration interaction (CI) calculations to obtain energies and the dipole moments in the CI basis using the Zerner's Intermediate Neglect of Differential Overlap (ZINDO) method. The CI approach adopted here has been extensively used in earlier works, and was found to provide excitation energies and dipole matrix elements in good agreement with experiments²⁸. We have chosen the reference determinants which are dominant in the description of the ground state and the lowest one-photon excited state. For the Hartree-Fock determinant, varying number of occupied and unoccupied molecular orbital has been used to construct the SCI space until a proper convergence is obtained. We have used the singles CI (CIS), because the first nonlinear optical coefficients are derived from second-order perturbation theory involving one-electron excitations. For each reference determinant, 8 occupied and 8 unoccupied molecular orbitals were used to construct a CI space with configuration dimension of 65. To calculate NLO properties, the correction vector method was used which

implicitly assumes all the excitations to be approximated by a correction vector.²⁹⁻³⁰ For the calculations of the optical coefficients, an excitation frequency of 1064nm (1.17eV), which corresponds to the frequency of the Nd-YAG laser, was used. Given the Hamiltonian matrix, the ground state wave function, and the dipole matrix, all in CI basis, it is straight forward to compute the dynamic nonlinear optical coefficients using either the first-order or the second-order correction vectors³¹⁻³⁴.

4. 2. 2. Experimental methods

The second harmonic generation efficiency of the polymers were analysed in the powder form by Kurtz Perry technique³⁵⁻³⁶. The well powdered sample was filled in a capillary tube of 0.8 mm thickness. The NLO responses of the materials were recorded using urea and KDP the references, filled in a similar capillary tube sealed at one end for comparison. The experimental set up for the second harmonic generation properties utilizes a Quanta Ray DCR II Nd/YAG laser with a 9 mJ pulse and 1064 nm wavelength, at a repetition rate of 5Hz. A Q-switched, mode-locked Nd: YAG laser was used to generate about 9 mJ pulse at 1064 nm fundamental radiation. The input laser beam was allowed to pass through an IR reflector and then directed on the micro-crystalline powdered sample packed in a capillary tube of diameter, 0.8 mm. The photodiode detector and oscilloscope arrangements measured the light emitted by the sample. The laser beam was split into two parts, one to generate the second harmonic signal in the sample and the other to generate the second harmonic signal in the reference. An output signal of 532 nm was measured at a 90° geometry using urea/KDP as the standard. The intensity of the second harmonic output from the sample was compared with that of the reference. The efficiency of the NLO activity of the polymers are expressed in percentage as

$$\text{SHG Efficiency (\%)} = \frac{\text{Signal of Sample}}{\text{Signal of Reference}} \times 100$$

4. 2. 3. Static molecular property calculations of chiral monomers

Ab initio calculations using Hartree-Fock CPHF level was used to predict the second-order NLO response. The results of *static* CPHF calculations are given in Table 4. 1. The selection of diastereomers was based on this dipolar

orientation. In one of the diastereomers (isomannide), the dipoles are oriented to the same direction, while in the other isomer (isosorbide), the orientation is through opposite direction. The dipolar orientations of isosorbide and isomannide are shown in **Figure 4. 2**.

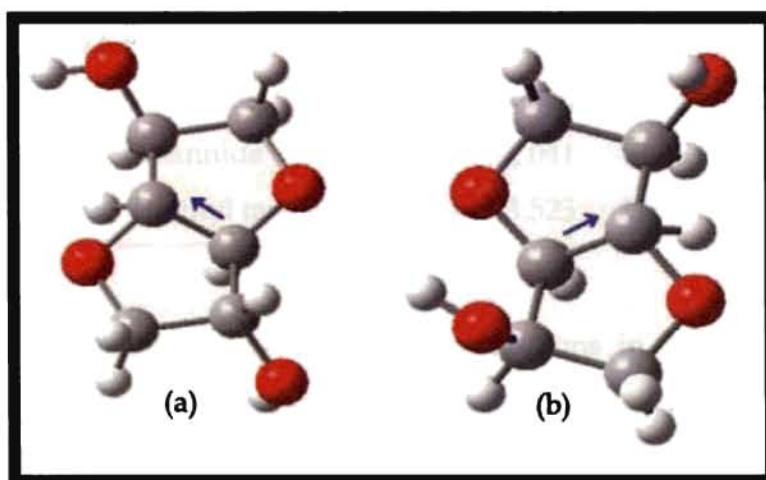


Figure 4. 2 .Optimized structure of Isosorbide (a) and Isomannide(b)

From **Table 4. 1** it can be seen that among the diastereomers, isosorbide and isomannide, one has higher dipole moment than the other. This is due to the orientation of the dipolar group. The expectation was that the diastereomers with oppositely oriented dipoles have smaller value of dipole moment. But while analyzing the geometries, after optimization, it could be found that the ground state dipole moment, μ_g of isosorbide (oppositely oriented dipoles) is greater than that of isomannide. This is because in isosorbide and isomannide diastereomers, the optimized output geometry is more stable with twist conformation, than the planar input geometry. In this twist conformation of isosorbide, the arrangement of oppositely oriented dipoles are in favor of the dipole moment through resultant direction, while in the twist conformation of isomannide, the orientation of dipoles is not in favor of the direction of resultant dipole moment vector.

Table 4. 1 gives the static polarizability values of chiral molecules. In *static* calculation, linear polarizability of diol molecule follows almost the same trend as that of dipole moment. For all pairs of diastereomers (isosorbide and isomannide), the polarizability is almost equal. Thus, it can be concluded that polarizability does not depend much on the dipolar orientation. The (2R, 3R)-diethyl tartrate possesses a higher α value than the isosorbide and isomannide stereo pairs.

Table 4. 1: HOMO-LUMO Gap (ΔE) in eV, Ground-State Dipole Moment (μ_g) in debye, Linear Polarizability (α) in units of 10^{-23} esu, and First Hyperpolarizability (β) in units of 10^{-30} esu for the diastereomers (ab initio CPHF static property calculations)

Diastereomers	ΔE	μ_g	α	β_{vec}
Isosorbide	0.457	2.540	1.111	0.337
Isomannide	0.463	2.041	1.105	0.694
(2R,3R) Diethyl tartrate	0.474	3.523	1.577	0.494

From the results of *static* CPHF calculations in **Table 4. 1**, it can be observed that, in spite of the similar values of α obtained for the isosorbide and isomannide monomers, the β values have been found to vary considerably according to the stereochemistry of the diastereomer. The (2R, 3R) diethyl tartrate has comparatively good β value because of the absence of reflection center (center of symmetry). In the case of isomannide and isosorbide, β value is almost doubled in isomannide compared to isosorbide.

The major contribution to β due to charge transfer can be explained by donor-acceptor concept. Thus, one will get higher β with the factors that enhance the charge transfer. The HOMO-LUMO gap in the molecular orbital picture plays a vital role in the charge transfer.³⁷ If the HOMO-LUMO gap is small, it is easy for the charge transfer to occur. Thus the HOMO largely dictates the source of charge transfer and the details of the molecular LUMO govern the acceptor portion of the excitation. The HOMO-LUMO gaps (ΔE) of the molecules are given in **Tables 4. 1**. There is not much difference in the HOMO-LUMO gap of each pairs of diastereomers with respect to their stereochemistry. Also, while examining the values of β with respect to corresponding μ values of the respective diastereomer, especially for isosorbide-isomannide pair, it can be seen that the HOMO-LUMO, charge transfer model is inadequate for explaining the difference in β value of chiral molecules in the perspective of stereochemistry.

4. 2. 4. Dynamic property calculations for chiral monomers

The frequency dependent dynamic properties were calculated by Sum Over States (SOS) calculations, which could give an idea about the two level

parameters of the chiral monomers. The CPHF method is a frequency independent model in which only the static fields are considered. Table 4. 2. reports the two-level parameters such as, magnitude of oscillator strength (f), the optical gap (δE), the difference between the dipole moments of ground-state and the excited state ($\Delta\mu$), the ground-state dipole moment (μ_g), the linear polarizability (α), and the first hyperpolarizability (β) of the *dynamic* SOS calculation. The SOS method provides the excited level properties by making use of the frequency equal to that of Nd: YAG laser which has been applied as the reaction field.

Table 4. 2: Oscillator strength (f), Optical Gap (δE) in eV, Ground-State Dipole Moment (μ_g) in debye, Difference in dipole moment between ground state and excited state ($\Delta\mu$), Linear Polarizability (α) in units of 10^{-23} esu, and First Hyperpolarizability (β) in units of 10^{-30} esu for the diastereomers (ZINDO-SOS dynamic property calculations)

Diastereomers	f	δE	$\Delta\mu$	μ_g	α	β_{exc}
Isosorbide	0.034	10.940	11.167	15.646	38.3	0.314
Isomannide	0.036	11.066	23.754	11.728	37.3	3.224
(2R,3R)-Diethyl tartrate	0.512	8.695	5.769	19.309	83.3	6.748

Even in the presence of strong applied field (Nd:YAG frequency), similar trends were observed like that of *static* calculations. In the case of isosorbide and isomannide pairs, the difference in β value is more prominent, in one order of magnitude as thrice the value of isosorbide. Since there is no inversion center in (2R, 3R) diethyl tartrate, and has comparatively large change in dipole moment and oscillator strength, it has got the highest β value.

While examining the isosorbide-isomannide pair, it can be seen that the β values vary drastically with respect to the stereochemistry of the diastereomer. In isomannide, the first hyperpolarizability is increased in one order of magnitude. Even though the ground state dipole moment μ_g , is large for isosorbide, the change in dipole moment $\Delta\mu$, is higher for isomannide, which mainly determines the value of β . In fact, the optical gap for isomannide is slightly larger than that of isosorbide, but the large difference in $\Delta\mu$ governs β . To get a clear picture about the dependence of stereochemistry on the β value, all

the determining parameters of β , (f , δE , $\Delta\mu$), have been observed thoroughly. It can be seen that for the diastereomer with large $\Delta\mu$ value, the β is also large. According to Lalama *et al.*³⁸ the dipole moment difference $\Delta\mu$, between the ground and excited state is the major contributing factor in determining the value of β vector. Hence, it can be concluded that all the three molecules act as potential chiral molecules for second order NLO applications. Thus, these are used as promising chiral molecules for constructing chiral media or incorporating in to a polymer chain to get a chiral medium with pronounced SHG.

4. 3. Polymer design

4. 3. 1. Bifunctional polymers

The chiral and achiral bifunctional polyurethanes were designed theoretically as the polyaddition products of 2, 4- toluene diisocyanate (TDI) with chiral and achiral molecules. The structures of bifunctional polymers designed are shown in **Figure 4. 3**.

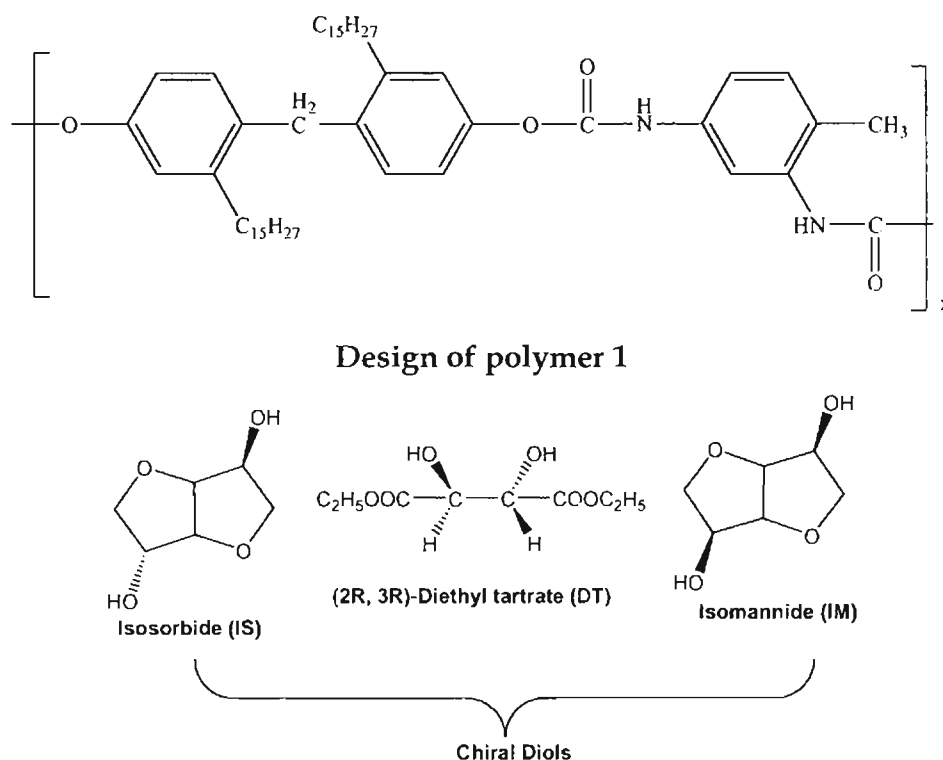


Figure 4. 3: Design of bifunctional polymers

The cardanol based polymers were designed as the combination of 2, 4-toluene diisocyanate (TDI) with achiral diol, bis (3-pentadecyl phenol) (BP) which is represented by the structure polymer 1. The cardanol incorporated

polymer **1**, possesses high value of oscillator strength and change in dipole moment compared to that of chiral polyurethanes. The optical gap ΔE , between the ground state and the lowest dipole allowed state is found to be too small for polymer **1** compared to chiral polymers. The charge transfer in polymer **1** will be much higher due to the small optical gap between the energy levels. All the determining factors of β have suggested that polymer **1** is an NLO active bifunctional polymer. The polarizability of **1** lies in the range of 19.689×10^{-23} esu, and possesses a high value of hyperpolarizability (5.047×10^{-30} esu). The two level parameters for polymer **1** are shown in **Table 4. 3**. All values are reported with respect to Nd:YAG laser frequency (1064nm). The optimized geometry of polymer **1**, is shown in **Figure 4. 4**.

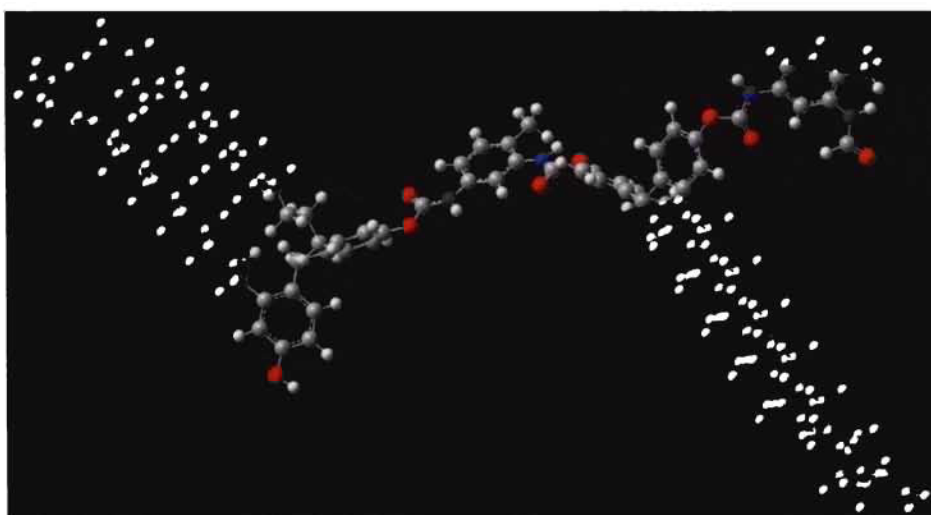


Figure 4. 4: Optimized geometry of polymer 1- TDIBP

The polymers **2**, **3**, and **4** represent the chiral bifunctional polyurethanes with isosorbide (IS), (2R, 3R) - diethyl tartrate (DT) and isomannide (IM) as chiral moiety. Two repeating units of the polymeric system have been chosen for structure optimization and nonlinear optical property calculations. Each repeating unit of the polyurethanes contains one molecule of TDI and one molecule of dihydroxy monomer (chiral diol). **Table 4. 3:** reports the two-level parameters such as, the ground-state dipole moment (μ_g), the difference between the dipole moments of ground-state and the excited state ($\Delta\mu$), the optical gap (ΔE), oscillator strength (f), the linear polarizability (α), and the first hyperpolarizability (β) of bifunctional polymers by the *dynamic* SOS calculations. While analyzing the geometries of bicyclic chiral molecules, it could be found

that the ground state dipole moment μ_g of isosorbide with oppositely oriented dipoles is greater than that of the isomannide. Even though the ground state dipole moment μ_g is large for isosorbide based polymers, the change in dipole moment $\Delta\mu$ is higher for isomannide based chiral polyurethanes. In the case of polyurethane with isomannide and isosorbide chiral moiety, the β value is almost doubled in **4** chiral polymer compared to **2**. Therefore, it can be concluded that the stereochemistry of the chiral monomer affects the polar ordering of the polymers which plays an important role in achieving highly active polymers capable of second harmonic generation. For the (2R, 3R)-diethyl tartrate based polymer **3**, a comparatively large change in dipole moment and oscillator strength are observed which cause the high β value for **3**.

Table 4. 3: Ground-State Dipole Moment (μ_g) in debye, Difference in dipole moment between ground state and excited state ($\Delta\mu$), Optical Gap (ΔE) in eV, Oscillator strength (f), Linear Polarizability (α) in units of 10^{-23} esu, and First Hyperpolarizability (β) in units of 10^{-30} esu for the polymers (ZINDO-SOS dynamic property calculations)

Polymer	μ_g	$\Delta\mu$	ΔE	f	a	β
1- TDIBP	4.765	10.765	6.178	2.393	19.689	5.047
2-TDIIS	11.958	8.029	6.113	1.244	19.982	1.523
3-TDIDT	6.740	9.570	6.641	1.466	18.952	3.039
4-TDIIM	6.141	9.977	6.298	1.404	19.984	3.894

Among the bifunctional polyurethanes (**2-4**), the polymer with isomannide as chiral diol (polymer **4**) and, achiral polymers with bis (3-pentadecyl phenol) (polymer **1**) are also found to show comparable SHG efficiency.

4.3.2. Multifunctional polymers

Dynamic (frequency dependent) SOS give an idea about the two level parameters. The nonlinear optical activity of the multifunctional polymers was thoroughly analyzed. Figure 4. 5 represents the design of multifunctional polymer **7**.

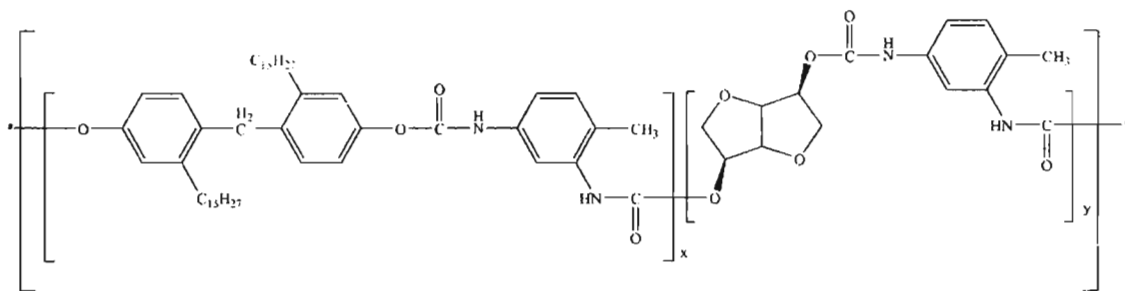


Figure 4. 5: Design of multifunctional polymer 7

The polymers are designed as the polyaddition products of the achiral diol, bis (3-pentadecyl phenol) (BP) and 2, 4- toluene diisocyanate (TDI) with the chiral moiety (Isosorbide, Isomannide and (2R, 3R)-diethyl tartrate). The polymer 5 represents the chiral multifunctional polyurethane with isosorbide (IS) as chiral moiety and **BP** as achiral diol. Similarly, polymer 6 represents multifunctional polymer with (2R, 3R)-diethyl tartrate (DT) as chiral monomer and the bis (3-pentadecyl phenol) as achiral diol molecule. The chiral polyurethanes 7 represent the isomannide derived multifunctional polymers with **BP** as achiral diol. Due to the computational cost, two repeating units of each polymer have been considered for the energy minimization and molecular property calculations. Each repeating unit contains one molecule of achiral diol (BP), two molecules of TDI and one chiral molecule (IS, IM or DT).

Table 4. 4: Ground-State Dipole Moment (μ_g) in debye, Difference in dipole moment between ground state and excited state ($\Delta\mu$), Optical Gap (ΔE) in eV, Oscillator strength (f), Linear Polarizability (α) in units of 10^{-23} esu, and First Hyperpolarizability (β) in units of 10^{-30} esu for the polymers (ZINDO-SOS dynamic property calculations)

Polymer	μ_g	$\Delta\mu$	ΔE	f	α	β
5-TDIISBP	9.206	21.484	4.277	2.522	22.187	12.392
6-TDIDTBP	8.643	24.967	4.242	2.526	26.012	19.104
7-TDIIMBP	9.563	26.112	4.182	2.541	29.926	26.926

Table 4. 4 reports the two-level parameters such as, the ground-state dipole moment (μ_g), the difference between the dipole moments of ground state and the excited state ($\Delta\mu$), the optical gap (ΔE), oscillator strength (f), the linear

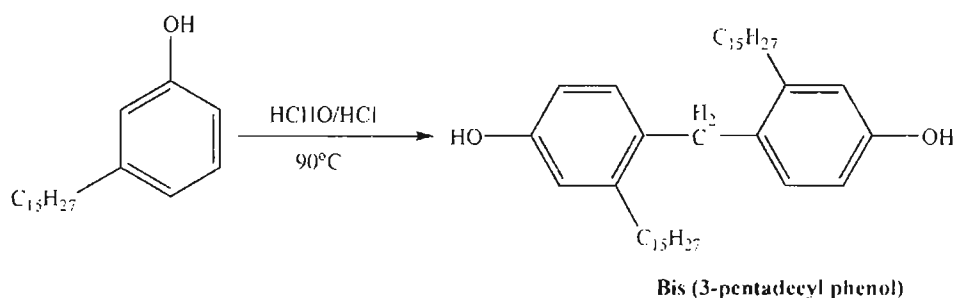
polarizability (α), and the first hyperpolarizability (β) of multifunctional polymers by the *dynamic* SOS calculations. The multifunctional polymer 7 with isomannide as chiral building unit and BP as achiral diol shows high NLO activity with high oscillator strength, change in dipole moment and low optical gap. In the case of polarizability parameters, significant changes are not observed for the multifunctional polymers even though there was prominent change in ground state dipole moment. Thus it can be concluded that the polarizability is not much influenced by the chiral and achiral molecules.

The factors that determine the parameters of β (f , ΔE , $\Delta\mu$) have been studied thoroughly by means of ZINDO/CV calculations. While examining the SHG efficiency of the polymers, it can be seen that all the multifunctional polymers (with chiral and achiral diol) have high β values than the bifunctional polymers. Among the chiral polyurethanes the isomannide-based polymers possess comparatively high value of hyperpolarizability. Both the bifunctional and multifunctional polymers show similar observations for isomannide. Helical structure of the optimized geometry ensures the macroscopic chirality and hence attains the spatial asymmetry. This is considered to be a major prerequisite for the second order nonlinear optical materials. Hence with all these factors, all the designed polymers (bifunctional and multifunctional) are recommended as good materials for nonlinear optical activity.

4.4. Synthesis of bis (3-pentadecyl phenol) monomers

4.4.1. Condensation of cardanol and formaldehyde

Purified cardanol (30 ml) was added to 3% HCl solution (20 ml). The mixture was heated to 90°C. To this mixture, HCHO (37%) solution (4.6 ml) was added dropwise for 1 h. Heating was continued for further 2 h with stirring. The product obtained was washed thoroughly with 1:1 benzene-methanol mixture and dried in vacuum. The synthetic route is shown in Scheme 4. 2.



Scheme 4. 2: Synthesis of achiral diol

The IR vibrations are observed at 1594 cm^{-1} (C=C stretching), 3010 cm^{-1} (CH stretching of alkene), and 778 cm^{-1} (C-H out-of-plane deformation). The bands at 3360 cm^{-1} are due to the presence of hydroxyl groups in the bis cardanol. The IR bands near 1458 and 994 cm^{-1} , are due to the ortho- and para-substituted aromatic rings. The appearance of peaks near 725 and 869 cm^{-1} are also indicative of ortho and para substitution in the phenyl ring.

In the ^1H NMR spectra of bis (3-pentadecyl phenol), the peak at 6.6–7.2 ppm is due to aryl protons of benzene nuclei, the peak around the region 6.4 ppm is due to the phenolic hydroxyl in the BP diol. The peak at 4.9–5.3 ppm is due to methylene (C=CH₂) proton of long alkyl side chain originally present in cardanol and the peak at 0.88–2.70 ppm is due to the long aliphatic side chain. The small peak at 0.80 ppm is due to terminal methyl group of the chain. The strong peak at 1.3 ppm is attributed to the long chain (more than five methylene groups) of the side chain. The peak at 3.6 ppm also indicates methylene proton of C₆H₅-CH₂-C₆H₅ for the bridge between the phenyl rings.

The ^{13}C NMR spectra showed carbon resonance at 14 ppm due to terminal CH₃ carbons of long chain in cardanol. Peaks observed at 22–39 ppm were due to the CH₂ of cardanol side chain (where (CH₂)_n). The C=C of side chain resonate in between 40–46 ppm. The aromatic carbons of cardanol resonate in the range of 120–157 ppm. Hence the proposed structure of the condensed product bis (3-pentadecyl phenol) was confirmed by spectral means.

4. 5. SYNTHESIS OF POLYMERS

The conditions for the synthesis of all polyurethanes were optimized from the synthesis of **PuA3**. Polymerization was done using 2, 4- toluene diisocyanate, IS as chiral diol and BP as achiral diol. Optimum conditions for the synthesis of polyurethanes were determined by varying the solvent, reaction time and temperature which are shown in **Table 4. 5**. For **PuA3**, the temperature variation studies showed that polyurethane with high yield was obtained at 70°C. The reaction was repeated with polar solvents like DMF and DMSO at 70°C for 24 h. Use of other solvents showed no improvement in the yield of product. In all cases few drops of DBTDL was used as catalyst. From these observations, the optimum condition for synthesis of all polyurethanes

incorporating chiral units was fixed as 24 h stirring of corresponding monomers in DMAc medium at 70°C.

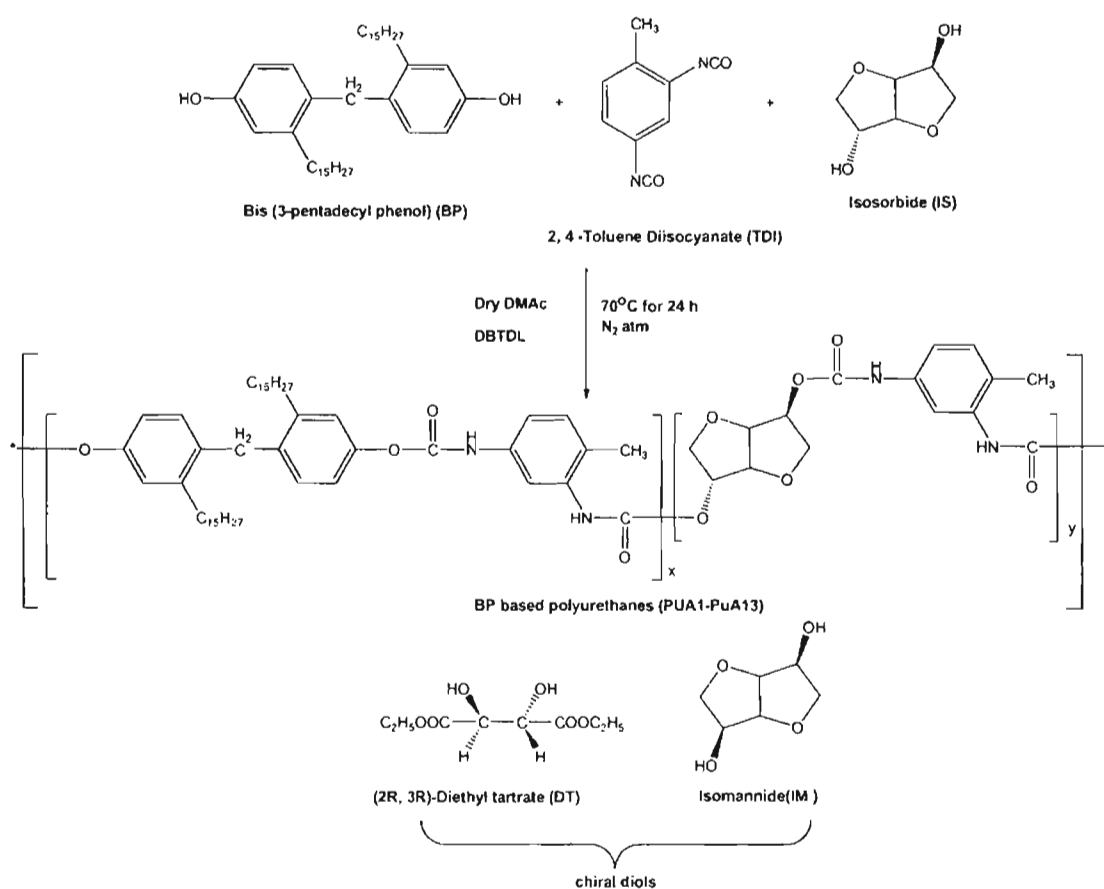
Table 4. 5: Optimization of reaction conditions

Solvent	Time(h)	Temperature (°C)	Yield (%)
DMAc	24	70	79
DMAc	24	100	63
DMAc	48	70	69
DMAc	48	100	73
DMSO	24	70	48
DMSO	24	100	57
DMF	24	70	58

4. 5. 1. General procedure³⁹⁻⁴⁰

A solution of achiral diol (BP) in HPLC grade DMAc (50 mL) was stirred in a flame dried R. B flask of 500 mL capacity equipped with a magnetic stirring bar, nitrogen inlet, a thermometer and a reflux condenser with a CaCl₂ guard-tube. A slight excess of the solution of 2, 4-toluene diisocyanate (TDI) in 10 mL DMAc and four drops of DBTDL were added with vigorous stirring. To this solution, appropriate mole percentage of chiral diols {isosorbide (IS) or isomannide (IM) or (2R, 3R)-Diethyl tartrate (DT)} were added. The stirring was continued at room temperature for 10 min and the mixture was heated at 70 °C for 24 h and cooled to room temperature. The viscous reaction mixture obtained was poured into 500 mL of water with stirring. The solid polymer was separated and washed with methanol. The polymer was dried under vacuum for 2 h.

A series of polyurethanes were synthesized by polyaddition reactions of chiral diols such as isosorbide (IS), isomannide (IM) and diethyl tartrate (DT), achiral diol such as BP with 2, 4-toluene diisocyanate (TDI) in the presence of di-n-butyl tin dilaurate (DBTDL) as catalyst in dimethyl acetamide solvent medium. The scheme of polymer synthesis is shown in Scheme 4. 3. All the chiral polyurethanes were characterized by IR, UV Vis, ¹H NMR, ¹³C NMR and MALDI-MS spectral techniques.



Scheme 4. 3: Scheme for the synthesis of polyurethanes

4. 5. 2. Experimental discussion

Different polymers with varying chiral (IS, DT & IM)-achiral composition were synthesized based on the above mentioned procedure. The polyurethane PuA1 is the one that has only achiral (BP) unit in polymer chain and considered as the mother polymer in the series. For PuA1, the ratio of TDI and BP are taken as 1:1. PuA2, PuA3, PuA4 and PuA5 are the polyurethanes with IS chiral diol having the TDI: BP: IS ratio as 1:0.75:0.25 (PuA2), 1:0.5:0.5 (PuA3), 1:0.25:0.75 (PuA4), 1:0:1 (PuA5), respectively. PuA6, PuA7, PuA8 and PuA9 are the polyurethanes with DT chiral diol in which TDI: BP: DT ratio is maintained as 1:0.75:0.25 (PuA6), 1:0.5:0.5 (PuA7), 1:0.25:0.75 (PuA8), 1:0:1 (PuA9), respectively. PuA10, PuA11, PuA12 and PuA13 are the polyurethanes with IM chiral diol having the ratio of TDI: BP: IM as 1:0.75:0.25 (PuA10), 1:0.5:0.5 (PuA11), 1:0.25:0.75 (PuA12), 1:0:1 (PuA13), respectively.

PuA1: FTIR (KBr), ν_{max} (cm^{-1}): 3350 (-NH str. of urethanes), 3000-2900 (CH stretching vibrations), 1733 (C=O str of urethanes), 1250 (C-O str of urethanes), 1540 (NH bending), 1410 (-CN str. of urethanes). $^1\text{H NMR}$ (DMSO- d_6), δ (ppm):

0.8 (t, -CH₃ of cardanol), 1.4 (s, -CH₃ of TDI), 1.9-2.6 (CH₂- of side chain of cardanol), 2.9 (CH-of cardanol), 6.8-7.3 (m, aromatic protons of cardanol) 7.5-8.2 (m, aromatic protons of TDI), 9.8 (s, -CONH- ortho to the -CH₃ of TDI), 10.5 (s, -CONH- para to the -CH₃ of TDI). ¹³C NMR (DMSO-d₆), δ (ppm): 170-175 (ester carbonyl in -OCONH- of urethane ortho and para to the -CH₃ of TDI), 130-160 (aromatic ring carbons), 72-78 (-CH- of achiral unit), 50-58 (CH₂-of side chain of cardanol), 28-33 (CH₂-of achiral unit) 18-14 (-CH₃ of TDI and cardanol).

PuA2-PuA4: FTIR (KBr), ν_{max} (cm⁻¹): 3300 (-NH stretching of urethanes), 3000-2850 (sp³ C-H stretching in both isosorbide and BP unit), 1740 (C=O str of urethane formed by BP) 1720 (C=O stretching in urethane formed by isosorbide); 1460 (C-H bend of chiral and achiral unit), 1400 (-CN stretching of urethane) 1210 (C-O stretching of isosorbide unit). ¹H NMR (DMSO-d₆), δ (ppm): 0.8 (t, -CH₃ of cardanol), 1.4 (s, -CH₃ of TDI), 1.9-3.0 (CH₂- of side chain of cardanol) 4.1 (q, -CH₂ in isosorbide unit), 4.3-4.5 (t, -CH- bridge protons of isosorbide unit), 5.3 (m, -CH in isosorbide unit), 6.8- 7.3 (m, aromatic protons of cardanol) 7.5-8.2 (m, aromatic protons of TDI), 9.8 (s, -CONH- ortho to the -CH₃ of TDI), 10.5 (s, -CONH- para to the -CH₃ of TDI). ¹³C NMR (DMSO-d₆), δ (ppm): 170-175 (ester carbonyl in -OCONH- of urethane ortho and para to the -CH₃ of TDI), 130-160 (aromatic ring carbons), 80-82 (-CH- bridge of isosorbide unit), 75-78 (-CH- of chiral and achiral unit), 60-62 (-CH₂ of isosorbide unit), 55-58 (CH₂-of side chain of cardanol), 28-33 (CH₂-of achiral unit) 18-14 (-CH₃ of TDI and cardanol).

PuA5: FTIR (KBr), ν_{max} (cm⁻¹): 3290 (-NH stretching of urethanes), 3000-2850 (sp³ C-H stretching in isosorbide unit), 1715 (C=O stretching in urethane formed by isosorbide); 1451 (C-H bend of -CH₂ group in isosorbide), 1415 (-CN stretching of urethane) 1230 (C-O stretching of isosorbide unit), 1055-1125 (C-O stretching vibrations of urethanes attached to phenyl group). ¹H NMR (DMSO-d₆), δ (ppm): 2.4-2.5 (s, -CH₃ of TDI), 4.1 (q, -CH₂ in isosorbide unit), 4.3-4.5 (t, -CH- bridge protons of isosorbide unit), 5.1 (m, -CH in isosorbide unit), 7.5-8.2 (m, aromatic protons of TDI), 9.8 (s, -CONH- ortho to the -CH₃ of TDI), 10.5 (s, -CONH- para to the -CH₃ of TDI). ¹³C NMR (DMSO-d₆), δ (ppm): 170-175 (ester carbonyl in -OCONH- of urethane ortho and para to the -CH₃ of TDI),

130-160 (aromatic ring carbons), 80-82 (-CH- bridge of isosorbide unit), 75-78 (-CH- of isosorbide unit), 40-42 (-CH₂- isosorbide unit), 18 (-CH₃ of TDI).

PuA6-PuA8: FTIR (KBr), ν_{\max} (cm⁻¹): 3280-3300 (NH str. of urethanes), 3000-2868 (sp³ CH str.), 1730-1740 (C=O str. of urethane by achiral diol), 1720-1725 (C=O str. in diethyl tartrate unit), 1690-1700 (C=O str in urethane by DT linkage), 1535 (-NH bending in urethane), 1468 (CN str. in urethanes), 1380 (-CH bend), 1055-1125 (C-O str. of urethane). **¹H NMR (DMSO-d₆), δ (ppm):** 0.8 (t, -CH₃ of cardanol), 1.4-1.8 (m, -CH₃ of TDI and DT), 2-2.9 (CH₂- of side chain of cardanol) 4.1 (q, -CH₂ in diethyl tartrate unit), 4.1-4.3 (t, -CH- of DT unit), 4.8 (m, -CH in cardanol unit), 6.6- 7.3 (m, aromatic protons of cardanol) 7.3-8.4 (m, aromatic protons of TDI), 9.7 (s, -CONH- ortho to the -CH₃ of TDI), 10.2 (s, -CONH- para to the -CH₃ of TDI). **¹³C NMR (DMSO-d₆), δ (ppm):** 174-179 (ester carbonyl in -OCONH- of urethane ortho and para to the -CH₃ of TDI), 170 (carbonyl group in DT), 135-155 (aromatic ring carbons), 75-78 (-CH- of chiral and achiral unit), 53-58 (CH₂-of side chain of cardanol), 30-32 (CH₂-of achiral unit) 20-14 (-CH₃ of TDI, DT and cardanol).

PuA9: FTIR (KBr), ν_{\max} (cm⁻¹): 3270-3300 (NH str. of urethanes), 3000-2890 (sp³ CH str.), 1736-1740, 1720-1725 (C=O str. in urethane), 1537 (NH bend), 1468, 1380 (-CH bend), 1055-1125 (C-O str. of urethane). **¹H NMR (DMSO-d₆), δ (ppm):** 1.2 (t, CH₃), 2.5 (s, CH₃), 4.1-4.3 (q, CH₂), 4.8 (s, CH), 7.2-7.6 (m, aromatic), 8.4 (s, CONH), 9.2 (s, CONH). **¹³C NMR (DMSO-d₆), δ (ppm):** 170-175 (-OCONH of urethane), 168 (C=O ester), 135 (aromatic), 68 (CH), 32 (CH₂), 18 (CH₃).

PuA10-PuA12: FTIR (KBr), ν_{\max} (cm⁻¹): 3300 (-NH stretching of urethanes), 3000-2850 (sp³ C-H stretching in both isomannide and BP unit), 1740 (C=O str. of urethane formed by BP) 1720 (C=O stretching in urethane formed by isomannide); 1460 (C-H bend of chiral and achiral unit), 1400 (-CN stretching of urethane) 1210 (C-O stretching of isomannide unit). **¹H NMR (DMSO-d₆), δ (ppm):** 0.8 (t, -CH₃ of cardanol), 1.4 (s, -CH₃ of TDI), 1.9-3.0 (CH₂- of side chain of cardanol) 4.1 (q, -CH₂ in isosorbide unit), 4.3-4.5 (t, -CH- bridge protons of isosorbide unit), 5.3 (m, -CH in isosorbide unit), 6.8- 7.3 (m, aromatic protons of cardanol) 7.5-8.2 (m, aromatic protons of TDI), 9.8 (s, -CONH- ortho to -CH₃ of TDI), 10.5 (s, -CONH- para to -CH₃ of TDI). **¹³C NMR (DMSO-d₆), δ (ppm):** 170-175 (ester carbonyl in -OCONH- of urethane ortho and para to the -CH₃ of

TDI), 130-160 (aromatic ring carbons), 80-82 (-CH- bridge of isomannide unit), 75-78 (-CH- of chiral and achiral unit), 40-43 (-CH₂- isomannide unit), 50-56 (CH₂-of side chain of cardanol), 28-33 (CH₂-of isomannide unit) 18-14 (-CH₃ of TDI and cardanol).

PuA13: FTIR (KBr), ν_{\max} (cm⁻¹): 3290 (-NH stretching of urethanes), 3000- 2850 (sp³ C-H stretching in isomannide unit), 1715 (C=O stretching in urethane formed by isomannide), 1537 (NH bend), 1451 (C-H bend of -CH₂ group in isomannide), 1415 (-CN stretching of urethane) 1230 (C-O stretching of isomannide unit), 1055-1125 (C-O stretching vibrations of urethanes attached to phenyl group). **¹H NMR (DMSO-d₆), δ (ppm):** 2.4-2.5 (s, -CH₃ of TDI), 4.1 (q, -CH₂ in isomannide unit), 4.3- 4.5 (t, -CH- bridge protons of isomannide unit), 5.1 (m, -CH in isomannide unit), 7.5 -8.2 (m, aromatic protons of TDI), 9.8 (s, -CONH- ortho to the -CH₃ of TDI), 10.5 (s, -CONH- para to the -CH₃ of TDI). **¹³C NMR (DMSO-d₆), δ (ppm):** 170-175 (ester carbonyl in -OCONH- of urethane ortho and para to the -CH₃ of TDI), 130-155 (aromatic ring carbons), 68 (-CH-bridge of isomannide unit), 32-35 (-CH₂- isomannide unit), 18 (-CH₃ of TDI). The ¹H NMR and ¹³C NMR spectra of PuA2-PuA4 are shown in **Figure 4. 6** and **Figure 4. 7**.

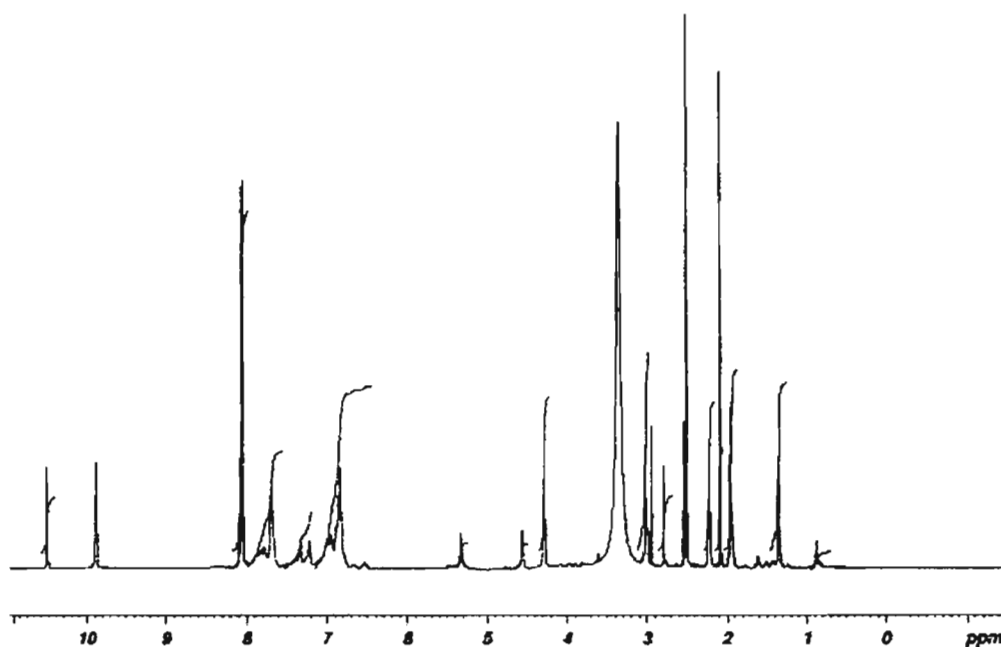


Figure 4. 6: ¹H NMR spectra of PuA2-PuA4

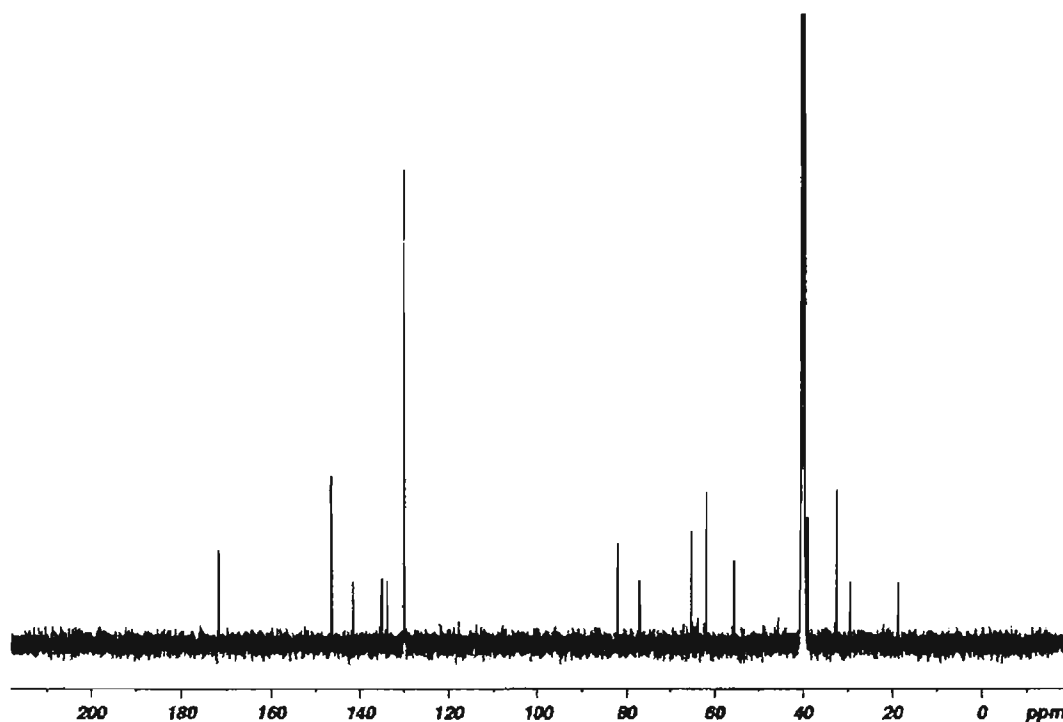


Figure 4. 7: ^{13}C NMR spectra of PuA2-PuA4

4. 5. 3. MALDI-MS of polymers

The molecular weight of the polyurethanes were analysed by using the MALDI mass spectrometry. From the spectrum it was found that the molecular weight of multifunctional polyurethanes were observed in the range 17500-19000, where the molecular weight of one repeating unit accounts to 1000-1100, which confirmed the proposed structure consisting of almost 16-20 repeating units. **Figure 4. 8.** represent the MALDI-MS spectrum of PuA3 polyurethane, which possess a molecular weight of 17848 with 1092 for each repeating unit. The polymer PuA3 possess 16 repeating units.

4. 5. 4. Absorption spectra

The UV-Vis absorption spectra of the polymers in DMAc were recorded and the maximal absorption wavelengths (λ_{max}) of the bifunctional chiral polymers are in the range of 269-272 nm, whereas bifunctional achiral polymer shows absorption at 295 nm. The λ_{max} values for multifunctional polymers are in the range of 280-295 nm. The data of λ_{max} are summarized in **Table 4. 6.** The peak positions in the UV-Vis absorption spectra of polymers were found to be similar to those of corresponding monomers. These results indicate that polar properties of the monomer part are not much decreased by the polymerization process. The

absorption maxima, λ_{\max} , of polymers with chiral monomers are lower than the multifunctional polymers with both chiral and achiral monomers.

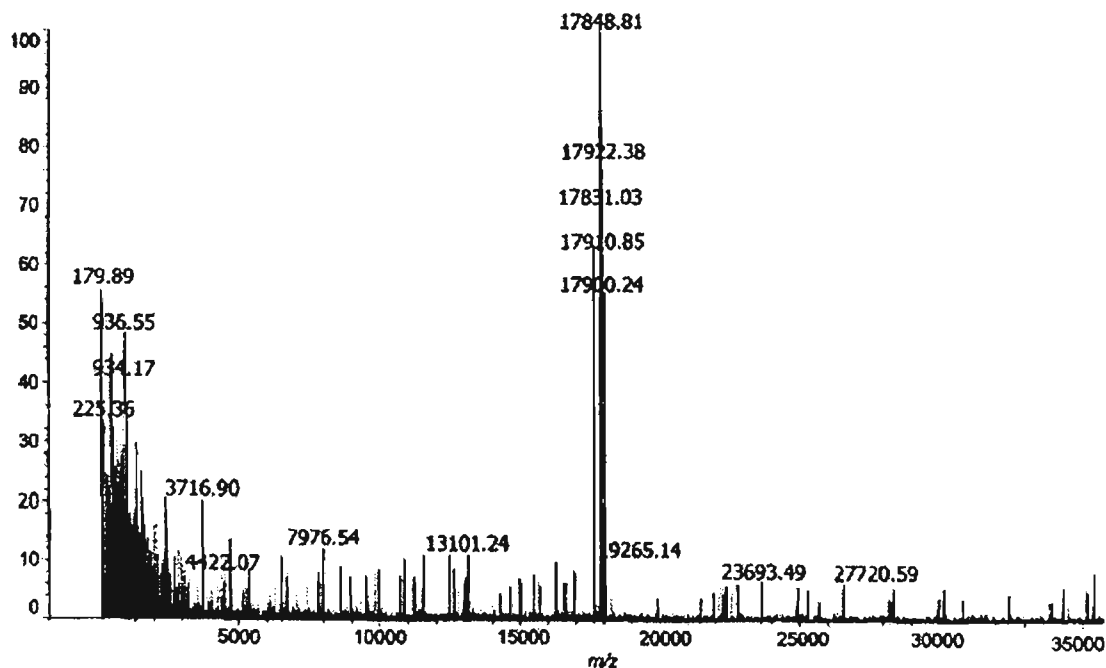


Figure 4. 8: MALDI-MS spectra of PuA3

4. 5. 5. Fluorescence spectra

For all the samples the excitation wavelengths and emission wavelengths were recorded by putting the corresponding absorption wavelengths and excitation wavelengths. The excitation wavelengths of multifunctional polymers were found to be between 350 and 365 nm and emission spectra in the range of 400–420 nm. The emission λ_{\max} values are reported in Table 4. 6.

4. 5. 6. Thermal characterization

The polymer samples were analyzed for their thermal stability by thermogravimetry (TG) and differential thermal analysis (DTA). Initial decomposition temperature (IDT) and glass transition temperature (T_g) of the polymer samples are given in Table 4. 6. The IDT and T_g are important criteria used to determine the thermal stability of polymers. The fact that, all the polyurethanes exhibited one step thermal decomposition behavior is noteworthy. Initial decomposition temperature (IDT) of polyurethanes were in the range of 230-270°C for the multifunctional polymers and 180-195°C for the

bifunctional polyurethanes. The glass transition temperature (T_g) of the polyurethanes were in the range 100-135°C indicating their good thermal stability. The high value of T_g generally corresponds to an increase in the rigidity as well as the polar order of polymers. The high T_g values contribute positively to the SHG efficiency. The polymer with higher T_g has shown higher SHG efficiency. This may be explained based on the higher polar order of the polymers⁴¹⁻⁴³. The polymer containing isosorbide has low value of T_g compared to the polymer containing its diastereomer, isomannide and this reflects the polar order in polymer containing isomannide. The weight residue of the polyurethanes when heated to 600°C in nitrogen was 30%. The high thermal stability offers polyurethanes a wide processing window.

Table 4. 6: Optical and thermal properties of Polyurethanes (PuA1- PuA13)

Polymer	% of chiral diol	Specific rotation ($[\alpha]_D^{20}$)	Absorption $\lambda_{max}(nm)$	Emission $\lambda_{max}(nm)$	IDT ($^{\circ}C$)	T_g ($^{\circ}C$)	Refractive Index
PuA1	0	0	295	419	195	102	1.6498
PuA2	25	29	295	416	240	115	1.6454
PuA3	50	34	292	415	238	108	1.6287
PuA4	75	38	285	410	236	104	1.5829
PuA5	100	43	270	403	190	105	1.5302
PuA6	25	32	292	410	254	112	1.6126
PuA7	50	35	290	419	252	106	1.6063
PuA8	75	39	284	412	249	104	1.5934
PuA9	100	43	272	406	190	101	1.5257
PuA10	25	78	294	418	262	134	1.6543
PuA11	50	80	283	415	257	130	1.6467
PuA12	75	82	280	417	247	129	1.5968
PuA13	100	84	269	401	180	125	1.5802

4. 5. 7. Specific Rotation

The polyurethanes (**PuA2-PuA13**) synthesized contained optically active monomers (**IS**, **DT** and **IM**). The specific rotation of **PuA2-PuA5** polymers was high when isosorbide (**IS**) molecules were incorporated. The specific rotation

$[\alpha]_D$ values measured for polymers varied from 29° to 43° . The polyurethanes **PuA6-PuA9** synthesized contained (2R, 3R)-diethyl tartrate (DT) as the optically active monomer. The optical activity of polymers increased with the increase in % incorporation of DT molecules. The specific rotation $[\alpha]_D$ values measured for polymers were observed in the range of 32° to 43° . For the **PuA10-PuA13** polymers, isomannide (IM) was taken as the optically active monomer for the synthesis, the activity of polymers was much higher compared to that of isosorbide and diethyl tartrate due to the larger specific rotation of IM. The polymers exhibited $[\alpha]_D$ values between 78° and 84° . The $[\alpha]_D$ value increased with the increase in the percentage of chiral component. The polyurethane without chiral molecules **PuA1** showed zero specific rotation. The specific rotation of the polyurethanes are shown in **Table 4. 6**. Relatively high values of specific rotation near to the specific rotation of optically active monomers were observed indicating that no considerable racemization occurred during the polymerization stage. The chiral unit has proved to be a highly stable building block which could impart molecular level chirality to the copolymers⁴³⁻⁴⁴.

4. 5. 8. Refractive index

For the refractive index measurements, distilled water with refractive index 1.33 was taken as the reference. The refractive index of the polymer samples lie in the range 1.52-1.66 which are shown in **Table 4. 6**.

4. 5. 9. X-ray diffraction

Crystallinity of the polyurethanes was evaluated using powder X-ray diffractometer. The polyurethanes showed a broad peak in a range of $2\theta=20-25^\circ$ indicating that the polymers are amorphous in nature. The amorphous characteristics could be explained in terms of the presence of pendent pentadecyl chains in the polymer backbone, which hindered the polymer chain packing and decreased the inter molecular forces, subsequently causing a decrease in crystallinity. The XRD pattern of polyurethanes PuP2-PuP4 is shown in **Figure 4. 9**. There is no prominent shift observed for the polyurethane materials with respect to change in the chiral monomers. The XRD studies also showed that the polyurethanes with and without chiral moiety possessed amorphous characteristics.

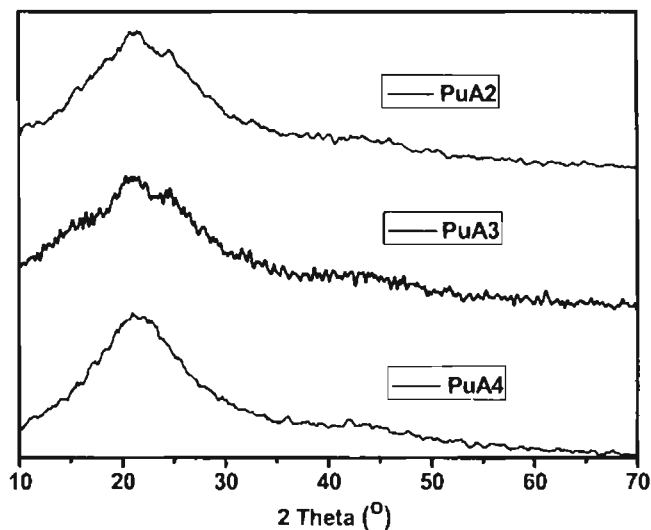


Figure 4. 9: XRD pattern for PuA2-PuA4

4.5.10. Solubility

Solubility studies of chiral polyurethanes were performed with solvents having different polarities. A number of solvents were used to check the solubility of polyurethanes. Most of the polymers synthesized were soluble in polar solvents like DMAc, DMSO, DMF etc. at room temperature and in THF upon heating. The polymers were not soluble in non-polar solvents like benzene, toluene, CCl₄, petroleum ether, ethyl acetate, chloroform etc.

4.5.11. Measurement of NLO activity

The second harmonic generation efficiency of the polyurethanes was examined by powder reflection technique of Kurtz and Perry³⁵⁻³⁶. A laser beam of 9 mJ pulse from an Nd:YAG laser was used for NLO study. The measurements were recorded in comparison with urea and KDP in which all samples were in well-powdered form filled in a capillary tube of 0.8 mm thickness. The second harmonic output was observed at 532 nm. The SHG intensity observed for urea and KDP are 640 mV and 72 mV respectively. The SHG efficiency with respect to urea and KDP are shown in Table 4. 7. The multifunctional polymers possessed high SHG efficiency compared to bifunctional polymers.

The SHG efficiency has shown similar trends in theoretical calculation and experimental measurements. Experimental observations showed that all the polymers showed good SHG efficiency compared to KDP and urea. The

polymers with isomannide chiral diol have the maximum SHG values in both theoretical calculation and experimental measurements. It can be concluded from theoretical calculation and experimental measurement that the second harmonic generation efficiency of bifunctional polymers is less efficient than that of the multifunctional polymers containing both chiral and achiral diols.

Table 4. 7: The SHG efficiency for polyurethanes

Polymer	SHG efficiency	SHG efficiency
	w. r. to urea (%)	w. r. to KDP (%)
PuA1	1.65	14.67
PuA2- PuA4	4.69	41.67
PuA6- PuA8	5.47	48.61
PuA10 -PuA12	6.09	54.17
PuA5	1.72	15.28
PuA9	1.83	16.22
PuA13	2.00	17.78

4. 6. Conclusions

Based on the quantum chemical calculations and comprehensive consideration of several factors, such as first hyperpolarizability, change in dipole moment, oscillator strength, optical gap, etc an effective series of polyurethanes (bifunctional and multifunctional) containing both chiral and achiral diols were designed and synthesized. In this chapter, cardanol- based achiral monomer, bis (3-pentadecyl phenol) was synthesized from cardanol, which is a well known renewable organic resource and a useful byproduct of cashew industry. The BP monomer successfully polymerized with 2, 4- toluene diisocyanate and a new series of high molecular weight polyurethanes were prepared by varying the chiral-achiral monomer (0-100%) compositions. The XRD patterns indicated that the polyurethanes containing bis 3-pentadecyl phenol and chiral diols were amorphous in nature. The high T_g and IDT values of polyurethanes indicated their good thermal stability. The experimental results showed that the polyurethanes exhibited high specific rotation with good thermal stability and nonlinear optical properties. The theoretical calculation is

in good agreement with the experimental results. In conclusion, the cardanol based polymers could be considered as very attractive renewable sources to be used in eco-friendly processes.

4. 7. References

1. More A S, Pasale S K, Wadgaonkar P P, *Euro Polym J*, 2010, **46**, 557.
2. Rekha N, Asha S K, *J Polym Sci, Part A: Polym Chem*, 2009, **47**, 2996.
3. Yadav R, Srivastava D, *J Appl Polym Sci*, 2009, **114**, 1670.
4. Cheriyan S, Abraham E T, *J of Hazardous Materials*, 2010, **176**, 1097.
5. Athawale V, Shetty N, *Pigment & Resin Technology*, 2010, **39**, 9.
6. Chen Q, Xue H, Lin J, *J Appl Polym Sci*, 2010, **115**, 1160.
7. Jyothish K, Vemula P K, Jadhav S R, Francesconi L C, John G, *Chem Commun*, 2009, **36**, 5368.
8. Yadav R, Aswathi P, Srivastava D, *J Appl Polym Sci*, 2009, **114**, 1471
9. Rios M A S, Nascimento T L, Santiago S N, Mazzetto S E, *Energy Fuels*, 2009, **23**, 5432.
10. Campaner P, D'Amico D, Longo L, Stifani C, Tarzia A, *J Appl Polym Sci*, 2009, **114**, 3585.
11. Kumar P S, Kumar N A, Sivakumar R, Kaushik C, *J Mater Sci*, 2009, **44**, 5894.
12. Scorzza C, Nieves J, Vejar F, Bullon J, *J Surfact Deterg*, 2010, **13**, 27.
13. Bruce I E, Mehta L, Porter M J, Stein B K, Tyman J H P, *J Surfact Deterg*, 2009, **12**, 337.
14. Radhakrishnan S, Rao C R K, Vijayan M, *J Appl Polym Sci*, 2009, **114**, 3125.
15. Noordover B A J, Heise A, Malanowksi P, Senatore D, Mak M, Molhoek L, Duchateau R, Koning C E, VanBenthen R A T M, *Progress in Organic Coatings*, 2009, **65**, 187.
16. Yokoe M, Okada M, Aoi K, *J Polym Sci, Part A: Polym Chem*, 2005, **43**, 3909.
17. Marin R, Guerra S M, *J Appl Polym Sci*, 2009, **114**, 3723.
18. Lee C H, Takagi H, Okamoto H, Kato M, Usuki A, *J Polym Sci, Part A: Polym Chem*, 2009, **47**, 6025.
19. Ghosh S, Banthia A K, Maiya B G, *Org Lett*, 2002, **4**, 3603.
20. Kohn W, Sham L, J, *Phys Rev*, 1965, **140**, 1133.
21. Salahub D R, Zerner M C, *The Challenge of d and f Electrons*; ACS: Washington, D C, 1989.

22. Parr R G, Yang W, *Density-Functional Theory of Atoms and Molecules*; Oxford Univ. Press: Oxford, 1989.
23. Bacon D, Zerner M C, *Theo Chim Acta*, 1979, **53**, 21.
24. Gerratt J, Mills I M, *J Chem Phys*, 1968, **49**, 1719.
25. Karna S P, Dupuis M, *J Comp Chem*, 1991, **12**, 487.
26. Karna S P, Dupuis M, *J Chem Phys Lett*, 2000, **319**, 595.
27. Dewar M J S, Zoebisch E G, Healy E F, Stewart J J P, *J Am Chem Soc* 1985, **107**, 3902.
28. Datta A, Pati S K, *J Molecular Structure, Theochem*, 2005, **756**, 97.
29. Datta A, Pati S K, *J Phys Chem A*, 2004, **108**, 320.
30. Ramasesha S, Shuai Z, Bredas J L, *Chem Phys Lett*, 1995, **245**, 224.
31. Albert I D L, Ramasesha S, *J Phys Chem*, 1990, **94**, 6540.
32. Ramasesha S, Albert I D L, *Phys Rev B*, 1990, **42**, 8587.
33. Pati S K, Marks T J, Ratner M A, *J Am Chem Soc*, 2001, **123**, 7287.
34. Pati S K, Ramasesha S, Shuai Z, Bredas J L, *Phys Rev B*, 1999, **59**, 14827.
35. Kurtz S K, Perry T T, *J Appl Phys*, 1968, **39**, 3798.
36. Jayaprakash M, Radhakrishnan T P, *Chem Mater*, 2006, **18**, 2943.
37. Kanis D R, Ratner M A, Marks T J, *Chem Rev*, 1994, **94**, 195.
38. Lalama S J, Garito A F, *Phys Rev A*, 1979, **20**, 20.
39. Elizabeth C V, Sreekumar K, *J Mater Sci*, 2010, **45**, 1912.
40. Sudheesh K K, Sreekumar K, *Int J Polym Mater*, 2009, **58**, 160.
41. Philip B, Sreekumar K, *J Polym Sci: Part A: Polym Chem*, 2002, **40**, 2868.
42. Davis D, Sreekumar K, Pati S K, *Synthetic Metals*, 2005, **155**, 384.
43. Philip B, Sreekumar K, *Designed Monomers & Polymers*, 2002, **5**, 115.
44. Bahulayan D, Sreekumar K, *J Mater Chem*, 1999, **9**, 1425.

Chapter 5

NONLINEAR OPTICAL PROPERTIES OF MAIN CHAIN CHIRAL POLYURETHANES CONTAINING BISAZO CHROMOPHORES: THEORETICAL AND EXPERIMENTAL INVESTIGATIONS

5.1. Introduction

Azo benzene based polymeric materials have attained great attention in the past decades because of their huge potential applications in high technology fields, such as wave guide switches, photo mechanical systems, data manipulation, nonlinear optical materials, holographic memories, optical limiting applications and information processing¹⁻³. NLO active polymers have many advantages superior to conventional inorganic materials such as light weight, low cost, ultrafast response, wide response wave band, high optical damage threshold, thermal stability and good processability to form optical devices. Although many kinds of nonlinear optical materials have been extensively studied, search for polymers with large nonlinear optical response is still in progress⁴. Among the polymers, the bisazo diols have found many advantages over other nonlinear optical materials. The main prerequisites for NLO activity are, excited states close in energy to the ground state, large oscillator strength for electronic transitions from ground to excited state and a large difference between ground and excited state dipole moments. Such requirements are best met by dipolar, highly polarizable donor- π -acceptor systems, showing charge transfer between electron donating and electron withdrawing groups⁵. One of the major challenges in the NLO research area is to design and synthesize the NLO chromophores exhibiting large molecular hyperpolarizability, high thermal stability and good compatibility to polymer matrix. Donor-acceptor substituted π -conjugated molecules have been synthesized as NLO chromophores because of their high hyperpolarizability⁶. In such dipolar molecules, the first order hyperpolarizability depends on the conjugated π -electronic structures, viz., its length and shape, and on the specific character of the donor and acceptor groups. Recent attention has been focused on designing and synthesizing new NLO chromophores that combine large

hyperpolarizability, good near-IR transparency, excellent photostability, improved processability, and synthetic efficacy⁷. Most of the designs for large β chromophores have been based on the optimization of conjugated "push-pull" molecules. Such chromophores consist of electron-donating and electron-withdrawing end groups interacting through a conjugated bridge (D- π -A) to create an intramolecular charge transfer (ICT) transition. It is known that β values of dipolar chromophores depend on the strength of the donor and acceptor groups, as well as the nature and length of the conjugated bridges⁸⁻¹⁰.

The starting point for the development of effective NLO active polymers is the design, synthesis and characterization of chromophore molecules which have a large molecular hyperpolarizability, which is then incorporated into a polymer chain either in the main chain or side chain by covalent linkages. Many optical polymer materials require either non-centrosymmetric or polar packing (space group) of the active material. However, controlling the organization/packing of the polymer molecule is a very difficult task to accomplish; an easier method is making a polymer candidate containing chiral units and uses its inherent chirality to prevent centrosymmetric packing. The noncentrosymmetric (both charge asymmetry and spatial asymmetry) environment can be attained by the incorporation of the chiral units and donor-acceptor building blocks in the main chain and hence induces a helical conformation in the macromolecular chain¹¹⁻¹⁶. In this chapter, an attempt has been made to synthesize new polyurethanes containing nitro substituted chromophores to achieve better NLO performance and processability.

5.2. Methodology

5.2.1. Computational methods

The number of atoms present in polyurethanes is much large therefore the cost of computation will be higher and hence 2 repeating units of polyurethanes were used for the optimization of multifunctional polymers. The AM1 parameterized Hamiltonian available in the Gaussian 03 set of codes was used for the energy minimization. However, for large systems, the accurate determination of the excitation characteristics for dynamic spectroscopic applications still relies on semiempirical methods with configuration interactions. The geometry optimized structures were used for configuration interaction (CI) calculations to obtain energies and the dipole moments in the CI

basis using the Zerner's Intermediate Neglect of Differential Overlap (ZINDO) method. The CI approach adopted here has been extensively used in earlier works, and was found to provide excitation energies and dipole matrix elements in good agreement with experiments¹⁷. We have chosen the reference determinants which are dominant in the description of the ground state and the lowest one-photon excited state. For the Hartree-Fock determinant, varying number of occupied and unoccupied molecular orbital has been used to construct the SCI space until a proper convergence is obtained. We have used the singles CI (CIS), because the first nonlinear optical coefficients are derived from second-order perturbation theory involving one-electron excitations. For each reference determinant, 8 occupied and 8 unoccupied molecular orbitals were used to construct a CI space with configuration dimension of 65. To calculate NLO properties, the correction vector method was used which implicitly assumes all the excitations to be approximated by a correction vector.¹⁸⁻¹⁹ For the calculations of the optical coefficients, an excitation frequency of 1064nm (1.17eV) which corresponds to the frequency of the Nd-YAG laser, was used. Given the Hamiltonian matrix, the ground state wave function, and the dipole matrix, all in CI basis, it is straightforward to compute the dynamic nonlinear optic coefficients using either the first-order or the second-order correction vectors²⁰⁻²³.

5.2.2. Experimental methods

The second harmonic generation efficiency of the monomers and polymers were analysed in the powder form by Kurtz Perry powder technique²⁴. The well-powdered sample was filled in a capillary tube of 0.8mm thickness. The NLO responses of the materials were recorded using urea and KDP as references, filled in a similar capillary tube. The experimental set up for the second harmonic generation properties utilizes a Quanta Ray DCR II Nd/YAG laser with a 9 mJ pulse and 1064 nm wavelength, at a repetition rate of 5Hz. The laser beam is split into two parts, one to generate the second harmonic signal in the sample and the other to generate the second harmonic signal in the reference. An output signal of 532nm was measured in a 90⁰ geometry using urea/KDP as the standard. The efficiency of the NLO activity of the compounds are expressed in percentage as

$$\text{SHG Efficiency (\%)} = \frac{\text{Signal of Sample}}{\text{Signal of Reference}} \times 100$$

5.3. POLYMER DESIGN

5.3.1. Bifunctional polymers

The chiral and chromophoric bifunctional polyurethanes were designed theoretically as the polyaddition products of 2, 4-toluene diisocyanate (TDI) with chiral and donor π -acceptor molecules. The azo polymers(D- π -A) were designed as the combination of 2, 4-toluene diisocyanate (TDI) with azo diols, {bis (4-hydroxyphenylazo)-2, 2'-dinitrodiphenylmethane (PH), bis (8-hydroxyquinolin azo)-2, 2' dinitrodiphenyl methane (HQ), bis (4-hydroxy-3-methyl phenylazo)-2, 2' dinitrodiphenyl methane (CR)}, which are represented as 1, 2 and 3 polymer molecules.

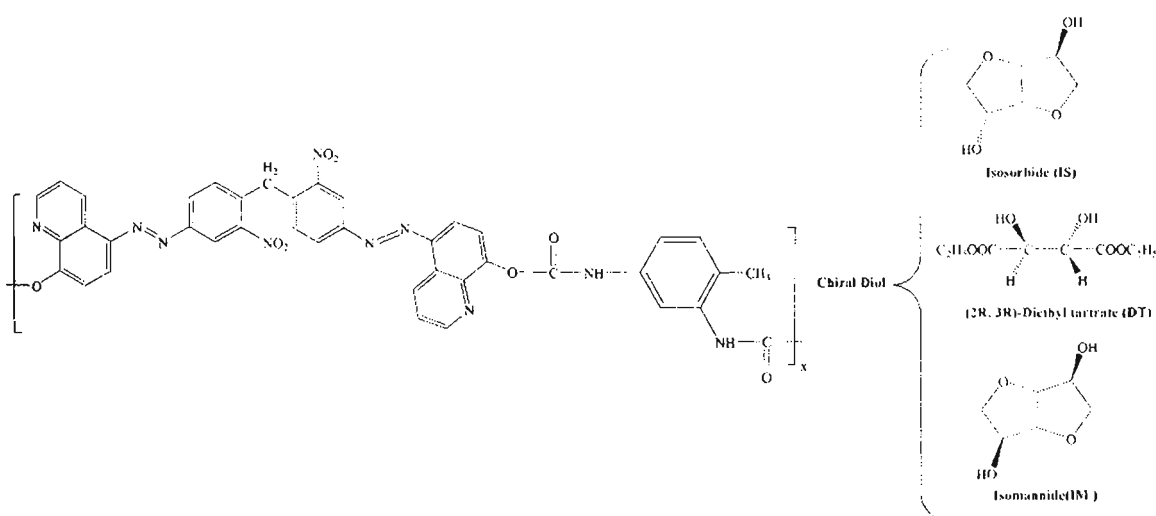


Figure 5. 1: Design of bifunctional polymers

The HQ substituted polymer **2**, possesses high value of oscillator strength and change in dipole moment compared to that of **1** and **3** polyurethanes. The optical gap ΔE , between the ground state and the lowest dipole allowed state is found to be too small for polymer **2**. The charge transfer in polymer **2** is much higher due to the small optical gap between the energy levels. All the determining factors of β - have been suggested that polymer **2** is the most NLO active one among the bifunctional series. The polarizability of **1-3** lie in the range of $22-24 \times 10^{-23}$ esu, which is higher than the polarizability values of **4-6** chiral polymers.

The polymers **4**, **5**, and **6** represents the chiral bifunctional polyurethanes with isosorbide (IS), (2R, 3R)-diethyl tartrate (DT) and isomannide (IM) as chiral moiety. Two repeating units of the polymeric system have been chosen for structure optimization and nonlinear optical property calculations. Each repeating unit of the polyurethanes contains one molecule of TDI and one molecule of dihydroxy monomer (chiral and donor- π -acceptor diol). **Table 5. 1** reports the two-level parameters such as, the ground-state dipole moment (μ_g), the difference between the dipole moments of ground-state and the excited state ($\Delta\mu$), the optical gap (ΔE), oscillator strength (f), the linear polarizability (α), and the first hyperpolarizability (β) of bifunctional polymers obtained by the *dynamic* SOS calculations. While analyzing the geometries of bicyclic chiral molecules, it could be found that the ground state dipole moment μ_g of isosorbide with oppositely oriented dipoles is greater than that of the isomannide. Eventhough the ground state dipole moment μ_g is large for isosorbide based polymers, the change in dipole moment $\Delta\mu$ is higher for isomannide based chiral polyurethanes²⁵.

Table 5. 1: Ground-State Dipole Moment (μ_g) in debye, Difference in dipole moment between ground state and excited state ($\Delta\mu$), Optical Gap (ΔE) in eV, Oscillator strength (f), Linear Polarizability (α) in units of 10^{-23} esu, and First Hyperpolarizability (β) in units of 10^{-30} esu for the polymers (ZINDO-SOS dynamic property calculations)

Polymer	μ_g	$\Delta\mu$	ΔE	f	α	β
1- TDIPH	12.505	12.784	4.202	1.492	22.717	39.059
2- TDIHQ	10.855	16.367	4.121	1.508	23.953	47.581
3-TDICR	11.895	14.846	4.123	1.501	23.121	40.184
4-TDIIS	11.958	8.029	6.113	1.244	19.982	1.523
5-TDIDT	6.740	9.570	6.641	1.466	18.952	3.039
6-TDIIM	6.141	9.977	6.298	1.404	19.984	3.894

The dipole moment difference $\Delta\mu$, between the ground and excited state is the major contributing factor in determining the value of β vector²⁶. In the case of polyurethane with isomannide and isosorbide chiral moiety, the β value is almost doubled in chiral polymer **6** compared to **4**. Therefore it can be concluded

that the stereochemistry of the chiral monomer affects the polar ordering of the polymers which plays an important role in achieving highly active polymers capable of second harmonic generation. For the (2R, 3R)-diethyl tartrate based polymer **5**, a comparatively large change in dipole moment and oscillator strength are observed which cause the highest β value for **5**.

Among the bifunctional polyurethanes, the polymer with isomannide as chiral diol (polymer **6**) and, achiral polymers with HQ azo diol (polymer **2**) are found to have high SHG efficiency.

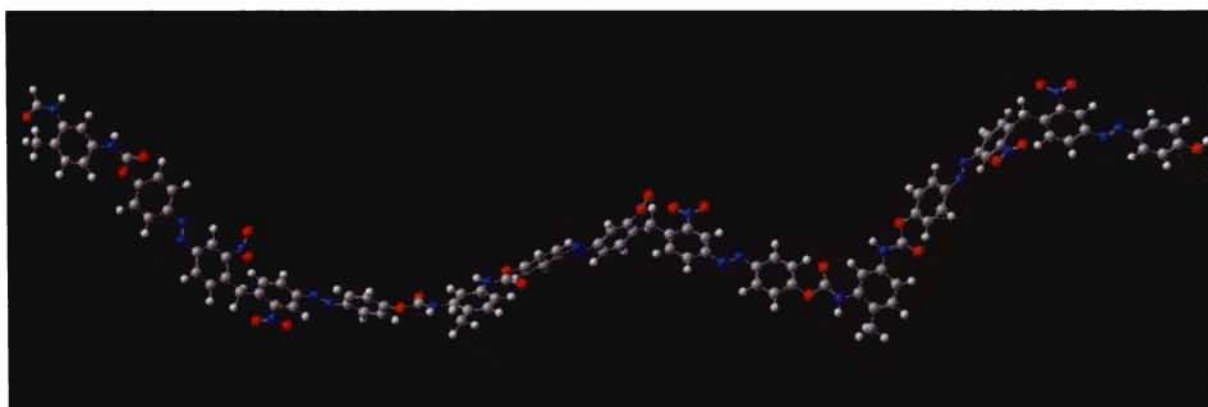


Figure 5. 2: Optimized geometry of polymer 1

5. 3. 2. Multifunctional polymers

The polymers are designed as the polyaddition products of the chromophore {bis (4-hydroxy phenylazo)-2, 2'-dinitrodiphenyl methane (PH), bis (8-hydroxy quinolinazo)-2, 2'-dinitrodiphenyl methane (HQ), bis (4-hydroxy-3-methyl phenyl azo)-2, 2'-dinitrodiphenyl methane (CR)} and 2, 4-toluene diisocyanate (TDI) with the chiral moiety (IS, IM and DT). The polymers **7**, **8** and **9** represent the chiral multifunctional polyurethanes with isosorbide (IS) as chiral moiety and **PH**, **HQ** and **CR** as achiral diols.

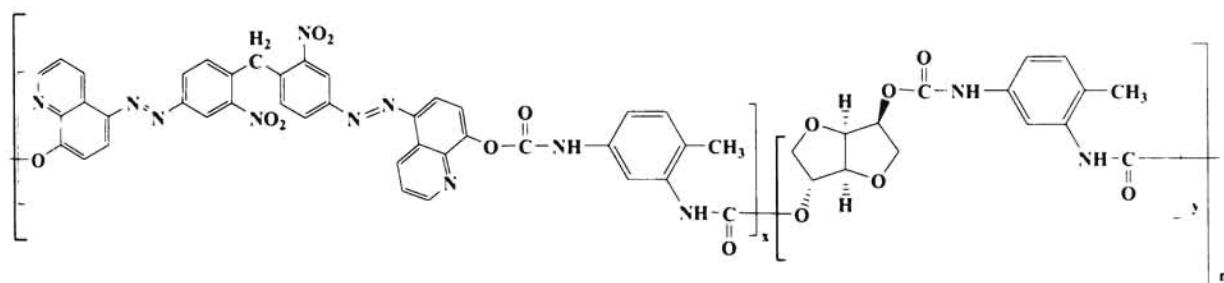


Figure 5. 3: Design of polymer **8** (multifunctional polymer)

Similarly **10**, **11** and **12** represent multifunctional polymers with diethyl tartrate (DT) as chiral monomer and the bisazo diol (PH, HQ & CR) as donor acceptor molecule. The chiral polyurethanes **13**, **14** and **15** represent the isomannide derived multifunctional polymers. Two repeating units of each polymer have been considered for the optimization and molecular property calculations. Each repeating unit contains one molecule of bis azo diol, two molecules of TDI and one chiral molecule (IS, IM and DT). The structures of the polymers are given in **Scheme 5. 5**. The energy minimized geometry of polymer **14** is shown in **Figure 5. 4**.

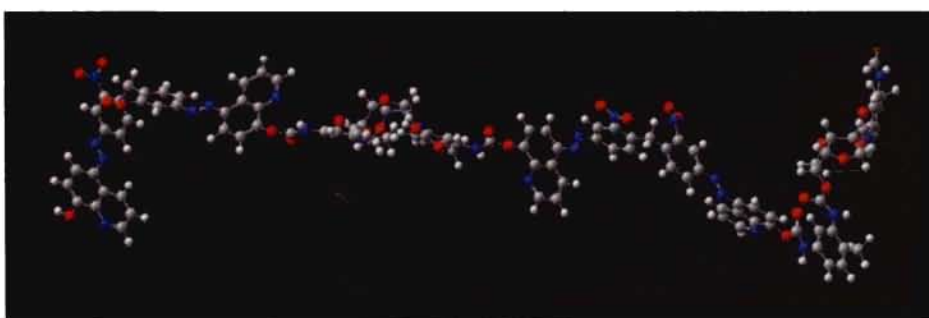


Figure 5. 4: Optimized geometry of polymer **14** (TDIIMHQ)

Table 5. 2. reports the two-level parameters such as, the ground-state dipole moment (μ_g), the difference between the dipole moments of ground-state and the excited state ($\Delta\mu$), the optical gap (ΔE), oscillator strength (f), the linear polarizability (α), and the first hyperpolarizability (β) of multifunctional polymers by the *dynamic* SOS calculations.

It is clear that the multifunctional polymer with isomannide as chiral substitution and HQ as chromophoric diol (**13-15**) shows more NLO activity with high oscillator strength, change in dipole moment and low optical gap. In the case of polarizability parameters, significant changes are not observed for the multifunctional polymers. Thus it can be concluded that the polarizability is not much influenced by the presence of chiral and achiral molecules.

All the determining parameters of β (f , ΔE , $\Delta\mu$) have been analysed thoroughly. While examining the efficiency of the polymers, it can be seen that all the multifunctional polymers (with chiral and chromophoric diols) have high beta values than the bifunctional polymers. Among the chiral polyurethanes, the isomannide based polymers possess comparatively high value of hyperpolarizability.

Table 5. 2: Ground-State Dipole Moment (μ_g) in debye, Difference in dipole moment between ground state and excited state ($\Delta\mu$), Optical Gap (ΔE) in eV, Oscillator strength (f), Linear Polarizability (α) in units of 10^{-23} esu, and First Hyperpolarizability (β) in units of 10^{-30} esu for the polymers (ZINDO-SOS dynamic property calculations)

Polymer	μ_g	$\Delta\mu$	ΔE	f	α	β
7-TDIISPH	9.206	21.484	4.277	1.522	32.184	59.392
8-TDIISHQ	8.808	22.046	4.190	1.537	36.011	66.485
9-TDIISCR	9.184	18.146	4.242	1.524	34.485	58.187
10-TDIDTPH	13.643	19.967	4.242	1.512	36.012	59.104
11-TDIDTHQ	16.845	22.185	4.121	1.544	34.458	68.487
12-TDIDTCR	13.998	20.018	4.284	1.526	32.798	60.910
13-TDIIMPH	6.563	20.112	4.182	1.541	33.926	66.926
14-TDIIMHQ	7.432	22.986	4.041	1.629	35.321	70.235
15-TDIIMCR	6.984	20.345	4.008	1.538	34.465	66.484

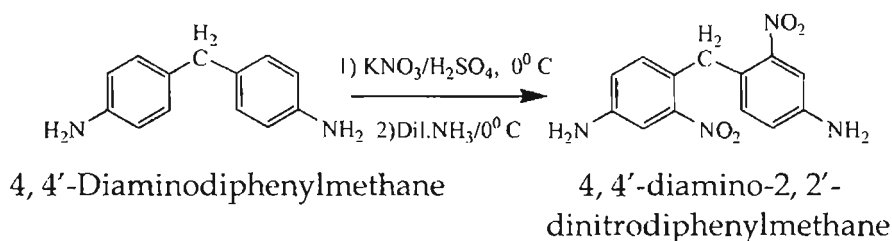
All the polymers have helically oriented conformation in the optimized geometry. The helical structure ensures the macroscopic chirality and hence attains the spatial asymmetry. This is the basic and essential requirement for second order nonlinear optical materials. Hence with all these factors, all the designed polymers are recommended as very good material for second harmonic generation.

5. 4. Synthesis of monomers

5. 4. 1. Synthesis of 4, 4' diamino-2, 2'-dinitrodiphenylmethane

4, 4'-diaminodiphenylmethane was nitrated using a mixture of anhydrous potassium nitrate and 98% sulphuric acid at 0°C. To an ice-cold solution (0-5°C) of 4, 4'-diaminodiphenylmethane (0.05 mole 9.9 g) in conc. sulphuric acid (18 M, 40 ml), a solution of potassium nitrate (0.1 mole 10.1 g) in conc. sulphuric acid (18 M, 15 ml) was added during a period of 1 h. The stirring was continued for 3 h, keeping the temperature below 5°C. The reaction mixture was poured into crushed ice and neutralized with ice-cold solution of ammonia. The yellow solid was collected on a filter, washed thoroughly with water. Crystallisation from a

mixture of dioxane–alcohol afforded orange yellow flakes of 4, 4'-diamino-2, 2'-dinitrodiphenylmethane¹¹⁻¹⁶.

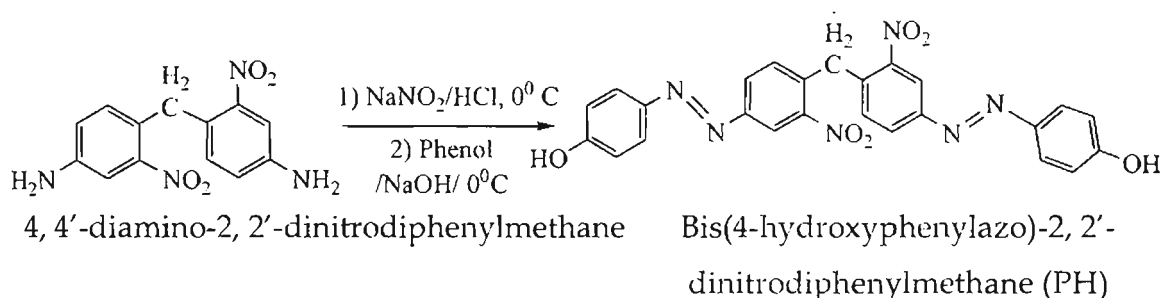


Scheme 5. 1: Synthesis of dinitro compound

FTIR (KBr), ν_{\max} (cm^{-1}): 1540 and 1350 (NO_2). **^1H NMR (300 MHz, CDCl_3):** 4.8 [4H (s), amino protons], 8.2 [2H (s), aromatic], 7.6 [2H (d), aromatic], 7.3 [2H (d), aromatic], 5 [2H (s), methylene]. **^{13}C NMR (CDCl_3):** 34 (methylene), 130- 157 (aromatic).

5. 4. 2. Synthesis of bis (4-hydroxyphenylazo)-2, 2'- dinitrodiphenylmethane

To an ice-cold solution of 3a (10 g, .035 mole) in HCl (6 M, $20 \times 10^{-6} \text{ m}^3$) was added aqueous sodium nitrate solution (6 g, $15 \times 10^{-6} \text{ m}^3$). The diazonium salt was added slowly to a cold alkaline solution of phenol (6.58 gm, 0.07 mol). The resulting solution on acidification gave a brown solid. It was collected, washed with water, dried and purified on a silica gel column using hexane and hexane-ethyl acetate mixture¹¹⁻¹⁶.

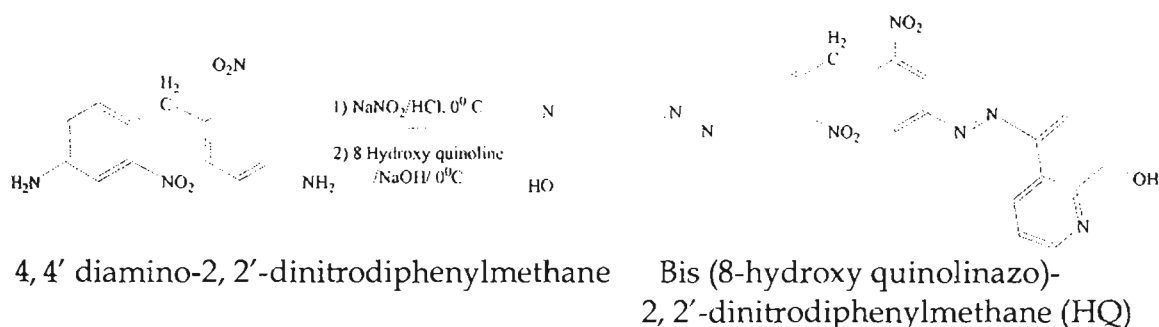


Scheme 5. 2: Synthesis of chromophore PH

FTIR (KBr), ν_{\max} (cm^{-1}): 1540, 1345 (NO_2), 1602 ($-\text{N}=\text{N}-$), 3400 (OH). **^1H NMR (CDCl_3): δ (ppm):** 3.8 [2H(s), CH_2], 6.93 [4H (d), Ha], 7.76 [4H(d), Hb], 9.2 [2H(d), Hc], 8.65 [2H(d), Hd], 7.9 [2H(d), He], 9.9 [2H(s), OH], **^{13}C NMR (CDCl_3): δ (ppm):** 32 (methylene), 140-160 (aromatic). **UV (λ_{\max} , nm):** 280 (NO_2), 400 ($\text{N}=\text{N}$).

5.4.3. Synthesis of bis (8-hydroxyquinolinazo)-2, 2' dinitrodiphenylmethane (HQ)

The HQ chromophore was prepared by reacting an ice cold solution of 4, 4'-diamino-2, 2'- dinitrodiphenylmethane (0.0218 mol, 6.3 g) in hydrochloric acid (6 M, 45mL) with aqueous sodium nitrite solution (4.4g, 70 mL). After complete addition of NaNO₂, sufficient amount of solid sodium acetate was added for attaining alkaline pH. To this, 10 ml of alcohol (99.5%) was added. 8-Hydroxy quinoline (7.48 gm, 0.065 mol) was dissolved in absolute alcohol in a dropping funnel and was slowly added to the mixture over a period of 1 h. The reaction mixture was stirred, for further 2 h. The product formed was washed thoroughly with water. It was dried and purified on a silica gel column using hexane and hexane-ethyl acetate mixture. Brick red coloured product was obtained¹¹⁻¹⁶.



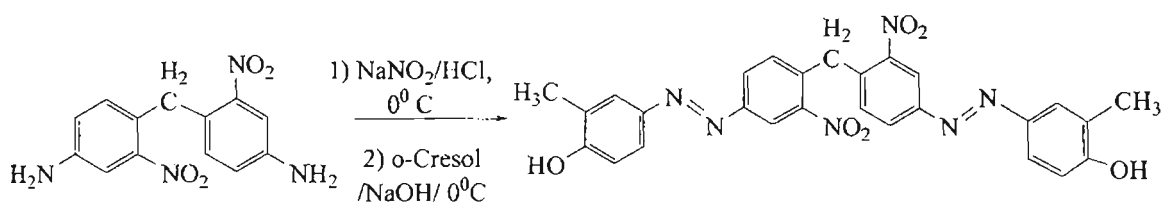
Scheme 5. 3: Synthesis of chromophore HQ

FTIR (KBr), ν_{\max} (cm⁻¹): 1540, 1345 (NO₂), 3400 (OH) 1602 (-N=N-). **¹H NMR (CDCl₃): δ (ppm):** 3.8 [2H(s), CH₂], 6.93 [4H (d)], 7.76 [4H(d)], 9.2 [2H(d)], 8.65 [2H(d)], 7.9 [2H(d)], 9.9 [2H(s), OH], **UV (λ_{\max} , nm):** 290 (NO₂), 410 (N=N).

5.4.3. Synthesis of bis (4-hydroxy -3-methylphenylazo)-2, 2' dinitrodiphenyl methane (CR)

The chromophore **CR** was prepared by reacting an ice cold solution of 4, 4'-diamino-2, 2'- dinitrodiphenylmethane (0.0218 mol, 6.3 g) in hydrochloric acid (6 M, 45mL) with aqueous sodium nitrite solution (4.4g, 70 mL). After complete addition of NaNO₂, sufficient amount of solid sodium acetate was added for attaining alkaline pH (7-7.5). To this, 10 ml of alcohol (99.5%) was added. O-cresol (6.46 gm, 0.068 mol) was dissolved in absolute alcohol in a dropping funnel and was slowly added to the mixture over a period of 1 hour. The reaction mixture was stirred, for further 2 hours. The product formed was

washed thoroughly with water. It was dried and purified on a silica gel column using hexane-ethyl acetate mixture. Brown coloured solid was obtained¹¹⁻¹⁶.



Scheme 5. 4: Synthesis of chromophore CR

FTIR (KBr), ν_{\max} (cm^{-1}): 1275 (C-O str. of Ph-OH) 1540, 1345 (NO_2), 1595(-N=N-), 2928, 2850 (- CH_2 str.) 3400 (OH). **^1H NMR ($\text{CD}_3\text{-CO-CD}_3$, δ (ppm)):** 2.29 (6H, two CH_3), 3.3 (2H, Ph- CH_2 -Ph), 9.2 (2H, OH), 7.77-7.72 (6H, aromatic), 8.77-8.1 (6H, aromatic). **^{13}C NMR (CDCl_3):** 20 (methyl), 34 (methylene), 132-157 (aromatic). **UV (λ_{\max} , methanol, nm):** 276 (NO_2), 402 (N=N). **Elemental Analysis:** Calculated for ($\text{C}_{27}\text{H}_{22}\text{N}_6\text{O}_6$): C-61.6; H-4.18; N-15.97. Found: C-61.12; H-4.15; N-15.94

5. 4. 4. SHG efficiency of monomers

The second harmonic generation efficiency of the monomers were analysed in the powder form by Kurtz Perry powder techniques.

Table 5. 3: SHG efficiency of monomers

Monomer	SHG intensity (mV)	SHG efficiency w. r. to urea (%)	SHG efficiency w. r. to KDP (%)
PH	40	6.25	55.56
HQ	48	7.5	66.67
CR	42	6.56	58.33

The SHG efficiencies of the chromophores were recorded with respect to urea and KDP and are reported in Table 5. 3. The HQ chromophore shows considerably high activity compared to the other two chromophore. Hence HQ based polyurethanes are predicted to be more NLO active.

5. 5. Synthesis of polymers

5. 5. 1. General procedure²⁷

A solution of chromophore (PH, HQ & CR) in HPLC grade DMAc (50

mL) was stirred in a flame dried R. B flask of 500 mL capacity equipped with a magnetic stirring bar, nitrogen inlet, a thermometer and a reflux condenser with a CaCl_2 guard-tube. To this, a slight excess of the solution of toluene diisocyanate (TDI) in 10 mL DMAc and four drops of DBTDL were added with vigorous stirring. To this solution, appropriate mole percentage of chiral diols {isosorbide (IS), isomannide (IM) and (2R, 3R)-Diethyl tartrate (DT)} were added. The stirring was continued at room temperature for 10 min and the mixture was heated at 70°C for 24 h and cooled to room temperature. The viscous reaction mixture obtained was poured into 500 mL of water with stirring. The solid polymer was separated and washed with methanol. The polymer was dried under vacuum for 2 h.

Table 5. 4: Optimization of reaction conditions

Solvent	Time(h)	Temperature ($^\circ\text{C}$)	Yield (%)
DMAc	24	70	75
DMAc	24	100	63
DMAc	48	70	68
DMAc	48	100	71
DMSO	24	70	48
DMSO	24	100	53
DMF	24	70	58

The optimum conditions for the synthesis of polyurethanes were determined by varying the solvent, time of reaction and temperature which are shown in **Table 5. 4**. Polymerization was done using 2, 4-toluene diisocyanate, DT as chiral diol and PH as chromophore. From these observations, the optimum conditions for the reaction are: temperature 70°C , time 24 h and DMAc as solvent.

The conditions for the synthesis of all polyurethanes were optimized from the synthesis of **PuP7**. The results of various conditions are summarized in **Table 5. 4**. For **PuP7**, the temperature variation studies showed that polyurethane of high yield was obtained at 70°C . The condition for synthesis of all polyurethanes incorporating chiral units was fixed as 24h stirring of corresponding monomers in DMAc medium at 70°C . The reaction was repeated with polar solvents like DMF and DMSO at 70°C for 24 h. The use of other

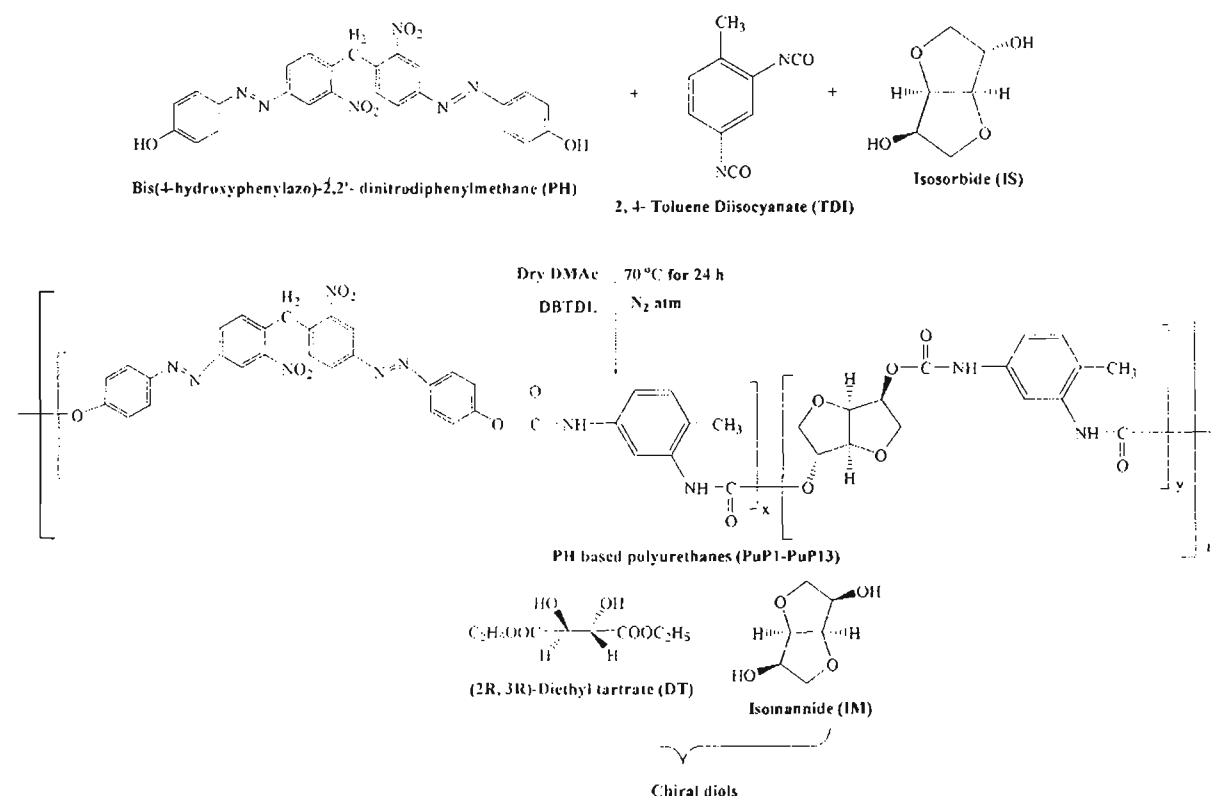
solvents showed no improvement. In all cases five drops of DBTDL was used as catalyst.

A series of nonlinear optically active polyurethanes were synthesized by polyaddition reactions of chiral diols such as isosorbide (IS), isomannide (IM) and diethyl tartrate (DT), azo diols such as PH, HQ and CR with 2, 4-toluene diisocyanate in the presence of di-n-butyl tin dilaurate (DBTDL) as catalyst in dimethyl acetamide solvent medium. All the polyurethanes were characterized by IR, UV-Vis, ^1H NMR, ^{13}C NMR and MALDI-MS spectral techniques.

5. 6. POLYURETHANES WITH BIS (4-HYDROXY PHENYLAZO)-2, 2'-DINITRO DIPHENYLMETHANE CHROMOPHORE

5. 6. 1. Experimental discussion

Different polymers with varying chiral diol (IS, DT & IM)-chromophore PH composition were synthesized. The polymer PuP1 is the one which has only chromophore (PH) unit in polymer chain and considered as the mother polymer in the series.



Scheme 5. 5: Synthesis of polyurethanes

For PuP1, the ratio of TDI and PH are taken as 1:1. PuP2, PuP3, PuP4 and PuP5 are the polyurethanes with IS chiral diol having the TDI: PH: IS ratio as

1:0.75:0.25 (PuP2), 1:0.5:0.5 (PuP3), 1:0.25:0.75 (PuP4), 1:0:1 (PuP5), respectively. PuP6, PuP7, PuP8 and PuP9 are the polyurethanes with DT chiral diol in which TDI:PH:DT ratio is maintained as 1:0.75:0.25 (PuP6), 1:0.5:0.5 (PuP7), 1:0.25:0.75 (PuP8), 1:0:1 (PuP9), respectively. PuP10, PuP11, PuP12 and PuP13 are the polyurethanes with IM chiral diol having the ratio of TDI:PH:IM as 1:0.75:0.25 (PuP10), 1:0.5:0.5 (PuP11), 1:0.25:0.75 (PuP12), 1:0:1 (PuP13), respectively. The scheme for polyurethane synthesis is shown in **Scheme 5.5**.

5.6.2. Spectral Characterization

PuP1: FTIR (KBr), ν_{\max} (cm^{-1}): 3318 (-NH), 2923, 2853 (-CH₂-), 1667 (urethane carbonyl), 1602 (-N=N-), 1531, 1347 (-NO₂), 1233 (-C-O-C- in -COOC of PU). **¹H NMR (DMSO-d₆), δ (ppm):** 10.6 (1H(s), -OCONH- para to the CH₃ of TDI), 9.0 (1H(s), -OCONH-ortho to the CH₃ of TDI), 8.77 (2H(s), phenyl), 8.2 (2H(d), phenyl), 8.0 (2H(d), phenyl), 8.47 (4H(d), phenyl), 8.15 (4H(d), phenyl), 7.0, 6.8, 6.6 (aromatic protons of TDI), 2.4 (3H(s), CH₃ of TDI), 2.95 (2H (s), Ph-CH₂-Ph). **¹³C NMR (DMSO-d₆), δ (ppm):** 153-154 (-OCONH, ortho and para to the CH₃ of TDI), 130- 170 (aromatic), 122-137 (C1-C6 of TDI), 32 (methylene), 18 (CH₃ of TDI).

PuP2-PuP4: FTIR (KBr), ν_{\max} (cm^{-1}): 3320 (-NH of urethanes), 2900-2800 (CH₂ of chromophore and isosorbide), 1725-1730 (C=O group of urethane formed by chromophore), 1710-1720 (C=O group formed by isosorbide), 1602 (-N=N-), 1454 (CH bend of CH₂ group), 1415 (-CN str. of urethane), 1540,1350 (-NO₂ group), 1220-1230 (-C-O-C- str. of isosorbide unit, -C-O-C- in polyurethane), 1050-1120 (C-O str. vibrations of urethanes attached to phenyl group). **¹H NMR (DMSO-d₆), δ (ppm):** 10.4 (s, -OCONH- para to CH₃ of TDI), 9.4 (s, -OCONH- ortho to CH₃ of TDI), 6.6-8.8 (m, aromatic protons), 5.2 (m, -CH in isosorbide unit), 4.3-4.5 (t, -CH bridge protons of isosorbide unit), 4 (q, -CH₂- in isosorbide unit), 2.95 (s, CH₂ of Ph-CH₂-Ph), 2.4 (s, -CH₃ of TDI). **¹³C NMR (DMSO-d₆), δ (ppm):** 178-170 (ester carbonyl in -OCONH- of urethane ortho and para to -CH₃ of TDI), 130-165 (aromatic ring carbons), 80-82 (-CH- bridge of isosorbide unit), 75-78 (-CH- of isosorbide unit), 40-42 (-CH₂- of isosorbide unit), 32 (methylene of chromophore), 18 (-CH₃ of TDI).

PuP5: FTIR (KBr), ν_{\max} (cm^{-1}): 3290 (-NH stretching of urethanes), 3000-2850 (sp³

C-H stretching in isosorbide unit), 1715 (C=O stretching in urethane formed by isosorbide); 1451 (C-H bend of -CH₂ group in isosorbide), 1415 (-CN stretching of urethane) 1230 (C-O stretching of isosorbide unit), 1055-1125 (C-O stretching vibrations of urethanes attached to phenyl group). ¹H NMR (DMSO-d₆), δ (ppm): 2.4-2.5 (s, -CH₃ of TDI), 4.1 (q, -CH₂ in isosorbide unit), 4.3-4.5 (t, -CH- bridge protons of isosorbide unit), 5.1 (m, -CH in isosorbide unit), 7.5-8.2 (m, aromatic protons of TDI), 9.8 (s, -CONH- ortho to the -CH₃ of TDI), 10.5 (s, -CONH- para to the -CH₃ of TDI). ¹³C NMR (DMSO-d₆), δ (ppm): 170-175 (ester carbonyl in -OCONH- of urethane ortho and para to the -CH₃ of TDI), 130-160 (aromatic ring carbons), 80-82 (-CH- bridge of isosorbide unit), 75-78 (-CH- of isosorbide unit), 40-42 (-CH₂- isosorbide unit), 18 (-CH₃ of TDI).

PuP6-PuP8: FTIR (KBr), ν_{max} (cm⁻¹): 3280-3000 (-NH str. of urethanes), 3000-2890 (CH str. of DT and chromophore), 1736-1740 (C=O formed by chromophore), 1725-1730 (C=O formed by DT), 1720-1722 (C=O str in DT), 1608 (-N=N-), 1539, 1345 (-NO₂ group), 1468, 1390 (-CH bend), 1100 (-C-O-C- of urethane), ¹H NMR (DMSO-d₆), δ (ppm): 10 (s, -OCONH- para to CH₃ of TDI), 9.3 (s, -OCONH- ortho to CH₃ of TDI), 7.2-8.5 (m, aromatic protons), 4.8 (s, CH), 4.1-4.3 (q, CH₂), 2.95 (Ph-CH₂-Ph), 2.5 (s, CH₃), 1.2 (t, CH₃). ¹³C NMR (DMSO-d₆), δ (ppm): 172-176 (-OCONH- ortho and para to the CH₃ of TDI), 169 (C=O of ester), 135-160 (aromatic carbons), 68 (CH), 32 (CH₂), 18 (CH₃)

PuP9: FTIR (KBr), ν_{max} (cm⁻¹): 3270-3300 (NH str.), 3000-2890 (sp³ CH str.), 1736-1740, 1720-1725 (C=O str.), 1537 (NH bend), 1468, 1380 (-CH bend), 1055-1125 (C-O str. of urethane). ¹H NMR (DMSO-d₆), δ (ppm): 1.2 (t, CH₃), 2.5 (s, CH₃), 4.1-4.3 (q, CH₂), 4.8 (s, CH), 7.2-7.6 (m, aromatic), 8.4 (s, CONH), 9.2 (s, CONH). ¹³C NMR (DMSO-d₆), δ (ppm): 170-175 (-OCONH of urethane), 168 (C=O ester), 135 (aromatic), 68 (CH), 32 (CH₂), 18 (CH₃).

PuP10-PuP12: FTIR (KBr), ν_{max} (cm⁻¹): 3320 (-NH of urethanes), 2900-2800 (CH₂ of chromophore and isomannide), 1725-1730 (C=O group of urethane formed by chromophore), 1710-1720 (C=O group formed by isomannide), 1602 (-N=N-), 1454 (CH bend of CH₂ group), 1415 (-CN str. of urethane), 1540, 1350 (-NO₂ group), 1220-1230 (-C-O-C- str of isomannide unit, -C-O-C- in polyurethane), 1050-1120 (C-O str vibrations of urethanes attached to phenyl group). ¹H NMR (DMSO-d₆), δ (ppm): 10.4 (s, -OCONH- para to CH₃ of TDI), 9.4 (s, -OCONH-

ortho to CH_3 of TDI), 6.6-8.8 (m, aromatic protons), 5.2 (m, $-\text{CH}$ in isomannide unit), 4.3-4.5 (t, $-\text{CH}$ bridge protons of isomannide unit), 4 (q, $-\text{CH}_2-$ in isomannide unit), 2.95 (s, CH_2 of $\text{Ph}-\text{CH}_2-\text{Ph}$), 2.4 (s, $-\text{CH}_3$ of TDI). ^{13}C NMR ($\text{DMSO}-d_6$), δ (ppm): 178-170 (ester carbonyl in $-\text{OCONH}-$ of urethane ortho and para to $-\text{CH}_3$ of TDI), 130-165 (aromatic ring carbons), 80-82 ($-\text{CH}-$ bridge of isomannide unit), 75-78 ($-\text{CH}-$ of isosorbide unit), 40-42 ($-\text{CH}_2-$ of isomannide unit), 32 (methylene of chromophore), 18 ($-\text{CH}_3$ of TDI).

PuP13: FTIR (KBr), ν_{max} (cm^{-1}): 3290 ($-\text{NH}$ stretching of urethanes), 3000- 2850 (sp^3 C-H stretching in isomannide unit), 1715 ($\text{C}=\text{O}$ stretching in urethane formed by isomannide), 1537 (NH bend), 1451 (C-H bend of $-\text{CH}_2$ group in isomannide), 1415 ($-\text{CN}$ stretching of urethane) 1230 (C-O stretching of isomannide unit), 1055-1125 (C-O stretching vibrations of urethanes attached to phenyl group). ^1H NMR ($\text{DMSO}-d_6$), δ (ppm): 2.4-2.5 (s, $-\text{CH}_3$ of TDI), 4.1 (q, $-\text{CH}_2$ in isomannide unit), 4.3- 4.5 (t, $-\text{CH}-$ bridge protons of isomannide unit), 5.1 (m, $-\text{CH}$ in isomannide unit), 7.5 -8.2 (m, aromatic protons of TDI), 9.8 (s, $-\text{CONH}-$ ortho to the $-\text{CH}_3$ of TDI), 10.5 (s, $-\text{CONH}-$ para to the $-\text{CH}_3$ of TDI). ^{13}C NMR ($\text{DMSO}-d_6$), δ (ppm): 170-175 (ester carbonyl in $-\text{OCONH}-$ of urethane ortho and para to the $-\text{CH}_3$ of TDI), 130-155 (aromatic ring carbons), 68 ($-\text{CH}-$ bridge of isomannide unit), 32-35 ($-\text{CH}_2-$ isomannide unit), 18 ($-\text{CH}_3$ of TDI).

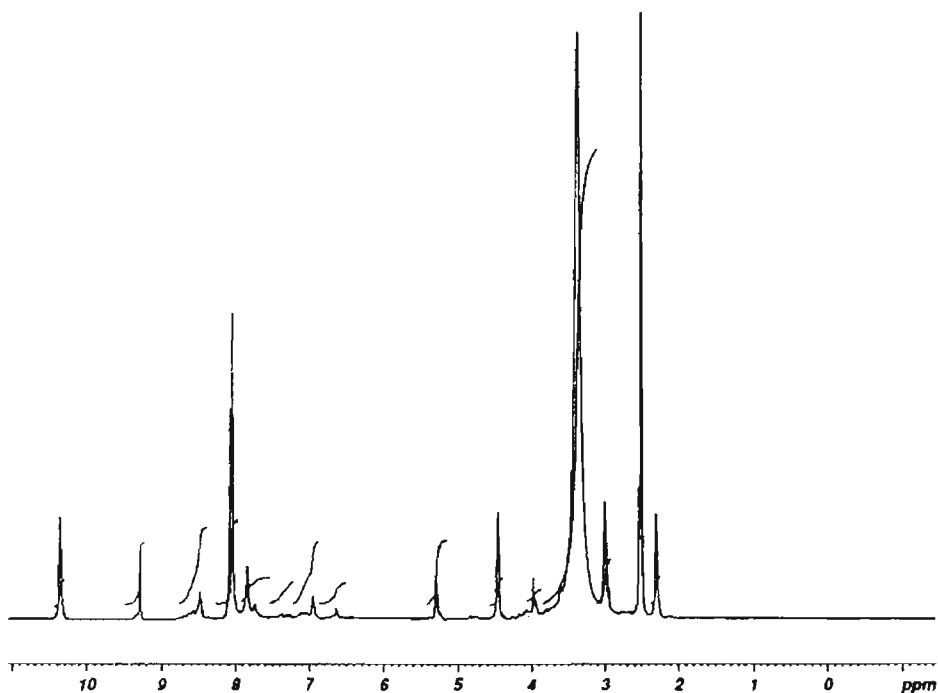


Figure 5. 5: ^1H NMR spectra of PuP2-PuP4

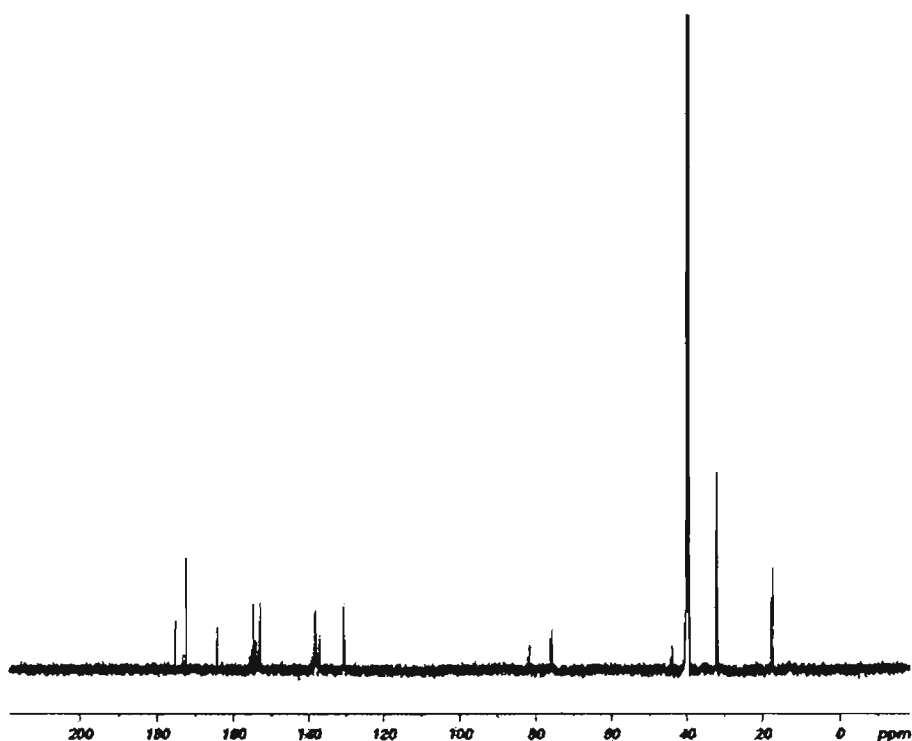


Figure 5. 6: ^{13}C NMR spectra of PuP2-PuP4

The molecular weight of the polyurethanes were analysed by using the MALDI mass spectrometry. From the spectrum it was found that the molecular weight of multifunctional polyurethanes were observed in the range 18000-19000, where the molecular weight of one repeating unit possess 900-1100, which confirmed the proposed structure consisting of almost 18-22 repeating units.

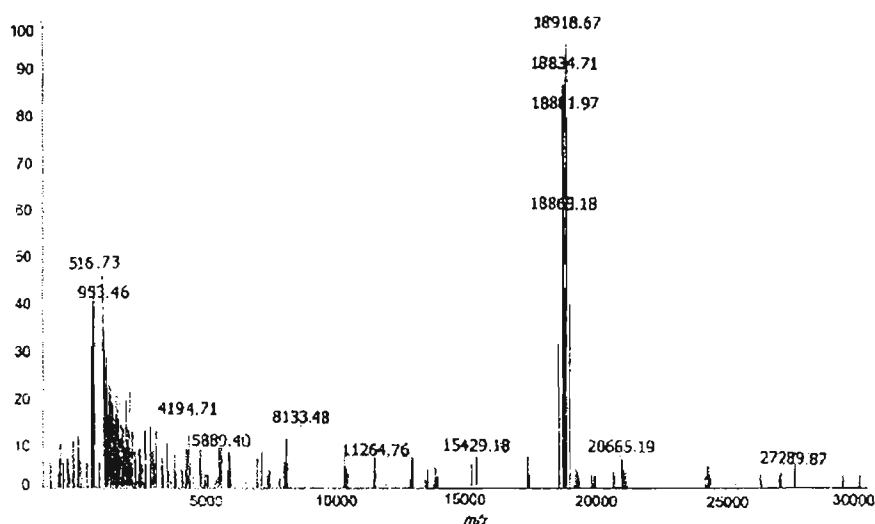


Figure 5. 7: MALDI MS of PuP2 polyurethane

Figure 5. 7. represent the MALDI MS of PuP2 polyurethane, which possess a molecular weight of 18918 with 992 for each repeating unit (19 repeating units).

5. 6. 3: Absorption spectrum

The UV-Visible absorption spectra of the polyurethanes were determined in DMAc. All multifunctional polyurethanes showed characteristic bands of nitro group at 275-285 nm ($n \rightarrow \pi^*$) and azo group ($\pi \rightarrow \pi^*$) at 380-400 nm. The peak positions in the UV-Vis absorption of polyurethanes were found to be similar to those of the corresponding chromophores. These results suggest that polar properties of chromophore part are not much decreased by polymerization process. However the absorption band due to the urethane carbonyl could not be observed. This might be due either to overlapping between the carbonyl and the nitro absorption or shortening of the absorption wavelength.

5. 6. 4. Fluorescence spectrum

For all the samples the excitation wavelengths and emission wavelengths were recorded in the fluorescence spectrum by putting the proper absorbance wavelengths and excitation wavelengths. The excitation wavelengths of multifunctional polymers were found to be between 440-455 nm and emission spectra in the range of 500-510 nm. The emission λ_{\max} values are reported in Table 5. 5.

5. 6. 5. Optical rotation

The polyurethanes (**PuP2-PuP13**) synthesized had optically active monomers (**IS**, **DT** and **IM**). The optical activity of **PuP2-PuP5** polymers, increased when chiral diol (**IS**) molecules were incorporated. The specific rotation $[\alpha]_D$ values measured for polymers varied from 30° to 43°. The polyurethanes **PuP6-PuP9** synthesized contained (2R, 3R)-diethyl tartrate (**DT**) as the optically active monomer. The optical activity of polymers increased with the increase in % incorporation of **DT** molecules. The specific rotation $[\alpha]_D$ values measured for polymers observed in the range 32° to 43°. For the **PuP10-PuP13** polymers, isomannide (**IM**) was taken as the optically active monomer for the synthesis, the activity of polymers was much higher compared to that of

isosorbide and diethyl tatrtrate due to the larger optical activity of **IM**. The polymers exhibited $[\alpha]_D$ values in between 65° to 84° . The $[\alpha]_D$ value increased with the increase in the % of chiral component. Low value of $[\alpha]_D$ is due to the low % incorporation of chiral diol. The polyurethane without chiral molecules **PuP1** shows zero specific rotation. The specific rotations of the polyurethanes are shown in **Table 5. 5**. Relatively high values of specific rotation near to the specific rotation of optically active monomers were observed indicating that no extensive racemization occurred during the polymerization stage¹³⁻¹⁵.

Table 5. 5: Optical and thermal properties of Polyurethanes (PuP1- PuP13)

Polymer	% of chiral diol	Specific rotation ($[\alpha]_D^0$)	Absorption $\lambda_{\max}(\text{nm})$	Emission $\lambda_{\max}(\text{nm})$	IDT ($^\circ\text{C}$)	T _g ($^\circ\text{C}$)	Refractive index
PuP1	0	0	398	506	200	142	1.5628
PuP2	25	30	392	504	280	155	1.5244
PuP3	50	38	390	500	289	161	1.5353
PuP4	75	40	389	501	300	168	1.5367
PuP5	100	43	270	403	190	105	1.5302
PuP6	25	32	389	501	285	158	1.5202
PuP7	50	35	387	504	292	161	1.5249
PuP8	75	38	384	500	299	165	1.5279
PuP9	100	43	272	346	190	101	1.5257
PuP10	25	65	393	505	295	155	1.5807
PuP11	50	72	390	504	299	165	1.5892
PuP12	75	78	388	501	305	170	1.5921
PuP13	100	84	269	401	180	125	1.5802

5. 6. 6. Refractive index

For the refractive index measurements, distilled water was taken as the reference which was having the refractive index-1.33. The refractive index of the polymer samples lie in the range 1.52-1.60 which are shown in **Table 5. 5**.

5. 6. 7. Thermal characterization

Thermal properties of the polyurethanes were examined by TG and DTA measurements. The polymer samples with chromophore alone exhibited a two

step degradation pattern while all other polymers with chiral diols exhibited a single step pattern. The initial weight loss of multifunctional polymers in the 280-305°C region may be due to the decomposition of azobenzene (N=N) double bonds and polyurethane back bone. Earlier studies on the thermal properties of polyurethanes demonstrated clearly that the cleavage of C-N bonds in the C-N=N-C group occurred in latter decomposition steps. All the polymers showed residual weight of more than 40% at 800°C in nitrogen atmosphere due to the presence of high percentage of aromatic rings in the polymer structure. From DTA, it was observed that glass transition temperature for the multifunctional polymers were in the range of 155-170°C. Polyurethanes containing chromophore alone exhibited relatively higher T_g values compared to those of polyurethanes containing chiral monomers. Hence polyurethanes with main chain azo chromophore obviously showed better thermal stability than those of polyurethanes containing chiral monomers. Among the chiral multifunctional polymers the isomannide incorporated polyurethanes possessed high thermal stability. The T_g and initial decomposition values are shown in **Table 5. 5**.

5. 6. 8. SHG Efficiency

The nonlinear optical properties of the polyurethanes were studied in powder form by Kurtz Perry powder techniques²⁴. The SHG responses of the samples were recorded using urea and KDP as references. The second harmonic signal generated by the polymer was confirmed by the emission of green radiation from the polymer. As expected from the electronic structure of the polymers, they showed much higher SHG efficiency.

Table 5. 6: SHG efficiency of polymers

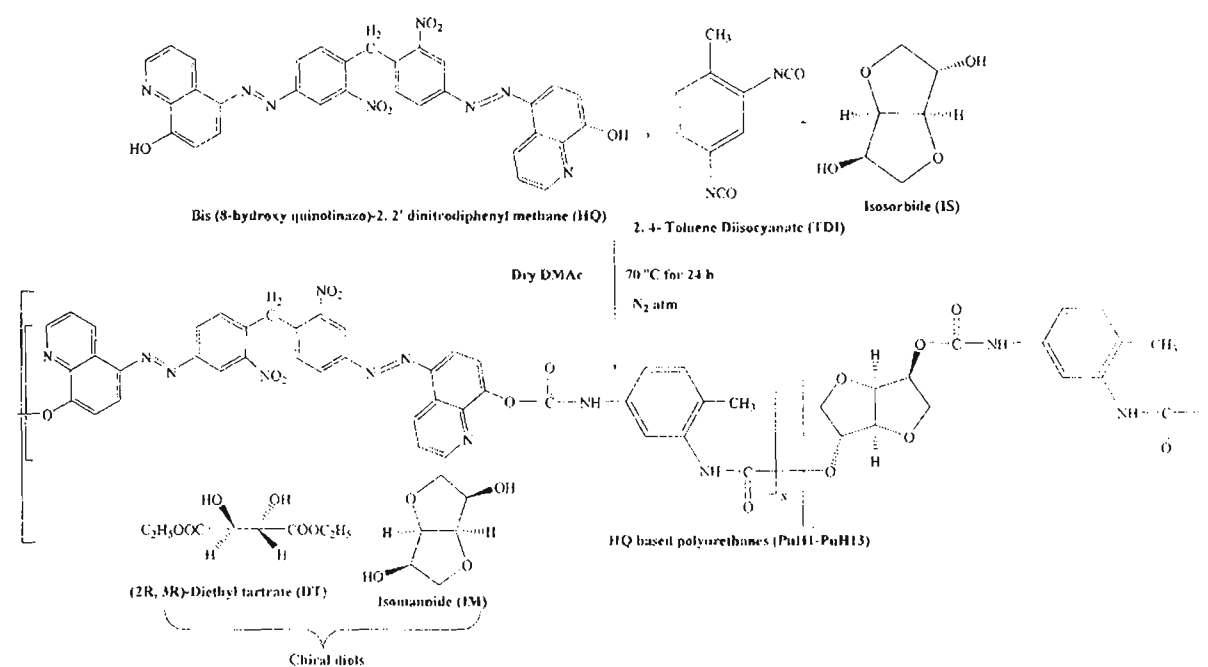
Polymer	SHG efficiency w. r. to urea (%)	SHG efficiency w. r. to KDP (%)
PuP1	5.35	46.64
PuP2- PuP4	9.84	87.5
PuP6- PuP8	10.63	94.45
PuP10 -PuP12	10.94	97.22
PuP5	1.72	15.28
PuP9	1.83	16.22
PuP13	2.00	17.78

Among the series of polyurethanes (PuP1-PuP13), the polymers with both chiral and chromophore groups showed much higher efficiency compared to bifunctional polymers. PuP2-PuP4, PuP6-PuP8 and PuP10-PuP12 systems had about 9.84%, 10.63% and 10.94% efficiency respectively that of urea, whereas, it showed efficiency of 87.5%, 94.45% and 97.22% respectively with KDP. The multifunctional polymers with high percentage of chromophore (75%) showed higher NLO activity. Even if there is an absence of π -conjugation in donor-acceptor systems, the polyurethane systems show considerable NLO activity. The bifunctional polymers PuP5 PuP9 and PuP13 showed much less SHG efficiency compared to PuP1. The chromophore incorporated bifunctional polymer PuP1, possessed high activity (5.35% w. r. to urea and 46.64% w. r. to KDP) due to the presence of highly delocalized electrons. The multifunctional polyurethanes synthesized with isomannide moiety possessed high SHG response as predicted in the theoretical results.

5. 7. POLYURETHANES WITH BIS (8-HYDROXY QUINOLINAZO)-2, 2' DINITRODIPHENYLMETHANE CHROMOPHORE

5. 7. 1. Experimental discussion

The polymer PuH1 is the one which has only HQ chromophore unit in polymer chain and considered as the mother polymer in the series.



Scheme 5. 6: Synthesis of polyurethanes

For PuH1, the ratio of TDI and HQ are taken as 1:1. PuH2, PuH3, PuH4 and PuH5 are the polyurethanes with IS chiral diol having the TDI: HQ: IS ratio as 1:0.75:0.25 (PuH2), 1:0.5:0.5 (PuH3), 1:0.25:0.75 (PuH4), 1:0:1 (PuH5), respectively. PuH6, PuH7, PuH8 and PuH9 are the polyurethanes with DT chiral diol in which TDI: HQ: DT ratio is maintained as 1:0.75:0.25 (PuH6), 1:0.5:0.5 (PuH7), 1:0.25:0.75 (PuH8), 1:0:1 (PuH9), respectively. PuH10, PuH11, PuH12 and PuH13 are the polyurethanes with IM chiral diol having the ratio of TDI: HQ: IM as 1:0.75:0.25 (PuH10), 1:0.5:0.5 (PuH11), 1:0.25:0.75 (PuH12), 1:0:1 (PuH13), respectively.

5.7.2. Spectral Characterization

PuH1: FTIR (KBr), ν_{\max} (cm^{-1}): 3318 (-NH), 2923, 2853 (-CH₂-), 1667 (urethane carbonyl), 1602 (-N=N-), 1531, 1347 (-NO₂), 1233 (-C-O-C- in -COOC of PU). **¹H NMR (DMSO-d₆), δ (ppm):** 10.6 (1H(s), -OCONH- para to the CH₃ of TDI), 9 (1H(s), -OCONH-ortho to the CH₃ of TDI), 8.77 (2H(s), phenyl), 8.2 (2H(d), phenyl), 8(2H(d), phenyl), 8.47 (4H(d), phenyl), 8.15 (4H(d), phenyl), 7, 6.8, 6.6 (aromatic protons of TDI), 2.4 (3H(s), CH₃ of TDI), 2.95 (2H (s), Ph-CH₂-Ph). **¹³C NMR (DMSO-d₆), δ (ppm):** 173-174 (-OCONH, ortho and para to the CH₃ of TDI), 121, 125, 127, 135, 137, 139, 144, 152, 153, 170 (aromatic), 122-137 (C1-C6 of TDI), 38 (methylene), 18 (CH₃ of TDI)

PuH2-PuH4: FTIR (KBr), ν_{\max} (cm^{-1}): 3320 (-NH of urethanes), 2900-2800 (CH₂ of chromophore and isosorbide), 1725-1730 (C=O group of urethane formed by chromophore), 1710-1720 (C=O group formed by isosorbide), 1602 (-N=N-), 1454 (CH bend of CH₂ group), 1415 (-CN str. of urethane), 1540,1350 (-NO₂ group), 1220-1230 (-C-O-C- str of isosorbide unit, -C-O-C- in polyurethane), 1050-1120 (C-O str vibrations of urethanes attached to phenyl group). **¹H NMR (DMSO-d₆), δ (ppm):** 10.4 (s, -OCONH- para to CH₃ of TDI), 9.4 (s, -OCONH- ortho to CH₃ of TDI), 6.6-8.8 (m, aromatic protons), 5.2 (m, -CH in isosorbide unit), 4.3-4.5 (t, -CH bridge protons of isosorbide unit), 4 (q, -CH₂- in isosorbide unit), 2.95 (s, CH₂ of Ph-CH₂-Ph), 2.4 (s, -CH₃ of TDI). **¹³C NMR (DMSO-d₆), δ (ppm):** 178-170 (ester carbonyl in -OCONH- of urethane ortho and para to -CH₃ of TDI), 130-165 (aromatic ring carbons), 80-82 (-CH- bridge of isosorbide unit), 75-78 (-CH- of isosorbide unit), 40-42 (-CH₂- of isosorbide unit), 32 (methylene of chromophore), 18 (-CH₃ of TDI).

PuH5: FTIR (KBr), ν_{\max} (cm^{-1}): 3290 (-NH stretching of urethanes), 3000-2850 (sp^3 C-H stretching in isosorbide unit), 1715 (C=O stretching in urethane formed by isosorbide); 1451 (C-H bend of $-\text{CH}_2$ group in isosorbide), 1415 (-CN stretching of urethane) 1230 (C-O stretching of isosorbide unit), 1055-1125 (C-O stretching vibrations of urethanes attached to phenyl group). ^1H NMR (DMSO- d_6), δ (ppm): 2.4-2.5 (s, $-\text{CH}_3$ of TDI), 4.1 (q, $-\text{CH}_2$ in isosorbide unit), 4.3-4.5 (t, $-\text{CH}-$ bridge protons of isosorbide unit), 5.1 (m, $-\text{CH}$ in isosorbide unit), 7.5-8.2 (m, aromatic protons of TDI), 9.8 (s, $-\text{CONH}-$ ortho to the $-\text{CH}_3$ of TDI), 10.5 (s, $-\text{CONH}-$ para to the $-\text{CH}_3$ of TDI). ^{13}C NMR (DMSO- d_6), δ (ppm): 170-175 (ester carbonyl in $-\text{OCONH}-$ of urethane ortho and para to the $-\text{CH}_3$ of TDI), 130-160 (aromatic ring carbons), 80-82 ($-\text{CH}-$ bridge of isosorbide unit), 75-78 ($-\text{CH}-$ of isosorbide unit), 40-42 ($-\text{CH}_2-$ isosorbide unit), 18 ($-\text{CH}_3$ of TDI).

PuH6-PuH8: FTIR (KBr), ν_{\max} (cm^{-1}): 3280-3000 (-NH str. of urethanes), 3000-2890 (CH str. of DT and chromophore), 1736-1740 (C=O formed by chromophore), 1725-1730 (C=O formed by DT), 1720-1722 (C=O str in DT), 1608 (-N=N-), 1539, 1345 ($-\text{NO}_2$ group), 1468, 1390 ($-\text{CH}$ bend), 1100 ($-\text{C}-\text{O}-\text{C}-$ of urethane), ^1H NMR (DMSO- d_6), δ (ppm): 10 (s, $-\text{OCONH}-$ para to CH_3 of TDI), 9.3 (s, $-\text{OCONH}-$ ortho to CH_3 of TDI), 7.2-8.5 (m, aromatic protons), 4.8 (s, CH), 4.1-4.3 (q, CH_2), 2.95 (Ph- CH_2 -Ph), 2.5 (s, CH_3), 1.2 (t, CH_3). ^{13}C NMR (DMSO- d_6), δ (ppm): 172-176 ($-\text{OCONH}-$ ortho and para to the CH_3 of TDI), 169 (C=O of ester), 135-160 (aromatic carbons), 68 (CH), 32 (CH_2), 18 (CH_3)

PuH9: FTIR (KBr), ν_{\max} (cm^{-1}): 3270-3300 (NH str.), 3000-2890 (sp^3 CH str.), 1736-1740, 1720-1725 (C=O str.), 1537 (NH bend), 1468, 1380 ($-\text{CH}$ bend), 1055-1125 (C-O str. of urethane). ^1H NMR (DMSO- d_6), δ (ppm): 1.2 (t, CH_3), 2.5 (s, CH_3), 4.1-4.3 (q, CH_2), 4.8 (s, CH), 7.2-7.6 (m, aromatic), 8.4 (s, CONH), 9.2 (s, CONH). ^{13}C NMR (DMSO- d_6), δ (ppm): 170-175 ($-\text{OCONH}$ of urethane), 168 (C=O ester), 135 (aromatic), 68 (CH), 32 (CH_2), 18 (CH_3)

PuH10-PuH12: FTIR (KBr), ν_{\max} (cm^{-1}): 3320 (-NH of urethanes), 2900-2800 (CH_2 of chromophore and isomannide), 1725-1730 (C=O group of urethane formed by chromophore), 1710-1720 (C=O group formed by isomannide), 1602 (-N=N-), 1454 (CH bend of CH_2 group), 1415 (-CN str. of urethane), 1540, 1350 ($-\text{NO}_2$ group), 1220-1230 ($-\text{C}-\text{O}-\text{C}-$ str of isomannide unit, $-\text{C}-\text{O}-\text{C}-$ in polyurethane), 1050-1120 (C-O str vibrations of urethanes attached to phenyl group). ^1H NMR

(DMSO- d_6), δ (ppm): 10.4 (s, -OCONH- para to CH_3 of TDI), 9.4 (s, -OCONH- ortho to CH_3 of TDI), 6.6-8.8 (m, aromatic protons), 5.2 (m, -CH in isomannide unit), 4.3-4.5 (t, -CH bridge protons of isomannide unit), 4 (q, - CH_2 - in isomannide unit), 2.95 (s, CH_2 of Ph- CH_2 -Ph), 2.4 (s, - CH_3 of TDI). ^{13}C NMR (DMSO- d_6), δ (ppm): 178-170 (ester carbonyl in -OCONH- of urethane ortho and para to - CH_3 of TDI), 130-165 (aromatic ring carbons), 80-82 (-CH- bridge of isomannide unit), 75-78 (-CH- of isosorbide unit), 40-42 (- CH_2 - of isomannide unit), 32 (methylene of chromophore), 18 (- CH_3 of TDI).

PuH13: FTIR (KBr), ν_{max} (cm^{-1}): 3290 (-NH stretching of urethanes), 3000- 2850 (sp^3 C-H stretching in isomannide unit), 1715 (C=O stretching in urethane formed by isomannide), 1537 (NH bend), 1451 (C-H bend of - CH_2 group in isomannide), 1415 (-CN stretching of urethane) 1230 (C-O stretching of isomannide unit), 1055-1125 (C-O stretching vibrations of urethanes attached to phenyl group). 1H NMR (DMSO- d_6), δ (ppm): 2.4-2.5 (s, - CH_3 of TDI), 4.1 (q, - CH_2 in isomannide unit), 4.3- 4.5 (t, -CH- bridge protons of isomannide unit), 5.1 (m, -CH in isomannide unit), 7.5 -8.2 (m, aromatic protons of TDI), 9.8 (s, - CONH- ortho to the - CH_3 of TDI), 10.5 (s, -CONH- para to the - CH_3 of TDI). ^{13}C NMR (DMSO- d_6), δ (ppm): 170-175 (ester carbonyl in -OCONH- of urethane ortho and para to the - CH_3 of TDI), 130-155 (aromatic ring carbons), 68 (-CH- bridge of isomannide unit), 32-35 (- CH_2 - isomannide unit), 18 (- CH_3 of TDI).

From the MALDI-MS analysis it was found that the molecular weight of the polyurethanes synthesized were in the range 17,000-20,000 (the molecular weight of one repeating unit is 900-1100) which confirmed the proposed structure consisting of almost 19-22 repeating units.

5. 7. 3. Absorption and fluorescence spectra

The UV spectra of the chiral polyurethanes were recorded in DMAc solvent and the observed λ_{max} values are reported in Table 5. 7. All the polyurethanes studied have strong bands in the range 275-400 nm, with λ_{max} lying between 390-400 nm. The spectra exhibited characteristic bands of nitro groups (275-280 nm, $n \rightarrow \pi^*$) and azo groups (390-400 nm, $\pi \rightarrow \pi^*$). The emission λ_{max} values are shown in Table 5. 7. The multifunctional polyurethanes exhibited the characteristically sharp emissions bands in between 500-515 nm.

5.7.4. Optical rotation

The polyurethanes (**PuH2-PuH13**) synthesized contained optically active monomers (**IS**, **DT** and **IM**). The specific rotation of **PuH2-PuH5** polymers was higher when isosorbide (**IS**) molecules were incorporated. The specific rotation $[\alpha]_D$ values measured for polymers varied from 35° to 43°. The polyurethanes **PuH6-PuH9** synthesized had (2R, 3R)-diethyl tartrate (**DT**) as the optically active monomer. The specific rotation of polymers with the increase in % incorporation of **DT** molecules. The specific rotation $[\alpha]_D$ values measured for polymers were observed in the range 32° to 43°. For the **PuH10-PuH13** polymers, isomannide (**IM**) was taken as the chiral monomer for the synthesis, the activity of polymers was higher compared to that of isosorbide and diethyl tartrate due to the larger optical activity of **IM**. The polymers exhibited $[\alpha]_D$ values in between 78° to 84°. The $[\alpha]_D$ value increased with the increase in the % of chiral component. Low value of $[\alpha]_D$ was due to the low % incorporation of chiral diol. The polyurethane without chiral molecules **PuH1** showed zero specific rotation. The specific rotation of the polyurethanes is shown in **Table 5.7**. Relatively high values of specific rotation near to the specific rotation of optically active monomers were observed indicating that no extensive racemization occurred during the polymerization stage¹²⁻¹⁵.

5.7.5. Refractive index

The refractive index of the polyurethanes was measured using prism method in which distilled water (the refractive index-1.33) was taken as the reference. The refractive index of the polymer samples lie in the range 1.42-1.62 which are shown in **Table 5.7**.

5.7.6. Thermal characterization

Thermal stability of the HQ based polymers was evaluated using TG/DTA. The polyurethanes with both chiral and chromophore unit showed two thermal decompositions. The initial decomposition of multifunctional polymers in the 290-320°C region may be due to the decomposition of azobenzene (N=N) double bonds and polyurethane back bone and the second decomposition is due to the cleavage of C-N bonds. The chromophore incorporated polyurethanes show a residual weight of 45% at 800°C. The Tg

values of multifunctional polymers were observed in the range of 168-175°C. The stability is maximum for the polymers with both chiral and chromophoric diols. Due to the high thermal stability, polyurethanes containing isomannide backbone exhibited higher IDT value. Polyurethanes containing chromophore monomer alone exhibited relatively higher T_g values compared to those of polyurethanes containing chiral monomers alone. The chiral multifunctional polymers showed better thermal stability than those of bifunctional polyurethanes. The glass transition temperature and initial decomposition values are shown in Table 5. 7.

Table 5. 7: Optical and thermal properties of Polyurethanes (PuH1- PuH13)

Polymer	% of Chiral diol	Specific rotation ($[\alpha]_D^{20}$)	Absorption $\lambda_{max}(nm)$	Emission $\lambda_{max}(nm)$	IDT ($^{\circ}C$)	Tg ($^{\circ}C$)	Refractive index
PuH1	0	0	395	507	210	155	1.580
PuH2	25	35	396	508	298	172	1.584
PuH3	50	38	394	503	295	168	1.589
PuH4	75	41	390	505	290	168	1.582
PuH5	100	43	270	403	190	105	1.530
PuH6	25	32	394	505	309	173	1.608
PuH7	50	38	394	508	305	170	1.603
PuH8	75	42	389	503	298	169	1.596
PuH9	100	43	272	346	190	101	1.526
PuH10	25	78	398	515	320	175	1.621
PuH11	50	80	395	508	315	172	1.604
PuH12	75	83	393	505	308	169	1.618
PuH13	100	84	269	401	180	125	1.580

5.7.7. SHG Efficiency

Kurtz Perry powder technique²⁴ was used for SHG efficiency measurement. The SHG responses of these samples were recorded using urea and KDP as references. Due to the presence of D-A chromophore, PuH1 possesses high activity as 62.34% w. r. to KDP. Among the series of polyurethanes (PuH1-PuH13), the polymers with both chiral and chromophore

groups showed high efficiency compared to bifunctional polymers. PuH2-PuH4, PuH6-PuH8 and PuH10-PuH12 systems had about 10.16%, 10.78% and 11.09% efficiency respectively that of urea, whereas it showed an efficiency of 90.28%, 95.83% and 98.61% respectively with KDP. The multifunctional polymers with 75% of chromophore possessed high SHG activity. The bifunctional polymers PuH5, PuH9 and PuH13 showed much less SHG efficiency nearly to 1-2% of SHG compared to urea and 15-18% as that of KDP. The multifunctional polyurethanes synthesized with isomannide moiety possessed high SHG activity as predicted in the theoretical results.

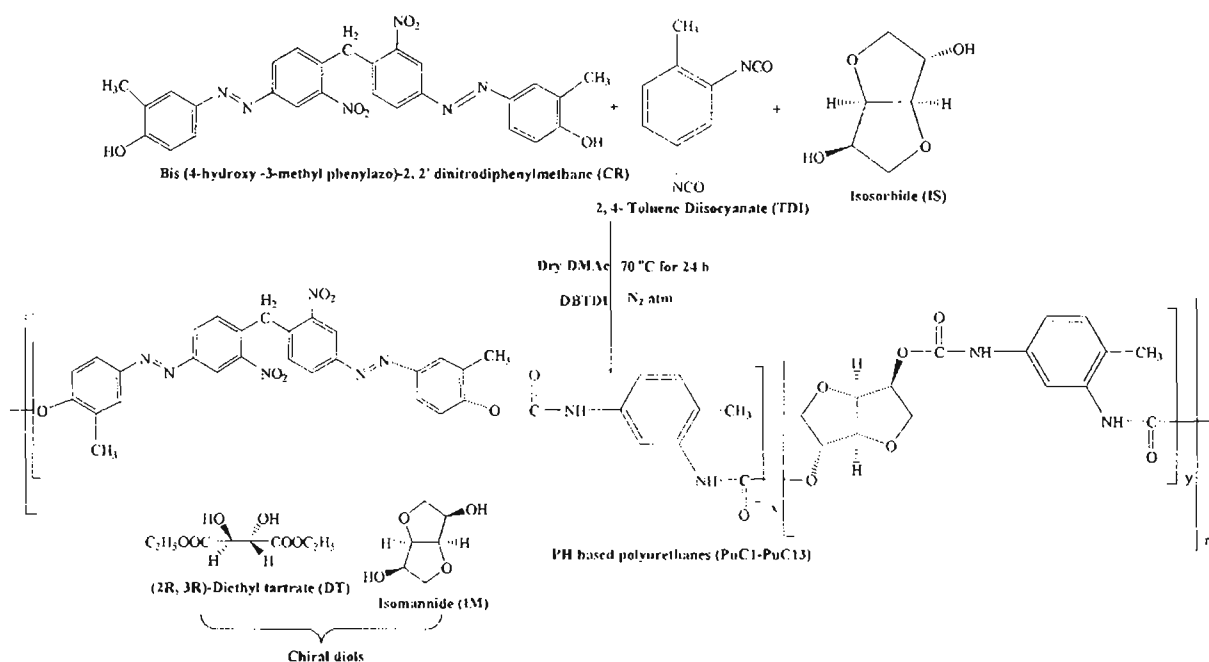
Table 5. 8: SHG efficiency of polymers

Polymer	SHG efficiency w. r. to urea (%)	SHG efficiency w. r. to KDP (%)
PuH1	7.02	62.34
PuH2- PuH4	10.16	90.28
PuH6- PuH8	10.78	95.83
PuH10 -PuH12	11.09	98.61
PuH5	1.72	15.28
PuH9	1.83	16.22
PuH13	2.00	17.78

5. 8. POLYURETHANES WITH BIS (4-HYDROXY-3-METHYLPHENYLAZO)-2, 2'- DINITRODIPHENYLMETHANE CHROMOPHORE

5. 8. 1. Experimental discussion

The polymer PuC1 is the one which has the CR chromophoric moiety in the polymer chain and considered as the mother polymer in the series. For PuC1, the ratio of TDI and CR are taken as 1:1. PuC2, PuC3, PuC4 and PuC5 are the polyurethanes with IS chiral diol having the TDI: CR: IS ratio as 1:0.75:0.25 (PuC2), 1:0.5:0.5 (PuC3), 1:0.25:0.75 (PuC4), 1:0:1 (PuC5), respectively. PuC6, PuC7, PuC8 and PuC9 are the polyurethanes with DT chiral diol in which TDI: CR: DT ratio is maintained as 1:0.75:0.25 (PuC6), 1:0.5:0.5 (PuC7), 1:0.25:0.75 (PuC8), 1:0:1 (PuC9), respectively. PuC10, PuC11, PuC12 and PuC13 are the polyurethanes with IM chiral diol having the ratio of TDI: CR: IM as 1:0.75:0.25 (PuC10), 1:0.5:0.5 (PuC11), 1:0.25:0.75 (PuC12), 1:0:1 (PuC13), respectively.



Scheme 5. 7: Synthesis of polyurethanes (PuC1-PuC13)

5. 8. 2. Spectral characterization

PuC1: FTIR (KBr), ν_{\max} (cm^{-1}): 3340 (N-H), 2924, 2854 ($-\text{CH}_2-$), 1686 (urethane carbonyl), 1620 ($-\text{N}=\text{N}-$), 1532, 1351 ($-\text{NO}_2$), 1244 ($-\text{C}-\text{O}-\text{C}-$ in $-\text{COOC}$ of PU). ^1H NMR ($\text{DMSO}-d_6$), δ (ppm): 10.6 (1H, $-\text{OCONH}$ para to the CH_3 of TDI), 9 (1H, $-\text{OCONH}$ -ortho to the CH_3 of TDI), 8.77 (2H, phenyl), 8.2 (2H, phenyl), 8 (2H, phenyl), 8.37 (2H, phenyl), 8.1 (2H, phenyl), 7, 6.8, 6.6 (aromatic protons of TDI), 2.95 (2H, $\text{Ph}-\text{CH}_2-\text{Ph}$), 2.4 (3H, CH_3 of TDI), 2.29 (6H, two CH_3). ^{13}C NMR ($\text{DMSO}-d_6$), δ (ppm): 174-179 ($-\text{OCONH}$, ortho and para to the CH_3 of TDI), 122, 128, 130, 131, 135, 137, 139, 146, 152, 154, 170, (aromatic), 32 (methylene), 20 (methyl), 18 (CH_3 of TDI)

PuC2-PuC4: FTIR (KBr), ν_{\max} (cm^{-1}): 3320 ($-\text{NH}$ of urethanes), 2900-2800 (CH_2 of chromophore and isosorbide), 1725-1730 ($\text{C}=\text{O}$ group of urethane formed by chromophore), 1710-1720 ($\text{C}=\text{O}$ group formed by isosorbide), 1602 ($-\text{N}=\text{N}-$), 1454 (CH bend of CH_2 group), 1415 ($-\text{CN}$ str. of urethane), 1540, 1350 ($-\text{NO}_2$ group), 1220-1230 ($-\text{C}-\text{O}-\text{C}-$ str of isosorbide unit, $-\text{C}-\text{O}-\text{C}-$ in polyurethane), 1050-1120 ($\text{C}-\text{O}$ str vibrations of urethanes attached to phenyl group). ^1H NMR ($\text{DMSO}-d_6$), δ (ppm): 10.4 (s, $-\text{OCONH}-$ para to CH_3 of TDI), 9.4 (s, $-\text{OCONH}-$ ortho to CH_3 of TDI)

TDI), 6.6-8.8 (m, aromatic protons), 5.2 (m, -CH in isosorbide unit), 4.3-4.5 (t, -CH bridge protons of isosorbide unit), 4 (q, -CH₂- in isosorbide unit), 2.95 (s, CH₂ of Ph-CH₂-Ph), 2.4 (s, -CH₃ of TDI). ¹³C NMR (DMSO-d₆), δ (ppm): 178-170 (ester carbonyl in -OCONH- of urethane ortho and para to -CH₃ of TDI), 130-165 (aromatic ring carbons), 80-82 (-CH- bridge of isosorbide unit), 75-78 (-CH- of isosorbide unit), 40-42 (-CH₂- of isosorbide unit), 32 (-CH₂ of chromophore), 18 (-CH₃ of TDI).

PuC5: FTIR (KBr), ν_{max} (cm⁻¹): 3290 (-NH stretching of urethanes), 3000-2850 (sp³ C-H stretching in isosorbide unit), 1715 (C=O stretching in urethane formed by isosorbide), 1451 (C-H bend of -CH₂ group in isosorbide), 1415 (-CN stretching of urethane) 1230 (C-O stretching of isosorbide unit), 1055-1125 (C-O stretching vibrations of urethanes attached to phenyl group). ¹H NMR (DMSO-d₆), δ (ppm): 2.4-2.5 (s, -CH₃ of TDI), 4.1 (q, -CH₂ in isosorbide unit), 4.3-4.5 (t, -CH- bridge protons of isosorbide unit), 5.1 (m, -CH in isosorbide unit), 7.5-8.2 (m, aromatic protons of TDI), 9.8 (s, -CONH- ortho to the -CH₃ of TDI), 10.5 (s, -CONH- para to the -CH₃ of TDI). ¹³C NMR (DMSO-d₆), δ (ppm): 170-175 (ester carbonyl in -OCONH- of urethane ortho and para to the -CH₃ of TDI), 130-160 (aromatic ring carbons), 80-82 (-CH- bridge of isosorbide unit), 75-78 (-CH- of isosorbide unit), 40-42 (-CH₂- isosorbide unit), 18 (-CH₃ of TDI).

PuC6-PuC8: FTIR (KBr), ν_{max} (cm⁻¹): 3280-3000 (-NH str. of urethanes), 3000-2890 (CH str. of DT and chromophore), 1736-1740 (C=O formed by chromophore), 1725-1730 (C=O formed by DT), 1720-1722 (C=O str in DT), 1608 (-N=N-), 1539, 1345 (-NO₂ group), 1468, 1390 (-CH bend), 1100 (-C-O-C- of urethane), ¹H NMR (DMSO-d₆), δ (ppm): 10 (s, -OCONH- para to CH₃ of TDI), 9.3 (s, -OCONH- ortho to CH₃ of TDI), 7.2-8.5 (m, aromatic protons), 4.8 (s, CH), 4.1-4.3 (q, CH₂), 2.95 (Ph-CH₂-Ph), 2.5 (s, CH₃), 1.2 (t, CH₃). ¹³C NMR (DMSO-d₆), δ (ppm): 172-176 (-OCONH- ortho and para to the CH₃ of TDI), 169 (C=O of ester), 135-160 (aromatic carbons), 68 (CH), 32 (CH₂), 18 (CH₃)

PuC9: FTIR (KBr), ν_{max} (cm⁻¹): 3270-3300 (NH str.), 3000-2890 (sp³ CH str.), 1736-1740, 1720-1725 (C=O str.), 1537 (NH bend), 1468, 1380 (-CH bend), 1055-1125 (C-O str. of urethane). ¹H NMR (DMSO-d₆), δ (ppm): 1.2 (t, CH₃), 2.5 (s, CH₃), 4.1-4.3 (q, CH₂), 4.8 (s, CH), 7.2-7.6 (m, aromatic), 8.4 (s, CONH), 9.2 (s, CONH). ¹³C

NMR (DMSO- d_6), δ (ppm): 170-175 (-OCONH of urethane), 168 (C=O ester), 135 (aromatic), 68 (CH), 32 (CH₂), 18 (CH₃)

PuC10-PuC12: FTIR (KBr), ν_{\max} (cm⁻¹): 3320 (-NH of urethanes), 2900-2800 (CH₂ of chromophore and isomannide), 1725-1730 (C=O group of urethane formed by chromophore), 1710-1720 (C=O group formed by isomannide), 1602 (-N=N-), 1454 (CH bend of CH₂ group), 1415 (-CN str. of urethane), 1540, 1350 (-NO₂ group), 1220-1230 (-C-O-C- str of isomannide unit, -C-O-C- in polyurethane), 1050-1120 (C-O str vibrations of urethanes attached to phenyl group). **¹H NMR (DMSO- d_6), δ (ppm):** 10.4 (s, -OCONH- para to CH₃ of TDI), 9.4 (s, -OCONH- ortho to CH₃ of TDI), 6.6-8.8 (m, aromatic protons), 5.2 (m, -CH in isomannide unit), 4.3-4.5 (t, -CH bridge protons of isomannide unit), 4 (q, -CH₂- in isomannide unit), 2.95 (s, CH₂ of Ph-CH₂-Ph), 2.4 (s, -CH₃ of TDI). **¹³C NMR (DMSO- d_6), δ (ppm):** 178-170 (ester carbonyl in -OCONH- of urethane ortho and para to -CH₃ of TDI), 130-165 (aromatic ring carbons), 80-82 (-CH- bridge of isomannide unit), 75-78 (-CH- of isosorbide unit), 70-72 (-CH₂- of isomannide unit), 32 (-CH₂ of chromophore), 18 (-CH₃ of TDI).

PuC13: FTIR (KBr), ν_{\max} (cm⁻¹): 3290 (-NH stretching of urethanes), 3000- 2850 (sp³ C-H stretching in isomannide unit), 1715 (C=O stretching in urethane formed by isomannide), 1537 (NH bend), 1451 (C-H bend of -CH₂ group in isomannide), 1415 (-CN stretching of urethane) 1230 (C-O stretching of isomannide unit), 1055-1125 (C-O stretching vibrations of urethanes attached to phenyl group). **¹H NMR (DMSO- d_6), δ (ppm):** 2.4-2.5 (s, -CH₃ of TDI), 4.1 (q, -CH₂ in isomannide unit), 4.3- 4.5 (t, -CH- bridge protons of isomannide unit), 5.1 (m, -CH in isomannide unit), 7.5 -8.2 (m, aromatic protons of TDI), 9.8 (s, -CONH- ortho to the -CH₃ of TDI), 10.5 (s, -CONH- para to the -CH₃ of TDI). **¹³C NMR (DMSO- d_6), δ (ppm):** 170-175 (ester carbonyl in -OCONH- of urethane ortho and para to the -CH₃ of TDI), 130-155 (aromatic ring carbons), 68 (-CH- bridge of isomannide unit), 32-35 (-CH₂- isomannide unit), 18 (-CH₃ of TDI).

From the MALDI-MS analysis it was found that the molecular weight of the polyurethanes synthesized were in the range 18,000-19,000 (the molecular weight of one repeating unit is 900-1100) which confirmed the proposed structure consisting of almost 18-22 repeating units.

5. 8. 3. Absorption spectra and fluorescence spectra

The UV-Vis spectra of polyurethanes showed the absorption bands attributed to the aromatic moiety and the azo conjugated unit ($\pi \rightarrow \pi^*$) in 385-395 nm range. In addition to the $\pi \rightarrow \pi^*$ transition one lower intense $n \rightarrow \pi^*$ transition of nitro group is also observed in 270-280 nm. The polymers exhibit an excitation λ_{\max} of 450-460 nm. The fluorescence emission λ_{\max} of corresponding azo polymers were observed in 499-510 nm range which falls in the green region of visible spectrum. The λ_{\max} values of absorption and emission spectra are shown in Table 5. 9.

5. 8. 4. Optical rotation

The polyurethanes (**PuC2-PuC13**) synthesized contained optically active monomers (**IS**, **DT** and **IM**). The specific rotation of **PuC2-PuC5** polymers, was higher when isosorbide (**IS**) molecules were incorporated. The specific rotation $[\alpha]_D$ values measured for polymers varied from 28° to 43° . The polyurethanes **PuC6-PuC9** synthesized had (2R, 3R)-diethyl tartrate (**DT**) as the optically active monomer. The specific rotation of polymers increased with the increase in % incorporation of **DT** molecules. The specific rotation $[\alpha]_D$ values measured for polymers were observed in the range 34° to 43° . For the **PuC10-PuC13** polymers, isomannide (**IM**) was taken as the specific rotation monomer for the synthesis, the activity of polymers was higher compared to that of isosorbide and diethyl tartrate due to the higher specific rotation of **IM**. The polymers exhibited $[\alpha]_D$ values in between 49° to 84° . The $[\alpha]_D$ value increased with the increase in the % of chiral component. The polyurethane without chiral molecules **PuC1** showed zero specific rotation. The specific rotation of the polyurethanes are shown in Table 5. 9. Relatively high values of specific rotation near to the specific rotation of optically active monomers were observed indicating that no extensive racemization occurred during the polymerization stage.¹²⁻¹⁵

5. 8. 5. Refractive index

The refractive index of the polyurethanes was measured by the prism method, in which distilled water (the refractive index-1.33) was taken as the reference. The refractive index of the polymer samples lie in the range 1.53-1.60, which are shown in Table 5. 9.

5. 8. 6. Thermal characterization

All the multifunctional polymers are thermally stable upto 300°C in contrast to bifunctional polyurethanes which decompose around 180-195°C. A two step degradation was observed; a small decomposition at 300°C followed by a significant decomposition at 500°C. Among the polyurethanes, the polymer with isomannide moiety exhibited higher T_g values in comparison with those of the IS and DT containing polymers. The π -delocalization causes the increase in thermal stability of polyurethanes due to the chain rigidity caused by the incorporation aromatic system in the form of chromophore. The isomannide based polyurethanes also possess high T_g values which is reflected in the NLO activity. The IDT and T_g values are reported in Table 5. 9.

Table 5. 9: Optical and thermal properties of Polyurethanes (PuC1- PuC13)

Polymer	% of Chiral diol	Specific rotation ($[\alpha]_D^{20}$)	Absorption $\lambda_{max}(nm)$	Emission $\lambda_{max}(nm)$	IDT ($^{\circ}C$)	Tg ($^{\circ}C$)	Refractive Index
PuC1	0	0	388	490	195	145	1.567
PuC2	25	28	392	505	306	160	1.545
PuC3	50	32	390	499	300	155	1.549
PuC4	75	37	386	502	308	150	1.536
PuC5	100	43	270	403	190	105	1.530
PuC6	25	34	389	501	298	158	1.589
PuC7	50	36	390	504	304	154	1.579
PuC8	75	39	385	499	305	161	1.580
PuC9	100	43	272	346	190	101	1.526
PuC10	25	49	394	510	315	168	1.589
PuC11	50	56	391	504	308	160	1.588
PuC12	75	59	386	501	310	162	1.594
PuC13	100	84	269	401	180	125	1.580

5. 8. 7. SHG efficiency

Kurtz Perry powder technique²⁴ was used for SHG efficiency measurement. The SHG responses of the polyurethanes were reported using urea and KDP as references. PuC1 possess a high activity as 48.02% with respect to KDP. Among the series of polyurethanes (PuC1-PuC13), the polymers with

both chiral and chromophore groups showed much higher efficiency compared to bifunctional polymers. PuC2-PuC4, PuC6-PuC8 and PuC10-PuC12 systems had about 9.06%, 9.53% and 9.84% efficiency respectively as that of urea. The multifunctional polymers show an efficiency of 80.56%, 84.72% and 87.5% respectively with respect to KDP. The highest activity was observed for 75% chromophore substituted systems. The bifunctional polymers PuH5 PuH9 and PuH13 showed much less SHG efficiency near to 1-2% of SHG compared to urea. As described in the above systems, the multifunctional CR-based polymers also possessed high SHG activity with isomannide moiety.

Table 5. 10: SHG efficiency of polyurethanes

Polymer	SHG efficiency w. r. to urea (%)	SHG efficiency w. r. to KDP (%)
PuC1	5.40	48.02
PuC2- PuC4	9.06	80.56
PuC6- PuC8	9.53	84.72
PuC10 -PuC12	9.84	87.50
PuC5	1.72	15.28
PuC9	1.83	16.22
PuC13	2.00	17.78

Solubility studies of chiral polyurethanes were performed with solvents having different polarity. A number of solvents were used to check the solubility of polyurethanes. Most of the polyurethanes synthesized were soluble in polar solvents like DMAc, DMSO, DMF etc. and not soluble in non-polar solvents like benzene, toluene, CCl₄, petroleum ether, ethyl acetate, chloroform etc. The polymers were found to be insoluble because of the polarity and rigidity due to hydrogen bonding.

The X-ray diffraction profiles of the polymers were used to analyze the crystalline nature of polymers¹²⁻¹⁵. The crystallinity of the prepared polymers was evaluated and strong diffraction peaks between the 2 θ range 10 and 30 degree were observed. The XRD pattern of polyurethanes PuP2-PuP4 is shown in the **Figure 5. 8**. Since the peaks were found to be broad, the polymeric system was considered to be amorphous in character. There is no prominent shift observed for the polyurethane materials with reference to chirality change. The

XRD studies showed that the polyurethanes with and without chiral moiety possessed amorphous characteristics.

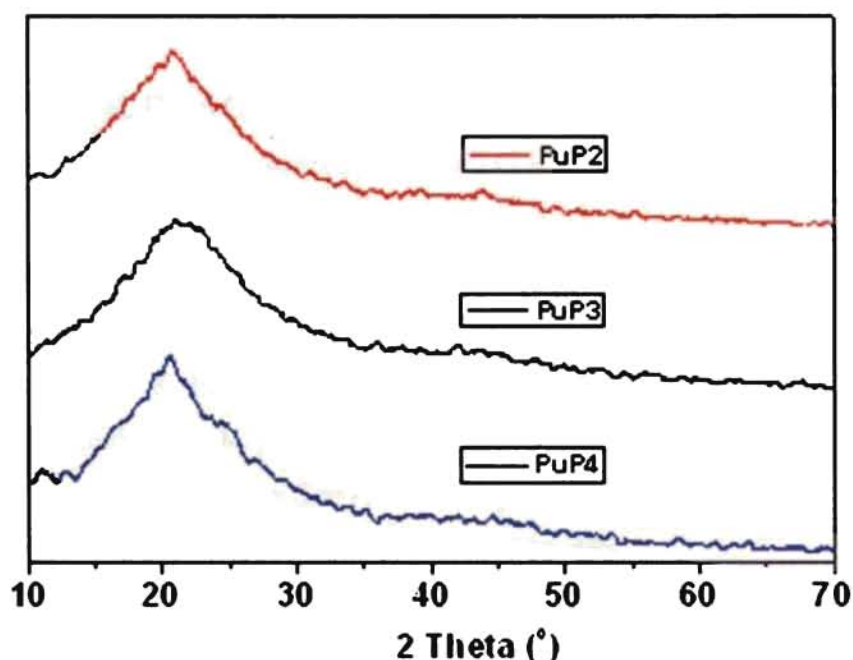


Figure 5. 8: XRD pattern of PuP2-PuP4

5. 9. Conclusions

A series of azodiol based polyurethanes were designed and their nonlinear optical responses were predicted. The polyurethanes synthesized possessed high T_g values with appreciably high thermal stability (high IDT). The various spectroscopic properties of the polymers were studied using standard techniques. The polyurethanes exhibited high NLO activity, especially the isomannide (chiral) and HQ (chromophore) substituted ones showed prominent efficiency. Experimental measurements of SHG were in good agreement with the theoretical predictions.

5. 10. REFERENCES

1. Qui F X, Xu H L, Cao Y L, Jiang Y, Zhou Y M, Liu J Z, Zhang X P, *Material Characterization*, 2007, **58**, 275.
2. Qui F X, Cao Y L, Xu H L, Jiang Y, Zhou Y M, Liu J Z, *Dyes and Pigments*, 2007, **75**, 454.
3. Qui F X, Yang D Y, Cao G R, Zhang R X, Li P P, *Sensors and Actuators B*, 2009, **135**, 449.

4. Aruna P, Rao B S, *Reactive and Functional Polymers*, 2009, **69**, 20.
5. Fengxian Q, Wei Z, Dongya Y, Minjian Z, Guorong C, Pingping L, *J Appl Polym Sci*, 2010, **115**, 146.
6. Zhong'an L, Li W, Bi X, Cheng Y, Jingui Q, Zhen L, *Dyes and Pigments*, 2010, **84**, 134.
7. Chattopadhyay D K, Dean C W, *Progress in Polymer Science*, 2009, **34**, 1068.
8. Tambe S M, Kittur A A, Inamdar S R, Mitchell G R, Kariduraganavar M Y, *Optical Materials*, 2009, **31**, 817.
9. Datta A, Pati S K, *Chem Soc Rev*, 2006, **35**, 1305.
10. Tero T, Jarkko L, Juhani H, Kari R, *Dyes & Pigments*, 2009, **80**, 34.
11. Davis D, Sreekumar K, Pati S K, *Synthetic Metals*, 2005, **155**, 384.
12. Bahulayan D, Sreekumar K, *J Mater Chem*, 1999, **9**, 1425.
13. Philip B, Sreekumar K, *J Polym Sci: Part A: Polym Chem*, 2002, **40**, 2868.
14. Philip B, Sreekumar K, *Colloid Polym Sci*, 2003, **281**, 485.
15. Philip B, Sreekumar K, *Designed Monomers and Polymers*, 2002, **5**, 115.
16. Philip B, *Studies on photorestructuring of synthetic polymers*, Ph. D thesis, Department of Chemistry, University of Kerala, India, 2001
17. Datta A, Pati S K, *J. Molecular Structure, Theochem*, 2005, **756**, 97.
18. Datta A, Pati S K, *J Phys Chem A*, 2004, **108**, 320.
19. Ramasesha S, Shuai Z, Bredas J L, *Chem Phys Lett*, 1995, **245**, 224.
20. Albert I D L, Ramasesha S, *J Phys Chem*, 1990, **94**, 6540.
21. Ramasesha S, Albert I D L, *Phys Rev B*, 1990, **42**, 8587.
22. Pati S K, Ramasesha S, Shuai Z, Bredas J L, *Phys Rev B*, 1999, **59**, 14827.
23. Pati S K, Marks T J, Ratner M A, *J Am Chem Soc*, 2001, **123**, 7287.
24. Kurtz S K, Perry T T, *J Appl Phys*, 1968, **39**, 3798.
25. Davis. D, *Nonlinear optical properties of polymers containing azomesogen and chiral molecules: Theoretical and experimental evaluations*, Ph. D thesis, Department of Applied Chemistry, Cochin University of Science And Technology, Kerala, India, 2005
26. Lalama S J, Garito A F, *Phys Rev A*, 1979, **20**, 20.
27. Sudheesh K K, Sreekumar K, *Int J Polym Mater*, 2009, **58**, 160.
28. Brydson J A, *Plastic Materials*, 7th edition, Iliffe Books, London, 1966.

Chapter 6

**MAIN CHAIN CHIRAL POLYESTERS WITH AMIDODIOL
MONOMERS DERIVED FROM γ -BUTYROLACTONE:
THEORETICAL AND EXPERIMENTAL INVESTIGATIONS****6. 1. Introduction**

The preparation, properties and application of chiral polymers remain an active area of research. An effective and easy way for synthesizing chiral polymers is to introduce chiral units into the polymer main chain or the side chains. When the polymer chains with helical structures pack together following symmetry operations to form ordered structures, the chirality may break the local mirror symmetry and lead to a helical morphology depending on the type of structural ordering formed¹. The chiral polymers have found potential applications in optical devices, signal transmission, data storage, optical switching, liquid crystals and biomedical devices because of the high nonlinear optical (NLO) response²⁻³. In the field of chemical synthesis, great effort has been made in order to obtain organic polymers with high SHG responses by enhancing the molecular hyperpolarizabilities of the constituting NLO active units⁴⁻⁵. Electrical poling is the most common way to break centrosymmetry in polymers. The second order nonlinear optical architecture can be constructed by synthesizing nonlinear optical molecules into supramolecular structure, which is found to be an alternative method⁶. Since the poling of polymers can be achieved through chemical synthesis, there is no need for external poling. The permanent dipole moment of such structures can be very large because of the coherent addition of dipole moments achieved by a high degree of polar order⁷⁻⁸.

This chapter discusses the design, synthesis and property studies of chiral polyesters incorporating amidodiol systems and chiral units that possess high T_g and thermal stability. The amidodiol systems selected for the study are N, N'- ethane- 1, 2- diyl bis (4-hydroxy butanamide) (**B1**), N, N'- butane- 1, 4- diyl bis (4-hydroxy butanamide) (**B2**) and N, N'- hexane- 1, 6- diyl bis (4-hydroxy butanamide) (**B3**), synthesized by the ring opening reaction of γ -butyrolactone by 1, 2-diaminoethane, 1, 4-diaminobutane, 1, 6-diaminohexane respectively.

6. 2. Methodology

6. 2. 1. Computational methods

All the polyesters (3 repeating units) were optimized using the AM1 parameterized Hamiltonian available in the Gaussian 03 set of codes. However, for large systems, the accurate determination of the excitation characteristics for dynamic spectroscopic applications still relies on semiempirical methods with configuration interactions. The geometry optimized structures were used for configuration interaction (CI) calculations to obtain energies and the dipole moments in the CI basis using the Zerner's Intermediate Neglect of Differential Overlap (ZINDO) method. The CI approach adopted here has been extensively used in earlier works, and was found to provide excitation energies and dipole matrix elements in good agreement with experiments⁹. We have chosen the reference determinants which are dominant in the description of the ground state and the lowest one-photon excited state. For the Hartree-Fock determinant, varying number of occupied and unoccupied molecular orbitals has been used to construct the SCI space until a proper convergence was obtained. We have used the singles CI (CIS), because the first nonlinear optical coefficients are derived from second-order perturbation theory involving one-electron excitations. For each reference determinant, 8 occupied and 8 unoccupied molecular orbitals were used to construct a CI space with configuration dimension of 65. To calculate NLO properties, the correction vector method was used which implicitly assumed all the excitations to be approximated by a correction vector¹⁰⁻¹¹. For the calculations of the optical coefficients, an excitation frequency of 1064nm (1.17eV) which correspond to the frequency of the Nd-YAG laser, was used. Given the Hamiltonian matrix, the ground state wave function, and the dipole matrix, all in CI basis, it is straightforward to compute the dynamic nonlinear optical coefficients using either the first-order or the second-order correction vectors¹²⁻¹⁵.

6. 2. 2. Experimental methods

The second harmonic generation efficiency of the polymers were analysed in the powder form by Kurtz Perry techniques¹⁶⁻¹⁷. The well powdered sample was filled in a capillary tube of 0.8 mm thickness. The NLO responses of the materials were recorded using urea and KDP as references, filled in a similar capillary tube sealed at one end, for comparison. The experimental set up for the

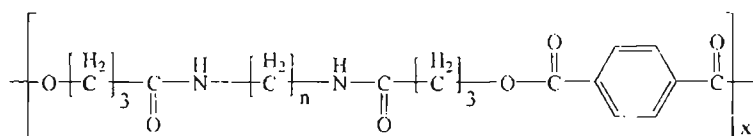
second harmonic generation properties utilizes a Quanta Ray DCR II Nd/YAG laser with a 9 mJ pulse and 1064 nm wavelength, at a repetition rate of 5 Hz. A Q-switched, mode-locked Nd:YAG laser was used to generate about 9 mJ pulse at 1064 nm fundamental radiation. The input laser beam was allowed to pass through an IR reflector and then directed on the micro-crystalline powdered sample packed in a capillary tube of diameter, 0.8 mm. The photodiode detector and oscilloscope arrangements measured the light emitted by the sample. The laser beam was split into two parts, one to generate the second harmonic signal in the sample and the other to generate the second harmonic signal in the reference. An output signal of 532 nm was measured at a 90° geometry using urea/KDP as the standard. The intensity of the second harmonic output from the sample was compared with that of the reference. The efficiency of the NLO activity of the polymers are expressed in percentage as

$$\text{SHG Efficiency (\%)} = \frac{\text{Signal of Sample}}{\text{Signal of Reference}} \times 100$$

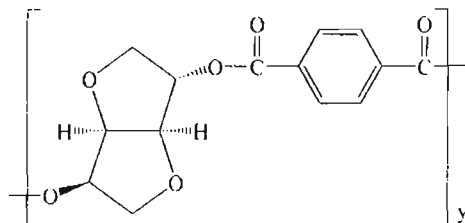
6. 3. Polymer design

6. 3. 1. Bifunctional polymers

The chiral and achiral bifunctional polyesters were designed theoretically as the polycondensation products of terephthaloyl chloride (TC) with chiral and achiral diol molecules. Three repeating units of the polymeric system have been chosen for structure optimization and nonlinear optical property calculations. Each repeating unit of the polyesters contains one molecule of TC and one molecule of dihydroxy monomer (chiral or achiral). The polymers **1**, **2**, and **3** represent the chiral bifunctional polyesters with isosorbide (IS), (2R, 3R)-diethyl tartrate (DT) and isomannide (IM) as chiral moiety. The achiral polymers were designed as the combination of terephthaloyl chloride (TC) with amidodiols, [N, N'-ethane-1, 2-diyl bis (4-hydroxy butanamide) (B1), N, N'-butane-1, 4-diyl bis (4-hydroxy butanamide) (B2) and N, N'-hexane-1, 6-diyl bis (4-hydroxy butanamide) (B3)] which are represented as **4**, **5** and **6** polymer molecules. The bifunctional polymers designed are shown in **Figure 6. 1**.



Polymer 4-6



Polymer 1

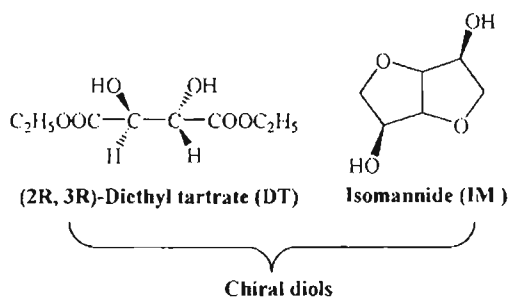


Figure 6. 1: Designed bifunctional polymers

Table 6. 1. reports the two-level parameters such as, the ground-state dipole moment (μ_g), the difference between the dipole moments of ground-state and the excited state ($\Delta\mu$), the optical gap (ΔE), oscillator strength (f), the linear polarizability (α), and the first hyperpolarizability (β) of bifunctional polymers by the *dynamic* SOS calculations. All the determining parameters of β (f , ΔE , $\Delta\mu$) have been studied thoroughly. While analyzing the geometries of dianhydridohexitol molecules (IS and IM), it was found that the ground state dipole moment μ_g of isosorbide with oppositely oriented dipoles is greater than that of the isomannide. Eventhough the ground state dipole moment μ_g is large for isosorbide based polymers, the change in dipole moment $\Delta\mu$ is higher for isomannide based chiral polyesters.

In the case of polyester with isomannide (polymer 3) and isosorbide (polymer 1) chiral moiety, the hyperpolarizability of 3 is almost ten times than that of polymer 1. The stereochemistry of the chiral monomer affects the polar ordering of the designed polymers which plays an important role in achieving highly active polymers with nonlinear optical activity. The dipole moment difference $\Delta\mu$, between the ground and excited state is the major contributing factor in determining the value of β vector¹⁸. The β value is associated with high

change in dipole moment, high oscillator strength and low optical gap which is the basic and essential requirement for the second order nonlinear optical materials. The polymer **3** possesses high $\Delta\mu$ and f values with low ΔE values which is considered to be a major contributing factor for high value of first hyperpolarizability. For the (2R, 3R)-diethyl tartrate based polymer **2**, a comparatively large dipole moment was observed with a less value of β . In case of polarizability parameters, significant changes are not observed for the chiral and achiral bifunctional polymers. Among the chiral polyesters, the isomannide based polymers possess comparatively high value of hyperpolarizability. For the polymers (**1**, **2**, **5** & **6**) the β values are very less compared to the polymers **3** and **4**. The low value of β for polymers **1**, **2**, **5** & **6** can be explained by the low (f , $\Delta\mu$) and high ΔE values. Among the polymer series from **4-6**, the polymer **4** possesses a high value of oscillator strength compared to that of **5** and **6** polyesters. Also the optical gap, the one which determines the energy gap between ground state and lowest dipole allowed state is smaller for polymer **4**. Because of the high oscillator strength and smaller optical gap, the charge transfer will be easier in polymer **4** compared to that of polymer **5** and **6**. Moreover, the polymer **4** exhibits large change in dipole moment compared to the others. The polarizability of all the bifunctional polyesters is in the range $18-21 \times 10^{-23}$ esu. Among the bifunctional polyesters, the polymer with isomannide as chiral diol (polymer **3**) is found to have high SHG efficiency.

Table 6. 1: Ground-State Dipole Moment (μ_g) in debye, Difference in dipole moment between ground state and excited state ($\Delta\mu$) in debye, Optical Gap (ΔE) in eV, Oscillator strength (f), Linear Polarizability (α) in units of 10^{-23} esu, and First Hyperpolarizability (β) in units of 10^{-30} esu for the bifunctional polymers (ZINDO-SOS dynamic property calculations)

Polymer	μ_g	$\Delta\mu$	ΔE	f	α	β
1-TCIS	3.791	10.384	6.819	2.146	20.840	0.539
2-TCDT	5.249	9.476	6.828	2.075	20.306	0.355
3-TCIM	3.132	12.589	6.779	2.527	19.556	5.633
4-TCB1	3.642	15.673	6.775	1.955	18.006	1.581
5-TCB2	3.340	10.674	6.847	1.547	20.793	0.640
6-TCB3	3.629	8.623	6.849	1.389	18.042	0.349

6.3.2. Multifunctional polymers

The polymers are designed as the polycondensation products of achiral diols [N, N' -ethane-1, 2-diyl bis (4-hydroxy butanamide) (B1), N,N' -butane-1, 4-diyl bis(4-hydroxy butanamide) (B2) and N,N' -hexane-1, 6- diyl bis(4-hydroxy butanamide) (B3)] and terephthaloyl chloride (TC) with the chiral moiety (IS, IM and DT). **Figure 6. 2.** represents one set of multifunctional polymers based on isomannide chiral substitution.

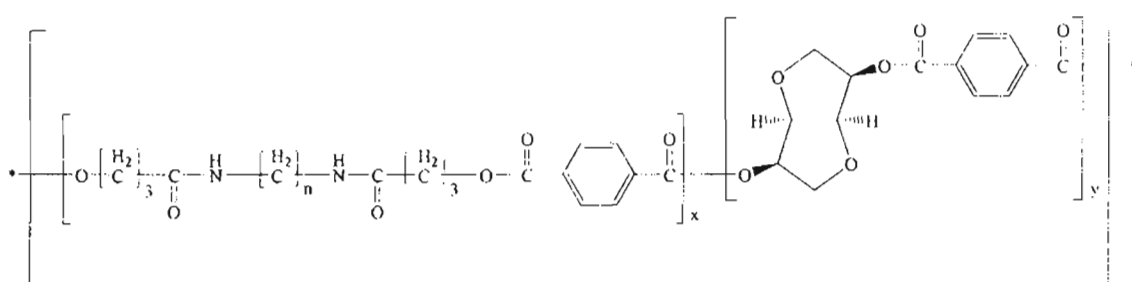


Figure 6. 2: Designed multifunctional polymers

The polymers 7, 8, and 9 represent the chiral multifunctional polyesters with isosorbide (IS) as chiral moiety and B1, B2 and B3 as achiral diols. Similarly 10, 11 and 12 represent multifunctional polymers with diethyl tartrate (DT) as chiral monomer and the amido groups (B1, B2 and B3) as achiral molecule. The chiral polyesters 13, 14 and 15 represent the isomannide derived multifunctional polymers. Three repeating units of each polymer have been considered for the optimization and molecular property calculations. Each repeating unit contains one molecule of achiral diol, two molecules of TC and one chiral molecule (IS, IM and DT).

Table 6. 2. reports the two-level parameters such as, the ground-state dipole moment (μ_g), the difference between the dipole moments of ground-state and the excited state ($\Delta\mu$), the optical gap (ΔE), oscillator strength (f), the linear polarizability (α), and the first hyperpolarizability (β) of multifunctional polymers by the *dynamic* SOS calculations. Dynamic hyperpolarizability values of multifunctional polymers which are found by ZINDO/CV method are given in table. A high value of ground state dipole moment was observed for the polyesters with (2R, 3R)-diethyl tartrate (10-12) and isosorbide (7-9) as chiral monomer. Even if the (2R, 3R)-diethyl tartrate based polymers have comparatively high ground state dipole moment, difference in dipole moment

between the ground state and the excited state $\Delta\mu$, is small compared to the isomannide based polymers. All these factors (lower $\Delta\mu$, higher ΔE and lower f) reduce the value of hyperpolarizability considerably in IS and DT substituted polymers. **Figure 6. 3** shows the AM1 optimized geometry of the polymer containing 3 repeating unit of polymer **14**.

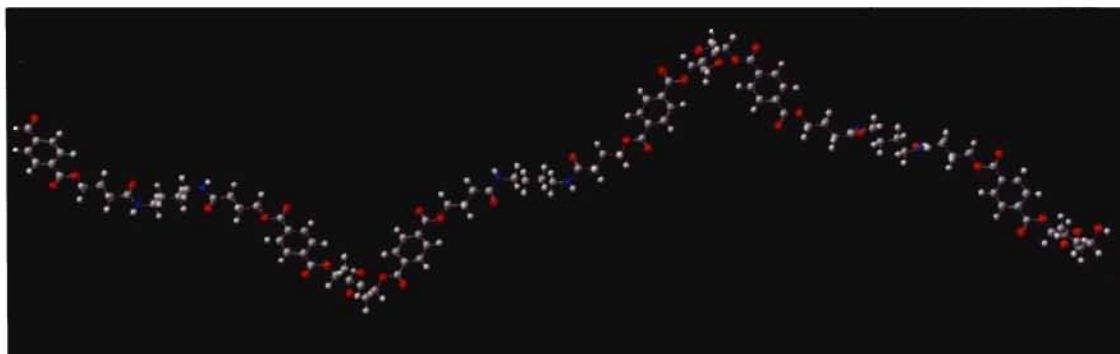


Figure 6. 3: Optimized geometry of polymer **14**

The helical structure ensures the macroscopic chirality and hence attains the asymmetry which is the basic and essential requirement for second order NLO material. While examining the effect of chiral molecule in the design of an efficient SHG material it can be seen that all the polymers (**13-15**) with isomannide chiral molecule have high β value than the polymer (**7-9**) with isosorbide and (**10-12**) with diethyl tartrate chiral monomers. For the isomannide based chiral polyesters (**13-15**), the oscillator strength (f), which determines the probability of transition from the ground state to the excited state was higher compared to the other polymers with isosorbide (**7-9**) and (2R, 3R)-diethyl tartrate (**10-12**) chiral monomers. The optical gap (ΔE), which determines the energy gap between the ground state and the lowest dipole allowed state is smaller for isomannide-based polyesters (**13-15**), compared to isosorbide and diethyl tartrate containing polyesters. For investigating the efficiency of the polyesters, all the determining parameters of β (f , ΔE , $\Delta\mu$) have been thoroughly analysed and it can be seen that all the chiral polyesters with isomannide substitution possess comparatively high value of hyperpolarizability.

For all the multifunctional polyesters, the polarizability lies in the same range ($14-16 \times 10^{-23}$ esu) even though they have different chiral and achiral monomers. Thus it can be concluded that the polarizability is not much influenced by the chirality of the building units. Among the bifunctional and

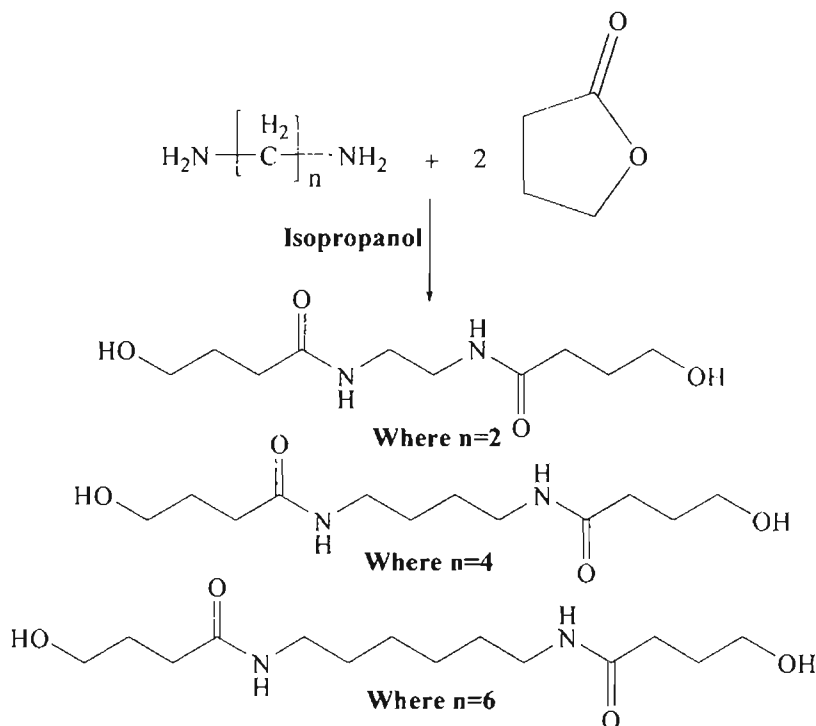
multifunctional polymers, the multifunctional polymers (with chiral and achiral diol) have high β values than the bifunctional polymers. The designed polymer with isomannide as chiral diol and B1 as achiral diol are found to possess high NLO activity. The theoretical results predict that all the designed polymers are good candidates for nonlinear optics.

Table 6. 2: Ground-State Dipole Moment (μ_g) in debye, Difference in dipole moment between ground state and excited state ($\Delta\mu$) in debye, Optical Gap (ΔE) in eV, Oscillator strength (f), Linear Polarizability (α) in units of 10^{-23} esu, and First Hyperpolarizability (β) in units of 10^{-30} esu for the multifunctional polymers (ZINDO-SOS dynamic property calculations)

Polymer	μ_g	$\Delta\mu$	ΔE	f	α	β
7-TCISB1	10.987	15.076	6.683	1.149	15.862	6.929
8- TCISB2	11.018	12.985	6.681	1.140	15.138	6.918
9- TCISB3	11.154	10.916	6.679	1.139	15.818	6.869
10-TCDTB1	12.543	13.285	6.614	1.282	14.810	7.985
11- TCDTB2	12.954	13.182	6.619	1.185	14.805	7.215
12- TCDTB3	12.712	13.135	6.629	1.180	14.803	7.212
13-TCIMB1	9.835	16.825	6.546	1.549	14.909	8.578
14- TCIMB2	10.883	15.918	6.546	1.546	15.186	8.549
15- TCIMB3	9.984	15.903	6.534	1.483	15.156	8.521

6. 4. Monomer Synthesis (B1, B2, B3): Synthesis of amidodiols¹⁹⁻²⁴

Diaminoalkanes (diaminoethane for **B1**, diaminobutane for **B2** and diaminohexane for **B3**) (0.1 mol) and γ - butyrolactone (0.2 mol) were taken in two separate conical flasks and both were dissolved in 50 ml isopropanol. The lactone solution was added to diamine solution over a period of 1 h and kept with stirring. White crystalline product was filtered and washed with isopropanol. It was recrystallised from methanol-acetone mixture (70:30 w/w) and further purified by column chromatography using ethyl acetate and hexane as solvent system (Scheme 6. 1).



Scheme 6. 1: Synthesis of monomers

The amidodiols N, N'-ethane-1, 2-diyl bis (4-hydroxy butanamide) (**B1**), N, N'-butane-1, 4-diyl bis (4-hydroxy butanamide) (**B2**) and N, N'-hexane-1, 6-diyl bis (4-hydroxy butanamide) (**B3**) were prepared from 1, 2-diaminoethane, 1, 4-diaminobutane and 1, 6-diaminohexane, respectively using the procedure. The aminolysis of γ -Butyrolactone with diaminoalkanes in isopropanol medium gave amidodiols in good yield and high purity.

Amidodiols prepared by the above method were shining crystals and had melting point around 100-120°C. The amidodiols were characterized by elemental analysis, ^1H NMR, ^{13}C NMR, FTIR etc. FTIR (KBr, ν_{max} , cm^{-1}): 1420 (C-N stretching in amidodiols), 1560 (N-H bending), 1649 (C=O str. of amidodiols), 3270 (N-H stretching), 3460 (-OH stretching in amidodiols). The amidodiols monomers showed ^1H NMR signals at 4.8 ppm corresponding to the proton of the hydroxyl group of $-\text{CH}_2\text{OH}$. The proton of $-\text{CH}_2$ of $-\text{CH}_2\text{OH}$ resonated at 3.3-3.4 ppm. The signals at 2.7-2.9 ppm corresponds to $-\text{CH}_2$ nearer to carbonyl carbon. The signals between 1.6 and 2.3 ppm corresponds to $-\text{CH}_2$ protons of the amidodiols. In the case of the ^{13}C NMR, the chemical shift values of the amide carbon appeared in the range from 172-178 ppm and the carbinol carbon resonated at 62-70 ppm and alkyl carbons gave signals at 24 ppm and the $-\text{CH}_2\text{NH}-$ appeared around 38 ppm.

6. 5. Polymer Synthesis

The reaction conditions for the synthesis of polyesters were optimized by varying the solvent, time of reaction and temperature which are shown in **Table 6. 3**. Polymerization was done using terephthaloyl chloride, IS as chiral diol and B1 as achiral monomer.

Table 6. 3: Optimization of reaction conditions

Solvent	Time (h)	Temperature (°C)	Yield (%)
DMAc	25	60	50
DMAc	25	120	62
DMAc	50	60	72
DMAc	50	120	76
DMF	50	120	65
DMSO	50	120	70

From these observations, the optimum conditions for the reaction chosen are temperature 120°C, time 50 h and DMAc as solvent (76%).

6. 5. 1. General procedure ^{6-8, 25-28}

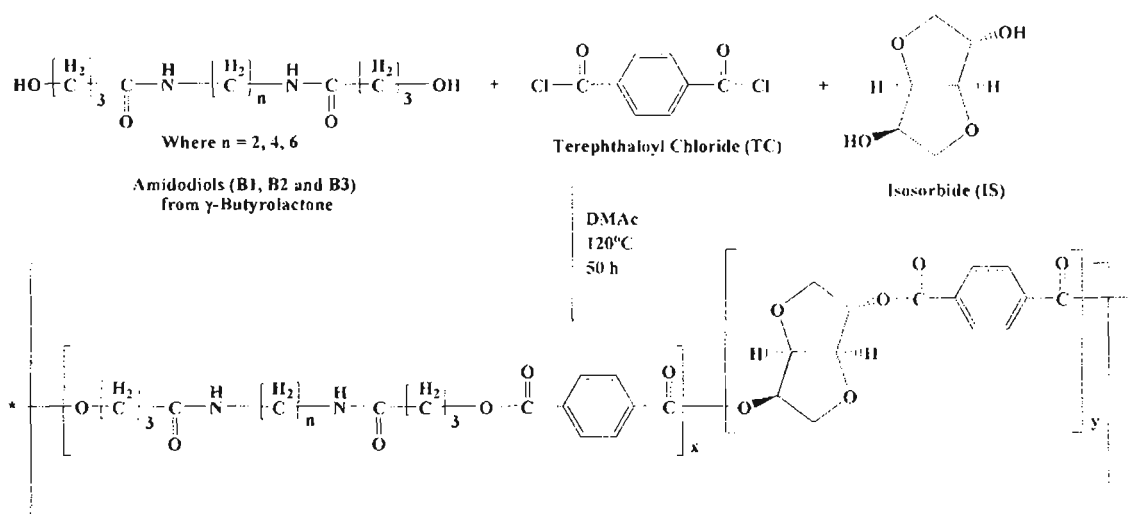
Terephthaloyl chloride (TC) was dissolved in hot DMAc. To this solution, appropriate mole percentage of amidodiols (B1, B2 and B3) and chiral diols, isosorbide (IS), (2R, 3R)-diethyl tartrate (DT) and isomannide (IM) were added. The mixture was heated under stirring for 50h at 120°C. The products were precipitated in cold methanol. The solid obtained was washed thoroughly with hot water and acetone, filtered, dried and the soxhlet extraction was done using methanol. A series of polymers containing the amidodiol and chiral building block in the main chain were synthesized.

6. 6. ISOSORBIDE BASED POLYESTERS

6. 6. 1. Experimental discussion

Different polymers with varying chiral (IS)-amidodiol (B1, B2 and B3) composition were synthesized based on the above mentioned procedure. The polymer PEA1 is the one which has only chiral unit (isosorbide) in polymer

chain and considered as the mother polymer in the series. For PEA1, the ratio of TC and IS are taken as 1:1. PEA2, PEA3, PEA4 and PEA5 are the polyesters with B1 amidodiols having the TC: IS: B1 ratio as 1:0.75:0.25 (PEA2), 1:0.5:0.5 (PEA3), 1:0.25:0.75 (PEA4), 1:0:1 (PEA5), respectively. PEA6, PEA7, PEA8 and PEA9 are the polyesters with B2 amidodiols in which TC: IS: B2 ratio is maintained as 1:0.75:0.25 (PEA6), 1:0.5:0.5 (PEA7), 1:0.25:0.75 (PEA8), 1:0:1 (PEA9), respectively. PEA10, PEA11, PEA12 and PEA13 are the polyesters with B3 amidodiols having the ratio of TC: IS: B3 as 1:0.75:0.25 (PEA10), 1:0.5:0.5 (PEA11), 1:0.25:0.75 (PEA12), 1:0:1 (PEA13), respectively. The polyester (PEA1-PEA13) synthesis is shown in **Scheme 6. 2**.



Scheme 6. 2: Synthesis of polyesters (PEA1-PEA13)

6. 6. 2. Spectral Characterization

PEA1: FTIR (KBr), ν_{max} (cm^{-1}): 3000-2950 (sp^3 C-H stretching in isosorbide unit), 1725 (C=O stretching of ester formed by isosorbide); 1460 (C-H bend of $-\text{CH}_2$ group in isosorbide), 1230 (C-O stretching of ester attached to isosorbide unit), 1050-1130 (C-O stretching vibrations of ester attached to phenyl group). **^1H NMR (DMSO- d_6), δ (ppm):** 4.2 (q, $-\text{CH}_2$ in isosorbide unit), 4.3-4.5 (t, $-\text{CH}$ -bridge protons of isosorbide unit), 5.1 (m, $-\text{CH}$ in isosorbide unit), 7.8-8.2 (d, aromatic protons of TC). **^{13}C NMR (DMSO- d_6), δ (ppm):** 170-175 (ester carbonyl of polyester), 130-160 (aromatic ring carbons), 80-82 ($-\text{CH}$ -bridge of isosorbide unit), 75-78 ($-\text{CH}$ -of isosorbide unit), 40-42 ($-\text{CH}_2$ - isosorbide unit).

PEA2-PEA4: FTIR (KBr), ν_{max} (cm^{-1}): 3290-3300 ($-\text{NH}$ stretching of amidodiols)

unit), 3000–2850 (C–H stretching of $-\text{CH}_2-$ in both isosorbide and amidodiol unit), 1730–1740 (C=O stretching in ester formed by amido group), 1710–1715 (C=O stretching in ester formed by isosorbide); 1650–1680 (C=O stretching of $-\text{CONH}$ group in amidodiol), 1530–1550 (NH bending in amidodiol), 1450–1470 (C–H bend of CH_2 groups), 1420–1425 ($-\text{C}-\text{N}$ stretching in amidodiol), 1220–1225 (C–O stretching of isosorbide unit) 1075–1118 (C–C–O stretching of ester).

^1H NMR (DMSO- d_6), δ (ppm): 1.2–3.2 (m, CH_2 of amido group), 3.5 ($-\text{NH}$ protons of amido group), 4.1–4.4 (q, $-\text{CH}_2$ in isosorbide unit), 4.6 (t, $-\text{CH}-$ bridge protons of isosorbide unit), 5.3 (m, $-\text{CH}$ in isosorbide unit), 7.1–7.6 (d, aromatic protons of TC). **^{13}C NMR (DMSO- d_6), δ (ppm):** 175 (ester carbonyl in polyester), 172 (C=O of amidodiol) 140–155 (aromatic ring carbons), 72 ($-\text{CH}-$ bridge of isosorbide unit), 60–67 ($-\text{CH}_2\text{O}-$ in amido unit), 39 ($-\text{CH}_2\text{NH}-$ in amidodiol), 35–38 ($-\text{CO}-\text{NH}-\text{CH}_2-\underline{\text{C}}\text{H}_2-$), 25–28 ($-\text{CO}-\text{CH}_2-\underline{\text{C}}\text{H}_2-$), 32–34 ($-\text{CH}_2-$ isosorbide unit).

PEA5: FTIR (KBr), ν_{max} (cm^{-1}): 3280–3300 ($-\text{NH}$ stretching of amidodiol unit), 1712–1728 (C=O stretching in ester formed by amidodiol), 1640–1650 (C=O stretching in amidodiol), 1541 ($-\text{NH}$ bending in amido group), 1410–1420 ($-\text{CN}$ stretching in amido unit), 1130–1180 (C–C–O stretching of ester). **^1H NMR (DMSO- d_6), δ (ppm):** 1.2–3.0 (m, $-\text{CH}_2$ of amidodiol unit), 3.5 ($-\text{NH}$ protons of amide), 7.8–8 (d, aromatic protons of TC). **^{13}C NMR (DMSO- d_6), δ (ppm):** 170–175 (ester carbonyl in polyester), 168 (C=O of amidodiol), 140–165 (aromatic ring carbons), 60–70, 39–42, 32–36, 28–30 ($-\text{CH}_2-$ of amido groups).

PEA6–PEA8: FTIR (KBr), ν_{max} (cm^{-1}): 3250–3300 ($-\text{NH}$ stretching of amidodiol unit), 3000–2900 (C–H stretching of $-\text{CH}_2-$ in both isosorbide and amidodiol unit), 1740–1750 (C=O stretching in ester formed by amidodiol), 1720–1725 (C=O stretching in ester formed by isosorbide), 1650–1680 (C=O stretching of $-\text{CONH}$ group in amidodiol), 1530–1545 (NH bending in amidodiol), 1455–1465 (C–H bend of CH_2 groups), 1415–1420 ($-\text{C}-\text{N}$ stretching in amido unit), 1220–1225 (C–O stretching of isosorbide unit), 1075–1135 (C–C–O stretching of ester).

^1H NMR (DMSO- d_6), δ (ppm): 1.2–3.3 (m, $-\text{CH}_2$ of amidodiol unit), 3.5 ($-\text{NH}$ protons of amido group) 4.02 (q, $-\text{CH}_2$ in isosorbide unit), 4.4 (t, $-\text{CH}-$ bridge protons of isosorbide unit), 4.8 (m, $-\text{CH}$ in isosorbide unit), 6.5–7.0 (d, aromatic protons of TC). **^{13}C NMR (DMSO- d_6), δ (ppm):** 175–178 (ester carbonyl in

polyester), 172 (C=O of amidodiol), 150-155 (aromatic ring carbons), 68 (-CH-bridge of isosorbide unit), 60-67 (-CH₂O-), 39 (-CH₂NH-), 31-36 (-CO-NH-CH₂-CH₂-), 32-35 (-CH₂- isosorbide unit), 25-28 (-CO-CH₂-CH₂-).

PEA9: FTIR (KBr), ν_{\max} (cm⁻¹): 3280-3300 (-NH stretching of amido unit), 1712-1728 (C=O stretching in ester formed by amidodiol), 1660- 1675 (C=O stretching in amidodiol), 1541 (-NH bending in amidodiol), 1410-1420 (-CN stretching in amido unit), 1130-1180 (C-C-O stretching of ester). **¹H NMR (DMSO-d₆), δ (ppm):** 1.3-3.2 (m, -CH₂ of amidodiol unit), 3.5 (-NH protons of amido group), 8.2 (d, aromatic protons of TC). **¹³C NMR (DMSO-d₆), δ (ppm):** 174-176 (ester carbonyl in polyester), 172 (C=O of amidodiol) 140-150 (aromatic ring carbons), 60-70, 39-42, 32-36, 25-30 (-CH₂- of amido groups).

PEA10-PEA12: FTIR (KBr), ν_{\max} (cm⁻¹): 3250-3300 (-NH stretching of amidodiol unit), 3000-2900 (C-H stretching of -CH₂- in both isosorbide and amidodiol unit), 1740- 1750 (C=O stretching in ester formed by amidodiol), 1720-1725 (C=O stretching in ester formed by isosorbide); 1650-1680 (C=O stretching of -CONH group in amidodiol), 1530-1550 (NH bending in amidodiol), 1455-1460 (C-H bend of CH₂ groups), 1415-1420 (-C-N stretching in amidodiol), 1220-1225 (C-O stretching of isosorbide unit) 1075-1135 (C-C-O stretching of ester). **¹H NMR (DMSO-d₆), δ (ppm):** 1.2-3.3 (m, -CH₂ of amidodiol unit), 3.5 (-NH protons of amido group), 4-4.3 (q, -CH₂ in isosorbide unit), 4.7 (t, -CH- bridge protons of isosorbide unit), 5.0-5.1 (m, -CH in isosorbide unit), 7.9-8.1 (m, aromatic protons of TC). **¹³C NMR (DMSO-d₆), δ (ppm):** 170-175 (ester carbonyl in polyester), 169 (C=O of amidodiol) 130-155 (aromatic ring carbons), 68 (-CH-bridge of isosorbide unit), 60-67 (-CH₂O-), 39 (-CH₂NH-), 31-36 (-CO-NH-CH₂-CH₂-), 32-35 (-CH₂- isosorbide unit), 25-28 (-CO-CH₂-CH₂-).

PEA13: FTIR (KBr), ν_{\max} (cm⁻¹): 3290-3300 (-NH stretching of amido unit), 1719-1730 (C=O stretching in ester formed by amidodiol, 1640- 1650 (C=O stretching in amido linkage), 1541 (-NH bending in amidodiol), 1410-1420 (-CN stretching in amidodiol), 1146-1178 (C-C-O stretching of ester). **¹H NMR (DMSO-d₆), δ (ppm):** 1.2-3.3 (m, -CH₂ of amidodiol unit), 3.5 (-NH protons of amido group), 7.2 (m, aromatic protons of TC). **¹³C NMR (DMSO-d₆), δ (ppm):** 173-175 (ester carbonyl in polyester), 171 (C=O of amidodiol), 130-155 (aromatic ring carbons), 60-70, 39-42, 32-36, 25-30 (-CH₂- of amido groups).

6. 6. 3. Mass spectra

From the MALDI-MS analysis, it was found that the molecular weight of the polyesters synthesized were in the range 17,000–20,000 (the molecular weight of one repeating unit=650–800) which confirmed the proposed structure consisting of almost 25–30 repeating units.

6. 6. 4. Absorption spectra

The spectra of polyesters were taken in DMAc solvent. All the polymers showed two absorbance peaks at 280–290 nm range (λ_{\max}) and 300–320 nm range. The absorption in the region 250–360 nm without any major absorption at shorter wavelengths (200–250 nm) usually indicate the $n \rightarrow \pi^*$ transition in the molecule containing a hetero atom. This type of transition includes the presence of $-C=O$, $-COOR$, $-CONH_2$ etc. Polyesters with amidodiols containing both π bonds and unshared electron pairs exhibit two absorptions, a low intensity shoulder like $n \rightarrow \pi^*$ transition at longer wavelength ~ 300 – 320 nm and a high intensity $\pi \rightarrow \pi^*$ band at a shorter wavelength of ~ 280 – 290 nm. The absorption λ_{\max} values are shown in **Table 6. 4**.

6. 6. 5. Fluorescence spectra

Fluorescence is particularly an interesting tool to probe the rigidity of the polymer backbone. The broadness of the fluorescence peak decreases with increasing rigidity. For all the samples, the excitation wavelengths and emission wavelengths were recorded in the fluorescence spectrum by inputting the proper absorbance wavelengths and excitation wavelengths. The excitation wavelengths were found to be between 350–365 nm and emission spectra in the range of 400–410 nm. The emission λ_{\max} values are summarized in **Table 6. 4**.

6. 6. 6. Specific rotation

The specific rotation of the polymers can be studied by the polarimetric technique. The specific rotation value is equivalent to the angle of rotation obtained by the measurement using a solution of 100% concentration in a 100 mm observation tube. The angle of rotation depends upon the concentration of the solution, the length of the tube, temperature and measurement wavelength which was taken as 589 nm. The polyesters synthesized contained optically active monomers. The optical activity of polymers increased when isosorbide

molecules was incorporated. The specific rotation $[\alpha]_D$ values measured for polymers varied from 0° to 43°. The $[\alpha]_D$ value increased with the increase in the % of isosorbide chiral component. The polymers with high % incorporation of chiral diol possess high value of $[\alpha]_D$. The polyesters without chiral molecule showed zero specific rotation. The specific rotations of the polyesters are summarized in **Table 6. 4**. Relatively high values of specific rotation near to the specific rotation of optically active monomers were obtained indicating that no extensive racemization occurred during the polymerization stage⁶⁻⁷.

6. 6. 7. Refractive index

To determine the refractive indices of the polymer samples, the well-known prism method was used. The measurements were carried out using ABBE Refractometer (ATAGO) DR M2 at a wavelength of 589 nm. Distilled water was taken as the reference which had the refractive index of 1.33. The refractive indices of the polyester systems lie in the range 1.42-1.58, which are reported in **Table 6. 4**.

6. 6. 8. Thermal properties

Knowledge of thermal stability of polyesters is an important aspect in determining their thermal performance. The thermal properties of the polymers were evaluated by thermogravimetry (TG) and differential thermal analysis (DTA). The thermal characteristics such as initial decomposition temperature (IDT) and glass transition temperature (T_g) measured under nitrogen atmosphere are given in **Table 6. 4**. The TG analysis gave the details of the degradation occurring via weight loss. Most of the polyesters were stable upto the temperature around 190-280°C. The results of thermogravimetry measurements demonstrated that the polymers showed a single stage decomposition pattern and have no weight loss below 190-280°C, where as the char yields at 600°C were in the range 30-40 % indicating their high thermal stability. The multifunctional polyesters showed glass transition temperature around 120 to 160°C where as bifunctional polyesters, including chiral and achiral diol based polymers, at a lower temperature of about 118°C to 135°C. Polymers with both chiral diol and amidodiols showed high T_g values compared to the polymers without chiral molecules.

Table 6. 4: Optical and thermal properties of polyesters (PEA1-PEA13)

Polymer	% of chiral diol	Specific rotation [α] _{D²⁰})	Absorption λ_{\max} (nm)	Emission λ_{\max} (nm)	IDT ($^{\circ}$ C)	T_g ($^{\circ}$ C)	Refractive index
PEA1	100	43	290	408	190	118	1.4692
PEA2	75	38	288	408	260	150	1.5794
PEA3	50	35	289	404	268	158	1.5743
PEA4	25	32	289	406	272	160	1.5762
PEA5	0	0	289	402	220	135	1.4219
PEA6	75	37	289	402	215	143	1.5087
PEA7	50	36	286	406	228	148	1.5154
PEA8	25	28	289	409	250	160	1.5243
PEA9	0	0	286	405	190	118	1.4876
PEA10	75	36	288	405	228	127	1.4962
PEA11	50	32	286	403	230	138	1.4994
PEA12	25	27	290	405	240	140	1.5115
PEA13	0	0	290	404	210	128	1.4997

6. 6. 9. SHG efficiency

The nonlinear optical properties of selected polyesters were studied in powder form by Kurtz -Perry method¹⁶⁻¹⁷. The SHG responses of these samples were recorded using urea and KDP as the reference. The reference materials for the measurement show SHG intensities of 640 mV and 72 mV for Urea and KDP respectively. The SHG activity for polymers was compared with the standards and the results of experimental SHG efficiency of polymers are reported in **Table 6. 5**. As expected from the designed polymers, they showed moderate SHG efficiency when compared with the reference compounds urea and KDP. Among the series of polyesters (PEA1-PEA13), the polymers with both chiral and amidodiol groups gave considerably high activity compared to bifunctional polymers. PEA2-PEA4, PEA6-PEA8 and PEA10-PEA12 polymers had about 2.5, 2.34 and 2.19 % efficiency respectively compared to that of urea and 22.22, 20.83 and 19. 44 % respectively as that of KDP standard. Even if there is an absence of π -conjugation in donor-acceptor systems, the polyester systems show considerably high NLO activity. The bifunctional polymers with chiral diol

PEA1 showed 1.41 % efficiency compared to urea and 12.5 % compared to KDP. PEA5, PEA9 and PEA13 showed SHG efficiency near to 2.08 % of SHG compared to urea and 18.69 % compared to KDP. The multifunctional polymers possess more SHG response compared to bifunctional polyesters.

Table 6. 5: SHG efficiency of polymers

Polymer	SHG efficiency	SHG efficiency
	w. r. to urea (%)	w. r. to KDP (%)
PEA1	1.41	12.50
PEA2- PEA4	2.50	22.22
PEA6- PEA8	2.34	20.83
PEA10 -PEA12	2.19	19.44
PEA5, PEA9, PEA13	2.08	18.69

6. 6. 10. Crystallinity

The crystalline nature of polymers was studied with the help of X-ray diffraction pattern. Strong diffraction peaks in XRD were observed between the 2θ range 15 and 30 degree.

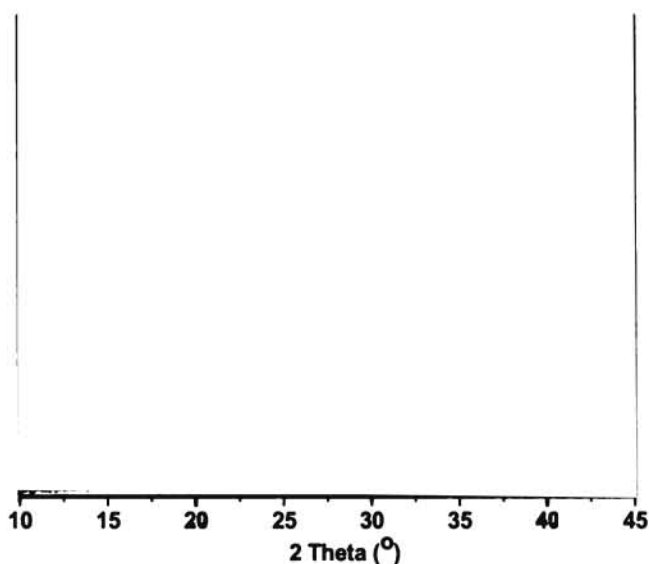


Figure 6. 4: XRD pattern for PEA2-PEA4

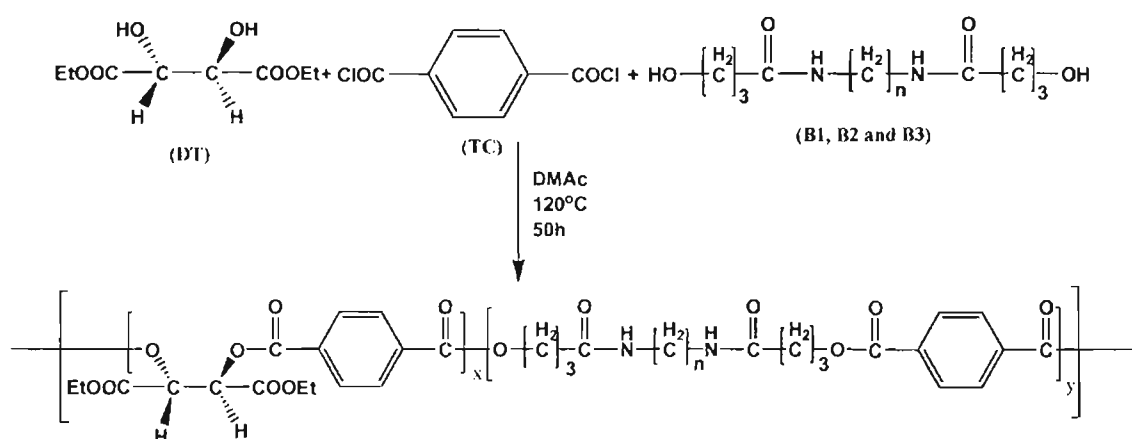
Sharp peaks were observed for multifunctional polyesters, which were assigned to be highly crystalline in nature. All sets of multifunctional polymers

showed strong reflection peaks, but there was no prominent shift observed for the polyesters with reference to chiral diol composition. The bifunctional polymers with only achiral diols possessed low intensity broad peaks which corresponded to the semicrystalline characteristics of the achiral bifunctional polymers. The bifunctional polymers with only chiral diols showed sharp crystalline peaks. The XRD pattern of multifunctional polymers is shown in Figure 6. 4.

6. 7. (2R, 3R)-DIETHYL TARTRATE BASED POLYESTERS

6. 7. 1. Experimental discussion

The polymer **PEB1** was the one which has only the chiral diol (2R, 3R-diethyl tartrate) in the polymer chain. For **PEB1**, the ratio of **TC** and **DT** are taken as 1: 1. **PEB2**, **PEB3**, **PEB4**, **PEB5** are the polyesters with **B1** achiral diol having the **TC: DT: B1** ratio as 1: 0.75: 0.25(**PEB2**), 1: 0.5: 0.5(**PEB3**), 1: 0.25: 0.75(**PEB4**), 1: 0: 1(**PEB5**) respectively. **PEB6**, **PEB7**, **PEB8** and **PEB9** are the polyesters with **B2** achiral diol in which **TC: DT: B2** ratio is maintained as 1: 0.75: 0.25(**PEB6**), 1: 0.5: 0.5(**PEB7**), 1: 0.25: 0.75(**PEB8**), 1: 0: 1 (**PEB9**) respectively. **PEB10**, **PEB11**, **PEB12**, **PEB13** are the polyesters with **B3** diol having the ratio of **TC: DT: B3** as 1: 0.75: 0.25(**PEB10**), 1: 0.5: 0.5(**PEB11**), 1: 0.25: 0.75(**PEB12**), 1: 0: 1 (**PEB13**) respectively. Another series of polyesters (**PEB1-PEB13**) were synthesized by the high temperature condensation of the chiral diol and amidodiols with the acid chloride, terephthaloyl chloride as shown in **Scheme 6. 3**. All the polymers were characterized by means of various spectroscopic techniques.



Scheme 6. 3: Synthesis of Polyesters (**PEB1- PEB13**)

6. 7. 2. Spectral characterization

For PEB1, FTIR (KBr in cm^{-1}): 3000, 2960, 2900 (sp^3 C-H str. in tartrate unit), 1736-1740($\text{C}=\text{O}$ str. ester group in diethyl tartrate); 1720-1725($\text{C}=\text{O}$ str. in ester formed by tartrate); 1468(C-H bend of CH_2 group), 1380(C-H bend of CH_3 group). ^1H NMR (DMSO- d_6), δ (ppm): 0.8 (t, $-\text{CH}_3$ in tartrate unit), 4.2 (q, $-\text{CH}_2$ in tartrate unit), 5.3 (s, $-\text{CH}$ in tartrate unit), 7.5 (d, aromatic protons). ^{13}C NMR (DMSO- d_6), δ (ppm): 172 (the ester formed by chiral diols), 162-164 (ester carbon in tartrate unit), 134 (aromatic ring carbons), 65 ($-\text{CH}-$ of tartrate unit), 32 ($-\text{CH}_2-$ tartrate unit), 18 (CH_3- tartrate unit).

PEB2-PEB4: IR (KBr in cm^{-1}): 3250-3300 NH str. of amidodiol unit, 3000-2900(sp^3 C-H str. in tartrate unit), 1740-1750($\text{C}=\text{O}$ str. in ester formed by amidodiol), 1730-1735($\text{C}=\text{O}$ str. ester group in diethyl tartrate); 1720-1725($\text{C}=\text{O}$ str. in ester formed by tartrate); 1650-1680($\text{C}=\text{O}$ str. ester group in amidodiol), 1530-1550(NH bending in amidodiol), 1455-1460(C-H bend of CH_2 group), 1420-1430(CN str. in amidodiol) 1380-1405(C-H bend of CH_3 group), 1220-1230(C-C-O str. of ester attached to diethyl tartrate group), 1130-1140(C-C-O str. of ester attached to amidodiol). ^1H NMR (DMSO- d_6), δ (ppm): 1.2 (t, $-\text{CH}_3$ in tartrate unit), 1.8-2.5, 2.8-3.1 (m, CH_2 of amidodiol unit), 3.5 ($-\text{NH}$ protons of amidodiol), 4.2 (q, $-\text{CH}_2$ in tartrate unit), 5.3 (s, $-\text{CH}$ in tartrate unit), 7.8 (d, aromatic protons). ^{13}C NMR (DMSO- d_6), δ (ppm): 175 (the ester formed by both chiral diols and amidodiols), 170 (ester carbon in tartrate unit), 167 (ester carbon in amido unit), 136 (aromatic ring carbons), 64 ($-\text{CH}-$ of tartrate unit), 39 ($-\text{CH}_2\text{O}-$), 36 ($-\text{CH}_2-$ tartrate unit), 32-34 ($-\text{CH}_2\text{NH}-$), 29-30 ($-\text{CO}-\text{NH}-\text{CH}_2-\underline{\text{C}}\text{H}_2-$), 25-28 ($-\text{CO}-\text{CH}_2-\underline{\text{C}}\text{H}_2-$), 16 (CH_3- tartrate unit).

PEB5: IR (KBr in cm^{-1}): 3250-3300 NH str. of amidodiol unit, 3000-2900(sp^3 C-H str.), 1740-1750($\text{C}=\text{O}$ str. in ester formed by amidodiol), 1710-1720($\text{C}=\text{O}$ str. ester group in amidodiol), 1530-1550(NH bending in amidodiol), 1455-1460(C-H bend of CH_2 group), 1420-1430(CN str. in amidodiol) 1380-1405(C-H bend of CH_3 group), 1220-1230(C-C-O str. of ester). ^1H NMR (DMSO- d_6), δ (ppm): 1.8, 2.3, 2.7, 3.0 (m, $-\text{CH}_2$ of amidodiol unit), 3.5($-\text{NH}$ protons of amidodiol), 8(d, aromatic protons). ^{13}C NMR (DMSO- d_6), δ (ppm): 174 ($\text{C}=\text{O}$ group of polyester), 170 ($\text{C}=\text{O}$ group of amidodiol), 146-160 (aromatic protons), 60-65, 39-42, 32-36, 28-30 (CH_2 of amidodiol).

PEB6-PEB8: IR (KBr in cm^{-1}): 3250-3300 NH str. of amidodiol unit, 3000-2900(sp^3 C-H str.), 1740-1750(C=O str. in ester formed by amidodiol), 1730-1735(C=O str. ester group in diethyl tartrate); 1720-1725(C=O str. in ester formed by tartrate unit); 1650-1680(C=O str. ester group in amidodiol), 1530-1550(NH bending in amidodiol), 1455-1460(C-H bend of CH_2 group), 1420-1430(CN str. in amidodiol) 1380-1405(C-H bend of CH_3 group), 1220-1230(C-C-O str. of ester from DT), 1130-1140(C-C-O str of ester from amidodiol). **^1H NMR (DMSO- d_6), δ (ppm):** 1.1 (t, $-\text{CH}_3$ in tartrate unit), 1.5, 1.9, 2.1, 2.8, 3.1 (m, $-\text{CH}_2$ of amidodiol unit), 3.5 (-NH protons of amidodiol) 4.2 (q, $-\text{CH}_2$ in tartrate unit), 5.3 (s, $-\text{CH}$ in tartrate unit), 7.5 (d, aromatic protons). **^{13}C NMR (DMSO- d_6), δ (ppm):** 175-178 (the ester formed by both chiral diols and amidodiols), 172-173 (ester carbon in tartrate unit), 150 (aromatic ring carbons), 72 ($-\text{CH}-$ of tartrate unit), 65-67 ($-\text{CH}_2\text{O}-$), 45 ($-\text{CH}_2-$ tartrate unit), 38-42 ($-\text{CH}_2\text{NH}-$), 30-35 ($-\text{CO}-\text{NH}-\text{CH}_2-\underline{\text{CH}_2-}$), 25-27 ($-\text{CO}-\text{CH}_2-\underline{\text{CH}_2-}$), 20 (CH_3- tartrate unit).

PEB9: IR (KBr in cm^{-1}): 3250-3300 NH str. of amidodiol unit, 3000-2900 (sp^3 C-H str in tartrate unit), 1740-1750 (C=O str. in ester formed by amidodiol), 1730-1735 (C=O str. ester group in diethyl tartrate); 1720-1725 (C=O str. in ester formed by tartrate); 1650-1680(C=O str. ester group in amidodiol), 1530-1550 (NH bending in amidodiol), 1455-1460 (C-H bend of CH_2 group), 1420-1430 (CN str. in amidodiol) 1380-1405 (C-H bend of CH_3 group), 1130-1230 (C-C-O str. of ester). **^1H NMR (DMSO- d_6), δ (ppm):** 1.2, 1.5, 2.3, 2.8, 3.1 (m, $-\text{CH}_2$ of amidodiol unit), 3.5 (-NH protons of amidodiol), 8 (d, aromatic protons). **^{13}C NMR (DMSO- d_6), δ (ppm):** 178 (C=O group of polyester), 172 (C=O group of amidodiol), 136-160 (aromatic protons), 60-65, 39-42, 32-36, 28-30 (CH_2 of amidodiol).

PEB10-PEB12: IR (KBr in cm^{-1}): 3250-3300 NH str. of amidodiol unit, 3000-2900(sp^3 C-H str. in tartrate unit), 1740-1750(C=O str. in ester formed by amidodiol), 1730-1735(C=O str. ester group in diethyl tartrate); 1720-1725(C=O str. in ester formed by tartrate); 1650-1680(C=O str. ester group in amidodiol), 1530-1550(NH bending in amidodiol), 1455-1460(C-H bend of CH_2 group), 1420-1430(CN str. in amidodiol) 1380-1405(C-H bend of CH_3 group), 1220-1230(C-C-O str. of ester attached to DT unit), 1130-1140(C-C-O str. of ester attached to amidodiol group). **^1H NMR (DMSO- d_6), δ (ppm):** 1.0 (t, $-\text{CH}_3$ in tartrate unit), 1.4, 1.8, 2.3, 2.7, 3.1 (m, $-\text{CH}_2$ of amidodiol unit), 3.5 (-NH protons of amidodiol), 4.2 (q, $-\text{CH}_2$ in tartrate unit), 5.3 (s, $-\text{CH}$ in tartrate unit), 8 (d, aromatic protons).

^{13}C NMR (DMSO- d_6), δ (ppm): 172-178 (the ester formed by both chiral diols and amidodiols), 162-164 (ester carbon in tartrate unit), 134 (aromatic ring carbons), 75 (-CH- of tartrate unit), 60-67 (-CH₂O-), 42 (-CH₂- tartrate unit), 39-40 (-CH₂NH-), 29-36 (-CO-NH-CH₂-CH₂-), 23-28 (-CO-CH₂-CH₂-), 18 (CH₃- tartrate unit).

PEB13: IR (KBr in cm^{-1}): 3250-3300 NH str. of amidodiol unit, 3000-2900(sp^3 C-H str in tartrate unit), 1740-1750(C=O str. in ester formed by amidodiol), 1650-1680(C=O str. ester group in amidodiol), 1530-1550(NH bending in amidodiol), 1455-1460(C-H bend of CH₂ group), 1420-1430(CN str. in amidodiol) 1380-1405(C-H bend of CH₃ group), 1130-1230(C-C-O str. of ester). ^1H NMR (DMSO- d_6), δ (ppm): 1.2, 1.5, 2.3, 2.8, 3.1 (m, -CH₂ of amidodiol unit), 3.5 (-NH protons of amidodiol), 8 (d, aromatic protons). ^{13}C NMR (DMSO- d_6), δ (ppm): 178 (C=O group of polyester), 172 (C=O group of amidodiol), 136-160 (aromatic protons), 60-65, 39-42, 32-36, 28-30 (CH₂ of amidodiol). The ^1H NMR and ^{13}C NMR spectra of PEB2-PEB4 are shown in Figure 6. 5 and Figure 6. 6.

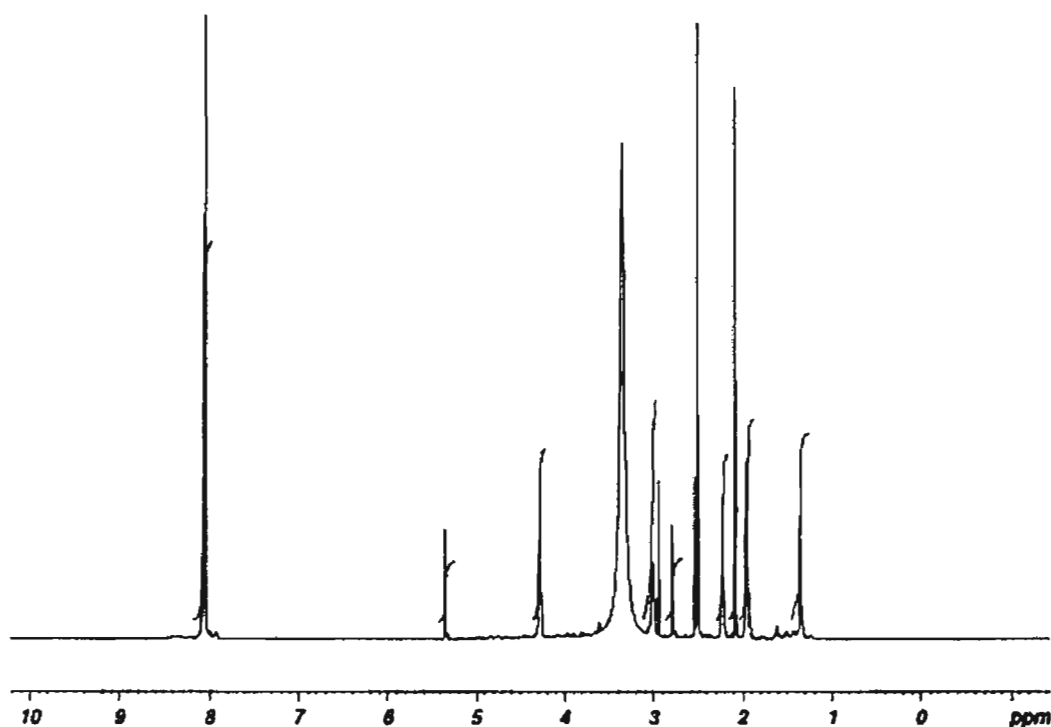
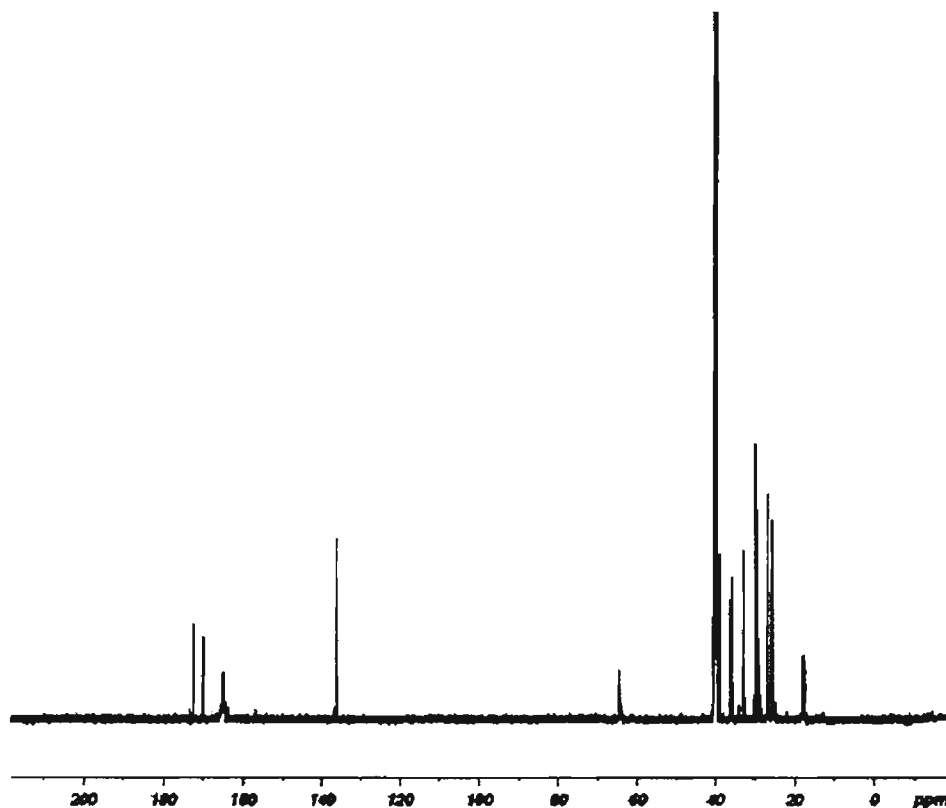


Figure 6. 5: ^1H NMR spectra of PEB2-PEB4

Figure 6. 6: ^{13}C NMR spectra of PEB2-PEB4

6. 7. 3. Mass spectra

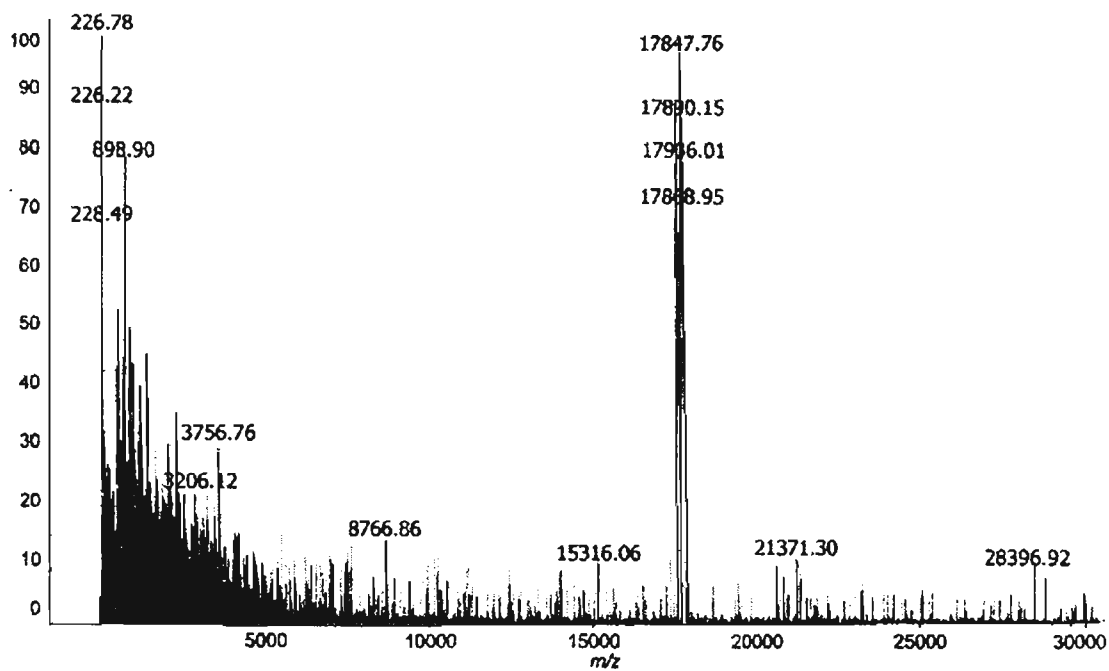


Figure 6. 7: MALDI Mass spectra of PEB3

From the MALDI MS analysis, it was found that the molecular weight of the polyesters synthesized were in the range 17,000-20,000, whereas the

molecular weight of the single repeating unit \approx 650-800, which confirmed the proposed structure consisting of almost 25-30 repeating units. One of the mass spectra of the series is shown (PEB3) in **Figure 6. 7.**, which possess a molecular weight of 17847 with 698 for each repeating unit (26 repeating units).

6. 7. 4. Absorption Spectra

The UV-Vis spectra of polyesters were taken in DMAc solvent. All polymers showed absorbance at a range of 265-295 nm and the absorption maxima are summarized in **Table 6. 6.** This type of $n \rightarrow \pi^*$ transition includes the presence of $-C=O$, $-COOR$, $-CONH_2$ etc.

6. 7. 5. Emission Spectra

For the fluorescence measurement, the excitation wavelength was chosen in a range of 340-360 nm and emission was observed in the range of 400-420 nm. For all the samples, the excitation wavelengths and emission wavelengths were recorded in the instrument by giving the proper absorption wavelengths and excitation wavelengths. The fluorescence emission λ_{max} values are shown in **Table 6. 6.**

6. 7. 6. Specific rotation

The molecular level chirality of the polymers can be studied by the polarimetric technique. The value of optical rotation of the polymers increased when the chiral diethyl tartrate molecule was incorporated. The specific rotation $[\alpha]_D$ values measured for polymers varied from 0° to 43° . The $[\alpha]_D$ value increased with increase in the percentage of chiral component. The polyesters without chiral molecule possess zero specific rotation. The fairly high values for specific rotation for polymers with higher % of chiral diols show that no racemization has occurred during the polymerization process. The specific rotation values of all the polyesters are summarized in **Table 6. 6.**

6. 7. 7. Refractive index

The prism method was used to determine the refractive index of the polymer samples. The measurements were carried out using Digital Refractometer (ATAGO) using the wavelength of 589 nm. Distilled water was

taken as the reference with refractive index of 1.33. The values of refractive index of the polyesters are obtained in the range 1.42-1.53, which are shown in Table 6.6.

Table 6.6: Optical and thermal properties of the polyesters (PEB1-PEB13)

Polymer	% of chiral diol	Specific rotation ($[\alpha]_{D^{20}}$)	Absorption $\lambda_{\max}(\text{nm})$	Emission $\lambda_{\max}(\text{nm})$	IDT ($^{\circ}\text{C}$)	T_g ($^{\circ}\text{C}$)	Refractive index
PEB1	100	43	293	416	180	105	1.4702
PEB2	75	40	288	418	200	118	1.4689
PEB3	50	35	289	414	270	150	1.4819
PEB4	25	12	289	406	280	165	1.4268
PEB5	0	0	289	402	220	135	1.4219
PEB6	75	32	289	412	218	135	1.4987
PEB7	50	28	286	410	220	148	1.5123
PEB8	25	14	289	409	250	160	1.5243
PEB9	0	0	286	405	190	118	1.4876
PEB10	75	33	288	415	240	109	1.5062
PEB11	50	28	284	410	246	140	1.4895
PEB12	25	25	295	408	250	157	1.5019
PEB13	0	0	290	404	210	128	1.4997

6.7.8. XRD pattern

The X-ray diffraction profiles of the polymers were used to analyze the crystalline nature of polymers. The crystallinity of the prepared polymers was evaluated by XRD pattern and strong reflection peaks between the 2θ range 15 and 30 degree were observed. Since the peaks were found to be sharp, the multifunctional polymeric systems were considered to be crystalline in nature. The XRD pattern of PEB6, PEB7 and PEB8 multifunctional polymers are shown in Figure 6.8. There is no prominent shift observed for the polyesters with reference to chiral diol composition. The bifunctional polymers with only achiral diols possessed low intensity broad peaks which corresponded to the semicrystalline characteristics of the achiral bifunctional polymers. The

semicrystalline XRD pattern of PEB5, PEB9 and PEB13 are also shown in the Figure 6. 9.

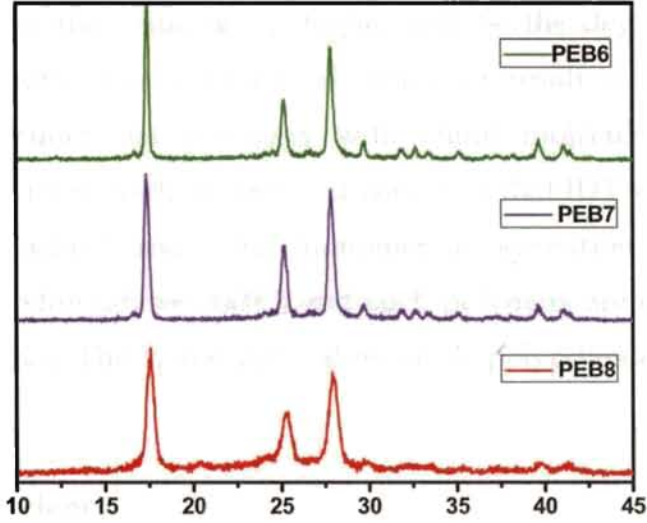


Figure 6. 8: XRD pattern for PEB6-PEB8

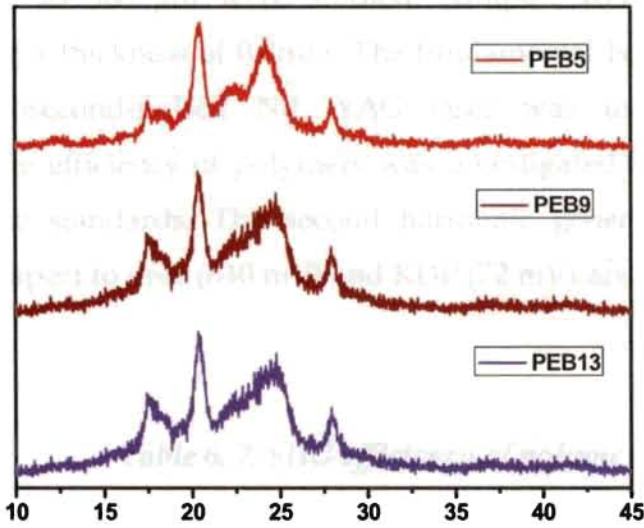


Figure 6. 9: XRD pattern of polyesters PEB5, PEB9 and PEB13

6. 7. 9. Thermal properties

The thermal stability of a polymer can give a sufficient temperature window for NLO measurement even at elevated temperatures. The T_g of a polymer depends largely on the thermal energy required to create internal segmental motion in the polymer chain. A transition from rigid to flexible structures is indicated by the glass transition (T_g) values for a polymer. The

flexible working behaviour of a polymer decreases below its T_g . The glass transition effects are relatively small in magnitude compared to the melting point. Higher the thermal energy and degree of polar order, higher will be the values of T_g ⁶⁻⁸. It was seen that the T_g values of the polymers range from 105°C to 165°C. The higher the value of T_g , higher will be the degree of polar order. Polymers with both chiral and achiral monomer resulted in a high T_g value compared to bifunctional polymers with chiral molecules. IDT values of polyester ranged from 180°C to 280°C. It was clear that IDT values of polyesters containing both achiral and chiral monomer incorporation were found to be having more stability (above 200°C) and such polymers are expected to exhibit high SHG efficiency. The T_g and IDT values of the polyesters are shown in **Table 6. 6**.

6. 7. 10. SHG efficiency

SHG from microcrystalline powders of polymer was examined using the Kurtz-Perry method¹⁶⁻¹⁷. Particles were graded using standard sieves; sizes ranging from 40 to 300 μm were studied. Samples were loaded in glass capillaries having a thickness of 0.8mm. The fundamental beam (1064 nm) of a Q-switched nanosecond-pulsed Nd: YAG laser was used for the NLO measurement. The efficiency of polymers was investigated by using KDP and urea as reference standards. The second harmonic generation efficiency of polymers with respect to urea (640 mV) and KDP (72 mV) are summarized in the **Table 6. 7**.

Table 6. 7: SHG efficiency of polymers

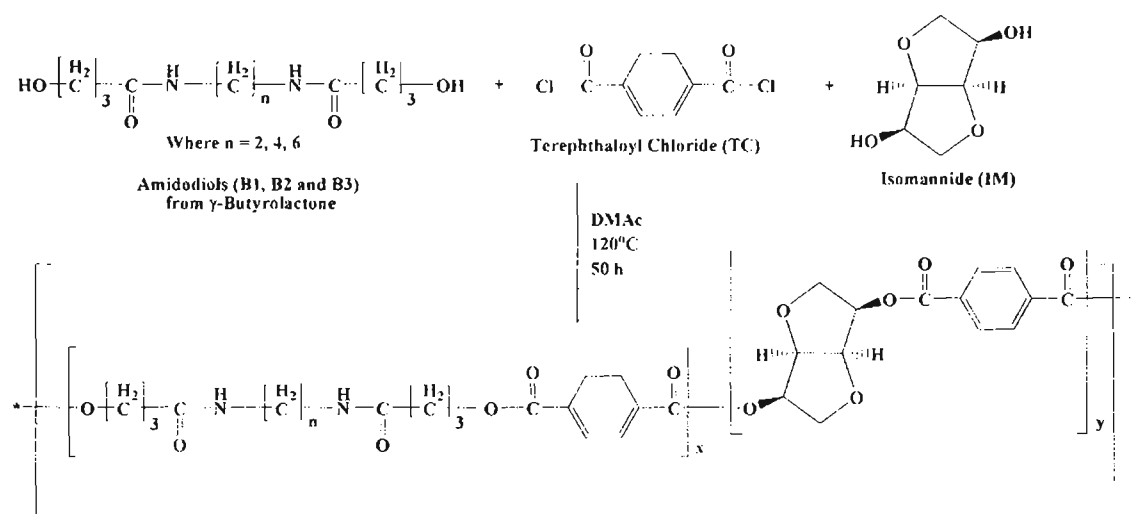
Polymer	SHG efficiency w. r. to urea (%)	SHG efficiency w. r. to KDP (%)
PEB1	1.72	15.28
PEB2- PEB4	2.81	25.00
PEB6- PEB8	2.50	22.22
PEB10 -PEB12	2.34	20.83
PEB5, PEB9, PEB13	2.08	18.69

Among the polyesters, the multifunctional polymers possessed more SHG efficiency compared to bifunctional polyesters. The multifunctional polymer with B1 amidodiols exhibited more SHG efficiency.

6. 8. ISOMANNIDE BASED POLYESTERS

6. 8. 1. Experimental discussion

The polymer PEC1 is the one which is having only chiral unit (isomannide unit) in polymer chain and considered as the mother polymer in the series. The ratio of TC and IM are taken as 1: 1. PEC2, PEC3, PEC4, PEC5 are the polyesters with B1 achiral molecule having the TC: IM: B1 ratio as 1: 0.75: 0.25, 1: 0.5: 0.5, 1: 0.25: 0.75, 1: 0: 1 respectively. PEC6, PEC7, PEC8, PEC9 are the polyesters with B2 amidodiols in which TC: IM: B2 ratio is maintained as 1: 0.75: 0.25, 1: 0.5: 0.5, 1: 0.25: 0.75, 1: 0: 1 respectively. PEC10, PEC11, PEC12, PEC13 are the polyesters with B3 achiral diol having the ratio of TC: IM: B3 as 1: 0.75: 0.25, 1: 0.5: 0.5, 1: 0.25: 0.75, 1: 0: 1 respectively. Scheme 6. 4 represent the synthesis of polyesters (PEC1-PEC13).



Scheme 6. 4: Synthesis of polyesters PEC1-PEC13

6. 8. 2. Spectral characterization

PEC1: FTIR (KBr), ν_{max} (cm^{-1}): 3045-2970 (sp^3 C-H stretching in isomannide unit), 1735 (C=O stretching in ester formed by isomannide), 1537 (NH bend), 1451 (C-H bend of $-\text{CH}_2$ group in isomannide), 1230 (C-O stretching of isomannide unit), 1055-1125 (C-O stretching vibrations of polyester). ^1H NMR (DMSO- d_6), δ

(ppm): 4.0 (q, -CH₂ in isomannide unit), 4.1- 4.3 (t, -CH- bridge protons of isomannide unit), 4.9 (m, -CH in isomannide unit), 8.2 (d, aromatic protons of terephthaloyl chloride). ¹³C NMR (DMSO-d₆), δ (ppm): 172-178 (ester carbonyl in ester), 150-155 (aromatic ring carbons), 72 (-CH- bridge of isomannide unit), 32-35 (-CH₂- isomannide unit).

PEC2-PEC4: FTIR (KBr), ν_{max} (cm⁻¹): 3250-3300 (-NH stretching of amidodiol unit), 3000-2900 (C-H stretching of -CH₂- in both isomannide and amidodiol unit), 1735-1744 (C=O stretching in ester formed by amidodiol), 1720-1725 cm⁻¹ (C=O stretching in ester formed by isomannide); 1670-1688 (C=O stretching of -CONH group in amidodiol), 1540-1552 (NH bending in amidodiol), 1450-1465 (C-H bend of CH₂ groups), 1415-1420 (-C-N stretching in amido linkage), 1220-1225 (C-O stretching of isomannide unit) 1075-1135 (C-C-O stretching of polyester). ¹H NMR (DMSO-d₆), δ (ppm): 1.2- 3.0 (m, CH₂ of amidodiol unit), 3.5 (-NH protons of amido unit), 4.1 (q, -CH₂ in isomannide unit), 4.3- 4.5 (t, -CH- bridge protons of isomannide unit), 4.8-4.9 (m, -CH in isomannide unit), 6.9 (d, aromatic protons of TC). ¹³C NMR (DMSO-d₆), δ (ppm): 172-175 (ester carbonyl in polyester), 170 (C=O of amidodiol), 140-150 (aromatic ring carbons), 68 (-CH- bridge of isomannide unit), 60-66 (-CH₂O-), 42 (-CH₂NH-), 36-39 (-CO-NH-CH₂-CH₂-), 25-28 (-CO-CH₂-CH₂-), 32-34 (-CH₂- isomannide unit).

PEC5: FTIR (KBr), ν_{max} (cm⁻¹): 3295-3300 (-NH stretching of amidodiol unit), 3000-2900 (C-H stretching in polyesters), 1712-1728 (C=O stretching in ester formed by amidodiol), 1648-1650 (C=O stretching in amidodiol), 1545-1550 (-NH bending in amidodiol), 1418-1425 (-CN stretching in amidodiol), 1130-1200 (C-C-O stretching of ester). ¹H NMR (DMSO-d₆), δ (ppm): 1.3-3.0 (m, -CH₂ of amidodiol unit), 3.5 (-NH proton of amidodiol), 7.8 (d, aromatic protons of TC). ¹³C NMR (DMSO-d₆), δ (ppm): 173-175 (ester carbonyl in polyester), 170 (C=O of amidodiol), 150-155 (aromatic ring carbons), 60-70, 39-42, 32-36, 25-30 (-CH₂- of amido groups).

PEC6-PEC8: FTIR (KBr), ν_{max} (cm⁻¹): 3240-3300 (-NH stretching of amidodiol unit), 3000-2950 (C-H stretching of -CH₂- in both isomannide and amidodiol unit), 1732-1740 (C=O stretching in ester formed by amidodiol), 1722-1728 (C=O stretching in amidodiol formed by isomannide); 1660-1675 (C=O stretching of -CONH group in amidodiol), 1530-1550 (NH bending in amidodiol), 1455-1460

(C-H bend of CH₂ groups), 1425-1430 (-C-N stretching in amidodiol), 1230-1234 (C-O stretching of isomannide unit) 1075-1135 (C-C-O stretching of ester). **¹H NMR (DMSO-d₆), δ (ppm):** 1.3-3.0 (m, -CH₂ of amidodiol unit), 3.5 (-NH of amido unit), 4.2 (q, -CH₂ in isomannide unit), 4.4-4.5 (t, -CH- bridge protons of isomannide unit), 4.9 (m, -CH in isomannide unit), 7.8 (d, aromatic protons of TC). **¹³C NMR (DMSO-d₆), δ (ppm):** 173-175 (ester carbonyl in polyester), 171 (C=O of amidodiol), 150-156 (aromatic ring carbons), 72 (-CH- bridge of isomannide unit), 60-67 (-CH₂O-), 49 (-CH₂NH-), 32-36 (-CO-NH-CH₂-CH₂-), 25-28 (-CO-CH₂-CH₂-), 22-24 (-CH₂- isomannide unit).

PEC9: FTIR (KBr), ν_{max} (cm⁻¹): 3280-3300 (-NH stretching of amidodiol unit), 3012-2980 (C-H stretching) 1712-1728 (C=O stretching in ester formed by amidodiol), 1660-1675 (C=O stretching in amidodiol), 1542-1550 (-NH bending in amidodiol), 1415-1423 (-CN stretching in amidodiol), 1145-1200 (C-C-O stretching of ester). **¹H NMR (DMSO-d₆), δ (ppm):** 1.3-3.0 (m, -CH₂ of amidodiol unit), 3.5 (-NH of amido unit), 8 (d, aromatic protons of TC). **¹³C NMR (DMSO-d₆), δ (ppm):** 174-177 (ester carbonyl in polyester), 172 (C=O of amidodiol), 146-159 (aromatic ring carbons), 65-70, 39-45, 32-37, 25-30 (-CH₂- of amido groups).

PEC10- PEC12: FTIR (KBr), ν_{max} (cm⁻¹): 3250-3300 (-NH stretching of amidodiol unit), 3000-2900 (C-H stretching of -CH₂- in both isomannide and amidodiol unit), 1740-1750 (C=O stretching in ester formed by amido group), 1731-1738 (C=O stretching in ester formed by isomannide), 1650-1680 (C=O stretching of -CONH group in amidodiol), 1530-1550 (-NH bending in amido unit), 1455-1460 (C-H bend of CH₂ groups), 1416-1427 (-C-N stretching in amidodiol), 1220-1225 due to (C-O stretching of isomannide unit), 1075-1135 (C-C-O stretching of ester). **¹H NMR (DMSO-d₆), δ (ppm):** 1.2-3.3 (m, -CH₂ of amidodiol unit), 3.5 (-NH of amido group), 4-4.2 (q, -CH₂ in isomannide unit), 4.8 (t, -CH- bridge protons of isomannide unit), 5.1-5.2 (m, -CH in isomannide unit), 6.7- 7.0 (d, aromatic protons of TC). **¹³C NMR (DMSO-d₆), δ (ppm):** 175-178 (ester carbonyl in ester), 172 (C=O of amidodiol), 145-155 (aromatic ring carbons), 68 (-CH-bridge of isomannide unit), 60-67 (-CH₂O-), 39 (-CH₂NH-), 31-36 (-CO-NH-CH₂-CH₂-), 25-28 (-CO-CH₂-CH₂-), 32-35 (-CH₂- isomannide unit).

PEC13: FTIR (KBr), ν_{max} (cm⁻¹): 3280-3300 (-NH stretching of amidodiol unit), 3000-2900 (C-H stretching in polyester), 1712-1728 (C=O stretching in ester

formed by amidodiol), 1660-1671 (C=O stretching in amidodiol), 1540-1553 (-NH bending in amidodiol), 1410-1420 (-CN stretching in amidodiol), 1145-1183 (C-C-O stretching of ester). ^1H NMR (DMSO- d_6), δ (ppm): 1.3-2.9 (m, $-\text{CH}_2$ of amidodiol unit), 3.5 (-NH protons of amidodiol) 7.2 (m, aromatic protons of polyester). ^{13}C NMR (DMSO- d_6), δ (ppm): 170-175 (ester carbonyl in polyester), 168 (C=O of amidodiol), 134-140 (aromatic ring carbons), 61-72, 39-43, 30-36, 25-28 ($-\text{CH}_2-$ of amido groups).

6. 8. 3. Mass spectra

From the MALDI-MS analysis it was found that the molecular weight of the polyesters synthesized were between 17,800-19,000, where as the molecular weight of one repeating unit \approx 650-800, which confirmed the proposed structure was made of almost 25-30 repeating units.

6. 8. 4. Absorption Spectra

The UV-Vis spectra of polyesters were taken in DMAc solvent. All the polymers showed two absorption peaks at 280-290 nm range (λ_{max}) and 300-320 nm range. The polyesters with amido units containing both π bonds and unshared electron pairs exhibit two absorptions, a low intensity shoulder like $n \rightarrow \pi^*$ transition at longer wavelength \sim 300-320 nm and a high intensity $\pi \rightarrow \pi^*$ band at a shorter wavelength of \sim 280-290 nm. The λ_{max} values are shown in Table 6. 8.

6. 8. 5. Fluorescence spectra

The excitation wavelengths were found to lie between 365-370 nm and emission spectra obtained were between 400-410 nm. For all the samples, the excitation wavelengths and emission wavelengths were recorded in the fluorescence spectrum by knowing the proper absorption wavelengths and excitation wavelengths. The emission maximum values are shown in Table 6. 8.

6. 8. 6. Specific rotation

Since isomannide was taken as the optically active monomer ($[\alpha]_D^{20} = +89$) for the polyester synthesis, the specific rotation of polymers was found to be higher compared to that of isosorbide and (2R, 3R)-diethyl tartrate containing

polyesters. The specific rotation of polyesters increased when more % of chiral molecules with more isomannide was incorporated. The specific rotation $[\alpha]_D$ values measured for polymers varied from 0° to 84° . The $[\alpha]_D$ value increased with increase in the % of chiral component. The polyesters with only achiral unit (bifunctional) possessed zero specific rotation. The values of specific rotation of the polyesters are shown in Table 6. 8.

6. 8. 7. Refractive index

For the refractive index measurements, distilled water was taken as the reference with the refractive index of 1.33. The refractive index of the polymer samples lie in the range 1.42-1.58, which are shown in Table 6. 8.

Table 6. 8: Optical and thermal properties of Polyesters (PEC1- PEC13)

Polymer	% of chiral diol	Specific Rotation ($[\alpha]_D^\theta$)	Absorption $\lambda_{\max}(\text{nm})$	Emission $\lambda_{\max}(\text{nm})$	IDT ($^\circ\text{C}$)	Tg ($^\circ\text{C}$)	Refractive index
PEC1	100	84	290	410	195	78	1.5619
PEC2	75	78	286	405	240	140	1.5573
PEC3	50	76	286	406	248	152	1.5683
PEC4	25	72	287	402	256	156	1.5732
PEC5	0	0	289	402	220	135	1.4219
PEC6	75	83	289	402	220	135	1.5683
PEC7	50	78	286	405	225	146	1.5692
PEC8	25	69	289	402	228	147	1.5672
PEC9	0	0	286	405	190	118	1.4876
PEC10	75	79	285	407	226	139	1.5534
PEC11	50	78	287	407	228	131	1.5532
PEC12	25	74	286	405	225	137	1.5423
PEC13	0	0	290	404	210	128	1.4997

6. 8. 8. Thermal properties

The thermal behaviour of the polymers was investigated using TG and DTA to determine the thermal degradation pattern and glass transition temperature. The results are summarized in the **Table 6. 8**. The multifunctional polymers are thermally stable upto 220-260°C according to its TGA thermogram. The bifunctional achiral polymers were stable upto 190-220°C and the chiral bifunctional polymers have thermal stability near to 195°C. The T_g value of chiral PEC1 polymer measured using DTA is near to 78°C. The T_g values of bifunctional achiral polymers are 118-135°C, lower than those of the multifunctional polyesters with both chiral and achiral blocks, which are in the range 130 to 160°C. The TG and DTA studies showed that the decomposition temperature and T_g of the polymers with both chiral diol and achiral diol were higher than their corresponding bifunctional polymers. This is due to the enhancement of the rigidity caused by the incorporation of both the monomer units. For most of the polymers, sharp endothermic peaks were observed in DTA. The sharpness of the endothermic peak showed the crystalline nature of the polymer²⁷⁻²⁸. The data obtained by thermal analysis showed that the polyesters were having good thermal stability.

6. 8. 9: Crystallinity

The X-ray diffraction profiles were used to analyze the crystalline nature of the polyesters. Strong XRD signals of PEC2-PEC4, PEC6-PEC8 and PEC10-PEC12 multifunctional polymers were observed in the range of $2\theta=15-30$ degree, which explained the crystalline characteristics of polyesters. The polymers were synthesized by varying their chiral-achiral diol composition. But there was no prominent shift observed for the polyesters with reference to chiral diol percentage. The bifunctional polymers containing only chiral diols also possessed high intensity sharp peaks which corresponded to the crystalline characteristics of the PEC1. The semicrystalline nature of PEC5, PEC9 and PEC13 were explained by the low intense peaks in XRD pattern.

6. 8. 10. SHG efficiency

Powder technique was used for investigating the nonlinear optical response of the polymers¹⁶⁻¹⁷. The second harmonic signal generated by the polymer was confirmed by the emission of green radiation from the polymer.

The SHG responses of the polymer samples were recorded using urea and KDP as references. The polyesters showed good SHG efficiency with respect to the reference compounds, urea (640 mV) and KDP (72 mV). Among the series of polyesters (PEC1-PEC13), the polymers with both chiral and amidodiols groups gave considerably high activity compared to bifunctional polymers. PEC2-PEC4, PEC6-PEC8 and PEC10-PEC12 systems have high efficiency as that of urea and KDP. The NLO responses of the polymers are reported in the **Table 6. 9**. Even if there is an absence of π -conjugation in donor-acceptor systems, the polyester systems showed considerable NLO activity. As predicted by theoretical results, the bifunctional polymers PEC1, PEC5, PEC9 and PEC13 showed comparatively good SHG efficiency with respect to urea and KDP.

Table 6. 9: SHG efficiency of polymers

Polymer	SHG efficiency w. r. to urea (%)	SHG efficiency w. r. to KDP (%)
PEC1	1.88	16.67
PEC2- PEC4	3.28	29.17
PEC6- PEC8	2.97	26.39
PEC10 -PEC12	2.81	25.00
PEC5, PEC9, PEC13	2.08	18.69

From the experimental measurements, it was found that the polyesters with isomannide moiety possessed good SHG efficiency compared to polymer containing other chiral moieties. The multifunctional polymers PEC2-PEC4, with B1-achiral monomer possessed more SHG response among the series.

The solubility behaviour of the polymers was tested qualitatively in various solvents. The polymers showed good solubility in aprotic solvents such as DMAc, DMSO, DMF etc. However, the polyesters showed very poor level of solubility in THF at room temperature and complete solubility while heating. The polymers were insoluble in organic solvents like CHCl_3 , hexane, toluene, benzene etc.

Both theoretical calculation and experimental measurements gave almost similar inferences about the SHG efficiency of polymers. Experimental observation showed that all the polymers have high SHG efficiency compared to KDP and urea. The polymers with isomannide chiral diol have the maximum SHG values in both theoretical calculation and experimental measurements. It can be concluded from both theoretical calculation and experimental measurement that the second harmonic generation efficiency of the multifunctional polymers with both chiral and achiral diols is more than the bifunctional polymers with either chiral or achiral monomers.

6. 9. Conclusions

A series of polyesters (bifunctional and multifunctional) containing chiral building blocks and amidodiols in the main chain have been designed and synthesized. All of them were characterized by various spectroscopic techniques. All sets of polyesters exhibited high T_g values with good thermal stability. The polyesters with both the chiral and achiral units demonstrated relatively high T_g and IDT values in comparison with those bifunctional polyesters with chiral or achiral units. The XRD pattern explained the crystalline nature of polyesters. The specific rotation was found to be less for the polymers with low % of chiral diols. All polyesters showed moderately good nonlinear optical activity by Kurtz-Perry Powder technique. From both the theoretical and experimental studies it can be concluded that the polymers which contained isomannide as the chiral monomer and **B1** as amidodiols, showed maximum second order response. Thus the polymers can be considered as good materials for practical photonic applications.

6. 10. References

1. Itsuno S, Devproshad K P, Salam M A, Haraguchi N, *J Am Chem Soc*, 2010, **132**, 2864.
2. Wang D, Zhang S, Zhang Y, Wang H, Mu J, Wang G, Jiang Z, *Dyes and Pigments*, 2008, **79**, 217.
3. Vembris A, Rutkis M, Zauls V, Laizane E, *Thin Solid Films*, 2008, **516**, 8937.
4. Krupka O, Elghayoury A, Rau I, Sahraoui B, Grote J G, Kajzar F, *Thin Solid Films*, 2008, **516**, 8932.
5. Prasad P N, Williams D J, *Introduction to Nonlinear Optical effects in Molecules*
204

- and Polymers*, John Wiley and Sons, New York, 1991.
6. Bahulayan D, Sreekumar K, *J Mater Chem*, 1999, **9**, 1425.
 7. Philip B, Sreekumar K, *J Polym Sci: Part A: Polym Chem*, 2002, **40**, 2868.
 8. Davis D, Sreekumar K, Pati S K, *Synth Metals*, 2005, **155**, 384.
 9. Datta A, Pati S K, *J Molecular Structure; Theochem*, 2005, **756**, 97.
 10. Datta A, Pati S K, *J Phys Chem A*, 2004, **108**, 320.
 11. Ramasesha S, Shuai Z, Bredas J L, *Chem Phys Lett*, 1995, **245**, 224.
 12. Albert I D L, Ramasesha S, *J Phys Chem*, 1990, **94**, 6540.
 13. Ramasesha S, Albert I D L, *Phys Rev B*, 1990, **42**, 8587.
 14. Pati S K, Ramasesha S, Shuai Z, Bredas J L, *Phys Rev B*, 1999, **59**, 14827.
 15. Pati S K, Marks T J, Ratner M A, *J Am Chem Soc*, 2001, **123**, 7287.
 16. Kurtz S K, Perry T T, *J Appl Phys*, 1968, **39**, 3798.
 17. Jayaprakash M, Radhakrishnan T P, *Chem Mater*, 2006, **18**, 2943.
 18. Lalama S J, Garito A F, *Phys Rev A*, 1979, **20**, 20.
 19. Elizabeth C V, Sreekumar K, *J Mater Sci*, 2010, **45**, 1912.
 20. Elizabeth C V, Sreekumar K, *J Appl Polym Sci*, 2010, xx, xxxx.
 21. Sandhya K Y, Pillai C K S, Sreekumar K, *J Polym Sci Part B, Polym Phys*, 2004, **42**, 1289.
 22. Pillai C K S, Sandhya K Y, Sudha J D, Saminathan M, *Pramana; J Phys*, 2003, **61**, 417.
 23. Sudha J D, *J Polym Sci, Part A, Polym Chem*, 2000, **38**, 2469.
 24. Sudha J D, Ramamohan T R, Pillai C K S, Scariah K J, *Eur Polym J*, 1999, **35**, 1637.
 25. Philip B, Sreekumar K, *Colloid Polym Sci*, 2003, **281**, 485.
 26. Philip B, Sreekumar K, *Designed Monomers and Polymers*, 2002, **5**, 115.
 27. Philip B, *Ph. D thesis, Studies on photorestructuring of synthetic polymers*, Department of Chemistry, University of Kerala, India, 2001
 28. Davis D, *Ph. D thesis, Nonlinear optical properties of polymers containing azomesogen and chiral molecules: Theoretical and experimental evaluations*, Department of Applied Chemistry, Cochin University of Science and Technology, Kerala, India, 2005.

Chapter 7

**MAIN CHAIN CHIRAL POLYURETHANES WITH AMIDODIOL
MONOMERS DERIVED FROM ϵ -CAPROLACTONE:
THEORETICAL AND EXPERIMENTAL INVESTIGATIONS****7. 1. Introduction**

Polyurethanes with donor-acceptor structures attached to the polymeric chains have attracted great interest in recent years because of the possibility of a broad range of applications. These materials have found many applications in the areas of adhesives, coatings, flexible and rigid foams, elastomers, fibres, water proofing, thermoset resins, thermoplastic molding compounds, rubber vulcanization, silicon and boron polymers¹⁻². In the last few years, research interest has grown in developing polymeric materials, which exhibit nonlinear optical (NLO) properties, for applications such as optical devices, optical signal processing and information storage³⁻⁴. Although the second order NLO polymers hold promising applications in electro-optic devices, a number of issues have to be addressed thoroughly before they possess commercial value. The crucial issues are the high thermal stability of the dipole orientation and large optical nonlinearity⁵. Many organic molecules and polymers which exhibit high second harmonic generation activity require special techniques like poling under an electric field to remove the centre of symmetry and orient themselves in a directional fashion so that they are practically applicable for device fabrication⁶⁻⁷. The centre of symmetry is necessarily broken when preferred helicity is achieved in supramolecular organization by the usage of chiral building blocks. (2R, 3R)-diethyl tartrate, and the dianhydrohexitols, isosorbide and isomannide are used as chiral building blocks which induce a helical conformation in the macromolecular chain that are reported to show high glass transition temperatures, excellent thermal stability and interesting physical properties⁸⁻⁹. The incorporation of donor-acceptor systems provides a pathway for redistribution of electronic charges across the entire length or parts or segments of the polymer molecule under the influence of an electric field (optical or electric). Polymers of such organized geometry are very interesting since they can supplement the directional order of donor-acceptor system and

the dipole units are tilted in one direction along the polymer axis which leads to high second harmonic generation ability¹⁰. It is reported that polymers that are synthesized from amidodiols as donor-acceptor groups, obtained by the aminolysis of lactones are highly stable¹¹⁻¹⁶. The stability is explained mainly due to the contributions from the extensive H-bonding between the amide-amide and amide-urethane linkages. In the present work, a series of polyurethanes were designed computationally as a polyaddition product of diisocyanate (2, 4-toluene diisocyanate) with diol molecules (chiral and achiral diols) and different combinations of polymers were synthesized experimentally.

7.2. Methodology

7.2.1. Computational methods

Because of the high cost of computation, all polyurethanes (3 repeating units) were optimized using the AM1 parameterized Hamiltonian available in the Gaussian 03 set of codes. However, for large systems, the accurate determination of the excitation characteristics for dynamic spectroscopic applications still relies on semiempirical methods with configuration interaction. The geometry optimized structures were used for configuration interaction (CI) calculations to obtain energies and the dipole moments in the CI basis using the Zerner's Intermediate Neglect of Differential Overlap (ZINDO) method. The CI approach adopted here has been extensively used in earlier works, and was found to provide excitation energies and dipole matrix elements in good agreement with experiments¹⁷. We have chosen the reference determinants which are dominant in the description of the ground state and the lowest one-photon excited state. For the Hartree-Fock determinant, varying number of occupied and unoccupied molecular orbital has been used to construct the SCI space until a proper convergence is obtained. We have used the singles CI (CIS), because the first nonlinear optical coefficients are derived from second-order perturbation theory involving one-electron excitations. For each reference determinant, 8 occupied and 8 unoccupied molecular orbitals were used to construct a CI space with configuration dimension of 65. To calculate

NLO properties, the correction vector method was used which implicitly assumes all the excitations to be approximated by a correction vector.¹⁸⁻¹⁹ For the calculations of the optical coefficients, an excitation frequency of 1064nm

(1.17eV) which corresponded to the frequency of the Nd-YAG laser, was used. Given the Hamiltonian matrix, the ground state wave function, and the dipole matrix, all in CI basis, it is straightforward to compute the dynamic nonlinear optic coefficients using either the first-order or the second-order correction vectors²⁰⁻²³.

7. 2. 2. Experimental methods

The second harmonic generation efficiency of the polymers were analysed in the powder form by Kurtz Perry technique³⁵⁻³⁶. The well powdered sample was filled in a capillary tube of 0.8 mm thickness. The NLO responses of the materials were recorded using urea and KDP as references, filled in a similar capillary tube sealed at one end for comparison. The experimental set up for the second harmonic generation properties utilizes a Quanta Ray DCR II Nd/YAG laser with a 9 mJ pulse and 1064 nm wavelength, at a repetition rate of 5Hz. A Q-switched, mode-locked Nd: YAG laser was used to generate about 9 mJ pulse at 1064 nm fundamental radiation. The input laser beam was allowed to pass through an IR reflector and then directed on the micro-crystalline powdered sample packed in a capillary tube of diameter, 0.8 mm. The photodiode detector and oscilloscope arrangements measured the light emitted by the sample. The laser beam was split into two parts, one to generate the second harmonic signal in the sample and the other to generate the second harmonic signal in the reference. An output signal of 532nm was measured at a 90° geometry using urea/KDP as the standard. The intensity of the second harmonic output from the sample was compared with that of the reference. The efficiency of the NLO activity of the polymers are expressed in percentage as

$$\text{SHG Efficiency (\%)} = \frac{\text{Signal of Sample}}{\text{Signal of Reference}} \times 100$$

7. 3. Polymer design

7. 3. 1. Bifunctional polymers

The chiral and achiral bifunctional polyurethanes were designed theoretically as the polyaddition products of 2, 4- toluene diisocyanate (TDI) with chiral and achiral diol molecules. The polymers 1, 2, and 3 represent the chiral bifunctional polyurethanes with isosorbide (IS), (2R, 3R)-diethyl tartrate

(DT) and isomannide (IM) as chiral moiety. The achiral polymers were designed as the combination of 2, 4- toluene diisocyanate (TDI) with amidodiol, {N, N'-ethane 1, 2-diyl bis (6-hydroxy hexanamide) (CED), N, N'-butane 1, 4-diyl bis (6-hydroxy hexanamide) (CBD) and N, N'-hexane 1, 6- diyl bis (6-hydroxy hexanamide) (CHD)}, which are represented as **4**, **5** and **6** polymer molecules. Three repeating units of the polymeric system have been chosen for structure optimization and nonlinear optical property calculations. Each repeating unit of the polyurethanes contains one molecule of TDI and one molecule of dihydroxy monomer (chiral and achiral). **Figure 7. 1** represents the designed bifunctional polymers **4-6**, whereas the polymers, **1-3** are obtained by the polyaddition of chiral molecules IS, DT and IM, which are also shown in **Figure 7. 1**.

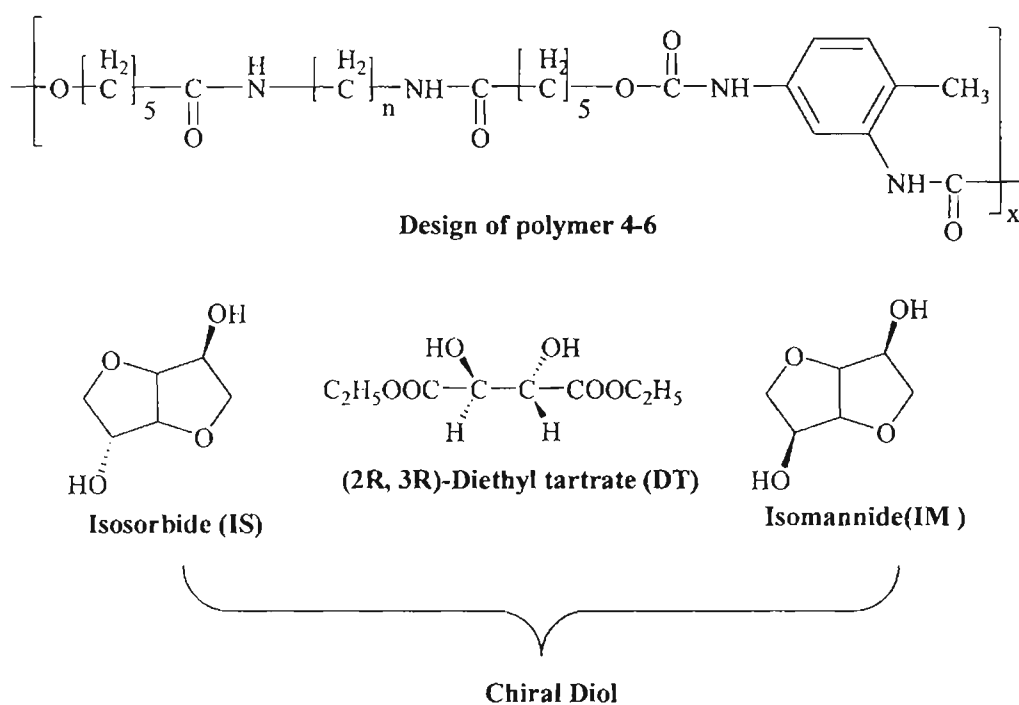


Figure 7. 1: Designed bifunctional polymers

Table 7. 1 reports the two-level parameters such as, the ground-state dipole moment (μ_g), the difference between the dipole moments of ground-state and the excited state ($\Delta\mu$), the optical gap (ΔE), oscillator strength (f), the linear polarizability (α), and the first hyperpolarizability (β) of bifunctional polymers by the *dynamic* SOS calculations. While analyzing the geometries of bicyclic chiral molecules, it could be found that the ground state dipole moment μ_g of isosorbide with oppositely oriented dipoles is greater than that of the

isomannide. Eventhough the ground state dipole moment μ_g is large for isosorbide based polymers, the change in dipole moment $\Delta\mu$ is higher for isomannide based chiral polyurethanes²⁵. The dipole moment difference $\Delta\mu$, between the ground and excited state is the major contributing factor in determining the value of β vector²⁶. In the case of polyurethane with isomannide and isosorbide chiral moiety, the β value is almost doubled in chiral polymer **3** compared to **1**. So it can be concluded that the stereochemistry of the chiral monomer affects the polar ordering of the polymers which plays an important role in achieving highly active polymers capable of second harmonic generation. For the (2R, 3R)-diethyl tartrate based polymer, **2**, a comparatively large change in dipole moment and oscillator strength are observed which causes the high β value for **2**.

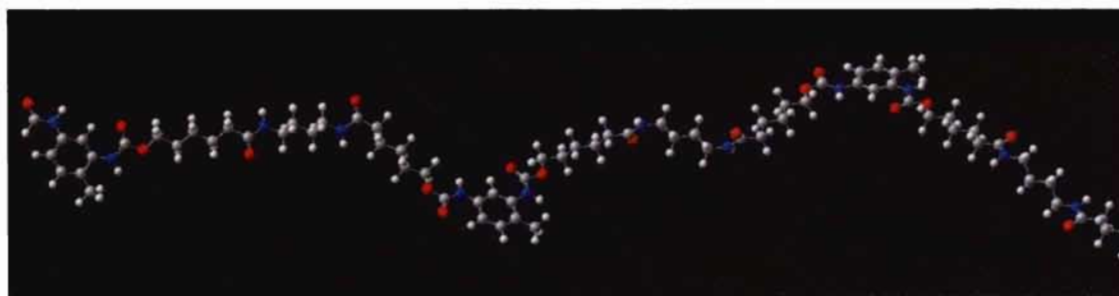


Figure 7. 2: Optimized geometry of polymer 5

Among the polymer series from **4-6**, the polymer **6** possesses a low value of oscillator strength compared to that of **4** and **5** polymers. Also the optical gap, the one which determines the energy gap between ground state and lowest dipole allowed state is large for polymer **6**. Because of the very small oscillator strength and large optical gap, the charge transfer will be difficult in polymer **6** compared to that of polymer **4** and **5**. Moreover, the polymer **6** exhibits a very small change in dipole moment compared to the others. For all the bifunctional polyurethanes, the polarizability lies in the range (14-20 $\times 10^{-23}$ esu).

Among the bifunctional polyurethanes, the polymer with isomannide as chiral diol (polymer **3**) and, achiral polymers with CED amidodiols (polymer **4**) are found to have high SHG efficiency.

Table 7. 1: Ground-State Dipole Moment (μ_g) in debye, Difference in dipole moment between ground state and excited state ($\Delta\mu$), Optical Gap (ΔE) in eV, Oscillator strength (f), Linear Polarizability (α) in units of 10^{-23} esu, and First Hyperpolarizability (β) in units of 10^{-30} esu for the polymers (ZINDO-SOS dynamic property calculations)

Polymer	μ_g	$\Delta\mu$	ΔE	f	α	β
1-TDIIS	11.958	8.029	6.113	1.244	19.982	1.523
2-TDIDT	6.7398	9.570	6.641	1.466	18.952	3.039
3-TDIIM	6.141	9.977	6.298	1.404	19.984	3.894
4-TDICED	12.386	9.544	6.300	1.788	19.325	3.751
5-TDICBD	10.981	8.006	6.329	1.266	14.881	2.673
6-TDICHD	9.8508	7.898	6.330	1.252	15.069	1.670

7. 3. 2. Multifunctional polymers

The polymers are designed as the polyaddition products of achiral diols {N, N' -ethane-1, 2-diyl bis (6-hydroxy hexanamide) (CED), N,N' -butane-1, 4-diyl bis(6-hydroxy hexanamide) (CBD) and N,N' -hexane-1, 6- diyl bis(6-hydroxy hexanamide) (CHD)} and 2, 4- toluene diisocyanate (TDI) with the chiral moiety (IS, IM and DT). The polymers **7**, **8**, and **9** represent the chiral multifunctional polyurethanes with isosorbide (IS) as chiral moiety and CED, CBD and CHD as achiral diols. Similarly **10**, **11** and **12** represents multifunctional polymers with diethyl tartrate (DT) as chiral monomer and the amidodiols (CED, CBD and CHD) as donor-acceptor molecule. The chiral polyurethanes **13**, **14** and **15** represent the isomannide derived multifunctional polymers. Three repeating units of each polymer have been considered for the optimization and molecular property calculations. Each repeating unit contains one molecule of achiral diol, two molecules of TDI and one chiral molecule (IS, IM and DT). The optimized geometry of multifunctional polymer **9** is given in **Figure 7. 3**.



Figure 7. 3: The optimized geometry of Polymer 9

Table 7. 2. reports the two-level parameters such as, the ground-state dipole moment (μ_g), the difference between the dipole moments of ground-state and the excited state ($\Delta\mu$), the optical gap (ΔE), oscillator strength (f), the linear polarizability (α), and the first hyperpolarizability (β) of multifunctional polymers by the *dynamic* SOS calculations. For all the multifunctional polyurethanes, the polarizability lies in the range (13-15 $\times 10^{-23}$ esu).

Table 7. 2: Ground-State Dipole Moment (μ_g) in debye, Difference in dipole moment between ground state and excited state ($\Delta\mu$), Optical Gap (ΔE) in eV, Oscillator strength (f), Linear Polarizability (α) in units of 10^{-23} esu, and First Hyperpolarizability (β) in units of 10^{-30} esu for the polymers (ZINDO-SOS dynamic property calculations)

Polymer	μ_g	$\Delta\mu$	ΔE	f	α	β
7-TDIISCED	11.3873	11.002	6.683	1.146	14.162	4.927
8- TDIISCBD	12.734	10.984	6.681	1.144	14.131	4.911
9- TDIISCHD	12.712	10.910	6.679	1.139	14.116	4.849
10-TDIDTCED	12.423	11.285	6.614	1.282	13.810	5.215
11- TDIDTCBD	12.734	11.182	6.619	1.175	13.805	5.215
12- TDIDTCHD	12.712	11.135	6.629	1.154	13.803	5.212
13-TDIIMCED	8.135	12.825	6.556	1.549	14.209	7.573
14- TDIIMCBD	5.883	12.591	6.556	1.546	15.186	7.547
15- TDIIMCHD	7.594	12.143	6.554	1.483	14.152	7.522

For the multifunctional polymers, the hyperpolarizability is observed to be high for **13**, **14** and **15** systems. The β value is much higher for polymer **13**, with isomannide and CED as monomers. Among the multifunctional polymers, $\Delta\mu$ has got highest contribution to **13**, **14** and **15** polymers. The polymer **13** possesses high $\Delta\mu$ and f values which are considered to be a major contributing factor for first hyperpolarizability. The optical gap ΔE is not very much varying for **13**, **14** and **15** systems. The diethyl tartrate based polymers (**10**, **11**, and **12**) also possess good NLO activity with high β values compared to the other sets of polymers. These polymers also show similar trends as isomannide based polymers. The β value associated with high change in dipole moment, oscillator strength and low optical gap is observed. For the polymers (**7**, **8**, **9**) the β values are very low compared to isomannide and diethyl tartrate based polymers. This low value of β can be explained by the low (f , $\Delta\mu$) and high ΔE values.

In the case of polarizability parameters, significant changes are not observed for the bifunctional and multifunctional polymers. Thus it can be concluded that the polarizability is not much influenced by the percentage of the chiral or achiral molecules.

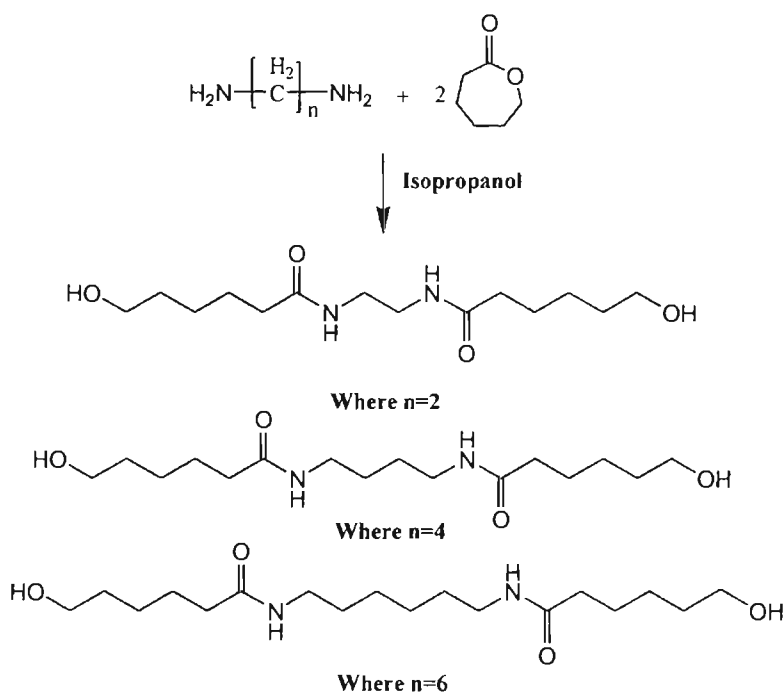
All the determining parameters of β (f , ΔE , $\Delta\mu$) have been analysed thoroughly. While examining the efficiency of the material, it can be seen that all the multifunctional polymers (with chiral and achiral diols) have high β values than the bifunctional polymers. Among the chiral polyurethanes the isomannide based polymers possess comparatively high value of hyperpolarizability. All the polymers have helically oriented conformation in the optimized geometry. The helical structure ensures the macroscopic chirality and hence attains the spatial asymmetry. This is the basic and essential requirement for second order nonlinear optical materials. Hence with all these factors, all the designed polymers are advised as good candidates for second harmonic generation.

7. 4. Synthesis of monomers (CED, CBD, CHD)

The amidodiols were synthesized according to the reported procedures. Diamine (1 eqv) and lactone (2 eqv) were taken in two separate conical flasks and both were dissolved in 50 mL isopropanol. The lactone solution was added to the diamine solution over a period of 1 h and stirred continuously for 2 h and the solution was heated (100°C) to reduce the volume

and cooled. The crystalline product was filtered and dried. It was further purified by column chromatography using hexane–ethyl acetate solvent system. The amidodiols N, N'-ethane-1, 2-diyl bis (6-hydroxy hexanamide) (CED), N, N'-butane-1, 4-diyl bis (6-hydroxy hexanamide) (CBD) and N, N'-hexane-1, 6-diyl bis (6-hydroxy hexanamide) (CHD) were prepared from 1, 2 diamino ethane, 1, 4 diamino butane and 1, 6 diamino hexane, respectively, using the reported procedure¹¹⁻¹⁶.

Different varieties of amidodiols monomers were synthesized by the aminolysis of ϵ -caprolactone, which are shown in **Scheme 7. 1**. The aminolysis of lactone with diamines in isopropanol medium gave amidodiols in good yield and high purity according to the reported procedures¹¹⁻¹⁶.



Scheme 7. 1: Synthesis of monomers

Amidodiols prepared by the above method were shining crystals and had a melting point around 100–130°C. The amidodiols were characterized by elemental analysis, ¹H NMR, ¹³C NMR, FT-IR etc. IR (KBr, cm⁻¹): 1413 (C–N stretching in amido linkage), 1556 (N–H bending), 1639 (C=O str of amidodiols), 3270 (N–H stretching), 3450 (–OH stretching in amidodiols). The amidodiols monomers showed ¹H NMR signals at 4.5 ppm corresponding to the proton of the hydroxyl group of –CH₂OH. The proton of –CH₂ of –CH₂OH resonated at 3.4–3.5 ppm. The signals at 2.7–2.9 ppm corresponds to –CH₂ nearer to carbonyl

group. The signals between 1.3 and 2.1 ppm corresponds to $-\text{CH}_2$ protons of the amidodiol. In the case of the ^{13}C NMR, the chemical shift values of the amide carbon appeared in the range from 174 to 178 ppm and the aldol carbon resonated at 67–68 ppm and alkyl carbons gave signals at 24 ppm and the $-\text{CH}_2\text{NH}-$ appeared around 32 ppm.

7. 5. SYNTHESIS OF POLYMERS

7. 5.1. General procedure

A solution of amidodiol (CED, CBD or CHD) in HPLC grade DMAc (50 mL) was stirred in a flame dried R.B flask of 500 mL capacity equipped with a magnetic stirring bar, nitrogen inlet, a thermometer and a reflux condenser with a CaCl_2 guard-tube. A slight excess of the solution of toluene diisocyanate (TDI) in 10 mL DMAc and four drops of DBTDL were added with vigorous stirring. To this solution, appropriate mole percentage of chiral diols {isosorbide (IS), isomannide (IM) and (2R, 3R) - Diethyl tartrate (DT)} were added. The stirring was continued at room temperature for 10 min and the mixture was heated at 70 °C for 24 h and cooled to room temperature. The viscous reaction mixture obtained was poured into 500 mL of water with stirring. The solid polymer was separated and washed with methanol. The polymer was dried under vacuum for 2 h²⁷.

The optimum conditions for the synthesis of polyurethanes were determined by varying the solvent, time of reaction and temperature which are shown in **Table 7. 3**.

Table 7. 3: Optimization of reaction conditions

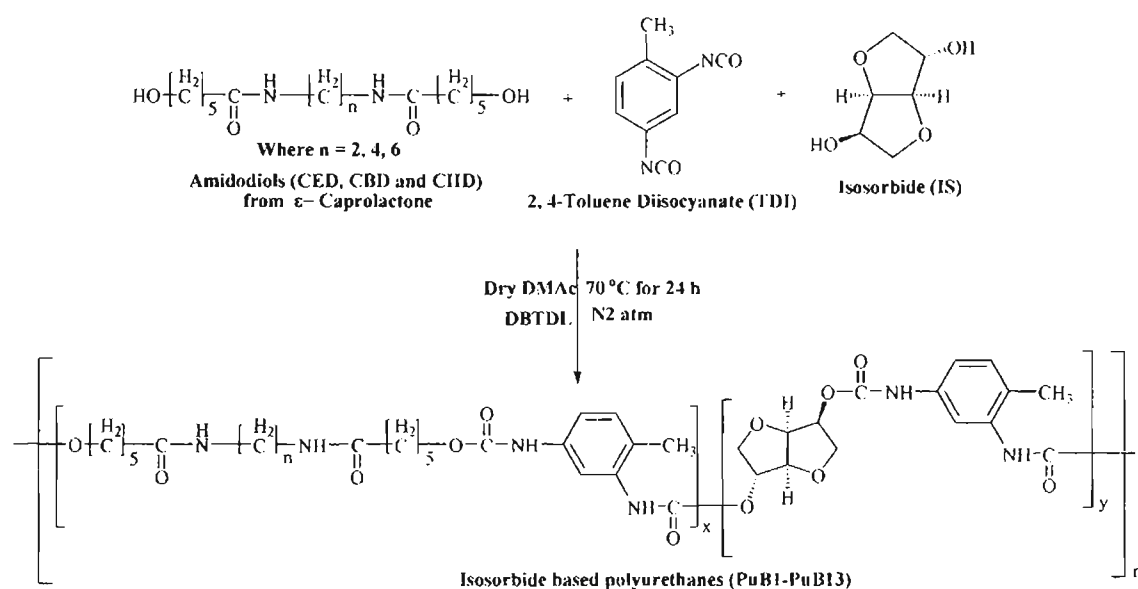
Solvent	Time(h)	Temperature (°C)	Yield (%)
DMAc	24	70	79
DMAc	24	100	60
DMAc	48	70	70
DMAc	48	100	72
DMSO	24	70	45
DMSO	24	100	52

Polymerization was done using 2, 4- toluene diisocyanate, IS as chiral diol and CED as chiral monomer. From these observations, the optimum conditions for the reaction are, temperature 70°C, time 24 h and DMAc as solvent. A series of polyurethanes were synthesized by the polyaddition reaction between achiral amidodiols (CED, CBD and CHD) and chiral diols, (IS, IM and DT) with the diisocyanate, toluene diisocyanate (TDI) in dimethyl acetamide solvent medium.

7. 6. ISOSORBIDE BASED POLYURETHANES

7. 6. 1. Experimental discussion

Different polymers with varying chiral (IS)-achiral (CED, CBD and CHD) composition were synthesized using the above mentioned procedure. The polymer PuB1 is the one which has only chiral unit in polymer chain and considered as the mother polymer in the series.



Scheme 7. 2: Synthesis of isosorbide based polyurethanes (PuB1-PuB13)

For PuB1, the ratio of TDI and IS are taken as 1:1. PuB2, PuB3, PuB4 and PuB5 are the polyurethanes with CED achiral diol having the TDI: IS: CED ratio as 1:0.75:0.25 (PuB2), 1:0.5:0.5 (PuB3), 1:0.25:0.75 (PuB4), 1:0:1 (PuB5), respectively. PuB6, PuB7, PuB8 and PuB9 are the polyurethanes with CBD amidodiol in which TC: IS: CBD ratio is maintained as 1:0.75:0.25 (PuB6), 1:0.5:0.5 (PuB7), 1:0.25:0.75 (PuB8), 1:0:1 (PuB9), respectively. PuB10, PuB11, PuB12 and PuB13 are the polyurethanes with CHD amidodiol having the ratio of TDI: IS: CHD as 1:0.75:0.25 (PuB10), 1:0.5:0.5 (PuB11), 1:0.25:0.75 (PuB12), 1:0:1

(PuB13), respectively. The scheme of polymer synthesis is shown in **Scheme 7. 2**.

7. 6. 2. Spectral Characterization

PuB1: FTIR (KBr), ν_{\max} (cm^{-1}): 3290 (-NH stretching of urethanes), 3000–2850 (sp^3 C-H stretching in isosorbide unit), 1715 (C=O stretching in urethane formed by isosorbide); 1451 (C-H bend of -CH₂ group in isosorbide), 1415 (-CN stretching of urethane) 1230 (C-O stretching of isosorbide unit), 1055–1125 (C-O stretching vibrations of urethanes attached to phenyl group). **¹H NMR (DMSO-d₆), δ (ppm):** 2.4–2.5 (s, -CH₃ of TDI), 4.1 (q, -CH₂ in isosorbide unit), 4.3–4.5 (t, -CH- bridge protons of isosorbide unit), 5.1 (m, -CH in isosorbide unit), 7.5–8.2 (m, aromatic protons of TDI), 9.8 (s, -CONH- ortho to the -CH₃ of TDI), 10.5 (s, -CONH- para to the -CH₃ of TDI). **¹³C NMR (DMSO-d₆), δ (ppm):** 178 (ester carbonyl in -OCONH- of urethane ortho and para to the -CH₃ of TDI), 130–160 (aromatic ring carbons), 80–82 (-CH- bridge of isosorbide unit), 75–78 (-CH- of isosorbide unit), 32–38 (-CH₂- isosorbide unit), 18 (-CH₃ of TDI).

PuB2–PuB4: FTIR (KBr), ν_{\max} (cm^{-1}): 3250–3300 (-NH stretching of both urethane and amidodiol unit), 3000–2900 (C-H stretching of -CH₂- in both isosorbide and amidodiol unit), 1740– 1750 (C=O stretching in urethane formed by amidodiol), 1720–1725 (C=O stretching in urethane formed by isosorbide); 1650–1680 (C=O stretching of -CONH group in amidodiol), 1530–1550 (NH bending in amidodiol), 1455–1460 (C-H bend of CH₂ groups), 1415–1420 (-C-N stretching in amidodiol), 1260–1280 (interaction between urethane carbonyl with amide of amidodiol), 1220–1225 (C-O stretching of isosorbide unit) 1075–1135 (C-C-O stretching of ester attached to aliphatic group). **¹H NMR (DMSO-d₆), δ (ppm):** 1.2–3.4 (m, CH₂ of amidodiol unit), 2.7 (s, -CH₃ of TDI), 4.1–4.4 (q, -CH₂ in isosorbide unit), 4.6 (t, -CH- bridge protons of isosorbide unit), 5.3 (m, -CH in isosorbide unit), 7.1–7.9 (m, aromatic protons of TDI), 8.7 (s, -CONH- ortho to the -CH₃ of TDI), 9.9 (s, -CONH- para to the -CH₃ of TDI). **¹³C NMR (DMSO-d₆), δ (ppm):** 172 (ester carbonyl in -OCONH- of urethane ortho and para to the -CH₃ of TDI), 169 (C=O group of amidodiol), 130–155 (aromatic ring carbons), 72 (-CH- bridge of isosorbide unit), 60–67 (-CH₂O-), 39 (-CH₂NH-), 35–38 (-CO-NH-CH₂-CH₂-), 25–28 (-CO-CH₂-CH₂-), 31 (-CH₂- isosorbide unit), 18 (-CH₃ of TDI).

PuB5: FTIR (KBr), ν_{\max} (cm^{-1}): 3280–3300 (-NH stretching of both amidodiol and

urethane unit), 1712-1728 (C=O stretching in urethanes formed by amidodiol), 1640- 1650 (C=O stretching in amidodiol), 1541 (-NH bending in amidodiol), 1410-1420 (-CN stretching in amidodiol unit), 1260-1280 (interaction between urethane carbonyl with amide of amidodiol), 1130-1180 (C-C-O stretching of ester attached to aliphatic group). $^1\text{H NMR (DMSO-d}_6\text{)}$, δ (ppm): 1.2, 2.3, 2.7, 3.0 (m, -CH₂ of amidodiol unit), 2.4-2.5 (s, -CH₃ of TDI), 7.8 (m, aromatic protons of TDI) 8.9 (s, -CONH- ortho to the -CH₃ of TDI), 9.3 (s, -CONH- para to the -CH₃ of TDI). $^{13}\text{C NMR (DMSO-d}_6\text{)}$, δ (ppm): 175-178 (ester carbonyl in -OCONH- of urethane ortho and para to the -CH₃ of TDI), 171 (C=O group of amidodiol), 130-155 (aromatic ring carbons), 50-55, 39-42, 32-36, 25-30 (-CH₂- of amidodiol unit), 16-18 (-CH₃ of TDI)

PuB6-PuB8: FTIR (KBr), ν_{max} (cm⁻¹): 3250-3300 (-NH stretching of both urethane and amidodiol unit), 3000-2900 (C-H stretching of -CH₂- in both isosorbide and amidodiol unit), 1740- 1750 (C=O stretching in urethane formed by amidodiol), 1720-1725 (C=O stretching in urethane formed by isosorbide); 1650-1680 (C=O stretching of -CONH group in amidodiol), 1530-1550 (NH bending in amidodiol), 1455-1460 (C-H bend of CH₂ groups), 1415-1420 (-C-N stretching in amidodiol), 1260-1280 (interaction between urethane carbonyl with amide of amidodiol), 1220-1225 (C-O stretching of isosorbide unit) 1075-1135 (C-C-O stretching of ester attached to aliphatic group). $^1\text{H NMR (DMSO-d}_6\text{)}$, δ (ppm): 1.2-3.4 (m, -CH₂ of amidodiol unit), 2.5 (s, -CH₃ of TDI), 4.02 (q, -CH₂ in isosorbide unit), 4.4 (t, -CH- bridge protons of isosorbide unit), 4.8 (m, -CH in isosorbide unit), 6.5-7.98 (m, aromatic protons of TDI), 8.75 (s, -CONH- ortho to the -CH₃ of TDI), 9.45 (s, -CONH- para to the -CH₃ of TDI). $^{13}\text{C NMR (DMSO-d}_6\text{)}$, δ (ppm): 170-175 (ester carbonyl in -OCONH- of urethane ortho and para to the -CH₃ of TDI), 130-155 (aromatic ring carbons), 78 (-CH- bridge of isosorbide unit), 60-67 (-CH₂O-), 39 (-CH₂NH-), 31-36 (-CO-NH-CH₂-CH₂-), 25-28 (-CO-CH₂-CH₂-), 32-35 (-CH₂- isosorbide unit), 18 (-CH₃ of TDI).

PuB9: FTIR (KBr), ν_{max} (cm⁻¹): 3280-3300 (-NH stretching of both amidodiol and urethane unit), 1712-1728 (C=O stretching in urethanes formed by amidodiol unit), 1640- 1650 (C=O str. in amidodiol), 1541 (-NH bending in amidodiol), 1410-1420 (-CN stretching in amidodiol), 1260-1280 (interaction between urethane carbonyl with amide of amidodiol), 1130-1180 (C-C-O stretching of

ester attached to aliphatic group). $^1\text{H NMR (DMSO-d}_6\text{)}$, δ (ppm): 1.3, 1.7, 2.3, 2.7, 3.2 (m, $-\text{CH}_2$ of amidodiol unit), 2.5 (s, $-\text{CH}_3$ of TDI), 8 (m, aromatic protons of TDI) 8.9 (s, $-\text{CONH-}$ ortho to the $-\text{CH}_3$ of TDI), 9.5 (s, $-\text{CONH-}$ para to the $-\text{CH}_3$ of TDI). $^{13}\text{C NMR (DMSO-d}_6\text{)}$, δ (ppm): 179 (ester carbonyl in $-\text{OCONH-}$ of urethane ortho and para to the $-\text{CH}_3$ of TDI), 172 (C=O group of amidodiol), 130-155 (aromatic ring carbons), 40-50, 39-42, 32-36, 25-30 ($-\text{CH}_2-$ of amidodiol units), 16-18 ($-\text{CH}_3$ of TDI).

PuB10-PuB12: FTIR (KBr), ν_{max} (cm^{-1}): 3250-3300 ($-\text{NH}$ stretching of both urethane and amidodiol unit), 3000-2900 (C-H stretching of $-\text{CH}_2-$ in both isosorbide and amidodiol unit), 1740- 1750 (C=O stretching in urethane formed by amidodiol), 1720-1725 (C=O stretching in urethane formed by isosorbide); 1650-1680 (C=O stretching of $-\text{CONH}$ group in amidodiol), 1530-1550 (NH bending in amidodiol), 1455-1460 (C-H bend of CH_2 groups), 1415-1420 ($-\text{C-N}$ stretching in amidodiol), 1260-1280 (interaction between urethane carbonyl with amide of amidodiol), 1220-1225 due to (C-O stretching of isosorbide unit) 1075-1135 (C-C-O stretching of ester attached to aliphatic group). $^1\text{H NMR (DMSO-d}_6\text{)}$, δ (ppm): 1.2-3.3 (m, $-\text{CH}_2$ of amidodiol unit), 2.4-2.5 (s, $-\text{CH}_3$ of TDI), 4-4.2 (q, $-\text{CH}_2$ in isosorbide unit), 4.76 (t, $-\text{CH-}$ bridge protons of isosorbide unit), 5.1-5.2 (m, $-\text{CH}$ in isosorbide unit), 6.7-8.7 (m, aromatic protons of TDI), 8.87 (s, $-\text{CONH-}$ ortho to the $-\text{CH}_3$ of TDI), 9.45 (s, $-\text{CONH-}$ para to the $-\text{CH}_3$ of TDI). $^{13}\text{C NMR (DMSO-d}_6\text{)}$, δ (ppm): 179 (ester carbonyl in $-\text{OCONH-}$ of urethane ortho and para to the $-\text{CH}_3$ of TDI), 172 (C=O group of amidodiol), 140-155 (aromatic ring carbons), 68 ($-\text{CH-}$ bridge of isosorbide unit), 50-53 ($-\text{CH}_2\text{O-}$), 39 ($-\text{CH}_2\text{NH-}$), 31-36 ($-\text{CO-NH-CH}_2\text{-CH}_2-$), 25-28 ($-\text{CO-CH}_2\text{-CH}_2-$), 32-35 ($-\text{CH}_2-$ isosorbide unit), 18 ($-\text{CH}_3$ of TDI).

PuB13: FTIR (KBr), ν_{max} (cm^{-1}): 3280-3300 ($-\text{NH}$ stretching of both amidodiol and urethane unit), 1712-1728 (C=O stretching in urethanes formed by amidodiol), 1640- 1650 (C=O stretching in amidodiol), 1541 ($-\text{NH}$ bending in amidodiol), 1410-1420 ($-\text{CN}$ stretching in amidodiol), 1260-1280 (interaction between urethane carbonyl with amide of amidodiol), 1130-1180 (C-C-O stretching of ester attached to aliphatic group). $^1\text{H NMR (DMSO-d}_6\text{)}$, δ (ppm): 1.2, 1.5, 2.3, 2.8, 3.3 (m, $-\text{CH}_2$ of amidodiol unit), 2.5 (s, $-\text{CH}_3$ of TDI), 7.2 (m, aromatic protons of TDI), 8.2 (s, $-\text{CONH-}$ ortho to the $-\text{CH}_3$ of TDI), 8.9 (s, $-\text{CONH-}$ para to the $-\text{CH}_3$ of TDI).

CONH- para to the $-\text{CH}_3$ of TDI). ^{13}C NMR ($\text{DMSO}-d_6$), δ (ppm): 172 (ester carbonyl in $-\text{OCONH}-$ of urethane ortho and para to the $-\text{CH}_3$ of TDI), 168 ($\text{C}=\text{O}$ group of amidodiol), 135-150 (aromatic ring carbons), 50-55, 39-42, 32-36, 25-30 ($-\text{CH}_2-$ of amidodiol unit), 16-18 ($-\text{CH}_3$ of TDI)

The ^1H NMR and ^{13}C NMR spectra of PuB2- PuB4 are shown in **Figure 7. 4** and **Figure 7. 5**.

The FTIR spectra of the polyurethanes showed a broad peak in the range of $3350\text{-}3050\text{ cm}^{-1}$ which is the characteristic peak of hydrogen bonded $-\text{NH}$ groups. The existence of broad band with overlaying shoulders between $3400\text{-}3300\text{ cm}^{-1}$ indicates the various types of hydrogen bonds with different bond distances for N-H groups present. The absorption bands in the region from $1800\text{-}1500\text{ cm}^{-1}$ are associated with the amide bands (two $-\text{CONH}-$ groups from amidodiol and two $-\text{OCONH}-$ from urethane linkages). Broad shoulder peaks were observed in the above mentioned region. The shoulder peaks observed at $1260\text{-}1280\text{ cm}^{-1}$ can be assigned to the H-bonding of urethane carbonyl with $-\text{NH}-$ hydrogen of amide linkage or vice versa. The low value of the $-\text{C}-\text{O}$ stretching vibration is due to the amide carbonyl groups involved in hydrogen bonding.

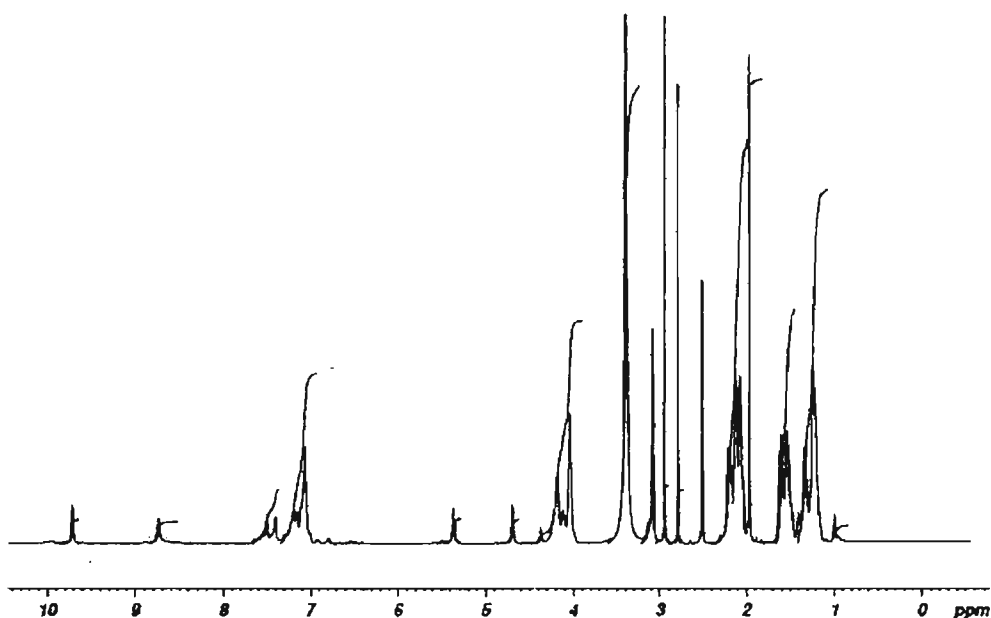


Figure 7. 4: ^1H NMR spectra of PuB2- PuB4

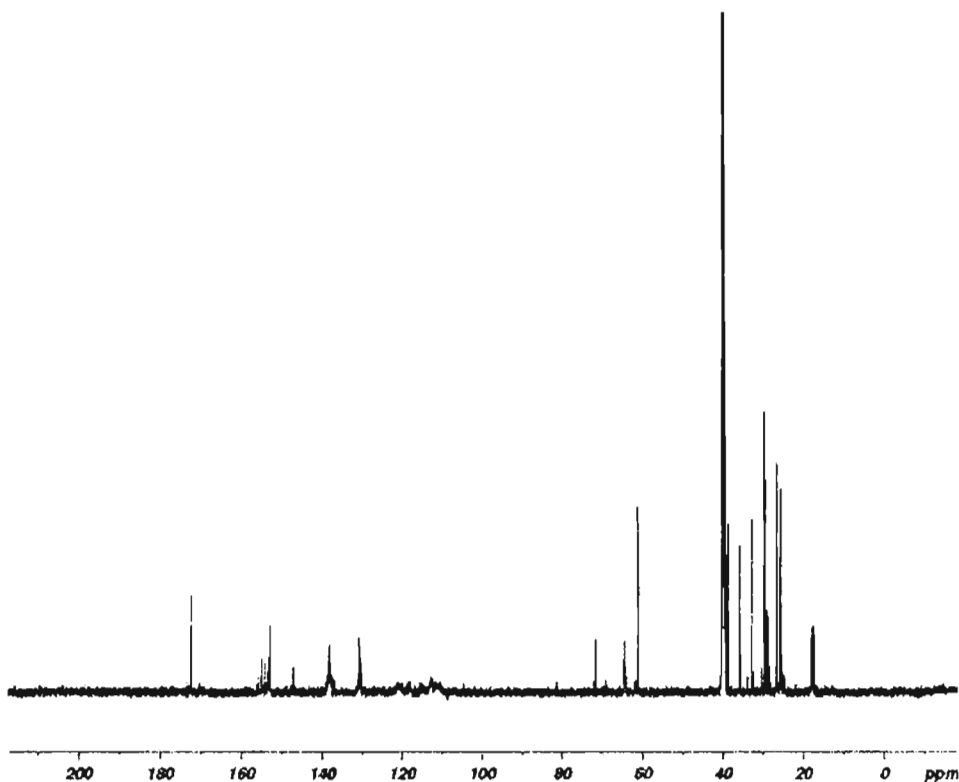


Figure 7. 5: ^{13}C NMR spectra of PuB2- PuB4

7. 6. 3. MALDI-MS spectra

From the MALDI-MS analysis, it was found that the molecular weight of the polyurethanes synthesized were in the range 17,000–20,000 (the molecular weight of one repeating unit=800–900), which confirmed the proposed structure consisting of almost 20–25 repeating units (Figure 7. 6).

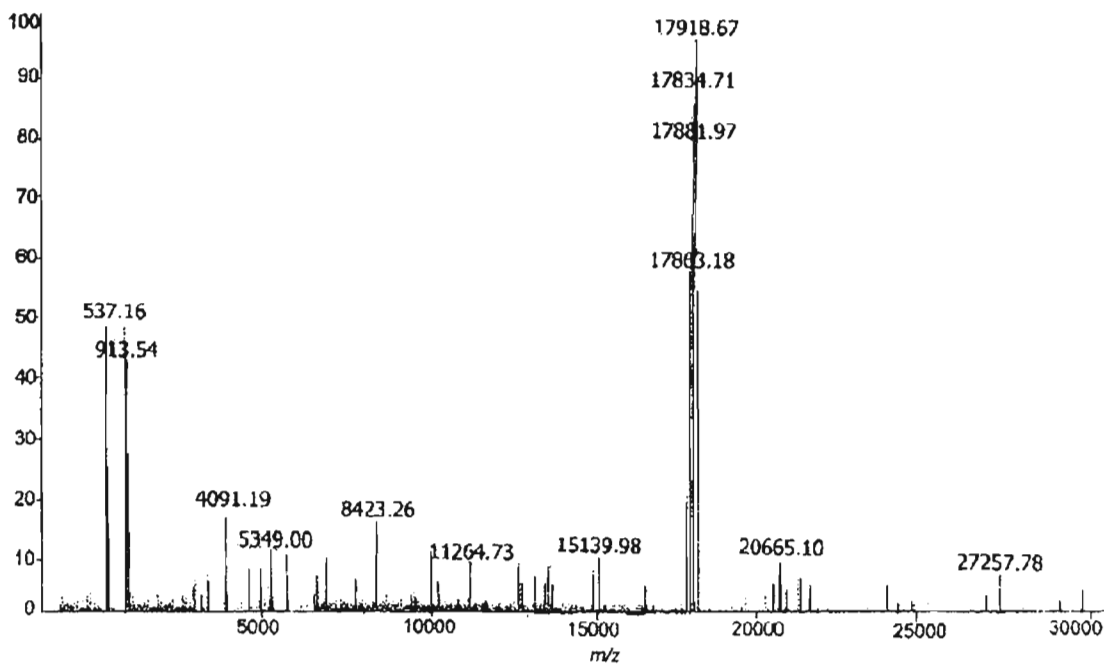


Figure 7. 6: MALDI-MS spectrum of PuB2 polyurethane

Figure 7. 6 represent the MALDI-MS spectrum of PuB2 polyurethane, which possess a molecular weight of 17918 with 835 for each repeating unit.

7. 6. 4. Absorption spectra

The spectra of polyurethanes were taken in DMAc solvent. All the polymers showed two absorbance peaks at 260-270 nm range (λ_{\max}) and 290-300 nm range. The absorption in the region 260-320 nm without any major absorption at shorter wavelengths (200-250 nm) usually indicate the $n \rightarrow \pi^*$ transition in the amidodiols containing a hetero atom. This type of transition includes the presence of $-C=O$, $-COOR$, $-CONH_2$ etc. Polyurethanes with amidodiol containing both π bonds and unshared electron pairs exhibit two absorptions, a low intensity shoulder like $n \rightarrow \pi^*$ transition at longer wavelength ~ 300 nm and a high intensity $\pi \rightarrow \pi^*$ band at a shorter wavelength of ~ 270 nm. The band gaps of the synthesized polymeric systems were determined from the $(\alpha h\nu)^2$ versus $h\nu$ plot. Where α is the absorption coefficient which is calculated by the equation, $\alpha = \lambda/t$, t is the pathlength of sample. The band gap of each polymer was calculated by extrapolating all the values and all the polymers were found to have band gap of approximately 4.6eV, which accounts for the insulating character of the polymer. The absorption λ_{\max} values are shown in Table 7. 4 and the UV-Vis spectra of PuB2-PuB4 are shown in Figure 7. 7.

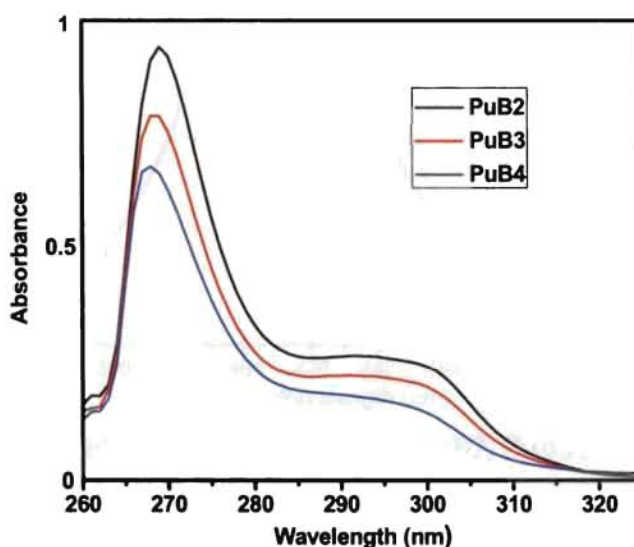


Figure 7. 7: Absorbance Spectra of PuB2- PuB4

7. 6. 5. Emission spectra

Fluorescence spectroscopy uses a beam of light, usually ultraviolet light,

that excites the electrons in molecules of certain compounds and makes them to emit light of a lower energy, typically, but not necessarily, visible light. In fluorescence spectroscopy, the molecule is first excited, by absorbing a photon, from its ground electronic state to one of the various vibrational states in the excited electronic state. The molecule then drops down to one of the various vibrational levels of the ground electronic state by emitting a photon in the process. As molecules may drop down into any of several vibrational levels in the ground state, the emitted photons will have different energies, and hence different frequencies. Therefore, by analysing the different frequencies of light emitted in fluorescent spectroscopy, along with their relative intensities, emission spectrum of polymers is obtained. Fluorescence is particularly an interesting tool to probe the rigidity of the polymer backbone. The broadness of the fluorescence peak decreases with increasing rigidity. The excitation wavelengths were found to be between 300–310 nm and emission spectra in the range of 400–410 nm. For all the samples the excitation wavelengths and emission wavelengths were recorded in the Fluorimeter by putting the proper absorbance wavelengths and excitation wavelengths. The emission λ_{max} values are reported in Table 7. 4 and spectra are shown in Figure 7. 8.

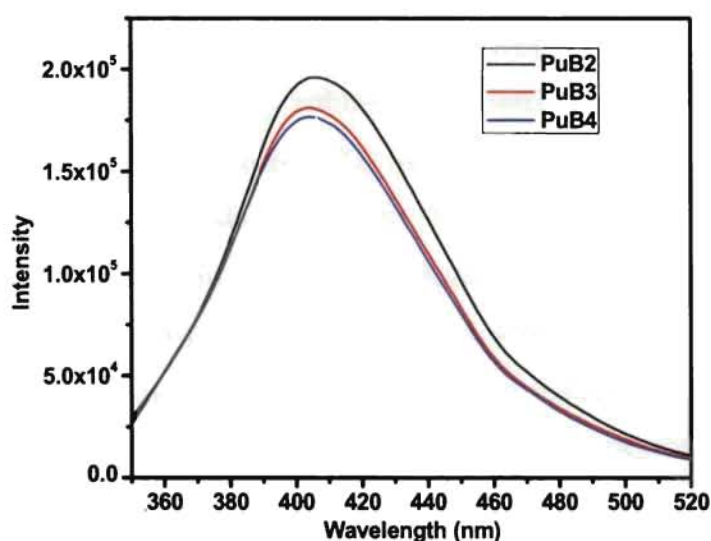


Figure 7. 8: Fluorescence Spectra of PuB2, PuB3 and PuB4

7. 6. 6. Specific rotation and Refractive index

The molecular level chirality of the polymers can be studied by polarimetric techniques. The angle of rotation depends upon the concentration of the solution, the length of the tube, temperature and measurement

wavelength which was taken as 589 nm. The polyurethanes synthesized contained optically active monomers. The optical activity of polymers increased with incorporation of isosorbide molecule. The specific rotation $[\alpha]_D$ values measured for polymers varied from 0° to 43° . The $[\alpha]_D$ value increased with the increase in the % of isosorbide chiral component. Low value of $[\alpha]_D$ is due to the low % incorporation of chiral diol. The polyurethanes without chiral molecule show zero specific rotation. The specific rotations of the polyurethanes are shown in **Table 7. 4**. Relatively high values of specific rotation near to the specific rotation of optically active monomers were obtained indicating that no extensive racemization occurred during the polymerization stage⁷⁻⁹. To determine the refractive indices of the polymer samples, the well-known prism method was used. The measurements were carried out using ABBE Refractometer (ATAGO) DR M2 at a wavelength of 589 nm. Distilled water with the refractive index of 1.33, was taken as the reference for the measurement. The refractive indices of the polyurethane systems lie in the range 1.42-1.62. The specific rotation and refractive index of the polymer samples are shown in **Table 7. 4**.

7. 6. 7. Thermal properties

While designing polymers for second harmonic generation, optimization of thermal properties like glass transition temperature and thermal stability are to be done. The T_g values were derived from DTA analysis and initial decomposition temperature (IDT) from thermogravimetric measurements. The T_g of a polymer depends largely on the thermal energy required to create internal segmental motion in the polymer chain. The stereochemical dependence of the polymers towards polar order can be proved from the T_g values of the polymeric systems. It is reported that isosorbide based polymers have shown very low T_g values compared to isomannide based polymeric systems⁷. The stereochemistry has played a major role in glass transition temperature through polar ordering. Usually the system with trans form shows lower T_g value than gauche form due to the flexibility of the trans. Also the molecule with symmetrically ordered polar groups has low T_g value than the one with asymmetrically placed polar group²⁸. In isosorbide, the -OH groups are more symmetrically placed than isomannide, hence the polymer containing isosorbide was found to be having low T_g values compared to isomannide. From

the structures of polymer containing isosorbide, it can be seen that the uniform stacking of isosorbide polymer is very difficult due to oppositely oriented -OH groups, hence reduce the polar order which causes the reduction in T_g values. All the samples were thermally stable up to the temperature around 190°C.

Table 7. 4: Optical and thermal properties of polyurethanes (PuB1-PuB13)

Polymer	Chiral diol %	Specific Rotation ($[\alpha]_D^{20}$)	Refractive Index	Absorption λ_{\max} (nm)	Emission λ_{\max} (nm)	IDT (°C)	T_g (°C)
PuB1	100	43	1.5302	270	403	190	105
PuB2	75	38	1.5569	268	402	210	115
PuB3	50	27	1.5287	268	403	250	108
PuB4	25	22	1.5230	269	404	280	120
PuB5	0	0	1.4219	268	402	190	60
PuB6	75	35	1.5499	269	404	280	114
PuB7	50	31	1.5928	268	404	278	105
PuB8	25	25	1.6087	269	402	200	98
PuB9	0	0	1.5876	269	405	195	82
PuB10	75	39	1.6176	268	407	280	102
PuB11	50	29	1.5582	269	402	220	118
PuB12	25	23	1.6079	268	406	230	97
PuB13	0	0	1.4697	268	403	190	78

Because of the high thermal stability, the IDT values of polyurethanes observed ranged from 190 to 280°C. It is clear that IDT values of polyurethanes containing both achiral and chiral monomers are found to be having more stability (250°C) and such polymers exhibit high SHG efficiency. It has been seen that the T_g values range from 60 to 120°C. The higher the value of T_g higher will be the degree of polar order. Polymers with both chiral diol and amidodiols result in high T_g values compared to the polymers without chiral molecules²⁸⁻³⁰.

A careful examination of DTA curves of all the polymers reveal endothermic peaks at around 280–380°C, which corresponds to a weight loss of 40–50% of the sample in TGA, which confirms that the decomposition of the

sample is more at the above mentioned temperature range. For most of the polymers very sharp endothermic peaks were observed in DTA. Hence the polymer material may be useful for making the NLO devices below its melting point. The thermal characterization data of polymers are given in **Table 7. 4**. The data obtained by thermal analysis showed that the polyurethanes were having good thermal stability due to the presence of hydrogen bonding and the presence of aromatic backbone in the polymer chain.

7. 6. 8. SHG efficiency

The nonlinear optical properties of selected polyurethanes were studied in powder form by Kurtz -Perry powder method. The SHG responses of these samples were recorded using urea and KDP as the reference. The second harmonic signal generated by the polymer was confirmed by the emission of green radiation from the polymer. As expected from the electronic structure of the polymers, they showed low SHG efficiency when compared with the reference compounds urea (640 mV) and KDP (72 mV).

Table 7. 5: SHG efficiency of polymers

Polymer	SHG efficiency	SHG efficiency
	w. r. to urea (%)	w. r. to KDP (%)
PuB1	1.72	15.28
PuB2- PuB4	1.93	17.16
PuB6- PuB8	1.92	17.09
PuB10 -PuB12	1.90	16.88
PuB5, PuB9, PuB13	1.88	16.67

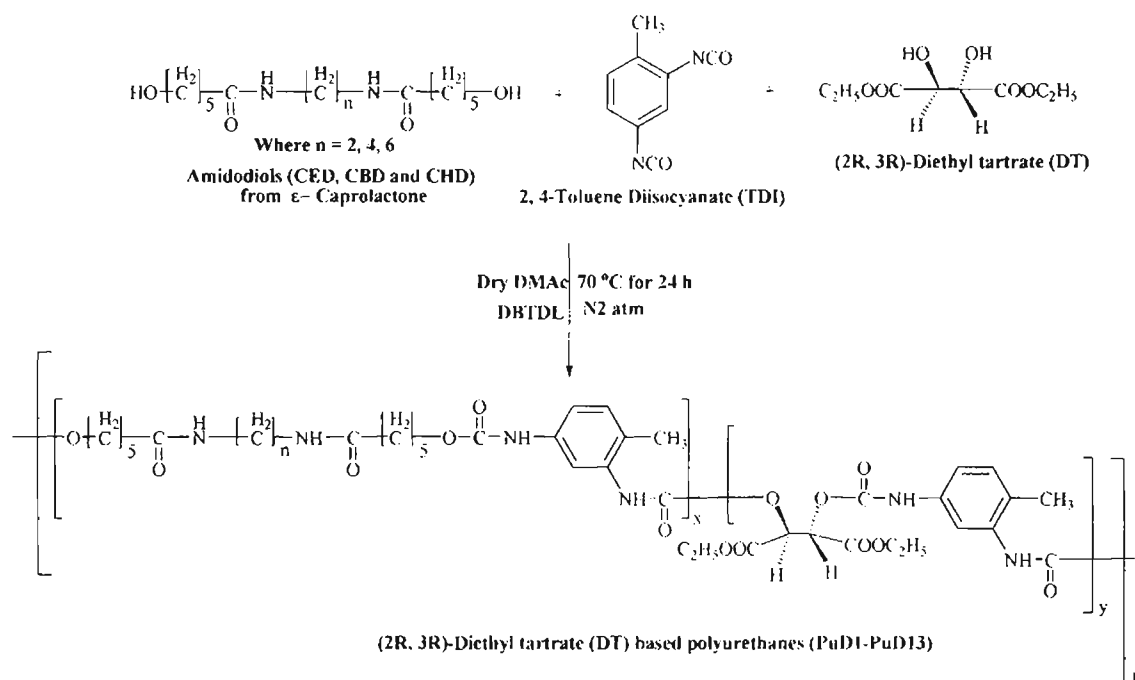
Among the series of polyurethanes (PuB1-PuB13), the polymers containing both chiral and amidodiols gave considerable activity compared to bifunctional polymers. PuB2-PuB4, PuB6-PuB8 and PuB10-PuB12 systems had about 1.93, 1.92, 1.90 % efficiency respectively as that of urea, whereas with KDP, PuB2-PuB4, PuB6-PuB8 and PuB10-PuB12 systems showed about 17.16, 17.09, 16.88 % efficiency respectively. Even if there is an absence of π -conjugation in donor-acceptor systems, the polyurethane systems show considerable NLO activity. The bifunctional polymers PuB5 PuB9 and PuB13 showed very low

SHG efficiency near to 1.88 % of SHG compared to urea and 16.67% with respect to KDP.

7. 7. (2R, 3R) DIETHYL TARTRATE BASED POLYURETHANES

7. 7. 1. Experimental discussion

The polymer **PuD1** is the one which has only the chiral diol in the polymer chain and the ratio of TDI and DT are taken as 1: 1. **PuD2**, **PuD3**, **PuD4**, **PuD5** are the polyurethanes with CED amidodiols having the TDI: DT: CED ratio as 1: 0.75: 0.25 (**PuD2**), 1: 0.5: 0.5 (**PuD3**), 1: 0.25: 0.75 (**PuD4**), 1: 0: 1(**PuD5**) respectively. **PuD6**, **PuD7**, **PuD8**, **PuD9** are the polyurethanes with CBD achiral diol in which TDI: DT: CBD ratio was maintained as 1: 0.75: 0.25(**PuD6**), 1: 0.5: 0.5 (**PuD7**), 1: 0.25: 0.75 (**PuD8**), 1: 0: 1 (**PuD9**) respectively. **PuD10**, **PuD11**, **PuD12**, **PuD13** are the polyurethanes with CHD amidodiols having the ratio of TDI: DT: CHD as 1: 0.75: 0.25 (**PuD10**), 1: 0.5: 0.5 (**PuD11**), 1: 0.25: 0.75 (**PuD12**), 1: 0: 1 (**PuD13**) respectively. Scheme of synthesis of (2R, 3R)-diethyl tartrate based polyurethane is shown in Scheme 7. 3.



Scheme 7. 3: Synthesis of (2R, 3R)-Diethyl tartrate based polyurethanes (PuD1-PuD13)

7. 7. 2. Spectral characterization

PuD1: FTIR (KBr), ν_{\max} (cm^{-1}): 3270-3300 (NH str.), 3000-2890 (sp^3 CH str.), 1736-1740, 1720-1725 (C=O str.), 1537 (NH bend), 1468, 1380 (-CH bend), 1055-1125 (C-O str. of urethane). **^1H NMR (DMSO- d_6), δ (ppm):** 1.2 (t, CH_3), 2.5 (s, CH_3), 4.1-4.3 (q, CH_2), 4.8 (s, CH), 7.2-7.6 (m, aromatic), 8.4 (s, CONH), 9.2 (s, CONH). **^{13}C NMR (DMSO- d_6), δ (ppm):** 170-175 (-OCONH of urethane), 168 (C=O ester), 135 (aromatic), 68 (CH), 32 (CH_2), 18 (CH_3)

PuD2- PuD4: FTIR (KBr), ν_{\max} (cm^{-1}): 3250-3300 (-NH str), 3000-2900 (sp^3 C-H str.), 1740-1750, 1720-1725, 1700-1710, 1640-1665 (C=O str.), 1530-1550 (NH bend), 1455-1460 (-CH bend), 1415-1420 (CN str.), 1220-1230 (interaction between C=O and NH), 1075-1116 (C-O str.). **^1H NMR (DMSO- d_6), δ (ppm):** 0.9 (t, CH_3 of tartrate), 1.2, 1.6, 2.2, 3.2 (m, CH_2), 2.5 (s, CH_3), 4.1-4.3 (q, CH_2), 4.8 (s, CH), 7.1-8 (m, aromatic), 8.8 (s, CONH), 9.4 (s, CONH). **^{13}C NMR (DMSO- d_6), δ (ppm):** 175 (-OCONH of urethane), 170 (C=O amide), 165 (C=O ester), 138 (aromatic), 62(CH), 33-39, 29-31, 24-28 (CH_2), 19, 15 (CH_3).

PuD5: FTIR (KBr), ν_{\max} (cm^{-1}): 3280-3300 (-NH str), 3000-2890 (C-H str.), 1708-1720, 1640-1650 (C=O str.), 1548 (NH bend), 1410-1420 (CN str.), 1260-1280 (interaction between C=O and NH), 1050-1060 (C-O str. in amidodiol). **^1H NMR (DMSO- d_6), δ (ppm):** 1.3, 1.7, 2.2, 3.2 (m, CH_2), 2.5 (s, CH_3), 8.1-8.9 (m, aromatic), 9.4 (s, CONH), 9.9 (s, CONH). **^{13}C NMR (DMSO- d_6), δ (ppm):** 172 (-OCONH of urethane), 169 (C=O amide), 138 (aromatic), 31-36, 23-29 (CH_2), 18 (CH_3).

PuD6-PuD8: FTIR (KBr), ν_{\max} (cm^{-1}): 3250-3300 (-NH str), 3000-2900 (sp^3 C-H str.), 1740-1750, 1720-1725, 1700-1710, 1640-1665 (C=O str.), 1530-1550 (NH bend), 1455-1460 (-CH bend), 1415-1420 (CN str.), 1220-1230 (interaction between C=O and NH), 1075-1116 (C-O str.). **^1H NMR (DMSO- d_6), δ (ppm):** 1.1 (t, CH_3) 1.3, 1.9, 2.1, 2.8, 3.4 (m, CH_2), 2.5 (s, CH_3), 4.1 (q, CH_2), 5.2 (S, CH) 6.5-7.9 (m, aromatic), 8.9 (s, CONH), 9.4 (s, CONH). **^{13}C NMR (DMSO- d_6), δ (ppm):** 173 (-OCONH of urethane), 170 (C=O amide), 168 (C=O ester), 135-155 (aromatic), 62-68 (CH), 36, 32, 28-31, 24-26 (CH_2), 19, 14 (CH_3)

PuD9: FTIR (KBr), ν_{\max} (cm^{-1}): 3280-3300 (-NH str), 3000-2890 (C-H str.), 1708-1720, 1640-1650 (C=O str.), 1548 (NH bend), 1410-1420 (CN str.), 1260-1280

(interaction between C=O and NH), 1050-1060 (C-O str. in amidodiol). ^1H NMR (DMSO- d_6), δ (ppm): 1.2-1.4, 1.6-1.8, 2-2.2, 3.2 (m, CH₂), 2.5 (s, CH₃), 6.9-7.3 (m, aromatic), 8.9 (s, CONH), 9.8 (s, CONH). ^{13}C NMR (DMSO- d_6), δ (ppm): 172 (-OCONH of urethane), 168 (C=O of amide) 138 (aromatic), 31-36, 23-29 (CH₂), 17 (CH₃)

PuD10-PuD12: FTIR (KBr), ν_{max} (cm^{-1}): 3250-3300 (-NH str), 3000-2900 (sp^3 C-H str.), 1740-1750, 1720-1725, 1700-1710, 1640-1665 (C=O str.), 1530-1550 (NH bend), 1455-1460 (-CH bend), 1415-1420 (CN str.), 1220-1230 (interaction between C=O and NH), 1075-1116 (C-O str.). ^1H NMR (DMSO- d_6), δ (ppm): 0.9 (t, CH₃), 1.2, 1.5, 2.1, 2.7, 3.2 (m, CH₂), 2.5 (s, CH₃), 4(q, CH₂), 5.3(s, CH), 6.7-8.7 (m, aromatic), 8.9 (s, CONH), 9.8 (s, CONH). ^{13}C NMR (DMSO- d_6), δ (ppm): 173-175 (-OCONH of urethane), 168 (C=O ester), 132-150 (aromatic), 60-65 (CH), 33-39, 30-31, 24-28 (CH₂), 19, 14 (CH₃)

PuD13: FTIR (KBr), ν_{max} (cm^{-1}): 3280-3300 (-NH str), 3000-2890 (C-H str.), 1708-1720, 1640-1650 (C=O str.), 1548 (NH bend), 1410-1420 (CN str.), 1260-1280 (interaction between C=O and NH), 1050-1060 (C-O str. in amidodiol). ^1H NMR (DMSO- d_6), δ (ppm): 1.2, 1.8, 2.2, 3.2 (m, CH₂), 2.5 (s, CH₃), 8.3-8.9 (m, aromatic), 9.5 (s, CONH), 9.9 (s, CONH). ^{13}C NMR (DMSO- d_6), δ (ppm): 175-177 (-OCONH of urethane), 172 (C=O of amidodiol) 133-158 (aromatic), 62-68, 42-45, 31-36, 23-29 (CH₂), 17(CH₃).

7.7.3. MALDI-MS spectra

From the MALDI-MS analysis it was found that the molecular weight of the polyurethanes synthesized were in the range 17,000-20,000 (the molecular weight of one repeating unit=800-900) which confirmed the proposed structure consisting of almost 20-25 repeating units.

7.7.4. Absorption spectra

The absorption spectra of polyurethanes were taken in DMSO solvent. All the polymers showed two absorbance peaks at 267-272 nm range (λ_{max}) and 290-300 nm range. The polyurethanes with amidodiol monomer containing both π bonds and unshared electron pairs exhibit two absorptions, a low intensity shoulder from $n \rightarrow n^*$ transition at longer wavelength ~ 300 nm and a high intensity $\pi \rightarrow \pi^*$ band at a shorter wavelength of $\sim 267-272$ nm. The band gaps of

the synthesized polymeric systems were determined by extrapolating all the values in the $(\alpha h\nu)^2$ versus $h\nu$ plot. The band gap of each polymer was calculated and all the polymers were found to be having band gap of approximately 4.43 to 4.68 eV, which accounts for the insulating character of the polymer. The absorption λ_{\max} values are shown in **Table 7. 6**.

7. 7. 5. Emission spectra

The emission λ_{\max} values are shown in **Table 7. 6**. The excitation spectra of all the polymers exhibited a wavelength maximum around 300-315 nm. The emission spectra of the polymers PuD4, PuD5, PuD6, PuD9, PuD10, PuD11, PuD12 and PuD13 display a broad band between 360-480 nm with a maximum around 385-430 nm (**Table 7. 6**) when excited at the 310 nm wavelength. PuD1, PuD2, PuD3, PuD7 and PuD8 exhibited the characteristically sharp band emissions in between 345-350 nm. For the polymers PuD10, PuD11 and PuD12, shoulder peaks were observed in the range of 425-490 nm.

7. 7. 6. Specific rotation

The polyurethanes synthesized contained (2R, 3R)-diethyl tartrate as the optically active monomer. The optical activity of polymers increased when chiral molecules were incorporated. The specific rotation $[\alpha]_D$ values measured for polymers varied from 0° to 43° . The $[\alpha]_D$ value was found to be increased with the increase in the % of chiral component. The polyurethanes without chiral molecule possess a zero specific rotation. The values of specific rotation of the polyurethanes are shown in **Table 7. 6**.

7. 7. 7. Refractive index measurements

For the refractive index measurements, distilled water was taken as the reference which had the refractive index-1.33. The refractive indices of the polyurethane systems showed a range in between 1.42-1.59. The refractive indices of the polymer samples are shown in **Table 7. 6**.

7. 7. 8. Thermal properties

High thermal stability is an important feature for a material to be usable in nonlinear optical applications²⁸⁻³⁰. The T_g of a polymer depends largely on the

thermal energy required to create internal segmental motion in the polymer chain. A transition from rigid to flexible structures is indicated by the glass transition (T_g) temperature for the polymer and a flexible working behaviour of the polymer was found to be decreased below its T_g . The glass transition effects are relatively small in magnitude compared to the melting point. Higher the thermal energy and degree of polar order, higher will be the values of T_g . For all the polymers studied some sort of similarities in thermal stability were observed. All the samples were thermally stable upto the temperature around 180°C-280°C. In all the polymeric systems one major thermal decomposition was observed. From the wt % graph of TGA, the temperature for different stages of weight loss (% weight loss) can be determined.

Table 7. 6: Optical and thermal properties of Polyurethanes (PuD1- PuD13)

Polymer	% of Chiral diol	Absorption $\lambda_{\max}(\text{nm})$	Emission $\lambda_{\max}(\text{nm})$	Specific rotation ($[\alpha]_{\text{D}}^0$)	Refractive index	IDT (°C)	T_g (°C)
PuD1	100	272	346	43	1.5257	190	101
PuD2	75	270	345	35	1.5107	180	158
PuD3	50	271	347	21	1.5012	185	203
PuD4	25	270	429	12	1.4570	270	210
PuD5	0	268	402	0	1.4219	190	60
PuD6	75	272	400	38	1.4725	280	108
PuD7	50	267	346	31	1.5152	260	180
PuD8	25	268	345	24	1.5211	250	197
PuD9	0	269	405	0	1.5876	195	82
PuD10	75	267	413	31	1.4771	240	106
PuD11	50	272	386	26	1.4910	185	118
PuD12	25	270	388	16	1.5151	230	205
PuD13	0	268	403	0	1.4697	190	78

The IDT values observed for the polyurethanes ranges from 180°C to 280°C. It is clear that IDT values of polyurethanes containing both amidodiol and chiral groups are found to be having more stability (~ 200°C) and such polymers

found to exhibit high SHG efficiency. It has been seen that the T_g values range from 60°C to 210°C. The higher the value of T_g higher will be the degree of polar order. Polymers with both chiral diol and achiral diols result in high T_g values compared to the polymers without chiral molecules.

A careful examination of DTA curves of all the polymers reveal endothermic peaks around 250°C-350°C, which corresponds to a weight loss of 60-20% of the sample in TGA, which confirms that the decomposition of the sample is more at the above mentioned temperature range. For most of the polymers broad endothermic peaks were observed in DTA thermogram. The thermal characterization data of polymers are given in the Table 7. 6. The data obtained by thermal analysis showed that the polyurethanes were having good thermal stability due to the presence of hydrogen bonding and the presence of aromatic backbone in the polyurethane chain²⁸⁻³⁰.

7. 7. 9. SHG efficiency

The second harmonic signal generated by the polymer was confirmed by the emission of green radiation from the polymer.

Table 7. 7: SHG efficiency of polyurethanes

Polymer	SHG efficiency w. r. to urea (%)	SHG efficiency w. r. to KDP (%)
PuD1	1.83	16.22
PuD2- PuD4	2.41	22.16
PuD6- PuD8	2.38	21.89
PuD10 -PuD12	2.27	20.88
PuD5, PuD9, PuD13	1.88	16.67

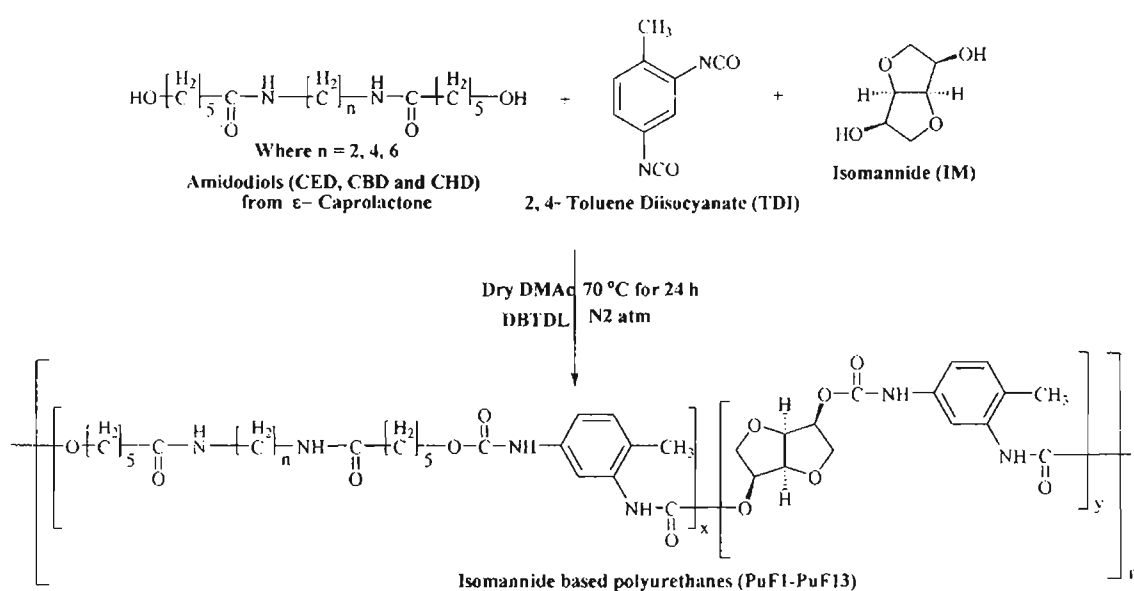
The polyurethanes showed very low SHG efficiency compared to the reference compounds urea (626 mV) and KDP (68 mV). Among the series of polyurethanes (PuD1-PuD13), the polymers with both chiral and achiral monomers gave considerably high activity compared to bifunctional polymers. PuD2-PuD4, PuD6-PuD8 and PuD10-PuD12 systems showed about 2.41, 2.38 and 2.27% efficiency as that of urea and 22.16, 21.89 and 20.88 % with respect to

KDP. The bifunctional polymer PuD1 showed much less SHG efficiency near to 1.83% of SHG compared to urea and 16.22% with respect to KDP.

7. 8. ISOMANNIDE BASED POLYURETHANES

7. 8. 1. Experimental discussion

The polymer **PuF1** is the one which is having only chiral unit in polymer chain and considered as the mother polymer in the series. The ratio of TDI and IM were taken as 1: 1. **PuF2, PuF3, PuF4, PuF5** are the polyurethanes with **CED** monomer having the **TDI: IM: CED** ratio as 1: 0.75: 0.25, 1: 0.5: 0.5, 1: 0.25: 0.75, 1: 0: 1 respectively. **PuF6, PuF7, PuF8, PuF9** are the polyesters with **CBD** amidodiol in which **TDI: IM: CBD** ratio was maintained as 1: 0.75: 0.25, 1: 0.5: 0.5, 1: 0.25: 0.75, 1: 0: 1 respectively. **PuF10, PuF11, PuF12, PuF13** are the polyesters with **CHD** achiral diol having the ratio of **TDI: IM: CHD** as 1: 0.75: 0.25, 1: 0.5: 0.5, 1: 0.25: 0.75, 1: 0: 1 respectively. The scheme for the synthesis of isomannide based polymers is shown in **scheme 7. 4**.



Scheme 7. 4: Synthesis of isomannide based polyurethanes (PuF1-PuF13)

7. 8. 2. Spectral characterization

PuF1: FTIR (KBr), ν_{max} (cm^{-1}): 3290 (-NH stretching of urethanes), 3000- 2850 (sp^3 C-H stretching in isomannide unit), 1715 (C=O stretching in urethane formed by isomannide), 1537 (NH bend), 1451 (C-H bend of - CH_2 group in isomannide), 1415 (-CN stretching of urethane) 1230 (C-O stretching of isomannide unit), 1055-1125 (C-O stretching vibrations of urethanes attached to phenyl group). ^1H NMR (DMSO- d_6), δ (ppm): 2.4-2.5 (s, - CH_3 of TDI), 4.1 (q, - CH_2 in isomannide)

unit), 4.3- 4.5 (t, -CH- bridge protons of isomannide unit), 5.1 (m, -CH in isomannide unit), 7.5 -8.2 (m, aromatic protons of TDI), 9.8 (s, -CONH- ortho to the -CH₃ of TDI), 10.5 (s, -CONH- para to the -CH₃ of TDI). ¹³C NMR (DMSO-d₆), δ (ppm): 172-178 (ester carbonyl in -OCONH- of urethane ortho and para to the -CH₃ of TDI), 170 (C=O group of amidodiol), 130-155 (aromatic ring carbons), 68 (-CH- bridge of isomannide unit), 32-35 (-CH₂- isomannide unit), 18 (-CH₃ of TDI).

PuF2- PuF4: FTIR (KBr), ν_{max} (cm⁻¹): 3250-3300 (-NH stretching of both urethane and amidodiol unit), 3000-2900 (C-H stretching of -CH₂- in both isomannide and amidodiol), 1740-1750 (C=O stretching in urethane formed by amidodiol unit), 1720-1725 (C=O stretching in urethane formed by isomannide), 1650-1680 (C=O stretching of -CONH group in amidodiol), 1530-1550 (NH bending in amidodiol), 1455-1460 (C-H bend of CH₂ groups), 1415-1420 (-C-N stretching in amidodiol), 1260-1280 (interaction between urethane carbonyl with amide of amidodiol), 1220-1225 (C-O stretching of isomannide unit) 1075-1135 (C-C-O stretching of ester attached to aliphatic group). ¹H NMR (DMSO-d₆), δ (ppm): 1.2- 3.4 (m, CH₂ of amidodiol unit), 2.4-2.5 (s, -CH₃ of TDI), 4.1 (q, -CH₂ in isomannide unit), 4.3- 4.5 (t, -CH- bridge protons of isomannide unit), 4.9-5.1 (m, -CH in isomannide unit), 6.7-7.8 (m, aromatic protons of TDI), 8.9 (s, -CONH- ortho to the -CH₃ of TDI), 9.9 (s, -CONH- para to the -CH₃ of TDI). ¹³C NMR (DMSO-d₆), δ (ppm): 178 (ester carbonyl in -OCONH- of urethane ortho and para to the -CH₃ of TDI), 176 (C=O group of amidodiol), 130-155 (aromatic ring carbons), 68 (-CH- bridge of isomannide unit), 60-67 (-CH₂O-), 39 (-CH₂NH-), 31-36 (-CO-NH-CH₂-CH₂-), 25-28 (-CO-CH₂-CH₂-), 32-35 (-CH₂- isomannide unit), 18 (-CH₃ of TDI).

PuF5: FTIR (KBr), ν_{max} (cm⁻¹): 3280-3300 (-NH stretching of both amidodiol and urethane unit), 3000-2900 (C-H stretching) 1712-1728 (C=O stretching in urethanes formed by amidodiol), 1640-1650 (C=O stretching in amidodiol), 1540-1550 (-NH bending in amidodiol), 1410-1420 (-CN stretching in amidodiol), 1260-1280 (interaction between urethane carbonyl with amide of amidodiol), 1130-1180 (C-C-O stretching of ester attached to aliphatic group). ¹H NMR (DMSO-d₆), δ (ppm): 1.2, 2.3, 2.7, 3.0 (m, -CH₂ of amidodiol unit), 2.4-2.5 (s, -CH₃ of TDI), 7.8 (m, aromatic protons of TDI) 8.9 (s, -CONH- ortho to the -CH₃ of TDI), 9.3 (s,

-CONH- para to the -CH₃ of TDI). ¹³C NMR (DMSO-d₆), δ (ppm): 173-176 (ester carbonyl in -OCONH- of urethane ortho and para to the -CH₃ of TDI), 170 (C=O group of amidodiol), 130-155 (aromatic ring carbons), 60-70, 39-42, 32-36, 25-30 (-CH₂- of amido groups), 16-18 (-CH₃ of TDI)

PuF6-PuF8: FTIR (KBr), ν_{max} (cm⁻¹): 3250-3300 (-NH stretching of both urethane and amidodiol unit), 3000-2900 (C-H stretching of -CH₂- in both isomannide and amidodiol unit), 1740-1750 (C=O stretching in urethane formed by amidodiol), 1720-1725 (C=O stretching in urethane formed by isomannide); 1650-1680 (C=O stretching of -CONH group in amidodiol), 1530-1550 (NH bending in amidodiol), 1455-1460 (C-H bend of CH₂ groups), 1415-1420 (-C-N stretching in amidodiol), 1260-1280 (interaction between urethane carbonyl with amide of amidodiol), 1220-1225 (C-O stretching of isomannide unit) 1075-1135 (C-C-O stretching of ester attached to aliphatic group). ¹H NMR (DMSO-d₆), δ (ppm): 1.2-3.4 (m, -CH₂ of amidodiol unit), 2.5 (s, -CH₃ of TDI), 4.02 (q, -CH₂ in isomannide unit), 4.4 (t, -CH- bridge protons of isomannide unit), 4.8 (m, -CH in isomannide unit), 6.5-7.98 (m, aromatic protons of TDI), 8.75 (s, -CONH- ortho to the -CH₃ of TDI), 9.45 (s, -CONH- para to the -CH₃ of TDI). ¹³C NMR (DMSO-d₆), δ (ppm): 176-179 (ester carbonyl in -OCONH- of urethane ortho and para to the -CH₃ of TDI), 172 (C=O group of amidodiol), 130-155 (aromatic ring carbons), 68 (-CH- bridge of isomannide unit), 60-67 (-CH₂O-), 39 (-CH₂NH-), 31-36 (-CO-NH-CH₂-CH₂-), 25-28 (-CO-CH₂-CH₂-), 32-35 (-CH₂- isomannide unit), 18 (-CH₃ of TDI).

PuF9: FTIR (KBr), ν_{max} (cm⁻¹): 3280-3300 (-NH stretching of both amidodiol and urethane unit), 3000-2900 (C-H stretching) 1712-1728 (C=O stretching in urethanes formed by amidodiol), 1640-1650 (C=O stretching in amidodiol), 1540-1550 (-NH bending in amidodiol), 1410-1420 (-CN stretching in amidodiol), 1260-1280 (interaction between urethane carbonyl with amide of amidodiol), 1130-1180 (C-C-O stretching of ester attached to aliphatic group). ¹H NMR (DMSO-d₆), δ (ppm): 1.3, 1.7, 2.3, 2.7, 3.2 (m, -CH₂ of amidodiol unit), 2.5 (s, -CH₃ of TDI), 8 (m, aromatic protons of TDI) 8.9 (s, -CONH- ortho to the -CH₃ of TDI), 9.5 (s, -CONH- para to the -CH₃ of TDI). ¹³C NMR (DMSO-d₆), δ (ppm): 170-175 (ester carbonyl in -OCONH- of urethane ortho and para to the -CH₃ of TDI), 168 (C=O

group of amidodiol), 130-155 (aromatic ring carbons), 60-70, 39-42, 32-36, 25-30 (-CH₂- of amidodiol groups), 16-18 (-CH₃ of TDI).

PuF10-PuF12: FTIR (KBr), ν_{\max} (cm⁻¹): 3250-3300 (-NH stretching of both urethane and amidodiol unit), 3000-2900 (C-H stretching of -CH₂- in both isomannide and amidodiol unit), 1740-1750 (C=O stretching in urethane formed by amidodiol), 1720-1725 (C=O stretching in urethane formed by isomannide); 1650-1680 (C=O stretching of -CONH group in amidodiol), 1530-1550 (NH bending in amidodiol), 1455-1460 (C-H bend of CH₂ groups), 1415-1420 (-C-N stretching in amidodiol), 1260-1280 (interaction between urethane carbonyl with amide of amidodiol), 1220-1225 (C-O stretching of isomannide unit) 1075-1135 (C-C-O stretching of ester attached to aliphatic group). **¹H NMR (DMSO-d₆), δ (ppm):** 1.2-3.3 (m, -CH₂ of amidodiol unit), 2.4-2.5 (s, -CH₃ of TDI), 4-4.2 (q, -CH₂ in isomannide unit), 4.76 (t, -CH- bridge protons of isomannide unit), 5.1-5.2 (m, -CH in isomannide unit), 6.7-8.7 (m, aromatic protons of TDI), 8.87 (s, -CONH- ortho to the -CH₃ of TDI), 9.45 (s, -CONH- para to the -CH₃ of TDI). **¹³C NMR (DMSO-d₆), δ (ppm):** 170-175 (ester carbonyl in -OCONH- of urethane ortho and para to the -CH₃ of TDI), 169 (C=O group of amidodiol), 130-155 (aromatic ring carbons), 68 (-CH- bridge of isomannide unit), 60-67 (-CH₂O-), 39 (-CH₂NH-), 31-36 (-CO-NH-CH₂-CH₂-), 25-28 (-CO-CH₂-CH₂-), 32-35 (-CH₂- isomannide unit), 18 (-CH₃ of TDI).

PuF13: FTIR (KBr), ν_{\max} (cm⁻¹): 3280-3300 (-NH stretching of both amidodiol and urethane unit), 3000-2900 (C-H stretching) 1712-1728 (C=O stretching in urethanes formed by amidodiol), 1640-1650 (C=O stretching in amidodiol), 1540-1550 (-NH bending in amidodiol), 1410-1420 (-CN stretching in amidodiol), 1260-1280 (interaction between urethane carbonyl with amide of amidodiol), 1130-1180 (C-C-O stretching of ester attached to aliphatic group). **¹H NMR (DMSO-d₆), δ (ppm):** 1.2, 1.5, 2.3, 2.8, 3.3 (m, -CH₂ of amidodiol unit), 2.5 (s, -CH₃ of TDI), 7.2 (m, aromatic protons of TDI), 8.2 (s, -CONH- ortho to the -CH₃ of TDI), 8.9 (s, -CONH- para to the -CH₃ of TDI). **¹³C NMR (DMSO-d₆), δ (ppm):** 170-175 (ester carbonyl in -OCONH- of urethane ortho and para to the -CH₃ of TDI), 168 (C=O group of amidodiol), 130-155 (aromatic ring carbons), 60-70, 39-42, 32-36, 25-30 (-CH₂- of amido groups), 16-18 (-CH₃ of TDI).

7. 8. 3. MALDI-MS Spectra

From the MALDI-MS analysis it was found that the molecular weight of the polyurethanes synthesized were between 17,000–20,000 (the molecular weight of one repeating unit accounts to 800–900) which confirmed the proposed structure was made almost 20–25 repeating units.

7. 8. 4. Absorption Spectra

The spectra of polyurethanes were recorded in DMAc solvent. All the polymers showed two absorption peaks at 260-270 nm range (λ_{\max}) and 290-300 nm range. The polyurethanes with amidodiols containing both π bonds and unshared electron pairs exhibited two absorptions, a low intensity shoulder like $n \rightarrow \pi^*$ transition at longer wavelength ~ 300 nm and a high intensity $\pi \rightarrow \pi^*$ band at a shorter wavelength of ~ 270 nm. The spectral values are shown in Table 7. 8. The band gap of each polymer was calculated by extrapolating all the values of $(\alpha h\nu)^2$ versus $h\nu$ plot and all the polymers were found to be having a band gap of approximately 4.6eV, which accounts for the insulating character of the polyurethanes.

Table 7. 8: Optical and thermal properties of Polyurethanes (PuF1- PuF13)

Polymer	% of Chiral diol	Specific rotation ($[\alpha]_D^{20}$)	Absorption $\lambda_{\max}(\text{nm})$	Emission $\lambda_{\max}(\text{nm})$	IDT ($^{\circ}\text{C}$)	Tg ($^{\circ}\text{C}$)	Refractive index
PuF1	100	84	269	401	180	125	1.5802
PuF2	75	70	268	402	182	128	1.5689
PuF3	50	55	268	397	245	151	1.5889
PuF4	25	44	268	401	280	155	1.5269
PuF5	0	0	268	402	190	60	1.4219
PuF6	75	72	269	407	280	120	1.5984
PuF7	50	58	268	409	287	108	1.6123
PuF8	25	46	268	402	220	124	1.6243
PuF9	0	0	269	405	195	82	1.5876
PuF10	75	73	268	406	199	106	1.6062
PuF11	50	48	269	392	205	122	1.5295
PuF12	25	45	268	406	211	150	1.6049
PuF13	0	0	268	403	190	78	1.4697

7. 8. 5. Fluorescence spectra

The excitation wavelengths were found to lie between 280-320 nm and emission spectra obtained were between 390-410 nm. For all the samples, the excitation wavelengths and emission wavelengths were recorded in the fluorescence spectrum using the proper absorption wavelengths and excitation wavelengths. The emission spectral values are shown in **Table 7. 8.**

7. 8. 6. Polarimetric measurements

Since isomannide was taken as the optically active monomer for the polyurethane synthesis and the activity of polymers was found to be higher compared to that of isosorbide and diethyl tatrtrate containing polymers. The specific rotation of polymers increased when chiral molecules were incorporated. The specific rotation $[\alpha]_D$ values measured for polymers varied from 0° to 75° . The $[\alpha]_D$ value increased with increase in the % of chiral component. The polyurethanes without chiral molecule possessed zero specific rotation. The values of specific rotation of the polyurethanes are shown in **Table 7. 8.**

7. 8. 7. Refractive index

For the refractive index measurements, distilled water was taken as the reference which was having the refractive index 1.33. The refractive index of the polymer samples lie in the range 1.42-1.62, which are shown in **Table 7. 8.**

7. 8. 8. Thermal properties

The T_g values and initial decomposition temperature (IDT) are given in **Table 7. 8.** The T_g of a polymer depends largely on the thermal energy required to create internal segmental motion in the polymer chain. A transition from rigid to flexible structures is indicated by the glass transition (T_g) values for a polymer. The flexible working behaviour of a polymer decreases below its T_g . The glass transition effects are relatively small in magnitude compared to the melting point. Higher the thermal energy and degree of polar order, higher will be the values of T_g ²⁸⁻³⁰. For all the polymers some sort of similarities in thermal stability were observed.

Due to the high thermal stability of the polymers, the initial decomposition temperatures (IDT) of polymers were found to be comparatively high. The observed IDT values of polyurethanes ranged from 180°C to 290°C. It is clear that IDT values of polyurethanes with both amidodiol and chiral units were found to be high (above 200°C) and such polymers exhibited high SHG efficiency. It has been seen that the T_g values range from 60°C to 160°C. The higher the value of T_g higher will be the degree of polar order. Polymers with both chiral diol and amidodiol resulted in high T_g values compared to the polymers without chiral molecules. The DTA curves of all the polymers revealed endothermic peaks at around 280°C-380°C, which corresponded to a weight loss of 70-20% of the sample in TGA. For most of the polymers broad endothermic peaks were observed in DTA³⁰⁻³¹. The data obtained by thermal analysis showed that the polyurethanes were having good thermal stability.

7. 8. 9. NLO activity measurements

The SHG responses of the polyurethane samples were recorded using urea and KDP as references. The second harmonic signal generated by the polymer was confirmed by the emission of green radiation from the polymer.

Table 7. 9: SHG efficiency of polymers

Polymer	SHG efficiency	SHG efficiency
	w. r. to urea (%)	w. r. to KDP (%)
PuF1	2.00	17.78
PuF2- PuF4	2.94	26.16
PuF6- PuF8	2.80	24.89
PuF10 -PuF12	2.83	23.88
PuF5, PuF9, PuF13	1.88	16.67

The polyurethanes showed low SHG efficiency compared to the reference compounds urea (640 mV) and KDP (72 mV). Among the series of polyurethanes (PuF1-PuF13), the polymers containing both chiral diol and amidodiol groups gave considerably high activity compared to bifunctional polymers. PuF2-PuF4, PuF6-PuF8 and PuF10-PuF12 systems showed about 2.94,

2.80 and 2.83 % efficiency as that of urea and 26.16, 24.89 and 23.88 % with respect to KDP. The bifunctional polymers PuF1 showed low SHG efficiency near to 2.00 % of SHG efficiency compared to urea and 17.78 % SHG efficiency as that of KDP. From the NLO measurements, it was found that the polyurethanes with isomannide moiety possessed good Second Harmonic Generation Efficiency.

7. 8. 10. Conductivity of chiral polyurethanes

The conductivity of the polymers was measured by using Keithley 2400 Sourcemeter by 2 probe method. The polymer materials studied were pelletized to measure the conductivity. The source meter was interfaced to a computer in which the measurements were done using a program developed in LABVIEW. The measured conductivity was found to be of the order of 10^{-9} S/cm, which related to the high insulating character of the material, which also confirmed the band gap studies that was already discussed.

7. 8. 11. Solubility of chiral polyurethanes

Solubility studies of polyurethanes with isomannide chiral moiety were performed with solvents having different polarity. A number of solvents were used to check the solubility of polyurethanes. Most of the polyurethanes synthesized were soluble in polar solvents like DMAc, DMSO, DMF etc. and not soluble in non-polar solvents like benzene, toluene, CCl_4 , petroleum ether, ethyl acetate, chloroform etc. The polymers were found to be insoluble because of the polarity and rigidity due to hydrogen bonding.

7. 8. 12. X-ray diffraction for chiral polyurethanes

The X-ray diffraction profiles of the polymers were used to analyze the crystalline nature of polymers²⁰⁻³¹. The crystallinity of the prepared polymers was evaluated and strong reflection peaks between the 2θ range 10 and 40 degree were observed. Since the peaks were found to be broad, the polymeric system was considered to be amorphous in character. There is no prominent shift observed for the polyurethane materials with reference to the nature of the chiral monomers present. The XRD studies showed that the polyurethanes with and without chiral moiety possessed amorphous characteristics. The XRD pattern for PuB2-PuB4 is shown in **Figure 7. 8.**

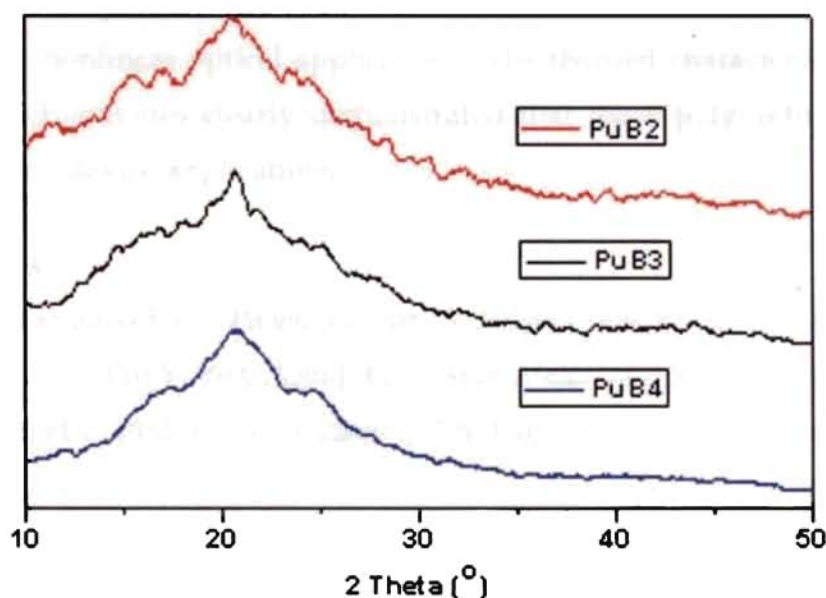


Figure 7. 8: XRD pattern for PuB2-PuB4

7. 9. Conclusions

From the theoretical designing it was concluded that the polymer which contained isomannide as the chiral monomer and CED as amidodiol, showed maximum second-order response. A series of optically active polyurethanes were synthesized by incorporating the isosorbide, isomannide and (2R, 3R)-diethyl tartrate chiral moieties and amidodiol molecules in the main chain. The amidodiol monomers were synthesized by the aminolysis of ϵ -caprolactone. All the series of polyurethanes were characterized by IR, UV-Vis, ^1H NMR, ^{13}C NMR and MALDI-MS spectroscopy. All the polymers showed absorption bands in ultraviolet region from 260 to 300 nm in which the absorption maximum λ_{max} values were between 260 and 275 nm. The band gap calculated for the polymeric systems was in between 4.4-4.7 eV, which was related to the insulating character of the polymers. The electronic excitation and emission of the polymers were studied systematically. From the polarimetric measurements, the specific rotation of the polymers was found to increase with the increase in percentage of chiral moiety. The amorphous nature of polymers were confirmed by the XRD studies and insulating behaviour by conductivity studies. From the thermal measurement it was found that the polymers were thermally stable ($\sim 200^\circ\text{C}$) and exhibited relatively high T_g values which assured a better stability of the induced polar order and the increase in polar order resulted in

high temporal stability. The Kurtz Perry technique showed that the efficiency of the polymers is comparable with that of the standard and hence the polymers can be used for nonlinear optical applications. The thermal characteristics and nonlinear optical activities clearly demonstrated that these polyurethanes are recommended for device applications.

7. 10. References

1. Buruiana T, Buruiana E C, *J Polym Sci: Part A: Polym Chem*, 2004, **42**, 5463.
2. Li Z, Wu W, Yu G, Liu Y, Ye C, Qin J, Li Z, *Appl. Mater. Interfaces*, 2009, **1**, 856.
3. Min J C, Dong H C, Philip A S, Andrew J P A, Larry R D, *Progr in Polym Sci*, 2008, **33**, 1013.
4. Vembris A, Rutkis M, Zauls V, Laizane E, *Thin Solid Films*, 2008, **516**, 8937.
5. Tambe S M, Kittur A A, Inamdar S R, Mitchell G R, Kariduraganavar M Y, *Optical Materials*, 2009, **31**, 817.
6. Tero T, Jarkko L, Juhani H, Kari R, *Dyes & Pigments*, 2009, **80**, 34.
7. Davis D, Sreekumar K, Pati S K, *Synthetic Metals*, 2005, **155**, 384.
8. Bahulayan D, Sreekumar K, *J Mater Chem*, 1999, **9**, 1425.
9. Philip B, Sreekumar K, *J Polym Sci: Part A: Polym Chem*, 2002, **40**, 2868
10. Najun L, Jianmei L, Xuwei X, Qingfeng X, Lihua W, *Dyes & Pigments*, 2009, **80**, 73 .
11. Elizabeth C V, Sreekumar K, *J Mater Sci*, 2010, **45**, 1912.
12. Elizabeth C V, Sreekumar K, *J Appl Pol Sci*, 2010 xx: xxxx.
13. Sudha J D, *J Polym Sci: Part A: Polym Chem*, 2000, **38**, 2469.
14. Pillai C K S, Sandhya K Y, Sudha J D, Saminathan M, *Pramana, J Phys*, 2003, **61**, 417.
15. Sandhya K Y, Pillai C K S, Sreekumar K, *J Polym Sci Part B, Polym Phys*, 2004, **42**, 1289.
16. Sudha J D, Ramamohan T R, Pillai C K S, Scariah K J, *Eur Polym J*, 1999, **35**, 1637.
17. Datta A, Pati S K, *J. Molecular Structure, Theochem*, 2005, **756**, 97.
18. Datta A, Pati S K, *J Phys Chem A*, 2004, **108**, 320.
19. Ramasesha S, Shuai Z, Bredas J L, *Chem Phys Lett*, 1995, **245**, 224.
20. Albert I D L, Ramasesha S, *J Phys Chem*, 1990, **94**, 6540.
21. Ramasesha S, Albert I D L, *Phys Rev B*, 1990, **42**, 8587.
22. Pati S K, Ramasesha S, Shuai Z, Bredas J L, *Phys Rev B*, 1999, **59**, 14827.

23. Pati S K, Marks T J, Ratner M A, *J Am Chem Soc*, 2001, **123**, 7287.
24. Jayaprakash M, Radhakrishnan T P, *Chem Mater*, 2006, **18**, 2943.
25. Davis. D, *Nonlinear optical properties of polymers containing azomesogen and chiral molecules: Theoretical and experimental evaluations*, Ph. D thesis, Department of Applied Chemistry, Cochin University of Science And Technology, Kerala, India, 2005
26. Lalama S J, Garito A F, *Phys Rev A*, 1979, **20**, 20.
27. Sudheesh K K, Sreekumar K, *Int J Polym Mater*, 2009, **58**, 160.
28. Brydson J A, *Plastic Materials*, 7th edition, Iliffe Books, London, 1966.
29. Philip B, Sreekumar K, *Colloid Polym Sci*, 2003, **281**, 485.
30. Philip B, Sreekumar K, *Designed Monomers & Polymers*, 2002, **5**, 115.
31. Philip B, *Studies on photorestructuring of synthetic polymers*, Ph. D thesis, Department of Chemistry, University of Kerala, India, 2001

Chapter 8

SUMMARY

The search for nonlinear optical materials with high optical nonlinearities is essential for potential application in the field of electro-optic devices including optical signal processing, optical limiting, telecommunication and optical storage. Though many kinds of nonlinear optical materials have been extensively studied, searching for high nonlinear optical response polymers are still in progress. Noncentrosymmetry is the main prerequisite for second-order nonlinear optical properties. The most common way to break centrosymmetry in polymers is through electrical poling with an electric field. Alternatively, second-order nonlinear optical devices can be constructed by synthesizing nonlinear optical molecules as chromophores into a noncentrosymmetric supramolecular structure. When such structures extend to macroscopic dimensions, the poling of chromophores can be achieved through chemical synthesis; hence there is no need for external poling. Another promising development in this field of nonlinear optical polymers is the use of chiral polymers. Incorporating chiral units into the main chain of polymers leads to noncentrosymmetric materials with helical supramolecular organization. Therefore, chiral polymers can provide a noncentrosymmetric media with nonvanishing second-order susceptibility. The chirality of the material is associated with the helical supramolecular configuration of the backbone, and a strong coupling exists between the backbone and chromophore. The present study is mostly concerned with improving the performance of NLO polymers for better thermal stability, orientational stability and processability.

The present thesis has discussed the design and synthesis of polymers suitable for nonlinear optics. Most of the molecules that were studied have shown good nonlinear optical activity. The second order nonlinear optical activity of the polymers was measured experimentally by Kurtz and Perry powder technique. The thesis comprises of eight chapters.

The theory of NLO phenomenon and a review about the various nonlinear optical polymers has been discussed in **chapter 1**. The review has provided a survey of NLO active polymeric materials with a general

introduction, which included the principles and the origin of nonlinear optics, and has given emphasis to polymeric materials for nonlinear optics, including guest-host systems, side chain polymers, main chain polymers, crosslinked polymers, chiral polymers etc. The influence of donor-acceptor chromophores and the influence of chirality for designing second order nonlinear optical materials has also been discussed in this chapter.

Chapter 2 has discussed the stability of the metal incorporated tetrapyrrole molecules, porphyrin, chlorin and bacteriochlorin. First principle calculations have been used to investigate the structural stability, electronic structure, and various spectroscopic properties of the free base as well as several metal (with +2 oxidation state Be, Mg, Ca, Sr, Ba, Zn and Cd) encapsulated porphyrin, chlorin and bacteriochlorin complexes. The effect of changes in geometry, bond order, and charge distribution on the stability of various metal encapsulated complexes have been explored, and also the signature in modulation of several spectroscopic properties (e.g., IR, Raman, UV) including nonlinear optical (NLO) properties by DFT and TD-DFT methods. The stability of the complexes are mainly explained based on the size of the metal, bond order between metal and nitrogen, formation energy and the π -electron delocalization of the macrocycle. It was found that the higher formation energy and aromatic character stabilized the complexes in the order, Be > Mg > Ca > Sr > Ba and Zn > Cd. Based on the theoretical findings, it has been predicted that the metal encapsulated complexes followed the order of stability as Be > Mg > Ca > Sr > Ba and Zn > Cd.

Chapter 3 has provided the NLO properties of certain organic molecules by computational tools. The chapter is divided into four parts. The first part has described the nonlinear optical properties of chromophore (D- π -A) and bichromophore (D- π -A-A- π -D) systems, which were separated by methylene spacer, by making use of DFT and semiempirical calculations. The second part of this chapter has discussed the odd-even effects in D-A groups of amidodiols obtained by the aminolysis of ϵ -caprolactone. The effect of spacer length enhancement on the second order NLO properties of twin donor-acceptor molecules having amido units bridged by the CH₂ spacers were thoroughly studied by ZINDO/CV semiempirical calculations. The third part has described

the odd even effect of D-A groups of amidodiols obtained by the aminolysis of γ -butyrolactone. The fourth part of the chapter has discussed the theoretical investigation on the Diels-Alder reactions of fulgides with maleic anhydride. The spectroscopic properties of fulgides obtained by the Stobbe condensation of acetone, acetophenone and benzophenone with diethyl succinate and the theoretical studies regarding the feasibility of Diels-Alder reaction with maleic anhydride were studied by computational methods. DFT/B3LYP/6-31G (d, p) was used for the computational studies for finding the transition state and activation energies.

Chapter 4: A series of polyurethanes was prepared from cardanol, a renewable resource and a waste of the cashew industry by previously designed bifunctional and multifunctional polymers using quantum theoretical approach. The chapter has discussed the importance of polymers derived from natural resources like sugar, cashew nut shell liquid etc. The achiral diol monomer bis 3-pentadecyl phenol used for polymer synthesis was prepared by the condensation of formaldehyde with cardanol. The bis 3-pentadecyl phenol monomer obtained from cashew nut shell liquid, was successfully polymerized with 2, 4- toluene diisocyanate and a new series of high molecular weight polyurethanes were prepared by varying the chiral-achiral monomer (0-100%) compositions. The experimental results showed that the polyurethanes synthesized exhibited large nonlinear optical activity with good thermal stability and optical properties. The theoretically predicted NLO activity was in good agreement with the experimental results. In conclusion the cardanol-based polymers could be considered as very attractive renewable biosources to be used in ecofriendly processes.

Chapter 5: A series of chiral polyurethanes with main chain bis azo diol groups in the polymer backbone was designed and NLO activity was predicted by ZINDO/CV methods. Computational study showed that all the polymers were highly efficient NLO active materials. The azo polymers were designed and synthesized as the polyaddition product of 2, 4-toluene diisocyanate (TDI) with the azo diols, bis (4-hydroxy phenylazo)-2, 2'- dinitrodiphenylmethane, bis (8-hydroxy quinolinazo)-2, 2'-dinitrodiphenylmethane, bis (4-hydroxy-3-methyl phenylazo)-2, 2'-dinitrodiphenylmethane and chiral diols (isosorbide, (2R, 3R)-

diethyl tartrate and isomannide). The bis azo diols were synthesized by the diazo coupling of 4, 4'-diamino-2, 2'-dinitrodiphenylmethane with phenol, 8-hydroxy quinoline and o-Cresol, in which 4, 4'-diamino-2, 2'-dinitrodiphenylmethane was obtained by the nitration of 4, 4'-Diamino diphenylmethane. The theoretical results correlated with the experimental SHG efficiency measurement of the polyurethanes with Kurtz Perry technique. The multifunctional polyurethanes with isomannide as chiral monomer showed maximum NLO activity.

Chapter 6: The chiral polyesters were computationally designed as the polycondensation product of terephthaloyl chloride with chiral diols and achiral diols and NLO properties of the bifunctional and multifunctional polymers were studied by using ZINDO/CV methods. The amidodiols selected for the study were N, N'- ethane- 1, 2- diyl bis (4-hydroxy butanamide), N, N'- butane- 1, 4- diyl bis (4-hydroxy butanamide) and N, N'-hexane- 1, 6- diyl bis (4-hydroxy butanamide), obtained by the ring opening reaction of γ -butyrolactone by 1, 2-diaminoethane, 1, 4-diaminobutane, 1, 6 diaminohexane respectively. The first part of the chapter has described the polyester synthesis using isosorbide as chiral moiety. The second and third parts of the chapter have dealt with synthesis of polyesters from (2R, 3R)-diethyl tartrate and isomannide as chiral molecules and the SHG efficiency of the synthesized polymers were evaluated and the correlation with theoretical results was explored.

In **Chapter 7**, polyurethanes were first designed by computational methods and the NLO properties were predicted by correction vector method. The designed bifunctional and multifunctional polyurethanes were synthesized by varying the chiral-achiral diol compositions. A series of nonlinear optically active polyurethanes was synthesized by incorporating isosorbide, isomannide and (2R, 3R)-diethyl tartrate chiral moieties and amidodiol molecules, N, N'-ethane-1, 2-diyl bis (6-hydroxy hexanamide) (CED), N,N'-butane-1, 4-diyl bis(6-hydroxy hexanamide) (CBD) and N,N'-hexane-1, 6- diyl bis(6-hydroxy hexanamide) (CHD) in the main chain. The amidodiol monomers were synthesized by the aminolysis of ϵ -caprolactone by using diaminoalkanes. The SHG efficiency of the polymers predicted by theoretical calculations correlated with the experimental measurements. 247

Compared to the already existing nonlinear optical polymers, the polymers described in the present study have many merits. The materials are important on account of their high efficiency, ease of fabrication, low cost and thermal stability. All the commercially available polymeric materials are very expensive, whereas most of the monomers used in the present study are very cheap and can be obtained from natural resources. The polymers designed and synthesized in the present thesis deserve special attention as they are economically cheaper. The study was a success in the sense that the aim was achieved along with some results which may find application in nonlinear optical research areas. In conclusion, within the scope of this thesis, different possibilities to obtain attractive nonlinear optical polymer systems were developed and investigated, especially methodologies for oriented system that displays polarized optical characteristics. Furthermore, some of the presented systems may find use in optical data storage media and some of the methodologies could allow the development of patterned electrically conducting or magnetic systems.

"I have not failed. I've just found 10,000 ways that won't work"-A famous quote from Thomas Edison. I won't call this piece of work as an extraordinary one, but the effort taken was nothing short of an extraordinary. As the saying goes, do whatever you do with all your heart and soul, I have put my all into the work to reach this far. I hope this will make a small difference in the study of the nonlinear optical properties of polymers.

PUBLICATIONS

Conference papers

1. Theoretical and experimental evaluations of nonlinear optical properties of chiral polyurethanes with bis (4-hydroxy phenylazo)-2, 2'-dinitrodiphenyl methane as donor acceptor system, Elizabeth C V, Sreekumar K, Presented at *the International Conference I2CAM 2010*, JNCASR, Bangalore, April 2010.
2. Nonlinear optical response of chiral polyurethanes with bis (8-hydroxy quinolinazo)- 2, 2'-dinitrodiphenyl methane as donor acceptor system: Theoretical and experimental evaluations, Elizabeth C V, Sreekumar K, Presented at *the International Conference MATCON 2010*, Cochin University of Science and Technology, Kerala, India, January 2010.
3. Isomannide based NLO active chiral polyurethanes with main chain amido chromophores, Elizabeth C V, Sreekumar K, Presented at *the National Conference MACRO 2009*, IIT Chennai, India, March 2009.
4. Nonlinear optical properties and thermal studies of polyesters with diethyl tartrate as chiral moiety, Elizabeth C V, Sreekumar K, Presented at *the International Conference SAMPADA 2008*, Pune, India, December 2008.
5. Synthesis and Charecterization of Polyurethanes with Isosorbide as Chiral Moiety, Elizabeth C V, Sreekumar K, Presented at *the International Conference POLYCHAR-16* at Lucknow, U. P. India, February 2008.
6. Study of Lennard Jones Fluid System Using Molecular Dynamics, Elizabeth C V, Sreekumar K, Presented at *the International Conference MATCON-2007* at Cochin University of Science and Technology, Kerala, India, March 2007.
7. Dendrimers and applications, Elizabeth C V, Sreekumar K Presented at *the International School on Frontiers in Polymer Chemistry-2006*, Indian Institute of Science, Bangalore, India June 2006.
8. Theoretical Investigation on the Diels-Alder reaction of Fulgide with Maleic Anhydride, Elizabeth C V, Sreekumar K, Presented at *the International Symposium on Theoretical Chemistry Symposium 2006*, Thiruchirappally, India. December 2006.

Journal papers

1. Isosorbide based chiral polyurethanes: optical and thermal studies, Elizabeth C V, Sreekumar K, *J Mater Sci*, 2010, **45**, 1912.
2. Optical and thermal properties of diethyl-(2R, 3R) (+)-tartrate based chiral polyurethanes with main chain amido chromophores, Elizabeth C V, Sreekumar K, *J Appl Polym Sci*, 2010, xx, xx (in press).
3. Hyperpolarizability studies of some nonconjugated twin donor-acceptor molecules, Elizabeth C V, Sreekumar K, *Bull Mater Sci*, 2010, xx, xx (in press).

--T 82--

